PROSPECT OF VERMICOMPOSTING ON TRANSFORMING OIL REFINERY SLUDGE INTO VALUABLE ORGANIC MANURE

A THESIS SUBMITTED IN PARTIAL FULFILLMENT OF THE REQUIREMENTS FOR THE DEGREE OF DOCTOR OF PHILOSOPHY

SNIGDHA NATH

MZU REGISTRATION NO.: 2200136

Ph.D. REGISTRATION NO.: MZU/PhD/1888 of 21/08/2021

DEPARTMENT OF ENVIRONMENTAL SCIENCE

SCHOOL OF EARTH SCIENCES AND NATURAL RESOURCES MANAGEMENT

FEBRUARY, 2026

PROSPECT OF VERMICOMPOSTING ON TRANSFORMING OIL REFINERY SLUDGE INTO VALUABLE ORGANIC MANURE

BY

SNIGDHA NATH

DEPARTMENT OF ENVIRONMENTAL SCIENCE

Supervisor

Dr. SUBHASISH DAS

Submitted

In partial fulfillment of the requirement of the Degree of Doctor of Philosophy in Environmental Science, Mizoram University, Aizawl.

CERTIFICATE

This is to certify that the thesis **"Prospect of vermicomposting on transforming oil refinery sludge into valuable organic manure"** submitted by Mr. Snigdha Nath for the award of Doctor of Philosophy in Environmental Science is carried out under my guidance and incorporates the student's Bonafide research and this has not been submitted for award of any degree in this or any other university or institute of learning.

Dr. Subhasish Das

(Supervisor)

Department of Environmental Science

Pachhunga University College

Mizoram University

Mizoram University

February, 2026

DECLARATION

I, Snigdha Nath, hereby declare that the subject matter of this thesis is the record of work done by me, that the contents of this thesis did not form basis of the award of any previous degree to me or to do the best of my knowledge to anybody else, and that the thesis has not been submitted by me for any research degree in any other University/Institute.

This is being submitted to the Mizoram University for the degree of Doctor of Philosophy in Environmental Science.

(Snigdha Nath)

(Head, Department of Environmental Science) (Supervisor)

Mizoram University

ACKNOWLEDGEMENT

First and foremost, I sincerely and wholeheartedly thank my supervisor, Dr. Subhasish Das, Professor, Assistant Professor, Department of Environmental Science, Pachhunga University College, Mizoram University, for his immense support and guidance throughout my doctoral journey. His insightful and constructive feedback enhanced the quality of my work. This work would not have been completed without his immense knowledge, expertise, and constant supervision. There were many times when it seemed impossible to continue, but his wise and motivational words inspired me to pursue and become a better scholar. The patience and understanding that he had shown me was truly tremendous. I am forever indebted for the guidance and inspiration that he had provided throughout this journey and will forever cherish the moments that had been shared between us in research and academics.

I am very thankful to Mr. Dibyajyoti Dutta, General Manager, Research and Development, Indian Oil Corporation Limited (IOCL), Noonmati, Guwahati, for providing me the oil refinery sludge samples to carry out the experimental works of my Ph.D. This work was possible only because he entrusted me with the oil refinery sludge samples to further my research and experimental pursuits. I am forever grateful for his kind gesture and consideration.

I would also like to thank the Principal Scientist, Horticulture Research Centre, Kahikuchi, Guwahati, for providing me the hybrid seeds of the two crops for my field experiment. Without this kind consideration, my experimental pursuits would not have been successful.

I express my sincere gratitude to Dr. Kulendra Chandra Das, Head of the Department of Environmental Science, Pachhunga University College, Mizoram University, for providing laboratory facilities for conducting my research. I am also thankful to the respected faculty and non-teaching staff of the Department for their encouragement, valuable inputs, and help in various aspects. I will forever cherish the times that I had spent in the Department, under their due support and guidance.

I would like to extend my heartfelt gratitude to the Head of the Department of Environmental Science, Mizoram University, as well as the teaching and non-teaching staff for all the valuable guidance and cooperation throughout the journey here in the university. I am deeply obliged to have the opportunity to sincerely thank all the staff of the Department.

I am also grateful to my colleagues John Lianngura, R. Lalruatdika, R. Laldinthari, M.C. Lalropeki, and B. Lalthlengliana for their support during my lab work. I would also like to thank my juniors Rahul Jairu, Lallawmsangi, and Lynette Ralte for always uplifting me.

I gratefully acknowledge the emotional and moral support provided by my dear friends Gautomi Basumatary, Pradipta Roy, Riku Dutta, Kruttika Rout, and Sudem Boro throughout my Ph.D. journey.

Lastly, I would extend my heartfelt gratitude to my parents Mr. Dharma Kanta Nath and Mrs. Meghali Devi, for their endless support, unconditional love, and sacrifices in educating me. I thank my father for being the very backbone of the person that I am. I pay my deepest love to my mother for nourishing the child in me and making me a responsible person.

I sincerely thank all those who have supported me, directly or indirectly, throughout my research journey. Each one of you has played an important role in helping me complete this work successfully.

I owe everything to God for His guidance and blessings.

I dedicate this thesis to my parents. Thank you, Maa and Deuta, for everything.

CONTENTS

LIST OF TABLES

LIST OF FIGURES

LIST OF PLATES

CHAPTER 1

INTRODUCTION

CHAPTER 1

1. INTRODUCTION

1.1. Industrial waste generation and issues

In the 21st century, waste production has become one of the most pertinent environmental problems, resulting from the ever-growing population and increased per capita consumption (Minelgaitė and Liobikienė, 2019). Consumerism has substantially increased over the recent years because of economic growth, which has consequently increased the rate of industrial waste generation on an extensive scale (Nath et al., 2024). Reports have illustrated that the industrial waste production is predicted to increase 3-fold before the end of the 21st century (Krishnan et al., 2021). The European Union (EU) produces ~482 kg per capita industrial sludge on average every year (Minelgaitė and Liobikienė, 2019). In Europe, the manufacturing units of industries generate about 280 million tons of waste alone (Shahbazi et al., 2013), while in China, the total aggregation of industrial waste for 2017 was approximately 60-70 billion tons, with an utilization rate of only 60% (Zhang et al., 2021). India also generates a significant volume of industrial waste, which is estimated to be about 160,000 tonnes per day (Chaudhary et al., 2021). In India, the industrial sectors produce ~290 million tons of organic wastes, of which 4.5 million tons are categorized as hazardous (Swain et al., 2018). About 0.10 to 0.15-fold of the global industrial waste are classified as harmful and non-biodegradable (Krishnan et al., 2021). In India and China, about 4.5 million tonnes (1.5%) and 11.6 million tonnes (1.1%) of the total industrial waste were classified as hazardous, respectively.

Industrial waste involves a wide array of industrial processed end-products, ranging from hazardous to non-hazardous, recyclable to non-recyclable, and reusable to non-reusable (Soliman and Moustafa, 2020). Primarily, industrial wastes constitute extremely high levels of toxic elements and other hazardous compounds. Several organic compounds such as polyaromatic hydrocarbons (PAHs), pyrenes, phenols, halides, etc., constitute some of the other major detrimental components of industrial waste (Johnson and Affam, 2019; Su et al., 2019). The three major industrial sectors that contribute significantly to the global industrial waste generation are food processing, metallurgy, and non-metallurgy industries (Arockiam JeyaSundar et al., 2020). In the recent decades, industrial waste management has become the most critical environmental problem, particularly in the developing and under-developed nations (Sandberg et al., 2019). Over 300 million tons of industrial waste consisting of various hazardous chemicals, heavy metals, radionuclides, toxic phenols, and hydrocarbons are released into the environment annually without any adequate treatment (Choudhary et al., 2022). According to a 2012 report by the United Nations Environment Programme (UNEP), about 650 million tonnes of industrial sludge is discarded of in the Mediterranean Sea every year. As a result, the marine environment and the adjacent coastal regions undergo detrimental ecological changes, resulting in a reduced economic growth (Bergmann et al., 2015). In addition, prevailing waste disposal processes, i.e., incineration and landfilling produce toxic leachates, hazardous pollutants, and gases in the environment, consequently affecting the terrestrial ecosystems (Gaur et al., 2020). Therefore, the need to effectively control and reduce industrial environmental pollutants should be realized, and effective remediation measures should be promptly implemented accordingly (Bilal and Iqbal, 2020).

1.2. Petroleum industries and oil refinery sludge (ORS)

The petroleum industries form a central pillar in the global economy, which mainly contributes through the production of fuels, lubricating oils, and petrochemical intermediates in large volumes. The exploitation of large quantities of water used in the extraction of crude oil and in the refining procedures lead to the generation of effluents, which are in volumes 0.4-1.6 times greater than the volume of crude oil (Nath et al., 2024). These liquid effluents are processed in different depuration plants, generating oil refinery sludge (ORS), a potentially hazardous waste (Jerez et al., 2021). The main composition of ORS consists of petroleum derived hydrocarbons (PHCs), BTEX (benzene, toluene, ethylbenzene, xylene), heavy metals, and suspended solids (Nath and Das, 2025). By weight, ORS usually contains 35-58% hydrocarbons, 25-31% water, 25-45% other impurities and 3-15% heavy metals (Tanirbergenova et al., 2024). Approximately 60×10^6 tons of ORS is produced worldwide year^{-1}, which is ~0.6% of the overall oil produced (Teng et al., 2021; Hasan et al., 2024). The volume of ORS produced in the refining operations is approximately one-third to one-quarter of the volume of oil processed (Said et al., 2021). In China, the production of ORS is over six million tons per annum, with a recovery rate between 10 to 30% (X. Li et al., 2020). The cumulative production of ORS in India from different refineries is ~28,220 tons year^{-1} (Singha and Deka, 2024). The Indian Oil Corporation Limited (IOCL, Noonmati) in Guwahati, India, alone accumulates more than 16 million kg of ORS, with an oil recovery rate of about 30% (Borah, 2015). Over the past three decades, various ORS treatment and disposal methods like sludge dewatering and drying (Chen et al., 2002), ultrasonic and microwave irradiation (Zhang et al., 2012), solvent extraction (Taiwo and Otolorin, 2009), thermo-chemical treatment (Song et al., 2019), gasification (Martínez

González et al., 2019), oxidation treatment (Ferrarese et al., 2008), bio-slurry treatment (Machín-Ramírez et al., 2008), bioremediation (Marin et al., 2005; Roy et al., 2018), and phytoremediation (Saleh et al., 2017, 2019) have been extensively utilized to evaluate their effectiveness in ORS pollution mitigation. These methods, however, are inherently limited by aspects like their high operational cost, fluctuating efficiency, and time constraints (Singh and Kumar, 2020). Additionally, conventional disposal methods of ORS like landfilling are not efficient as they produce toxic leachates that seep into the underground soil strata or profiles, thereby polluting the ground water, as well as irrigated soils with hydrocarbons and heavy metals. These pollutants also lead to bioaccumulation through food chains, thus posing enormous threats to the overall health of people (Niu et al., 2022). These contaminants impart adverse effects in human beings due to their mutagenic and carcinogenic properties (Wang et al., 2012). The severe toxicological profile of ORS classify it as a critical environmental pollutant, underlining the urgent need for sustainable remediation and valorization methods to reduce its impacts on the ecosystems and humans (Nath et al., 2024).

1.3. Bioremediation avenues for waste management

The recent decades have observed a systematic shift from traditional disposal to resource-recovery approaches under the paradigms of waste management. Reutilization of industrial sludge and effluents constitutes a feasible pathway in waste management system, which follows the principles of circular economy and fulfils the United Nations Sustainable Development Goal 6 (Al-Hazmi et al., 2023). Within this framework, bioremediation strategies have emerged as viable and economically feasible methods to address the undesirable effects of environmental pollution caused by industrial wastes (Verma and Kuila, 2019). Bioremediation mainly deals with the utilization of different biological agents *viz*., enzymes, microorganisms, or multicellular organisms that help in transforming or degrading the harmful pollutants from waste streams (Ramírez-García et al., 2019). Different organisms including animals, plants, fungi, bacteria, cyanobacteria, algae, and yeasts have been utilized in heavy metal remediation (Jasrotia et al., 2017; Jariyal et al., 2020). Microorganisms are extensively used in bioremediation as they are more feasible and easier to work with as compared to the others (Massoud et al., 2019). Moreover, enzymes derived from microorganisms, especially marine microorganisms, have been reported to be more efficient in waste biodegradation (Sivaperumal et al., 2017). However, as the issue of industrial waste management has become more relevant, the very need to find more feasible and environmental friendly technologies that biodegrade industrial waste has been gaining momentum (Bhat et al., 2018b).

1.4. Vermicomposting technology in industrial waste management

Although bioremediation has been extensively used in waste valorization, the potential of earthworms vis-à-vis vermicomposting technology has not yet been examined adequately for the sanitization of a potentially hazardous waste like ORS. Vermicomposting is an inexpensive modern-day technique in which industrial sludge is biodegraded or bio-transformed with the help of earthworms, which act as natural bioreactors during the decomposition process (Paul et al., 2020). It is a non-thermophilic technique that converts organic residues through the complementary mechanisms of earthworms and their gut microbiota into a fortified product known as vermicompost (Pegu et al., 2024). The earthworms accelerate and enhance the biological degradation of these wastes while maintaining aerobic conditions. They do this by influencing the substratum through processes such as fragmentation, turnover, and aeration, and as potential natural blenders, they also increase the surface area in cooperation with microbes (Nath et al., 2023). The produced vermicompost is also considered as one of the nutrient-rich natural organic fertilizers, containing essential plant nutrients (N, P, K, and Ca) (Rorat and Vandenbulcke, 2019). Furthermore, earthworms have high metal bioconversion potential and are able to detoxify heavy metals more efficiently because of their strong metabolic system, anti-oxidative mechanisms, gut microflora, various enzymes, and chloragocyte cells (Das et al., 2016). Under metal stress, earthworms release extracellular polymeric substances through their skin, which facilitate chelation and accumulation of heavy metals (Khan et al., 2019). These exopolymers constitute enzymes, proteins, nucleic acids, humic acids, lipids, etc. (Costa et al., 2018). An investigation showed that the strain KX657843 (*Bacillus licheniformis*) isolated from the gut of *Metaphire posthuma* produced an extracellular polymeric substance that bioaccumulates Cu and Zn ions (Biswas et al., 2020). Earthworms help in heavy metal bioremediation through the bioaccumulation of these metal contaminants in their specialised gut tissues, known as chloragogenous tissues, while also changing the availability of these metals during the vermicomposting process (Paul et al., 2022). The resultant vermicompost, therefore, not only functions as a nutrient-rich organic manure but also a soil conditioner, which improves the structure, water infiltration, and biological activity of soil, resulting in a conducive plant growth environment (Mulatu and Bayata, 2024).

1.5. Utilization of vermi-converted industrial waste in agriculture

The utilization of organic waste derived vermicompost has proven its potential in agriculture because of its rich nutrients and diverse microbial population, making it a suitable organic amendment (Bhat et al., 2018a). Physically, vermicompost serves as an effective soil conditioner due to its adhesive humic compounds and mucus-dense castings that transform soil particles into water-stable clumps, thereby significantly increasing the porosity, aeration, and drainage of compacted clay matrices, as well as simultaneously increasing the water retention characteristics of sandy soils by increasing their organic matter content (Chatterjee et al., 2020). For example, Aksakal et al. (2016) showed that vermicompost application improved the soil macro-aggregation up to 31.2%. Chemically, vermicompost is a balanced and slow-release organic fertilizer containing macronutrients (N, P, and K), and micronutrients (Zn, Mg, and Bo) in plant-available forms. Because of its high levels of humic and fulvic acids, vermicompost suppresses the leaching of the essential nutrients and encourages their slow buildup over time in plant tissues. Another beneficial property of vermicompost is that it demonstrates efficient buffering capacity, which allows it to regulate soil pH toward a neutral value, making it favourable to diverse types of agricultural crops (Kumar et al., 2018). Das et al. (2012) illustrated that the utilization of vermicompost adjusted the soil pH to neutral levels, Yadav et al. (2017) illustrated the effectiveness of vermicompost in increasing the contents of soil organic carbon (SOC), and Olougou et al. (2025) reported that vermicompost application augmented key nutrients including nitrogen (N), phosphorus (P) and potassium (K) in the soil. In a similar manner, Ramnarain et al. (2019) and Sahariah et al. (2015a) have reported that vermicompost maintains high levels of secondary micronutrients. Biologically, vermicompost acts as an effective stimulant, bringing a wide variety of beneficial microorganisms into the soil system, often containing bacteria, fungi, and actinomycetes, and enzymes that inhibit soil pathogens through competitive exclusion and antimicrobial effects (Oyege and Balaji Bhaskar, 2023). Przemieniecki et al. (2021) reported a significant growth in beneficial bacteria due to vermicompost, increasing the abundance from 8.61×10^7 to 37.9×10^7 CFU g^{-1}. In addition to the positive impacts of vermicompost on soil, it also plays a crucial role in the growth and development of plants. It has been shown empirically that vermicompost prevents numerous diseases in plants by stimulating the expression of certain anti-oxidant enzymes and hormones (Hussain *et al*., 2017). Moreover, it has been demonstrated that plant growth-promoting regulators (PGPRs), including auxin, cytokinin, and gibberellin, are produced in vermicompost and mediated by the beneficial microbial communities (Lamichhane, 2017).

The use of vermi-transformed industrial wastes, particularly organic-based sludge of agro-processing, food, and paper industries has been fruitful in terms of promoting sustainable agricultural (Vyas et al., 2022). For instance, vermicomposting of anaerobic sludge from wastewater treatment and agro-industrial co-digested mixtures of olive mill wastewater and cheese whey showed significant N increment of 22-38.7% and 14.1-51.8% increment in P (Vavouraki and Kornaros, 2023). Vermicomposting of composite palm oil waste water has also demonstrated considerable increases in the concentrations of macronutrients, while reducing the carbon-to-nitrogen (C:N) ratio to a balanced 17.2 (Rupani et al., 2017). Moreover, a two-year field study applying vermicompost from liquid waste treatment reported significant increases in total soil C, total N, potentially mineralizable N, and particulate organic matter (Malal et al., 2024). Vermi-processed spent drilling fluid through *Eisenia fetida* showed better C:N ratio, mineral availability, and nutrient load (Z. Wang et al., 2021).

The application of vermicompost obtained from organic wastes has also shown positive results for different crop species (Oyege and Balaji Bhaskar, 2023). A meta-analysis has demonstrated that soil amendment with vermicompost resulted in a 0.26-fold boost in marketable yield of crops, 0.13-fold increase in total weight, 0.78-fold increase in shoot biomass, and 0.57-fold increment in root biomass (Blouin et al., 2019). Specific reports on potted vegetable soybeans showed that a 2% (w/w) soil amendment rate of vermicompost was optimal for enhancing the growth and yield benefits (Nonthapa et al., 2024). Bai et al. (2025) reported that vermicompost increased the fruit yield of strawberries up to 19.6% and Zhang et al. (2023) demonstrated vermicompost to increase fresh pod pepper yield from 24.4% to 88.9%. Studies have also demonstrated its positive effects on the growth and nutrient constitution of paddy crops like maize, barley, and buckwheat (Ozyazici and Turan, 2021; Khalifa et al., 2022). Moreover, vermicompost application at different rates has shown varying trends in crop production. For example, when vermicompost was applied at 0 to 250 tonnes ha^{-1}, the highest yield and biomass in the production of barley was achieved at 250 tonnes ha^{-1} (Shen et al., 2022). Contrastingly, Sengupta et al. (2021) observed that vermicompost applied at 3 tonnes ha^{-1} was sufficient for enhancing rice cultivation. The application of vermicompost primarily increases the soil nutrient availability and humic content, which boosts plant elongation, leaf broadening, and leaf area (Singh and Misal, 2022). For instance, humic substances from vermicompost along with arbuscular mycorrhizal fungi enhanced dry shoot and root biomass, increased plant elongation, and nutrient constitution in corns (Pinos et al., 2019).

Vermicompost application in soil has shown to modulate membrane proteins, stimulate plant defence mechanisms, and improve photosynthesis rates and phytoextraction potential of plants (Santos et al., 2022). The disease-suppressive traits of vermicompost have been observed to be species-specific; for instance, vermicompost derived from *Eudrilus eugeniae* has shown to inhibit the mycelial growth of the pathogen *Athelia rolfsii* by 50% *in vitro*, outperforming *E. fetida*-derived compost (16% inhibition) in soybean seedlings (Nonthapa et al., 2024). In terms of pollution mitigation, vermicompost also showed reduced accumulation of Cd content in soil and crops, particularly in rice cultivation (Liu et al., 2021a). Although the positive effects of vermicompost application are widely observed in agriculture, yet the negative impacts on soil and plants are not negligible. The usage of vermicompost may bring in heavy metals into soil and plants, especially when produced from waste streams such as municipal waste and sewage effluents (Mousavi et al., 2010). This type of contamination may pose serious risks to the soil biota, vegetation, as well as human beings, depending on the relative heavy metal concentrations. For instance, Shen et al. (2022) demonstrated that the application of vermicompost contaminated with heavy metals increased the concentrations of those heavy metals in soils and barley crops. However, it is worth mentioning that these concentrations were still within the permissible limits of the National Environmental Quality Standard (NEQS), suggesting no immediate risks to the environment (Oyege and Balaji Bhaskar, 2023). Large-scale applications of vermicompost have also proven its feasibility. For example, New Zealand had transformed about 80,000 tonnes per year of blended dairy processing sludge and pulp/paper mill refuse into vermicast, which was then applied on pastures, resulting in improved soil health and nutrient uptake (Quintern et al., 2016).

1.6. Research gaps and scope of the study

Although waste management is a widely investigated topic, yet there is a huge gap in the knowledge regarding oil refinery sludge (ORS) bioremediation. In recent years, investigations have been primarily focused on microbial-assisted remediation of ORS, however, the potential of earthworms in bio-transforming ORS is an underexplored research area that requires thorough investigations, considering the successful precedent works in industrial sludge vermiremediation. Specifically, the lack of systematic species-specific data on the remediation efficiency and metabolic performance of the different earthworm species with regards to ORS mitigation serves as the major research gap of this study.

This proposed study aims to fill these gaps holistically by carrying out systematic research on the vermiremediation of ORS for waste management and resource recovery with the following scopes:

a) Process optimization: To evaluate and optimize the vermicomposting process of ORS by using it as the primary feedstock.

b) Species-specific performance: To conduct a comparative analysis of the ORS remediation potential and differences of two earthworm species *Eisenia fetida* and *Eudrilus eugeniae*.

c) Product validation: To characterize the produced ORS vermicompost through chemical, ecotoxicological, and agronomic tests to ensure its safety as an organic manure.

1.7. Objectives of the study

To address the research gaps and scopes mentioned above, the present study was carried out with three main objectives:

i. To convert the oil refinery sludge through vermicomposting.

ii. To compare the potential of *Eisenia fetida* and *Eudrilus eugenia*e to produce vermicompost.

iii. To analyze the impact of vermicompost on the growth and yield of Cabbage and Tomato plant.

1.8. Structure of the thesis

The present thesis is divided into five chapters along with appendices and references:

CHAPTER 1 – INTRODUCTION

CHAPTER 2 – REVIEW OF LITERATURE

CHAPTER 3 – MATERIALS AND METHODS

CHAPTER 4 – RESULTS AND DISCUSSION

CHAPTER 5 – SUMMARY AND CONCLUSION

APPENDICES

REFERENCES

CHAPTER 2

REVIEW OF LITERATURE

CHAPTER 2

2. REVIEW OF LITERATURE

2.1. Waste generated from oil refining activities

The various processes in the petroleum refineries produce a wide variety of refinery wastes. Among these wastes, oil refinery sludge (ORS) constitute an extensive portion and is paid more attention to regarding its treatment and disposal (Hu et al., 2013). The petroleum wastes are mainly derived from three activities: i) exploration and production (E&P), ii) hydrocarbon processing, and iii) storage, transport, and distribution. Among the E&P activities, drilling, construction, development, production, and maintenance generate air pollutants, toxic effluents, and solid wastes (Jafarinejad, 2017). Contaminated soils, tank and piping wastes, production materials, pigging sludges, and incinerator ash constitute majority of the solid wastes in the E&P activities (Bashat, 2002). The solid wastes produced during the hydrocarbon processing activities are mainly of three types: i) sludge (oily and non-oily), ii) other refinery wastes (miscellaneous wastes), and iii) non-refinery wastes (European Commission and Joint Research Center, 2013). As a consequent of the steam-cracking and other refining processes, wastes such as coke, spent adsorbents, spent catalyst, oil filters, cartridges, etc., are generated. In addition, the storage, transport, and distribution operations of oil refining are integrated with the other sectors and produce wastes in the different terminals. The solid wastes generated during this phase mainly include sludges from the storage and transportation tanks (Jafarinejad, 2017). However, oil refinery sludges (ORS) are produced from all the three major refining activities including the production, storage, and transportation of crude oil (Deng et al., 2016; J. Liang et al., 2017) (Figure 1). These sludges are also derived from drilling processes, oil wells, emulsified solids, and storage tanks (Viana et al., 2015).

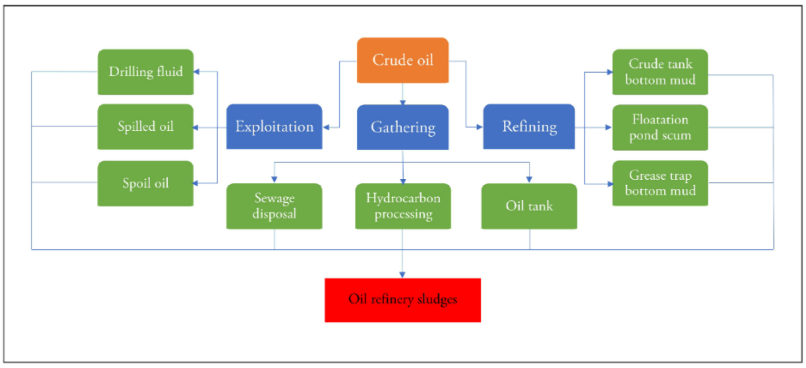

Figure 1. Sources of oil refinery sludge during petroleum refining activities

2.2. *Oil refinery sludge – global generation*

The global generation of ORS has substantially increased as a result of the growing energy demands (Hu et al., 2020). The ORS produced from petroleum refineries depends on various factors, such as the physical properties of the crude oil, refinery processing strategies, oil storage methods, and refining capacities (Hu et al., 2013). As per the Energy Institute Statistical Review of World Energy (2023), the global petroleum production is >14,000,000 m^3 per day, generating approximately 30,000 m^3 of ORS per day (Corrochano et al., 2025). Annually, approximately 30,000 tons of sludge can be produced with refining capacities varying in between 12,000-15,000 m^3 per day (Hu et al., 2020; Paul Choudhury and Kalamdhad, 2021). Globally, about 1.5% of the total oil processed in refineries is discarded of as oily sludge (Laurelta and Ernest, 2020). According to the reports of United States Environmental Protection Agency (US EPA), an average of 30,000 tons of ORS is produced by the United States annually (Hu et al., 2013). In Greece, petroleum refineries produce around 34,000 tonnes of ORS per year, while ORS produced in Europe was estimated to be around 1 million tonnes (Table 1). In China, approximately 3 million tons of oily sludge is discarded of by the petroleum refineries (Wang et al., 2012; Nath et al., 2024). The overall amassment of oily sludge in China had reached ~143 million tons based on business statistics (X. Li et al., 2020). As per the National Environmental Engineering Research Institute's report (NEERI, 1999), the Numaligarh oil refinery in India generates a total volume of ~1,400 tons $year^{-1}$ of ORS, followed by Bongaigaon oil refinery (~940 tons $year^{-1}$), Guwahati oil refinery (~400 tons $year^{-1}$), and Digboi oil refinery (~260 tons $year^{-1}$) (Bhattacharyya and Shekdar, 2003).

Table 1. An overview on the annual generation of oil refinery sludge

Country/Region	**Annual ORS Generation (million metric tons)**	**Source**
United States (U.S.)	~1.0 MMT	Hasan et al. (2024)
European Union (EU)	0.3–1.0 MMT	Jerez et al. (2021)
China	3.0–6.22 MMT	Dal Mas et al. (2021); Chen et al. (2024)
India	>0.028 MMT	Singha and Deka (2024)

2.3. Oil refinery sludge – chemical composition and heterogeneity

The constitution of ORS is highly heterogenous, depending on various factors such as the crude oil source, processing methods, and specific equipment and chemicals employed during the crude oil production. The total petroleum hydrocarbons (TPHs) concentration in ORS may vary between 15-50% (w/w), while total water and solid content could be between 30-85% (w/w) and 5-46% (w/w), respectively (Jerez et al., 2021). ORS may also contain up to 0.3-fold hydrocarbons and 0.3-fold solids by weight (Mokhtar et al., 2011). The hydrocarbons and organic matter in ORS mainly consist of saturates, aromatics, resins, and asphaltenes (SARA-fractions), comprising 5-60% of the overall mass. The dominating long-chain hydrocarbons (asphaltenes) mainly contributes to the viscosity of ORS, while the lighter toxic fractions (benzene, toluene, ethylene, and xylene - BTEX) are often minimal due to weathering (Hasan et al., 2024). In general, ORS contains ~50% alkanes, ~33% aromatics, ~10% asphaltenes, and ~22% resins by weight (Liu et al., 2019). The chemical heterogeneity of ORS results in variations in its physical characteristics including viscosity, density, and heating value. Oliveira et al. (2024) reported that the viscosity of ORS was approximately 34,793 centipoises, with 36.41% carbon, 56.80% oxygen, and 43.21% ash content (w/w). In addition, the heating value of ORS was in the range of 17.49–19.04 MJ/kg. The nitrogen content of ORS is generally less than 3%, sulphur content is within 0.3-10%, and oxygen level is less than 5%.

However, the observed properties of ORS procured from one source may not be similar to those procured from another source, and to those acquired at the same source at different times and location (Jerez et al., 2021). Abdulqader et al. (2021) demonstrated that ORS consisted 79% moisture content, 5% ash, 6% volatile matter, and 11% solid carbonaceous compounds. In contrast, Alexandrovich and Sergeevich (2018) reported that ORS was constituted of 72% organic components, 19.2% moisture content, 1.8% sulphur, and 16% mineral portion. Corrochano et al. (2025) found that ORS was composed of three phases: solid (1.6-8.2%), aqueous (7.7-98.4 %), and oily (35.6-88.3%). Similarly, Liang et al. (2014) reported that ORS contains water, oil, and solids in the range of 30-50%, 29-50%, and 10-12%, respectively. In addition, the presence of metals such as lead (Pb), nickel (Ni), zinc (Zn), chromium (Cr), copper (Cu), cadmium (Cd), vanadium (V), and arsenic (As) in ORS has been reported (Singh and Kumar, 2020; Hasan et al., 2024). The heavy metals in ORS also vary over a wide range as procured from different sources (Hu et al., 2013). In India, the concentrations of the different heavy metals (Ni, Cr, Zn, Mn, Cd, Cu, and Pb) present in ORS are mainly in the range of 0.001 to 120 mg kg^{-1} (Bhattacharyya and Shekdar, 2003).

2.4. Oil refinery sludge – environmental impacts

Various components of ORS viz., hydrocarbons, toxic metals, along with waxes and asphaltenes, are detrimental constituents for the ecosystem, as well as human health (Vdovenko et al., 2015). Because of the high concentrations of these toxic compounds, inefficient handling and disposal of ORS might pose a serious threat to the environment by contaminating groundwater, soil, and air (Hu et al., 2013; Jasmine and Mukherji, 2015). The petroleum derived hydrocarbons (PHCs) found in ORS could alter the properties, functions, and biological activities of the soil after enter into terrestrial ecosystems via leaching (Robertson et al., 2007). Most of the petroleum sludge contaminated soils are found to be lacking in essential nutrients, thus restricting seed growth, as well as inhibiting plant development (Al-Mutairi et al., 2008; Nath et al., 2024). The PHCs also lower the activity of soil enzymes and have negative effects on the soil microorganisms and nematodes (Suleimanov et al., 2005). As ORS is highly viscous, these sludges form a thick oil cover on the soil surfaces, minimizing water infiltration, hydraulic conductivity, and moisture content of the soils (Nath et al., 2024). These PHCs trickle through the different soil layers into underground aquifers, thus affecting the associated aquatic systems (Hu et al., 2013). Polyaromatic hydrocarbons (PAHs) found in ORS are of major concern as they are highly recalcitrant, owing to their tight molecular bonds, molecular weight, and hydrophobicity (Johnson and Affam, 2019).

2.5. Vermicomposting technique

Vermicomposting is an inexpensive modern-day technique that converts or biodegrades organic wastes with the help of earthworms, that act as natural bioreactors during the decomposition process. The earthworms accelerate and enhance the biological degradation of these wastes while maintaining aerobic conditions (Wang et al., 2009). They do it so by influencing the substratum through processes such as fragmentation, turnover, and aeration, and they also increase the surface area while in cooperation with microbes (Edwards and Lofty, 1977). The decomposition of substances is accelerated as a consequence of their enzymatic activity and nutrient enrichment (Ndegwa and Thompson, 2001). Moreover, earthworms have high bioconversion potential for heavy metals because of their active metabolism, presence of gut microbiota, enzymes, and chloragocyte cells (Srivastava et al., 2005).

2.5.1. Interplay of natural bulking materials

Bulking materials are substances that contain high carbon content, facilitating structural integrity to compost pile, control air supply to the compost, maintain moisture of the compost, and balance different vermicomposting parameters (Adhikari et al., 2008). Examples of bulking materials include cow manure, rabbit manure, poultry manure, agricultural residues, sawdust, rice husk, sugarcane trash, and household wastes (Manish et al., 2013). These substances help in adjusting the composting process conditions such as moisture, nitrogen content, C:N ratio, and air supply during the composting process (Nath et al., 2023) (Table 2).

Bulking agents such as cotton waste and maize straw have shown to enhance the nutritive values during the composting of olive mill sludge (Paredes et al., 1996). Usage of cow manure and sawdust have demonstrated to balance the C:N ratio and water levels in compost produced from water hyacinth (Singh and Kalamdhad, 2012). Madejón et al. (2001) observed that adding cotton gin and grape marc in the composting of sugar beet vinasse helped in obtaining a high-quality compost. Composting sewage sludge with the amendment of saw dust illustrated reduction in the concentrations of aromatic compounds by 88% (Oleszczuk, 2006). Vermicomposting of pre-consumer processing vegetable wastes (PPVW) spiked with cow manure showed a reduction in the C:N ratio by 45-69%, while it also stabilized the pH content and reduced heavy metal load (within permissible limits) (Garg and Gupta, 2011a). Vermiconversion of coal fly ash with the amendment of press mud resulted in an overall reduction in pH, C:N ratio, and organic C of the vermicompost (Karwal and Kaushik, 2020).

Table 2. Influence of various bulking materials in the composting and vermicomposting process

Sl. No.	Bulking materials	Types of wastes/substrates	Process	Functions	References
1.	Biochar	Poultry manure	Composting	Reduces loss of N	(Dias et al., 2010)
2.	Clinoptilolite and saw dust	Sewage sludge	Composting	Heavy metal uptake and boosts humic component	(Zorpas and Loizidou, 2008)
3.	Cotton gin and grape marc	Sugar beet vinasse	Composting	Maintains temperature, pH, and boosts quality of compost	(Madejón et al., 2001)
4.	Cotton and maize residues	Olive mill wastewater sludge	Composting	Minimized N loss, increases N fixation, and organic matter	(Paredes et al., 1996)
5.	Cow dung	Water hyacinth	Vermicomposting	Better earthworm proliferation	(Gajalakshmi et al., 2002)
6.	Cow dung	Textile mill sludge	Vermicomposting	Balances C:N ratio	(Kaushik and Garg, 2003)

7.	Cow dung	Water hyacinth	Vermicomposting	Boosts activation of enzymes	(Pramanik, 2010)
8.	Cow dung	Vegetable wastes	Vermicomposting	Minimizes heavy metals	(Garg and Gupta, 2011a)
9.	Cow dung	Paper mill wastes	Vermicomposting	Increases growth and proliferation in earthworms	(Kumar Badhwar et al., 2020)
10.	Cow dung	Biowastes	Vermicomposting	Balances C:N ratio and increases NPK	(Biruntha et al., 2020)
11.	Cow dung and saw dust	Water hyacinth	Composting	Maintains pH, bulk density, and C	(Singh and Kalamdhad, 2012)
12.	Fly ash and saw dust	Sewage sludge	Composting	Mitigates polyaromatic hydrocarbons	(Oleszczuk, 2006)
13.	Grape stalk and olive leaf	Alperujo (olive oil extraction by-product	Composting	Maintains air supply, temperature, C:N ratio, and pH	(Alburquerque et al., 2006)
14.	Onion peel	Kitchen wastes	Composting	Balances C:N ratio	(Abdullah et al., 2013)
15.	Press mud	Coal fly ash	Composting and vermicomposting	Maintains pH, C, C:N ratio, and facilitates reproduction of earthworms	(Karwal and Kaushik, 2020)
16.	Rice husk	Food wastes	Composting	Maintains temperature and moisture	(Chang and Chen, 2010)
17.	Rice straw	Swine manure	Composting	Reduces organic carbon and matter	(Zhu, 2007)
18.	Saw dust	Food wastes	Composting	Maintains pH, moisture, and air supply	(Adhikari et al., 2008)
19.	Star grass and sugarcane bagasse	Municipal solid wastes	Composting	Improves pH and total organic carbon	(Oviedo-Ocaña et al., 2015)

20.	Sugarcane trash	Different organic wastes	Composting	Maintains pH and C content	(Goyal et al., 2005)
21.	Waste paper and plant residue	Waste paint sludge	Composting	Reduces organic matter, trace elements, and C:N ratio	(Tian et al., 2012)

Thesis data published in the review paper: Nath, S., Qureshi, A., Das, S., 2023. Role of bulking agents, process optimization, and different earthworm species in the vermiremediation process of industrial wastes: A review. Not. Sci. Biol. 15, 11490.

2.5.2. Interplay of abiotic or climatic factors

Temperature, humidity/moisture, and light play crucial roles in the production of good quality compost, while maintaining health and reproduction of earthworms (Zhang et al., 2021; Zhou et al., 2021). Warmer temperature facilitates an increase in microbial population, thus maintaining high temperature for longer periods facilitates the effectiveness of the decomposition process (Chinakwe et al., 2019). *Proteo-bacteria* and fungi heightened the biodegradation activity at mesophilic temperatures (35°C to 37°C) during cattle manure composting. Organic matter degradation was also high at similar temperatures (Tang et al., 2007). Vermicomposting of pig manure showed that earthworms demonstrated higher enzymatic activity of catalases in mesophilic temperatures, while increasing the NPK content (Zhou et al., 2021). During dewatered sludge vermicomposting, temperature increase accelerated the rate of decomposition, carbon mineralization, and nitrogen assimilation. Also, an optimum temperature of 25°C resulted in high organic matter degradation and high nitrate content (Zhang et al., 2020). Another study showed that organic matter degradation by *E. fetida* and increment in TKN was more in the colder days as compared to warmer days, showing variation in seasons. Also, the reproductive activity of the earthworms were favoured more during the winter season (Garg and Gupta, 2011b).

Hossen et al. (2022) showed that moisture levels of about 70% were effective in crude fiber decomposition and production of crude protein. The decomposition and reaction kinetics were highest at ~75% moisture level, while a decrease in C:N ratio at same moisture levels was observed (Palsania et al., 2008). Yeh et al. (2020) studied the effect of initial moisture content and found that moisture in the range of 55-70% was more appropriate for successful composting of wastes. Moreover, earthworms are photophobic and sensitive to different light intensity and color (Harper, 1905; Naimpally and Nayak, 1978; Lin et al., 2018). Ultra-violet radiations have shown to reduce growth and reproductive rates, and inhibit cocoon fertility rate of *E. fetida* by 70% (Hamman et al., 2003). Lin et al. (2018) examined the impacts of monochromic lights and intensities on the photophobic behavior of earthworms (Table 3). It was found that light at higher intensities, particularly 270 lx, significantly increased earthworm movement away from the source, while red light elicited the weakest photophobic response.

Table 3. Effects of abiotic factors in the vermicomposting process

Abiotic factors	Process	Effects	References
Temperature	Vermicomposting	Enzyme activity and nutrient (N, P, K) levels were highest at 30°C	(Zhou et al., 2021)
	Vermicomposting	High EC and nitrate levels, combined with low organic matter, at 25°C	(Zhang et al., 2020)
	Vermicomposting	High organic matter decomposition during winter lowered the C:N ratio and raised total Kjeldahl nitrogen levels	(Garg and Gupta, 2011b)
	Vermicomposting	Optimal earthworm growth and high-quality compost production occur at temperatures between 15°C and 25°C	(Rostami et al., 2009)
	Vermicomposting	Enhanced vermicompost turnover, earthworm population, and biomass under low-temperature conditions	(Gopal et al., 2004)
	Vermicomposting	Peak activity for *E. eugeniae* occurs between 25°C and 28°C	(Shagoti et al., 2001)
	Vermicomposting	Sustained reproductive efficiency of *E. eugeniae* in cold environments	(Amoji et al. 1999)

Moisture	Vermicomposting	At 70% moisture content, crude fiber degradation was high and crude protein increased	(Hossen et al., 2022)
	Vermicomposting	Optimal earthworm growth and compost quality occur within a 65-75% moisture range	(Rostami et al., 2009)
	Vermicomposting	Moisture levels of 75 ± 5% resulted in a greater reduction in the C:N ratio, decomposition rate, and kinetic reaction rate	(Palsania et al., 2008)
	Vermicomposting	Higher relative humidity improved vermicompost processing, increased the population of *Eudrilus sp.* earthworms, and boosted worm biomass	(Gopal et al., 2004)
Light	Vermicomposting	Higher light intensities elicit a stronger negative phototaxis in earthworms	(Lin et al., 2018)
	Vermicomposting	*Hyperiodrilus africanus* exhibited its highest casting rate under red light and its lowest emigration rate in darkness	(Owa et al., 2008)
	Vermicomposting	High-frequency light (UV) exposure led to a reduction in both the growth rate and reproductive rate of the earthworm *E. fetida*	(Hamman et al., 2003)

Thesis data published in the review paper: Nath, S., Qureshi, A., Das, S., 2023. Role of bulking agents, process optimization, and different earthworm species in the vermiremediation process of industrial wastes: A review. Not. Sci. Biol. 15, 11490.

2.5.3. Role of different earthworm species – epigeic, endogeic, and anecic

Earthworms are terrestrial oligochaetes that mainly inhabit soil and constitute the largest animal biomass in temperate ecosystems (Martin, 1976). Earthworms can be grouped into three main ecological categories based on where they live in the soil: epigeic, endogeic, and anecic.

(Domínguez, 2018). And on the basis of their feeding habit, they are divided into two major groups: detrivores and geophagous (Hendrix, 1995).

Epigeic earthworms, which primarily inhabit the soil surfaces and organic horizon (Domínguez, 2018), primarily facilitate in decomposing organic matter, thereby accelerating decomposition rates and nutrient cycling (Gomez-Brandon et al., 2011). *E. fetida* imparted a reduction in pH and increased electrical conductivity, total N, and other available nutrients during vermicomposting of patchouli bagasse (Ahmed and Deka, 2022) (Table 4). Vermicomposting of spent drilling fluid by *E. fetida* reported a reduction in C:N ratio, and increment in EC and total NPK content (Z. Wang et al., 2021). Vermicomposting of brewery spent grain by *E. fetida* showed increased mineralization rate and stabilization of the mixture (Saba et al., 2019). Another investigation showed that *E. andrei* could successfully convert aquatic weed *Salvinia* into vermicast without amendment of bulking agents or pre-treatment (Channgam et al., 2015). *E. eugeniae* is also known for its vermicomposting ability, wherein this species was employed in the vermicomposting of hazardous coir pith. The results showed an increment in EC and total NPK content and a reduction in organic matter, TOC, and phenolic composition in the vermicompost (Jayakumar et al., 2022).

Endogeic earthworms inhabit deeper profiles of soil and primarily ingest on soils dense in organic residues (Domínguez, 2018). While epigeic and anecic earthworms are commonly utilized in vermicomposting, endogeic earthworms see far less application. This limited use may be explained by their ecological niche: as non-detritivores, they do not primarily consume surface litter or debris, instead inhabiting and feeding within deeper soil layers (Das et al., 2020). Nevertheless, the vermicomposting capacity of endogeic earthworms remains an understudied area, with only limited research conducted to date. For instance, Das et al. (2016) explored the use of *Metaphire posthuma* in processing jute mill waste. Their findings indicated that the resulting vermicompost exhibited increased availability of total NPK, humic and fulvic fractions of carbon, and microbial biomass carbon. Sahariah et al. (2015) examined the efficacy of *M. posthuma* in processing municipal solid waste through vermicomposting and demonstrated its potential to bioaccumulate heavy metals (Table 4).

Anecic earthworms are deep-dwelling species that create permanent vertical tunnels reaching depths of several meters (Domínguez, 2018; Das et al., 2020). In cadmium-contaminated soils, the anecic earthworm *Lampito mauritii* increased soil enzymatic activity (Sivakumar et al., 2015). Rajadurai et al. (2022) investigated the vermiremediation efficiency of *L. mauritii* on engine oil contaminated soils and demonstrated reduction of PAHs and TPHs by 68.6% and 34.3% respectively. Prashija et al. (2017) found that vermicomposting lignocellulosic waste with *L. mauritii* resulted in a final product with reduced pH, C:P ratio, and lower concentrations of lignocellulosic biomass and phenols (Table 4). During tea factory coal ash decomposition, *L. mauritii* efficiently accumulated heavy metals including Mn, Zn, Cu, and As (Goswami et al., 2014).

Table 4. Role of epigeic, endogeic, and anecic earthworms in vermicomposting

Category	Earthworm species	Wastes (organic/inorganic)	Effects	References
Epigeic	*Eisenia fetida*	Patchouli bagasse from oil industry	Key changes included reductions in organic C, C: N, C:P, and total K, alongside rises in total P and Ca and the uptake of heavy metals	(Ahmed and Deka, 2022)
	Eisenia fetida	Spent drilling fluid from Nature-gas industry	A decline in total organic carbon and the C:N ratio was observed, concomitant with a rise in total NPK content	(Wang et al., 2021)
	Eisenia fetida	Paper mill sludge + citronella bagasse	Lowering of the C:N ratio and degree of humification	(Boruah et al., 2019)
	Eisenia fetida	Spent grains from brewery	A decrease in organic carbon occurred with increases in nitrogen and humic substances	(Saba et al., 2019)
	Eisenia fetida	Sewage sludge	-	(Malińska et al., 2016)
	Eisenia fetida	Fruits and vegetable wastes	A decline in total organic carbon and a concurrent rise in total nitrogen	(Huang et al., 2016)
	Eisenia fetida	Tannery sludge	-	(Cunha et al., 2016)
	Eisenia fetida	Filter cake	Reduction in total organic carbon and total nitrogen	(Busato et al., 2016)
	Eisenia fetida	Wastewater sludge	Lower pH, total organic carbon, and C:N ratio, but higher total available phosphorus	(Xie et al., 2016)

Eisenia fetida	Fly ash	Reduction in C:N ratio	(Mupambwa et al., 2016)
Eisenia fetida	Press mud	Total organic carbon, the C:N ratio, and K decreased, while N, P, and Na increased	(Bhat et al., 2016)
Eisenia fetida	Apple pomace wastes	Rise in the concentration of plant-available N, P, K, and Mg	(Hanc and Chadimova, 2014)
Eisenia fetida	Dyeing sludge	Electrical conductivity, C:N ratio, organic carbon, and K content decreased, while N, P, and Na content increased	(Bhat et al., 2013)
Eisenia fetida	Sewage sludge	A gain in total nitrogen and phosphorus was accompanied by a reduction in metal content.	(Hait and Tare, 2012)
Eisenia fetida	Beverage sludge	Levels of electrical conductivity, organic C, and K declined, while levels of N, P, and Na increased	(Singh et al., 2010)
Eisenia fetida	Textile sludge	A decrease in the C:N ratio accompanied by an increase in nitrogen and phosphorus content	(Garg and Kaushik, 2005)
Eisenia andrei	Apple pomace wastes	Reduction of pathogenic *E. coli* and *Enterococcus*	(Procházková et al., 2018)
Eisenia andrei	Sewage sludge and kitchen wastes	-	(Hanc and Dreslova, 2016)
Eisenia andrei	Dairy sludge and paper mill sludge	Higher N and P content coupled with low heavy metal levels	(Elvira et al., 1998)
Eudrilus eugeniae	Coir pith	A decline in organic matter, total organic carbon, C:N ratio, C:P ratio, and phenolic content was observed, alongside an increase in electrical conductivity and total levels of NPK and calcium	(Jayakumar et al., 2022)
Eudrilus eugeniae	Lignocellulosic organic wastes	A consistent C:N ratio of 15 to 1	(Pandit et al., 2020)

Eudrilus eugeniae	Pressmud	The pH, total organic carbon, C:N ratio, water-soluble organic carbon, and C:P ratios all decreased, while the NPK content and microbial population increased	(Balachandar et al., 2020)
Eudrilus eugeniae	Biowastes	Reduced inorganic matter, organic carbon, lignin, cellulose, C: N, and C:P ratios, and elevated NPK levels	(Biruntha et al., 2020)
Eudrilus eugeniae	Municipal solid waste	Reduction in C:N ratio	(Soobhany et al., 2017)
Eudrilus eugeniae	Fermented tannery waste	Levels of heavy metals and total organic carbon decreased, while total Kjeldahl nitrogen increased	(Ravindran et al., 2016)
Eudrilus eugeniae	Kitchen waste	Lower levels of organic matter and carbon, but higher levels of electrical conductivity, nitrogen, phosphorus, and potassium	(Taeporamaysamai and Ratanatamskul, 2016)
Eudrilus eugeniae	Food waste	A concurrent increase in total nitrogen and decrease in total potassium	(Lalander et al. ,2015)
Eudrilus eugeniae	Tannery waste	Reduction in total organic carbon and C:N ratio	(Ravindran et al., 2015)
Perionyx excavatus	Seaweed	A decrease in organic carbon alongside an increase in NPK	(Ananthavalli et al., 2019)
Perionyx excavatus	Paper mill sludge	A decrease in pH, total organic carbon, C: N ratio, and C:P ratio, alongside an increase in electrical conductivity, total nitrogen, total phosphorus, and total potassium	(Yuvaraj et al., 2018)
Perionyx excavatus	Guar gum industry waste	Organic carbon declined as total N and P increased	(Suthar, 2006)
Perionyx simlaensis	Organic waste	Reduction in C:N ratio	(Bhardwaj and Sharma, 2015)

	Lumbricus rubellus	Sugarcane industry waste	Higher concentrations of vital nutrients (N, P, K, Ca, and Na)	(Shah et al., 2015)
	Lumbricus rubellus	Sewage sludge	Decline in the concentrations of Cr, Cd, and Pb	(Azizi et al., 2013)
	Eudrilus eugeniae + *Perionyx excavatus*	Textile mill wastewater sludge	Simultaneous reduction of heavy metal content with an increase in NPK nutrients	(Yuvaraj et al., 2020)
Endogeic	*Metaphire posthuma*	Jute mill waste	A decline in total organic C and pH coincided with increased N, P, and K availability	(Das et al., 2016)
	Metaphire posthuma	Municipal solid waste	The pH and total organic carbon decrease, while total nitrogen and the availability of phosphorus, potassium, and iron increase	(Sahariah et al., 2015)
	Metaphire posthuma	Organic waste	Reduction in C:N ratio	(Bhardwaj and Sharma, 2015)
	Pheretima elongata	Potato peels	-	(Munnoli et al., 2000)
Anecic	*Lampito mauritii*	Lignocellulosic organic waste	Decreases occurred in pH, organic C, C: N and C:P ratios, lignin, cellulose, hemicellulose, and phenols, while N, P, K, dehydrogenase, and humic acid increased	(Prashija et al., 2017)
	Lampito mauritii	Tea factory coal ash	Total organic carbon declined, while total nitrogen content and heavy metal accumulation increased	(Goswami et al., 2014)
	Lampito mauritii	Metal treated soil	A reduction in the C:N ratio coupled with increased availability of phosphorus and potassium	(Maity et al., 2008)
	Lampito mauritii	Sago sludge	A decline in organic carbon coupled with an increase in nitrogen and phosphorus content	(Banu et al., 2008)

Lampito mauritii	Kitchen waste	The C: N and C:P ratios decreased, while the contents of N, P, and K increased	(Tripathi and Bhardwaj, 2004)

Thesis data published in the review paper: Nath, S., Qureshi, A., Das, S., 2023. Role of bulking agents, process optimization, and different earthworm species in the vermiremediation process of industrial wastes: A review. Not. Sci. Biol. 15, 11490.

2.6. Earthworms' metal detoxification mechanism

The two ways via which earthworms acquire potentially toxic metals include dermal absorption and ingestion (Xiao et al., 2021; Nath et al., 2023). Firstly, the digestion of organic matter by the earthworms mobilizes the heavy metals by liberating them from their ions and carbonates. These bioavailable and mobile fractions are then subsequently accumulated in the cutaneous tissues as a stress response (Li et al., 2009; Swati and Hait, 2017). Biodegradation of organic residues also leads to the mineralization and humification of the wastes, generating low-molecular-weight organic acids (humic and fulvic acids). These acids react with the soluble metals and silicate fractions to form stable metal-organic and organo-silicate complexes (Hait and Tare, 2012). To adapt and survive in the metal-contaminated environments, earthworms maintain a internal balance by excreting metals at a higher rates that exceed the uptake, therefore mitigating tissue accumulation and stress (Swati and Hait, 2017). In addition, the metal accumulation and binding mechanisms in earthworms are influenced by different factors, including the concentration of metal, species, physiology, age of earthworm, induction of metal-chelating proteins, and characteristics of the surrounding matrix (Nannoni et al., 2011). Metal chelation is mainly facilitated by metallothionein (MT), a cysteine-rich low-molecular-weight protein. MT uses its thiol groups to bind metals and subsequently transports the metal ions to the chloragogenous tissues (Homa et al., 2016). In earthworms, the intestinal expression of MT is up-regulated in response to exposure to toxic elements such as cadmium and mercury (Colacevich et al., 2011; Nath et al., 2023). However, the relationship between the overall metal uptake in earthworms and the upregulation of intestinal MT is not always consistent (Goswami et al., 2016). The production of different non- metallothionein proteins that accumulate toxic elements has also been reported (Hussain et al., 2021; Nath et al., 2023).

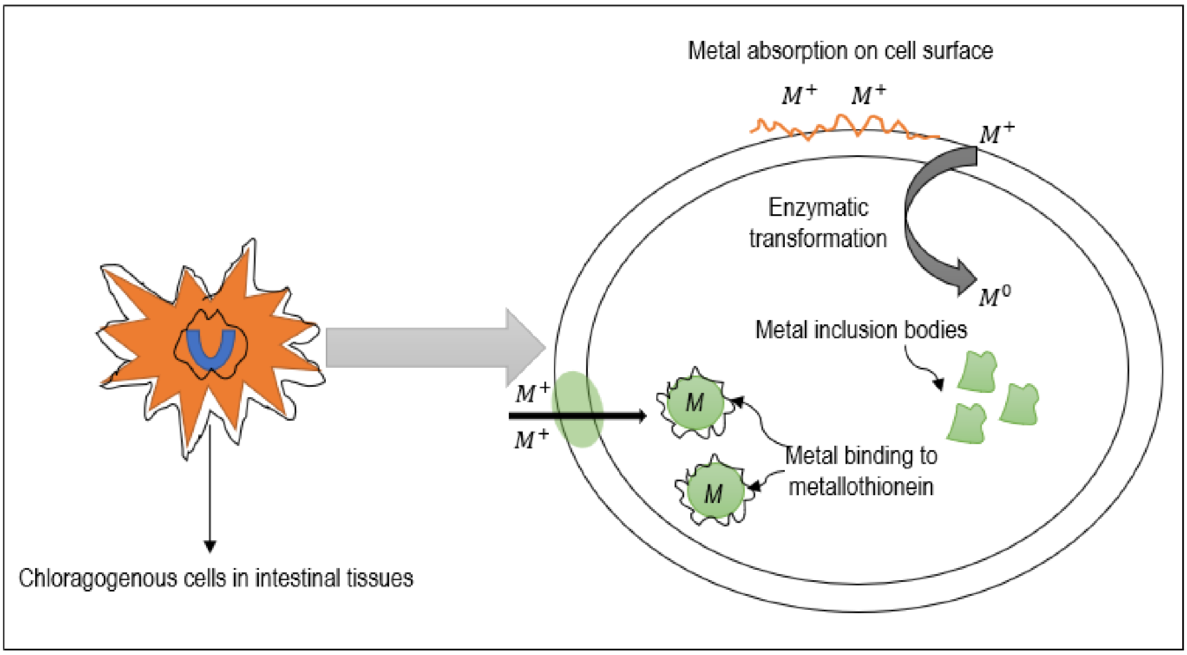

Figure 2. Metal detoxification mechanism used by earthworms (Thesis data published in the review paper: Nath, S., Qureshi, A., Das, S., 2023. Role of bulking agents, process optimization, and different earthworm species in the vermiremediation process of industrial wastes: A review. Not. Sci. Biol. 15, 11490.)

CHAPTER 3

MATERIALS AND METHODS

CHAPTER 3

3. MATERIALS AND METHODS

3.1. Overview of the experimental work

The transformation of oil refinery sludge (ORS) into a fortified organic fertilizer via vermicomposting was carried out through four systematic phases:

Phase I: *Characterization experiment*

Phase II: *Bioconversion experiment*

Phase III: *Large-scale composting experiment*

Phase IV: *Field experiment*

The characterization experiment was conducted to counter-balance the chemical and structural heterogeneity of ORS via mixing with two natural bulking substances: rice husk (RH) and cow dung manure (CDM). This experiment provided insights into the nutritional, physicochemical, and thermal characteristics of ORS, after mixing with RH and CDM. It also highlighted the variability in the pollution capacity of the two bio-amended ORS samples. The characterization experiment helped us in selecting the most appropriate bulking material required for the bioconversion experiment (Phase II).

The bioconversion experiment was carried out to optimize the ORS vermicomposting process and evaluate the ORS bioremediation efficiency of different bioconversion systems (with and without earthworms). Accordingly, a microcosm experiment was employed with ORS under the presence of earthworms and without them for 90 days. Two earthworm species *Eisenia fetida* and *Eudrilus eugeniae* were selected for the experiment. The resulting composts were further assessed for ecotoxicological and human health risks through the analysis of their aqueous extracts. Based on the comprehensive evaluation, the two most effective treatments were identified and advanced to the large-scale composting experiment (Phase III).

The large-scale composting experiment was carried out in a mesocosm with the two best treatments (from Phase II) to compare the performance of *E. fetida* and *E. eugeniae* in ORS transformation at a systematic scale, focussing mainly on heavy metal speciation dynamics, carbon fractionation patterns, and metal bioaccumulation. Through the large-scale experiment, we aimed to overcome the limitations of the previous microcosm experiment in providing reproducible insights. Additionally, this phase generated two ORS vermicomposts necessary for the subsequent field experiment (Phase IV).

The field experiment was conducted to ascertain the conditions in which bio-transformed ORS could be incorporated in a fully-integrated soil-plant system. A field-based comparative evaluation of the effects of the two bio-transformed ORS composts on soil conditions and on two morphologically different crops: tomato (*Solanum lycopersicum*) and cabbage (*Brassica oleracea* var. *capitata*) was carried out.

3.2. Phase I - Characterization experiment

3.2.1. Collection of oil refinery sludge, bulking materials, and experimental design

ORS samples were collected from the IOCL, Noonmati refinery, Guwahati (26.1807° N and 91.8154° E) and transported to the Department of Environmental Science, Pachhunga University College, in Aizawl, Mizoram (23.7233° N and 92.7271° E). The ORS samples were carried in metal containers (dimensions: 24 cm × 13 cm × 33 cm, volume: 5L) following all necessary protocols (Spinosa and Molinari, 2023). RH and CDM were procured from an agricultural farm in Aizawl.

Before characterization, a feasibility test was conducted by amending ORS in different ratios (3:1, 2:1, 1:1, and 1:2) with RH and CDM. Each mixture had a total weight of 5 kg (Table 5). The prepared substrates ORS + RH and ORS + CDM were then spread on tarpaulin sheets for a week to allow volatile organic compounds (VOCs) to dissipate. Key parameters including degree of compactness and moisture content were evaluated to determine substrate feasibility. For both substrate types, the degree of compactness decreased in the order: 3:1 > 2:1 ≥ 1:2 > 1:1. The 1:1 ratio had the highest moisture content for both mixtures. Based on these results, the 1:1 ratio was selected for further characterization. After this, 100 g samples were collected from each 1:1 substrate for subsequent analysis (Plate 1).

Table 5. Feasibility assessment of the different ratios of RH and CDM-amended ORS substrates

Sl. No.	Ratio	Particulars of mixture (5 kg)	Degree of compactness (%)	Moisture Content (%)
1	3:1	ORS (3.8 kg) + RH (1.2 kg)	64.44 ± 0.96	43.00 ± 2.00
2	2:1	ORS (3.3 kg) + RH (1.7 kg)	58.89 ± 1.73	44.00 ± 2.65
3	1:1	ORS (2.5 kg) + RH (2.5 kg)	47.22 ± 2.10	51.67 ± 1.53
4	1:2	ORS (1.7 kg) + RH (3.3 kg)	57.22 ± 1.73	48.67 ± 1.53
5	3:1	ORS (3.8 kg) + CDM (1.2 kg)	68.83 ± 2.20	40.33 ± 1.53

6	2:1	ORS (3.3 kg) + CDM (1.7 kg)	59.72 ± 2.55	42.67 ± 1.53
7	1:1	ORS (2.5 kg) + CDM (2.5 kg)	50.00 ± 5.00	47.67 ± 1.53
8	1:2	ORS (1.7 kg) + CDM (3.3 kg)	58.33 ± 3.63	45.33 ± 1.53

**ORS – oil refinery sludge; RH – rice husk; CDM – cow dung manure*

Plate 1. ORS sample before and after amendment with rice husk and cow dung manure

3.2.2. Physicochemical assessment of the RH and CDM-amended ORS substrates

The two blended samples were analyzed according to Page et al. (1982) for their pH, electrical conductivity (EC), water holding capacity (WHC), and bulk density (BD). Carbon, hydrogen, and nitrogen content of the samples were estimated using a PerkinElmer CHN analyzer (Series II 2400, USA). Phosphorus and potassium were colorimetrically estimated using spectrophotometer (Liu et al. 2021). For metal analysis, the two samples were processed in reverse aqua regia (HCl: HNO_3 = 1:3), diluted with deionized water (1:30, v/v), and thoroughly filtered (Whatman 42 filter paper). The filtrates were then quantified for heavy metals using an atomic absorption spectrophotometer (Shimadzu AA-7000, Japan).

3.2.3. Structural and elemental composition through SEM-EDX

The sample microstructure, surface cohesiveness, and elemental composition were characterized via Scanning Electron Microscope (Zeiss SIGMA) associated with an Energy Dispersive X-ray Spectroscopy (EDX) system. To mitigate charging effects, the samples were first smeared with a thin conductive gold layer via an Edwards Sputter Coater, following standard guidelines (ASTM E1508-12). Imaging and elemental mapping were performed at an accelerating voltage of 20 kV to optimize resolution and signal quality. EDX spectral data were acquired and processed using Zeiss SmartPI® software in accordance with ASTM E766-14 guidelines for compositional evaluation.

3.2.4. Thermal and combustion characteristics through TGA-DTG and van Krevelen

The thermal degradation behavior of the samples was investigated using TGA-DTG analysis. Analyses were performed on a TGA-4000 instrument (Perkin Elmer, USA) under a constant nitrogen rate of 40 cm^3 min^{-1} and 101 kPa pressure. The temperature was raised at a rate of 10°C min^{-1} (30°C 800°C). Data acquisition and processing were carried out using Pyris™ software v.11 (Perkin Elmer, USA) (Bhat et al., 2017).

To assess the fuel and combustion characteristics of the samples, a Van Krevelen diagram was constructed based on atomic H/C and O/C ratios. These ratios were estimated following the method of Kumar et al. (2019). Furthermore, the comprehensive combustibility index (CCI) was estimated for both samples to assess their combustion behavior using equation 1 according to Xu et al. (2021):

$$\text{CCI } (\%^2\,{}^{\circ}\text{C}^{-3}\,\text{min}^{-2}) = \frac{R_{\max}\,(\%/\text{min}) \times R_a\,(\%/\text{min})}{T_i^2\,(^{\circ}\text{C}) \times T_b\,(^{\circ}\text{C})} \quad (1)$$

Where R_{max}, R_a, T_i, and T_b represent the maximum combustion rate, average combustion rate, ignition temperature, and burnout temperature, respectively.

In addition, the ignition index (D_i) and the burnout index (D_b) were estimated according to Vasileiadou (2023) by equation 2 and 3, respectively.

$$D_i\ (\%/\text{min}^3) = \frac{R\text{max}\ (\%/\text{min})}{ti\ (\text{min}) \times tmax\ (\text{min})} \quad (2)$$

$$D_b\ (\%/\text{min}^4) = \frac{Rmax\ (\%/\text{min})}{\frac{\Delta t1}{2}\ (\text{min}) \times tmax\ (\text{min}) \times tb(\text{min})} \quad (3)$$

Where t_{max} represents the combustion rate time (maximum), t_i is the ignition time, t_b is the burnout time, and $\Delta t_{1/2}$ is DTG/DTG_{max} time zone = ½.

3.2.5. Assessment of functional groups through FTIR

The functional groups of the samples were characterized by Fourier Transform Infrared (FTIR) spectroscopy (Spectrum Two™, PerkinElmer, USA) following ASTM E1252-98. Samples were prepared as potassium bromide (KBr) pellets according to ASTM E168-16 by homogenizing 1 mg sample with 100 mg KBr (spectroscopic-grade) and compressing the mixture at 1 MPa into a transparent 10 mm diameter disc. Spectra were obtained at 4 cm^{-1} resolution over 4000-400 cm^{-1} waveband range using a deuterated triglycine sulfate detector with baseline correction applied. The resulting spectra were interpreted to identify functional groups and evaluate compositional differences of the samples (Nath and Das, 2025).

3.2.6. Chemical footprint and pollution potential through GC-MS

100 mL mixture of CH_3OH and water (9:1, v/v) was used from 5 mg aliquots of both samples. After overnight equilibration to maximize analyte solubilization, the mixture was filtered through a 0.45 micrometre membrane. The filtrates were concentrated to dry using a vacuum evaporator. The dried samples were mixed in CH_3OH to ensure optimal solubility of compounds. For analysis, 1 µL of the prepared samples was injected into a GC-MS system (TQ 8030, Shimadzu Corp., Japan) operating in electron ionization mode. Instrumental parameters were optimized for sensitivity and accuracy. Compound identification was achieved by matching the obtained mass spectra against the Wiley online spectral library. To confirm identities, authentic standards of relevant hydrocarbon derivatives and known ORS contaminants were analyzed under the same conditions, with retention times and spectral data used for their verification (Nath and Das, 2025).

The pollution capacity of the compounds found in both the blended ORS samples was assessed using the ATSDR (https://www.atsdr.cdc.gov/) and PubChem (https://pubchem.ncbi.nlm.nih.gov/) databases (Nath and Das, 2025).

3.3. Phase II - Bioconversion experiment

3.3.1. Initial preparation and conditioning of ORS for the composting process

Based on the characterization results (Phase I), the chemical and structural inconsistencies of ORS were amended using RH at a 1:1 ratio (w/v). This ORS + RH blend was then aerobically stabilized under shaded conditions for 7 days. Following this pre-treatment step, the stabilized ORS + RH was used to devise out distinct composting feed piles. These were prepared by further amending ORS + RH with farmyard manure (FYM) in the following dry weight ratios: 1:1, 1:2, and 2:1 (ORS + RH: FYM, w/w).

3.3.2. Composting operation, earthworms, and sample collection

The combined feedstock of ORS + RH and FYM was placed into earthen pots (dimensions: 25 cm × 25 cm × 19 cm, volume: 3 L capacity). Nine experimental treatments in triplicates were established based on feedstock combinations and the presence or absence of *E. fetida* and *E. eugeniae*. The description is provided in Table 6. For clarity and better presentation, the nine treatments were grouped into three distinct systems categorized by the type of composting process used: the *Eisenia*-system (utilizing *E. fetida*), the *Eudrilus*-system (utilizing *E. eugeniae*), and a non-earthworm system.

Table 6. Details of the composting treatments utilized during bioconversion of ORS

		Weight of the feedstock (kg)		
Treatment ID	**Treatment particulars**	**ORS***	**FYM**	**Total**
EF_1	*E. fetida* in ORS* + FYM (1:1)	1.5	1.5	3
EF_2	*E. fetida* in ORS* + FYM (1:2)	1	2	3
EF_3	*E. fetida* in ORS* + FYM (2:1)	2	1	3
EE_1	*E. eugeniae* in ORS* + FYM (1:1)	1.5	1.5	3
EE_2	*E. eugeniae* in ORS* + FYM (1:2)	1	2	3
EE_3	*E. eugeniae* in ORS* + FYM (2.1)	2	1	3
AC_1	Aerobic composting of ORS* + FYM (1:1)	1.5	1.5	3
AC_2	Aerobic composting of ORS* + FYM (1:2)	1	2	3
AC_3	Aerobic composting of ORS* + FYM (2:1)	2	1	3

Here, ORS denotes oil refinery sludge mixed with rice husk; FYM = Farm yard manure*

The earthworm specimens were sourced from Pabhoi Greens, Biswanath Chariali, Assam, India (26.7266° N, 93.1478° E). A 90-day composting was carried out, during which the feedstock was turned and moistened daily. 100 g samples were procured from each treatment of the three composting systems on days 0, 45, and 90. These samples were then air-dried, sieved (2-4 mm), and finely ground to a 1 mm particle size for subsequent analysis.

Plate 2. ORS compost produced during the bioconversion experiment (Phase II)

3.3.3. Earthworm health and growth assessment

The growth and reproduction of earthworms were monitored at regular intervals during the bioconversion experiment (Nath et al., 2025). After every 45 days, data were collected on earthworm count, biomass, body length, and cocoon number manually. The feedstock from each earthen pot was emptied onto aluminum trays and earthworms were manually separated using a 4-6 mm metallic sieve. Following each assessment, earthworms and feedstock were carefully returned to their respective pots. The net biomass and reproductive rates were then calculated according to Karwal and Kaushik (2020).

Plate 3. Periodic monitoring of earthworms during bioconversion experiment (Phase II)

3.3.4. Assessment of physicochemical characteristics

Samples collected at 0, 45, and 90 days were analyzed (pH, EC, WHC, BD, TP and TK, and heavy metals) as mentioned in section 3.2.2. The total organic carbon (TOC) was determined via wet digestion method (Walkley-Black method) (Nelson and Sommers, 1996), while total Kjeldahl nitrogen (TKN) was quantified by Kjeldahl digestion method.

3.3.5. Assessment of microbial proliferation

Microbial enumeration was performed using a serial dilution and plate count method. Samples were serially diluted (up to 10^{-7}). For total bacterial counts, 100 µL aliquots were plated on nutrient agar. Similarly, nitrogen-fixing and phosphate-solubilizing bacteria were assessed on Jensen's medium and Picovskaya's agar, respectively. All plates were incubated for 24 hours at 37°C, and formed colonies were counted with a colony counter. Bacterial populations were represented as colony-forming units per gram of compost (CFU g^{-1}) (Kaundal et al., 2016).

3.3.6. Assessment of enzymatic activity

Urease, dehydrogenase, and alkaline phosphatase activities were determined spectrophotometrically using established methods (Casida Jr et al., 1964; Tabatabai and Bremner, 1969; Milotić and Hoffmann, 2016). For urease activity, 1 g of sample was treated with toluene, 10% urea solution, citrate buffer (pH 6.7), and incubated at 35°C for 3 h, and the ammonium-N produced was quantified at 578 nm. Dehydrogenase activity was measured by incubating 1 g of sample with Triphenyl Tetrazolium Chloride and $CaCO_3$, with the resulting formazan extract read at 485 nm. Alkaline phosphatase activity was assessed by incubating the sample with toluene, phosphate buffer, and p-nitrophenyl phosphate, and quantifying the liberated p-nitrophenol at 410 nm (Nath et al., 2025).

3.3.7. Assessment of compost quality

Several quality indices were used to evaluate the maturity and quality of ORS composts, following Saha et al. (2010) and Nath et al. (2025).

The clean index (CI) was calculated using the equation 4:

$$CI = \frac{\sum SjWj}{\sum Wj} \qquad (4)$$

where S_j = score value and W_j = weighing factor assigned to the j^{th} metal (Cd, Cr, Cu, Ni, Pb, Zn). Cd received the highest weighing factor of 5, while the other metals were assigned values ranging from 1 to 5.

The fertility index (FI) was calculated using the equation 5:

$$FI = \frac{\sum SiWi}{\sum Wi} \qquad (5)$$

where S_i = score value and W_i = weighing factor for the i^{th} parameter (TOC, TKN, TP, TK, and C:N ratio). TOC was assigned the maximum weight of 5, with other parameters weighted between 1 and 5.

The humification index (HI) was estimated spectrophotometrically to reflect the degree of organic matter humification (Gieguzynska, 1998). 1 gram of sample was extracted with 50 mL of 1 M NaOH by shaking vigorously for 3 h, followed by overnight equilibration.

Following centrifugation at 3000 rpm for 40 min, absorbances at 470 nm (A470) and 660 nm (A660) were recorded. HI was calculated as the ratio A470/A660.

The relative germination index (RGI) was assessed through a seed germination bioassay using *Vigna radiata* (mung bean), chosen for its availability and common use (Das et al., 2016). Compost extracts were prepared by mixing 10 g of compost with 50 mL deionized water (1:5, w/v), shaken at 120 rpm for 1 h, and filtered. Ten seeds were placed on filter paper in petri dishes, moistened with the extract, and incubated at 25°C. Germination and root elongation were measured, and seed germination rate (SGR) and root elongation rate (RER) were calculated using equations 6 and 7. Following this, the RGI was calculated with equation 8 (Nath et al., 2025):

$$\text{SGR (\%)} = \frac{\text{No.of seeds germinated with composted ORS extract}}{\text{No.of seeds germinated in distilled water}} \times 100 \quad (6)$$

$$\text{RER (\%)} = \frac{\text{Mean root length of seeds with composted ORS extract}}{\text{Mean root length of seeds in distilled water}} \times 100 \quad (7)$$

$$\text{RGI (\%)} = \frac{\text{SGR} \times \text{RER}}{100} \quad (8)$$

Finally, the compost quality index (CQI) of the samples was calculated by equation 9 (Bera et al., 2013):

$$\text{CQI} = \frac{\text{NPK x MP x RGI}}{\text{C:N ratio}} \quad (9)$$

Where, NPK is total NPK percent, MP represents log10 value of total microbial population, and RGI is the relative germination index.

3.3.8. Cost-benefit of the compost systems

Net present value (NPV), benefit-to-cost ration (BCR), and pay-back time (PBT) were calculated to evaluate the cost-viability of the compost systems with equations 10, 11, and 12 respectively

$$\text{NPV} = -\text{Inv} + \sum_{k-1}^{n} [\frac{CF_k}{(1+i)^k}] \quad (10)$$

$$\text{BCR} = \frac{\text{P}}{\text{N}} \quad (11)$$

$$\text{PBT} = \frac{\text{Inv}}{\text{CF}} \quad (12)$$

Where, Inv = total investment, CF = cash flow in a given year, CF_k = net cash flow, k = discounted rate, n = time period, and i = depreciation rate.

3.3.9. Preparation of ORS compost teas (ORS compost aqueous extracts)

Compost teas (CTs) were prepared from periodically collected samples. For each preparation, 50 g of compost was dissolved in 200 mL of distilled water and stirred. The suspensions were agitated on a mechanical shaker (120 rpm, 2 h), then incubated at room temperature for 7 days. Finally, the suspensions were filtered through Whatman No. 42 paper, and the resulting filtrates (CTs) were analyzed for their heavy metal concentrations via di-acid digestion in reverse aqua regia as per section 3.2.2.

Plate 4. Compost tea prepared from ORS compost samples (Phase II)

3.3.10. Ecotoxicology assessment of the ORS compost teas

To assess the environmental and health risks associated with the prepared compost teas (CTs), several established indices for contamination and ecological risk were calculated following Nath and Das (2024).

The relative mobility (RM) of a metal is the ratio of its metal concentration in the compost tea (C_{sample}) to its total concentration in the environment ($C_{environment}$). The total relative mobility (RMc) for each CT sample was taken as the sum of the RM values for all measured metals (equations 13-14).

$$RM = \frac{C_{Sample}}{C_{environment}} \tag{13}$$

$$RM_c = \sum \frac{C_{Sample}}{C_{environment}} \tag{14}$$

The contamination factor for an individual metal (CF_i) was calculated as the ratio of its concentration in the CT (C_{Sample}) to its background concentration ($C_{Background}$) (equation 15) Varol (2011):

$$CF_i = \frac{C_{Sample}}{C_{Background}} \tag{15}$$

The overall degree of contamination (CD) for a CT sample was then determined as the sum of all individual contamination factors (equation 16).

$$CD = \sum \frac{C_{Sample}}{C_{Background}} \tag{16}$$

The enrichment factor (EF) was used to identify anthropogenic pollution by normalizing a target metal's concentration to a reference element (Sinex and Helz, 1981). The EF was calculated with equation 17 according to Sutherland (2000):

$$EF = \frac{\left(\frac{C_n}{C_{Ref}}\right)_{Sample}}{\left(\frac{C_n}{C_{Ref}}\right)_{Background}} \tag{17}$$

where C_n = concentration of metal in the CT and C_{Ref} = concentration of reference metal. Iron was selected as the reference due to its relatively uniform concentration in nature (Bhuiyan et al., 2010). The composite enrichment factor (EFc) for each CT was calculated as the sum EF values for all measured metals (equation 18).

$$EF_c = \sum \frac{\left(\frac{C_n}{C_{Ref}}\right)_{Sample}}{\left(\frac{C_n}{C_{Ref}}\right)_{Background}} \tag{18}$$

A multi-element pollution index (PI) was estimated to evaluate the overall pollution effects of the CT samples (equation 19) (Sahariah et al. 2015a):

$$PI = \frac{\frac{Cr}{100}+\frac{Pb}{100}+\frac{Cu}{100}+\frac{Cd}{100}+\frac{Zn}{300}}{5} \tag{19}$$

The adopted tolerance limits were: Cr, Pb, and Cd = 100 mg kg^{-1}; Cu and Zn = 300 mg kg^{-1}. PI greater than 1 shows high contamination risks (Mondal et al., 2017).

Single (ERI) and potential ecological risk (PERI) indices were estimated to quantify the risk posed by heavy metals in the CT samples, following Hakanson (1980). The equations 20 and (21) were used for the assessment:

$$\text{ERI} = T_r \times CF_i \quad (20)$$

$$\text{PERI} = \sum(T_r \times CF_i) \quad (21)$$

Here, CF_i is the contamination factor for a given metal, and T_r is its corresponding toxic response factor: Cr = 2, Pb = 5, Cu = 5, Cd = 30, and Zn = 1.

3.3.11. Health hazard assessment of the ORS compost teas

The health hazard quotient serves as a tool for assessing the impacts of pollutants that enter humans via three primary pathways: oral ingestion, inhalation of particulates, and dermal absorption. The equation 22 was used to calculate the hazard quotient (HQ) (Chabukdhara and Nema, 2013):

$$\text{HQ} = \frac{\text{Intakes (ingestion or inhalation or dermal)}}{R_f D} = \quad (22)$$

The Reference Dose (RfD) is the estimated maximum daily intake of a pollutant likely to be without harmful effects over a person's lifetime (Sahariah et al., 2015a). Furthermore, this allows for the determination of the non-cancerous hazard index (HI) in adults and children using equation 23 (Sahariah et al., 2015a).

$$\text{HI} = \sum \frac{\text{Intakes (ingestion or inhalation or dermal)}}{R_f D} \quad (23)$$

HI greater than 1 indicates a potentially high risk of non-carcinogenic toxicity. For carcinogenic risk, the intake for adults and children were multiplied with the cancer potency factor (CPF) specific to each metal (Chabukdhara and Nema, 2013).

3.4. Phase III - Large-scale composting experiment

3.4.1. Details of the experimental site and selection of treatments

The large-scale composting experiment was set up in Morigaon, Assam, India. The details of the experimental site are provided in the Table 7:

Table 7. Description of the experimental site

Aspect	Details
Coordinates	26.2514° N, 92.3423° E
Elevation	50-60 meters above mean sea level
Climate (Köppen)	Cwa - Subtropical, with dry winter and hot summer
Climate description	Hot/humid summers, mild winters, high annual rainfall
Mean annual precipitation	1319 mm
Temperature range (summer)	32°C to 38°C
Temperature range (winter)	8°C to 9°C
Soil type	Alluvial (formed by Brahmaputra River and tributaries)
Soil characteristics	Fertile, loamy to silty texture, suitable for agriculture (Gogoi et al., 2024)

The treatments EF_2 (*E. fetida*) and EE_2 (*E. eugeniae*) were selected as the two best treatments based on the overall results of the bioconversion experiment (from Phase II).

3.4.2. Collection of ORS and earthworms

ORS samples and earthworm specimens were collected and transported to the experimental site as mentioned in the previous sections 3.2.1 and 3.3.2.

3.4.3. Upscaling of the two best treatments through composting process

The two 1:2 (ORS + RH: FYM) treatments EF_2 and EE_2 were upscaled following the methods mentioned in sections 3.3.1 and 3.3.2. Accordingly, the mesocosm was set up with HDPE vermibeds (370 g per square meter - gsm). Both EF_2 and EE_2 were prepared in three replicates (n = 3) for 90 days. Sample collection and processing were done as per section 3.3.2. The vermicomposts prepared were stored in air-tight polybags for field application in Phase IV.

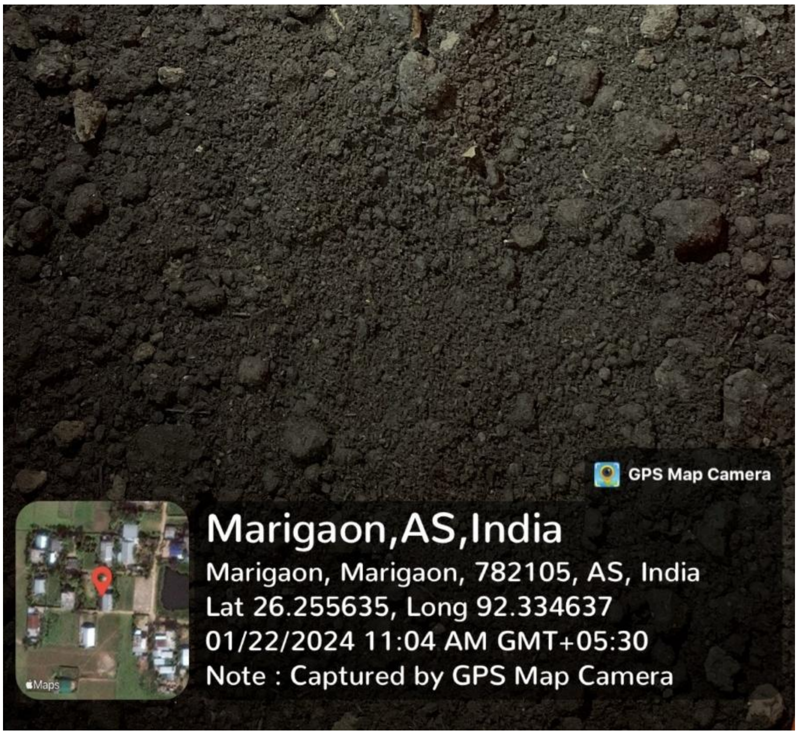

Plate 5. ORS vermicompost produced in large-scale experiment (Phase III)

3.4.4. Physicochemical assessment of the two composts

The physicochemical assessment of the samples was carried out as per the methods mentioned in sections 3.2.2. and 3.3.4. In addition, available nitrogen was determined through alkaline permanganate distillation (Armstrong, 1963). The quantity of Phosphorus was assessed using the molybdenum blue method (Pradhan and Pokhrel, 2013) and available potassium was measured by flame photometry ((Pavan and Jyothi, 2019; Nath and Das, 2026).

3.4.5. Speciation of heavy metals in the two composts

An speciation protocol (Tessier et al., 1979) was used to speciate the heavy metals into six operationally defined fractions: F1 = water-soluble, F2 = exchangeable, F3 = carbonate-bound, F4 = Fe–Mn oxide-bound, F5 = organic matter-bound, and F6 = residual. 1 g of air-dried compost was sequentially processed in acid-washed centrifuge tubes by following:

F1: 20 mL deionized water, 30 min shaking, 12 h equilibration.

F2: 8 mL 1 M $MgCl_2$ (pH 7), 1 h.

F3: 8 mL 1 M NaOAc (pH 5), 5 h.

F4: 20 mL 0.04 M $NH_2OH{\cdot}HCl$ in 25% (v/v) HOAc, 96 °C, 6 h.

F5: 3 mL 30% H_2O_2, 85 °C, 5 h; then 5 mL 3.2 M NH_4OAc in 20% (v/v) HNO_3.

F6: Residual digested in reverse aqua regia (HNO_3: HCl, 3:1).

Between each step, centrifugation was done (10,000 rpm, 30 min). After which, the sample was filtered and acid-preserved, and the residue was washed to minimize inter-fraction carryover. Metal concentrations in all fractions were quantified using AAS (Shimadzu AA-7000).

3.4.6. Carbon dynamics of the two compost samples

Humic substances in the composts were fractionated following Das et al. (2016). 5 g of compost was combined with 100 mL of 0.1 N $Na_4P_2O_7$–NaOH in acid-washed bottles. The mixture was shaken at 30 rpm for 16 h to achieve complete solubilization. For the determination of exchangeable carbon, 5 mL of the filtered extract was subjected to wet oxidation with 10 mL of 1 N $K_2Cr_2O_7$ and 20 mL H_2SO_4 (96%). The mixture was then titrated with 0.5 N $(NH_4)_2 \cdot Fe(SO_4)_2 \cdot 6H_2O$, using ortho-phosphoric acid (85%) and diphenylamine indicator. Fulvic acid carbon (FAC) was estimated from the filtrate after acidification with 10 mL of H_2SO_4 (96%) and precipitating for 12 h. After filtration, 5 mL aliquot of the acid-soluble fraction was analyzed using the same oxidation-titration procedure as for exchangeable carbon. Humic acid carbon (HAC) was estimated by collecting the membrane's precipitate in centrifuge tubes, washing with 20 mL of 0.1 N NaOH to dissipate FAC, and re-suspending the precipitate for oxidation-titration analysis.

3.4.7. Earthworm growth and health assessment

The assessment was done following the methods mentioned in the section 3.3.3.

3.4.8. Metal accumulation by earthworms

To quantify metal in the gut tissues, five mature and clitellated earthworms from each vermibed were randomly selected. Following a 24-hour depuration period on moist filter paper to clear gut contents, the gut of each specimen was surgically extracted. The isolated tissues were then rinsed with deionized water, blot-dried, and subjected to acid digestion (Kandaswamy et al., 2024; Nath and Das, 2026). Gut tissues were digested in a 4:1 (v/v) HNO_3:H_2O_2 mixture and analyzed via atomic absorption spectrophotometry for Cd, Cr, Cu, Pb, Ni, and Zn concentrations. Compost to earthworm heavy metal transfer was assessed by the bioaccumulation factor (BAF) with equation 24 (Wang et al., 2018):

$$BAF = M_{Earthworm}/M_{Compost} \tag{24}$$

Where, $M_{Earthworm}$ = metal content in gut tissue (mg kg^{-1}) and $M_{Compost}$ = metal content in the compost samples (mg kg^{-1}).

Plate 6. Surgically dissected gut of the earthworms after 24 hours depuration

3.4.9. Overall benefit assessment of the two earthworms

The performance of the two earthworms was evaluated using three distinct metrics: (i) Vermiremediation Benefit Index (VBI), a novel composite indicator developed in this study to assess overall compost quality and remediation efficacy; (ii) the Benefit Ratio (BR); and (iii) Removal Efficiency (RE). The VBI was calculated with the following equation 25:

$$VBI = \log_{10}[(NI + 1) \times (MR + 1) \times (EH + 1) \times (1 + 1/BAF)] \quad (25)$$

VBI is a composite measure that evaluates remediation success by combining four weighted components. The nutrient increment (NI) is the total NPK enrichment calculated as:

$$NI = \sum (C_{final} - C_{initial}) / \sum C_{initial}$$

where C_{final} and $C_{initial}$ are final and initial NPK, respectively.

The overall remediation efficiency of the various heavy metals studied is directly calculated as metal reduction (MR):

$$MR = \sum (M_{initial} - M_{final}) / \sum M_{initial}$$

where $M_{initial}$ and M_{final} are the concentration of the heavy metal before and after remediation.

Earthworm health (EH) is internally weighted with 60% in proliferation rate (increase in earthworm numbers and cocoon production) and 40% in biomass gain (increase in body weight) and calculated as:

$$EH = 0.6 \times \text{proliferation rate} + 0.4 \times \text{biomass gain}$$

A greater weightage on proliferation is applied as stable population of adults, juveniles, and cocoons are the major contributors of the long-term processing of the waste organic matter. On the contrary, short-term biomass gain in a dwindling population cannot be enough to sustain the degradation process.

Finally, the average gut bioaccumulation factor of the metals is calculated. This is inversely (1 + 1/BAF) included in VBI to penalize greater metal uptake, which may be an indication of metal stress in earthworms.

The BR was calculated using pH, EC, WHC, available N, P, and K as key variables with equation 26 (Sahariah et al., 2015):

$$BR = \frac{Average\ concentration\ (90D) - Average\ concentration\ (0D)}{Average\ concentration\ (0D)} \quad (26)$$

The RE for heavy metals was calculated with equation 27 (Sahariah et al., 2015):

$$RE = \frac{Average\ metal\ concentration\ (0D) - Average\ metal\ concentration\ (90D)}{Average\ metal\ concentration\ (0D)} \quad (27)$$

3.5. Phase IV - Field experiment

3.5.1. Details of the experimental site and ORS vermicompost

The field experiment was conducted during the winter season from November 2024 to March 2025 in a farmer's field in the Morigaon district of Assam, India. The details of the experimental site are mentioned in the section 3.4.1.

The two ORS vermicomposts (EF_2 and EE_2) produced from the large-scale composting experiment (Phase III) were utilized in the field experiment.

3.5.2. *Experimental design, treatments, and cultivars employed*

The study employed a randomized block design comprising eight treatments, each replicated three times for a total of 24 experimental units. These treatments included a negative control (no fertilizer) and a positive control (inorganic fertilizer). The inorganic control followed the recommended dosage of $N:P_2O_5:K_2O$ (urea, single superphosphate - SSP, and muriate of potash - MOP) at 120:60:60 as per the prescription of the Department of Agriculture, Government of Assam (AAU and DOA, 2015). To evaluate the produced vermicomposts (EF_2 and EE_2), they were applied at volumes supplying 25%, 50%, and 100% of the equivalent NPK found in the full inorganic recommendation. The trial was conducted in 24 individual sub-plots, each measuring 5 m x 6 m and physically separated by bunds to ensure treatment isolation and prevent runoff between plots (Goswami et al., 2024).

Table 8. Details of the treatments utilized in the field experiment

Sl. No	Treatments	Treatment details	Recommended dose
1	Control	No organic/inorganic amendment applied in soil	120:60:60
2	NPK_{100}	100% of recommended dose supplemented by $N-P_2O_5-K_2O$	
3	EF_{25}	25% of recommended dose supplemented by *E. fetida* processed ORS VC	
4	EF_{50}	50% of recommended dose supplemented by *E. fetida* processed ORS VC	
5	EF_{100}	100% of recommended dose supplemented by *E. fetida* processed ORS VC	
6	EE_{25}	25% of recommended dose supplemented by *E. eugeniae* processed ORS VC	
7	EE_{50}	50% of recommended dose supplemented by *E. eugeniae* processed ORS VC	
8	EE_{100}	100% of recommended dose supplemented by *E. eugeniae* processed ORS VC	

**ORS - oil refinery sludge; VC – vermicompost*

Plate 7. Nursery preparation for tomato and cabbage during field experiment (Phase IV)

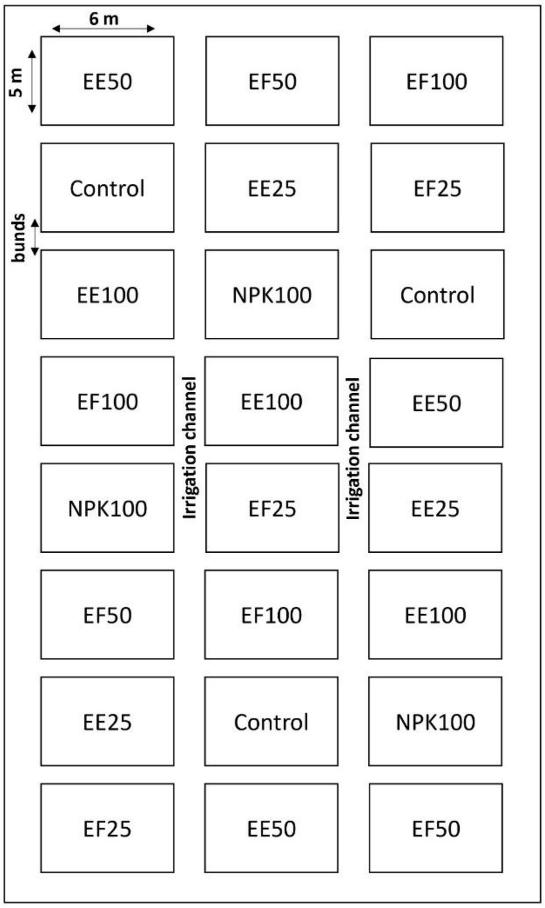

Figure 3. Randomized block design (RBD) employed for the treatments in the field experiment for tomato and cabbage cultivation

This investigation utilized two hybrid varieties: *Solanum lycopersicum* (tomato - Rocky F1) and *Brassica oleracea* var. *capitata* (cabbage - Early-ball F1). Seeds for both cultivars, procured from the nearby Horticulture Research Centre in Guwahati, India, were sterilized in a 0.2% mancozeb solution and sown in nursery beds (Plate 6) in October 2024. The resulting seedlings were transplanted one month later, in November 2024, into prepared experimental plots. Standard spacing protocols were followed: 60 cm x 45 cm for tomato and 45 cm x 45 cm for cabbage. Inorganic nitrogen was supplied as urea in two split applications, first half applied as pellets at transplantation and the remaining half as an emulsion 45 days later. Uniform irrigation and pest management were employed during the cutivation (AAU and DOA, 2015).

3.5.3. Soil sample collection, processing, and physicochemical assessment

Soil samples (0-15 cm depth) were collected from each sub-plot before transplantation and post-harvest for both the crop cycles. After collection, small pebbles and organic debris (roots and twigs) were removed using manual sorting. The resulting samples were thoroughly ground and sieved through a metal mesh (2mm) in order to get a uniform particle size for their subsequent analysis.

The physicochemical assessment of soil samples was carried out as per the protocols mentioned in the sections 3.3.4. and 3.4.4.

3.5.4. Heavy metal assessment of soil and plant metal uptake

The quantification of heavy metals in soil was done per the protocols mentioned in 3.3.4.

Heavy metal concentrations in the foliage of tomato and cabbage plants were determined using a wet digestion technique. Oven-dried leaf samples (1g each) were weighed and digested in a two-step acid process. Initial digestion with concentrated nitric acid (HNO_3) broke down organic matter, followed by treatment with hydrogen peroxide (H_2O_2) to complete oxidation, yielding a clear digestate. This solution was then volumetrically diluted to 25 mL, filtered to remove any residual particulates, and analyzed using AAS (Gong et al., 2020).

3.5.5. Soil quality assessment

The soil quality across various treatments was evaluated with two quantitative metrics: the Soil Quality Index (SQI) and the Degradation Index (DI). The SQI synthesized key physicochemical properties and heavy metal levels into a single comparable score, calculated by assessing a weighted quality index according to Temjen et al. (2022) using equation 28:

$$\text{SQI} = \sum WiSi \qquad (28)$$

Where, SQI demonstrates a score ranging from 0 to 1, S_i represents the score of the variable in the data set, and W_i is the value of the weighted factor, respectively. Based on the SQI values, the soils can be classified into five distinct categories: very bad (SQI < 0.40); bad

(0.55 ≥ SQI ≥ 0.40); moderate (0.70 ≥ SQI ≥ 0.55); good (0.85 ≥ SQI ≥ 0.70), and very good (SQI ≥ 0.85) (Eduah et al., 2025).

The Degradation Index (DI) was derived by evaluating soil properties in fertilized plots against a natural reference, specifically undisturbed forest soil. A single numerical value between 0 and 1 was then used to quantify the overall degree of positive or negative degradation. The DI was estimated by following Gebresamuel et al. (2010) using equation 29:

$$DI = \frac{(X-U)}{U} \times 100 \quad 0 \qquad (29)$$

Where, X represents soil properties (X) in fertilized soil with the mean soil properties (U) in an undisturbed primary forest.

3.5.6. Morphological and phytochemical assessment of the crops

For the morphometric analyses, the weight (g), head diameter (cm), length (cm), and width (cm) were noted manually for the harvested crops (Özer et al., 2021). For chlorophyll estimation, 0.1 g portion of fresh sample (leaf) was homogenized in 80% acetone (10 mL) and centrifuged (10 min, 5000 rpm). The absorbance of supernatants was spectrophotometrically estimated at 663 nm and 645 nm. The observed values were substituted in the equations 30, 31, and 32 according to Pérez-Patricio et al. (2018):

$$\text{Chlorophyll A (mg/g)} = (12.7 \times A663) - (2.59 \times A645) \qquad (30)$$

$$\text{Chlorophyll B (mg/g)} = (22.9 \times A645) - (4.7 \times A663) \qquad (31)$$

$$\text{Chlorophyll total (mg/g)} = \text{Chlorophyll A} + \text{Chlorophyll B} \qquad (32)$$

The total carotenoid content was estimated spectrophotometrically (at 470 nm) following the standard protocol of Kotecha and Ram (2023) with the equation 33:

$$\text{Carotenoid (mg/g)} = \frac{1000 \times A470 - 1.82 \times ChlA - 85.02 \times ChlB}{198} \qquad (33)$$

β-Carotene and lycopene were estimated by the dried methanol extract method according to Setyorini et al. (2018). 100 mg of extract was mixed with 10 ml of acetone-hexane mixture (4:6) for 1 min and filtered. The absorbance was recorded at three different wavelengths (453, 505 and 663 nm) and substituted in the equations 34 and 35:

$$\beta - \text{Carotene (mg/g)} = 0.216 \times A663 - 0.304 \times A505 + 0.452 \times A453 \qquad (34)$$

$$\text{Lycopene (mg/g)} = -0.0458 \times A663 + 0.372 \times A505 - 0.0806 \times A453 \quad (35)$$

An $AlCl_3$ colorimetric assay was used to determine the total flavonoid content. About 2.5 mL of the catechin standard (100-1000 µg/mL) was taken and mixed with 10 mL deionized water in a 25 mL volumetric flask. Then, 5% $NaNO_2$ solution (0.75 mL) was added, to which another 0.75 ml of $AlCl_3$ (10%) was added after 5 minutes. Then, 1M NaOH (1 mL) was added and 25 mL with deionised water to make up the volume. The solution was homogenised and the absorbance of the solution was estimated at 510 nm (Kumar et al., 2014).

The Folin-Ciocalteu assay was used for total phenolic content. A 25 mL flask was loaded with 1 mL of sample or a standard solution of gallic acid (50-250 µg/mL) and was diluted with 9 mL de-ionized water. A 1 mL Folin-Ciocalteu reagent was added and mixed properly. The solution was incubated after 5 minutes following 10 mL addition of Na_2CO_3 solution (7%) and deionised water was used to bring the mixture to a total volume of 25 mL. The sample was kept at room temperature for 90 minutes, and then the absorbance was read at 750 nm against a reagent blank (Kumar et al., 2014).

3.6. Multivariate statistical analyses

Normality of the various datasets obtained from the different phases of the experimental work was assessed using Q-Q plots prior to their statistical analysis. For the bioconversion experiment (Phase II), a three-way ANOVA was conducted to evaluate the effects of three independent factors: i) time (0^{th} day, 45^{th} day, and 90^{th} day) ii) technique (with earthworms and without earthworms) and iii) feed mixtures (1:1, 1:2, and 2:1 (w/w) ratios - ORS + RH: FYM) on the different response variables. To identify the key contributors to compost quality index (CQI) of the compost systems, Pearson's correlation, principal component analysis (PCA), and regression analysis were conducted. Moreover, step-down regression analysis and hierarchical cluster analysis (HCA) were done to understand the association of the different compost tea parameters with carcinogenic risk (CI) in humans.

In the large-scale composting experiment (Phase III), a two-way ANOVA was conducted to assess the effects of two independent factors: i) time (0^{th} day and 90^{th} day) and earthworm species (*E. fetida* and *E. eugeniae*) on the response variables. Moreover, a two-tailed t-test was conducted to compare the species performance in terms of growth and reproduction. Additionally, Pearson's correlation and PCA were done to determine the key factors influencing the vermiremediation benefit index (VBI) of the compost systems.

For the field experiment (Phase IV), physicochemical parameters and heavy metal data were analyzed via a two-way ANOVA with two independent factors: i) treatments and ii) time (pre-harvest and post-harvest). In crop-related responses such as metal uptake, morphometric traits, and phytochemical attributes, treatments and crop type (tomato and cabbage) were used as the two independent factors. To determine the complex relationships between soil characteristics, overall soil health, and crop performance, Pearson's correlation, PCA, and structural equation modelling (SEM) were done accordingly.

To evaluate the significant differences statistically, a least significant difference (LSD) post-hoc test was conducted. All of the statistical analyses were carried out using SPSS version 21.0 (IBM Corp., USA) (Bryman and Cramer, 2009). The graphical interpretations of correlation matrices and regression analysis were visualized using the "corrplot" and "ggplot2" packages and structural equation modelling (SEM) was visualized using the "lavaan" package in R-Studio (version 4.2.1) (R Core Team, 2021).

CHAPTER 4

RESULTS AND DISCUSSION

CHAPTER 4

4. RESULTS AND DISCUSSION

4.1. Phase I - Characterization experiment

4.1.1. Physicochemical and heavy metal characteristics of the blended ORS samples

Compared to ORS + CDM, the pH was lower (more acidic) in ORS + RH along with corresponding higher EC (Table 9). This could be associated with an accelerated conversion of cellulose and lignin into inorganic matter, facilitating higher production of anions and organic acids in the sample (Nath and Das, 2024). The amendment of rice husk to ORS might have also triggered a thermal hydrolysis reaction, leading to the synthesis of volatile fatty acids (Sun et al., 2023). An increased WHC and a decreased BD in ORS + RH suggests it to be an appropriate potting media for composting (Nath and Das, 2025). The low specific weight of the particles in rice husk and their high porosity were the contributing factors that enhanced the water retention of ORS + RH (Y. Liang et al., 2017). Carbon (C), nitrogen (N), phosphorus (P), and potassium (K) concentrations were significant in ORS + RH (Table 9), reflecting optimized C: N and C:P ratios of 113:1 and 17:1, respectively (Table 9). Higher silica and lignin content of rice husk could have contributed to stronger cohesive binding and nutrient holding in ORS + RH (Li et al., 2023). These results agree with Aydın Temel (2023) who demonstrated minimized loss of nutrients in a sewage sludge substrate by rice husk.

Table 9. Physicochemical and heavy metal characteristics of the blended ORS samples

Parameters	ORS + RH	ORS + CDM	Raw ORS (India)	Permissible limits		
				US EPA (40 CFR) 503, 503.13	EU (86/278/EEC)	China (GB 18918-2002)
pH	5.43 (0.21)	6.53 (0.25)	6.33 - 7.94	6.5 - 8.5	6.0 - 8.0	–
EC (µS cm^{-1})	549.04 (2.02)	413.06 (10.64)	89 - 590	2000	–	–
WHC (%)	55.70 (0.80)	50.63 (0.60)	–	–	–	–
BD (g cm^{-3})	0.58 (0.04)	0.62 (0.03)	–	–	–	–
C (%)	53.25 (0.05)	34.01 (0.04)	34.25 - 51.69	–	–	–
H (%)	7.17 (0.08)	4.30 (0.10)	_	–	–	–
N (%)	0.47 (0.04	0.36 (0.03)	0.14 - 0.24	–	–	–
P (%)	3.15 (0.15)	–	–	–	–	–
K (%)	0.59 (0.09)	–	0.000063 - 0.0023	–	–	–
Cd (mg kg^{-1})	14.22 (0.18)	15.51 (0.21)	7.6 - 100	85	20 - 40	5.0 - 20
Zn (mg kg^{-1})	253.26 (0.06)	764.07 (0.18)	267 - 688	7500	2500 - 4000	500 - 1000
Pb (mg kg^{-1})	153.48 (0.42)	163.30 (0.41)	40 - 850	840	750 - 1200	300 - 100
Fe (mg kg^{-1})	456.76 (0.20)	684.24 (0.22)	–	–	–	–

Mn (mg kg^{-1})	50.71 (0.01)	185.24 (0.75)	30 -305	–	–	_
Cr (mg kg^{-1})	49.16 (0.89)	59.01 (0.36)	13 - 24	3000	–	600 - 1000
Cu (mg kg^{-1})	41.41 (0.59)	45.55 (9.14)	22 - 650	4300	1000 - 1750	250 - 500
As (mg kg^{-1})	bdl	bdl	0.1 - 0.5	75	–	_

bdl = below detection level
**Sources*: (Bhattacharyya and Shekdar, 2003; Singh and Kumar, 2020; Singha and Deka, 2024)
Thesis data published in the research paper: Nath, S., Das, S., 2025. Exploring the Reusability of Oil Refinery Sludge Post Blending With Natural Bulking Agents: Comparing the Suitability of Rice Husk and Cow Dung Manure. Environ. Qual. Manag. 35, e70203.

The heavy metals varied from 14.22 to 764.07 mg kg^{-1} in both the samples. The bioavailability of metallic elements was considerably less in ORS + RH. As per global regulatory standards, both the blended samples showed lower heavy metal content in comparison to raw ORS (Table 9). It was seen that rice husk had enhanced metal retention capability relative to cow dung manure, due to its distinguishing composition and integrate structure. This could be because silica (SiO_2) in rice husk undergoes further hydration in the presence of water and available calcium ions (Ca^{2+}), generating hydrated calcium silicate and aluminosilicates, that facilitate adsorption of metals. The presence of hydroxyl and carbonyl functional groups in RH also serves as metal binding sites (Yefremova et al., 2023; Nath and Das, 2025). The results are consistent with Meretin (2021) who showed high metal adsorption ability of rice husk. In contrast, organic matter in CDM initially sequester heavy metals, but may get released into the matrix during decomposition (Nath and Das, 2025).

4.1.2. Structural and elemental traits of the blended ORS samples

In general, raw ORS's external surfaces are rough and porous with a pore volume of 0.056 cm^3/g and surface areas of 10.59 m^2/g (Zhang et al., 2022). In this study, ORS + RH demonstrated heterogenous cylindrical structures with large surfaces (Figure 4c). Numerous orifices were also seen on the exterior surfaces of ORS + RH, reflecting on its high porosity (Nath and Das, 2025). It was found that the structural integrity of the ORS + RH substrate was primarily preserved by the presence of the SiO_2. These align with Zainal et al. (2018) who also reported the appearance of coarse and hardy structures in raw rice husk, implying that ORS + RH is highly cohesive and structurally stable. In contrast, ORS + CDM displayed highly disoriented amorphous surfaces with low structural cohesion (Figure 4d-4f). This could linked to a reduced bonding of the ORS and CDM because of weaker augmentation of their interfacial surface areas (Yusefi et al., 2018; Nath and Das, 2025).

The EDX analysis determined that the ORS + RH sample had higher C, O, K and Si proportions (Figure 4g) and some traces of Al and Fe (Figure 4h). Rice husk retained most of the elements as it was highly fibrous, particularly SiO_2 that formed major part of the sample's composition. This further contributed to the sturdiness of ORS + RH through adhesive Si-layer production (Nath and Das, 2025). However, the ORS + CDM sample had fewer elements in its microstructure (mostly C and O) (Figures 4i-4j). The proportions of degradable organic matter in cow dung manure may have reacted with the petroleum hydrocarbons found in ORS. This may had slowed the mineralization, reducing the retention of elements (Douglas et al., 2024).

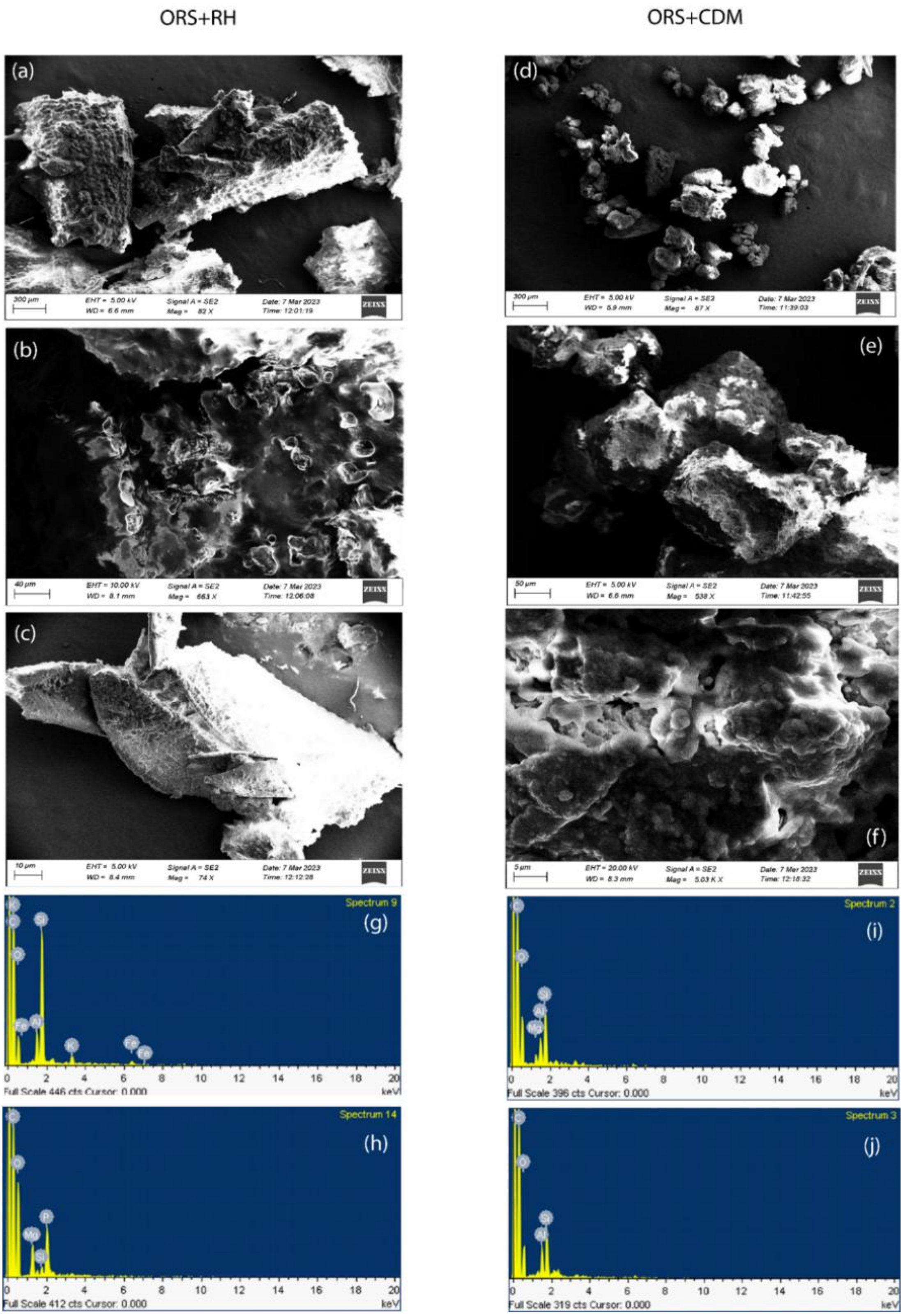

Figure 4. SEM and EDX profiles of ORS + RH and ORS + CDM (Thesis data published in the research paper: Nath, S., Das, S., 2025. Exploring the Reusability of Oil Refinery Sludge Post Blending With Natural Bulking Agents: Comparing the Suitability of Rice Husk and Cow Dung Manure. Environ. Qual. Manag. 35, e70203.)

4.1.3. Thermal behaviour of the blended ORS samples

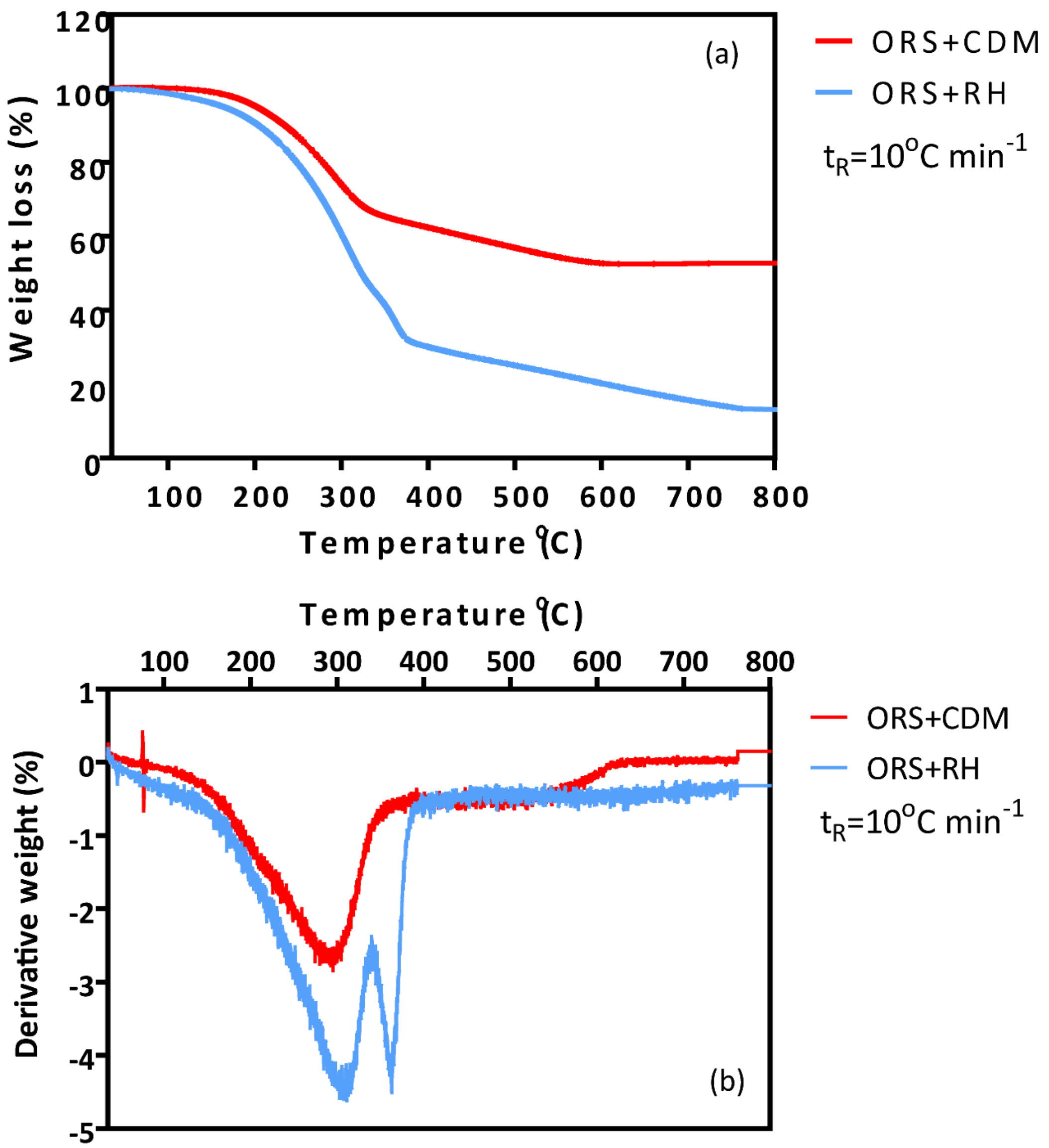

Figure 5. Mass loss behaviour of the samples through TGA-DTG curves (Thesis data published in the research paper: Nath, S., Das, S., 2025. Exploring the Reusability of Oil Refinery Sludge Post Blending With Natural Bulking Agents: Comparing the Suitability of Rice Husk and Cow Dung Manure. Environ. Qual. Manag. 35, e70203.)

The TGA curves showed three distinct stages of mass loss for both the samples (Figure 5a). The 1st stage (110-115°C) demonstrated a minor weight loss of 1-2%, attributing to the evaporation of moisture and low molecular solvents (Abdulqader et al., 2021). A slower mass loss phase occurred between 130-190°C, in which the samples lost 3-5% of their masses, attributing to oil volatilization (Zhang et al., 2022; Nath and Das, 2025). The 2nd stage (200-600°C) involved a rapid decomposition, with ORS + RH losing 79.77% of its mass, while ORS

+ CDM lost about 52.73%. Similar studies confirm that rapid pyrolysis of ORS occurs primarily in the 2nd stage (115-410°C) (Song et al., 2022). The DTG profiles showed derivative weight loss rates of 1-1.60% min^{-1} in ORS + RH and ORS + CDM (Figure 5b). Although DTG curves typically demonstrate three peaks for fuel substrates (Vasileiadou, 2023), the ORS + RH displayed two distinct peaks, while ORS + CDM showed only one (Figure 5b). The first peak (< 220°C) mainly attributed to moisture loss and the second (220-600°C) reflected devolatilization of major biopolymers in RH (Nath and Das, 2025). The fibrous structure and SiO_2 in RH enhance the thermal reactivity by lowering the activation energy required for combustion (Yefremova et al., 2023). At 600°C, cumulative mass losses reached 0.8-fold for ORS + RH and 0.5-fold for ORS + CDM. The 3rd stage (600-800°C) proceeded more steadily and could be attributed to the decomposition of carbonaceous matter (Syed Hassan et al., 2021). Overall, ORS + RH exhibited greater thermal susceptibility, losing 87% of its initial mass compared to ORS + CDM (Nath and Das, 2025).

4.1.4. *Fuel and combustion characteristics of the blended ORS samples*

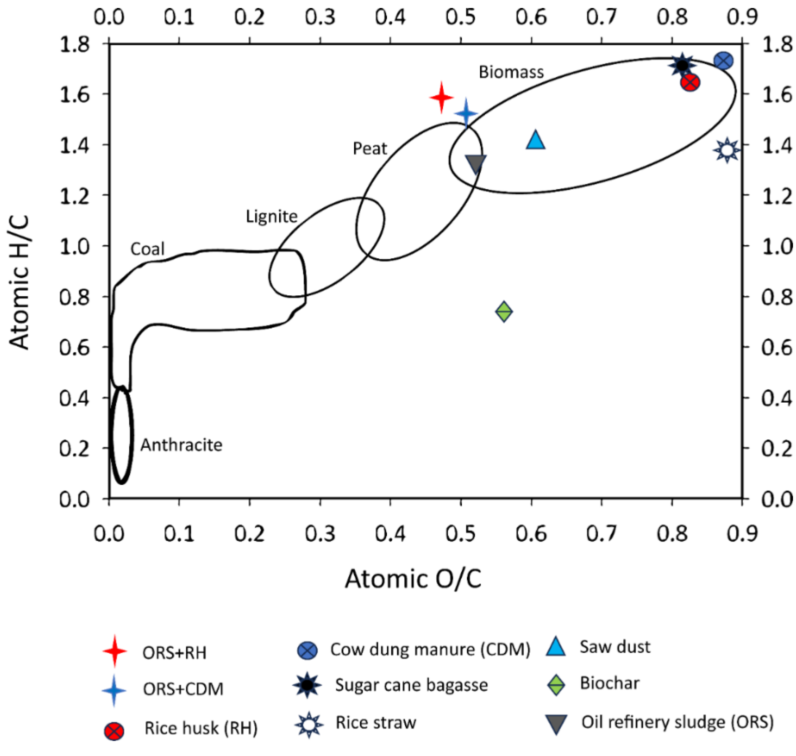

Figure 6. Van Krevelen plot ORS + RH and ORS + CDM along with raw ORS (Thesis data published in the research paper: Nath, S., Das, S., 2025. Exploring the Reusability of Oil Refinery Sludge Post Blending With Natural Bulking Agents: Comparing the Suitability of Rice Husk and Cow Dung Manure. Environ. Qual. Manag. 35, e70203.)

The van Krevelen plot illustrated the elemental ratios of H/C and O/C of the samples (Figure 6). Both the samples exhibited atomic ratios consistent with the typical biomass substrates (H/C = 1.2-1.6 and O/C = 0.5-0.9), with ORS + RH at H/C = 1.60 and O/C = 0.40) and ORS + CDM at H/C = 1.50 and O/C = 0.45 (Nath and Das, 2025). These ratios differed from raw ORS, which mainly is within the petrographic area of the van Krevelen plot (Figure 6). The shift toward the biomass region is likely due to the induction of oxygen-containing functional groups from RH and CDM, which increased the overall O/C ratio (Nath and Das, 2025).

The ignition temperature (T_i) was estimated from the intersection of tangents to the initial TGA curve, implying the onset of energy release (Nath and Das, 2025). The T_i values for ORS + RH (180.10°C) and ORS + CDM (181.32°C) were similar, suggesting minimal differences in volatile matter content. A lower T_i generally indicates improved ignition performance, which was favoured in ORS + RH (Table 10). The high surface area to volume ratio of both RH and CDM facilitates efficient heat transfer and improves oxygen accessibility to facilitate ignition at relatively low temperatures (Osibuamhe et al., 2024). The burnout temperature (T_b) of ORS + RH was 0.05-fold higher than ORS + CDM. This difference aligns with reports that suggest that RH exhibits higher activation energies (137.83 to 143.99 kJ mol^{-1}) (Yiga et al., 2023). The CCI value for ORS + RH was 0.5-fold higher than ORS + CDM. This improvement can be linked to the fuel properties of RH such as high calorific value and low moisture (Kumar & Patel, 2014). These findings are consistent with Xu et al. (2021) who observed that RH elevated the burnout rate and CCI of the mixture. Both the D_i and D_b were higher for ORS + RH than ORS + CDM (Nath and Das, 2025), implying rice husk addition improved the he ignition behavior and burnout efficiency (Kumar and Nandi, 2022).

Table 10. Combustion efficiencies of the blended ORS samples

	T_i (°C)	T_b (°C)	R_{max} (%/min)	R_a (%/min)	T_i^2 (°C)	CCI (%^{2} °C^{-3} min^{-2}) (× 10^{-07})	t_i (min)	t_b (min)	t_{max} (min)	$\Delta t_{1/2}$	D_i (%/min^3) (× 10^{-4})	D_b (%/min^4) (× 10^{-4})
ORS + RH	180.10	311.51	4.617203	1.1430427	32436.01	5.22	18	31	80	2.50	32.1	7.4
ORS + CDM	180.32	295.25	2.842447	0.7856574	32515.3	2.32	18	29	80	2.75	19.7	4.4

*T_i = ignition temperature; T_b = burnout temperature; R_{max} = maximum combustion rate; R_a = average combustion rate; CCI = comprehensive combustibility index; t_i = ignition time; t_b = burnout time; t_{max} = time of the maximum combustion rate; $\Delta t_{1/2}$ = time zone of DTG/DTG$_{max}$ = ½; D_i = ignition index; D_b =burnout index

Thesis data published in the research paper: Nath, S., Das, S., 2025. Exploring the Reusability of Oil Refinery Sludge Post Blending With Natural Bulking Agents: Comparing the Suitability of Rice Husk and Cow Dung Manure. Environ. Qual. Manag. 35, e70203.

4.1.5. Functional groups present in the blended ORS samples

The samples confirmed the presence of multiple functional groups (Figure 7). A broad absorption band between 3550-3200 cm^{-1} was observed in both samples with greater intensity in ORS + CDM, consistent with the O-H stretching frequency of alcoholic hydroxyl groups (Das et al., 2016; Nath and Das, 2025). The amine salt samples exhibited characteristic N-H stretching bands in the 3000-2800 cm^{-1} region. Aliphatic hydrocarbon chains and fatty acids were indicated by the absorption bands at 2900-2800 cm^{-1} (Aguelmous et al., 2016). The detection of fatty acids in this study is supported by the earlier findings of Polak et al. (2009). Prominent infrared absorptions in the 2600-1800 cm^{-1} region were observed for the ORS + CDM sample and were assigned to thiol, isocyanate, and alkene moieties (Nath and Das, 2025). The presence of an imine (C=N) linkage in ORS + CDM was evidenced by an infrared absorption band at 1690-1640 cm^{-1}. Aromatic C-H bending was also established near 1500 cm^{-1}, corroborating with presence of C-H groups within 1600-1500 cm^{-1} (Duan et al., 2018). C-Cl, C-Br, C-I (halogens) were prominently identified between 800-550 cm^{-1} in ORS + CDM, implying toxicological risks that warrant attention (Haider et al., 2024; Nath and Das, 2025). Also, ORS + CDM showed C-H bending of hydrocarbons at 650-500 cm^{-1}, attributing to CDM's higher humic content (Nath and Das, 2025).

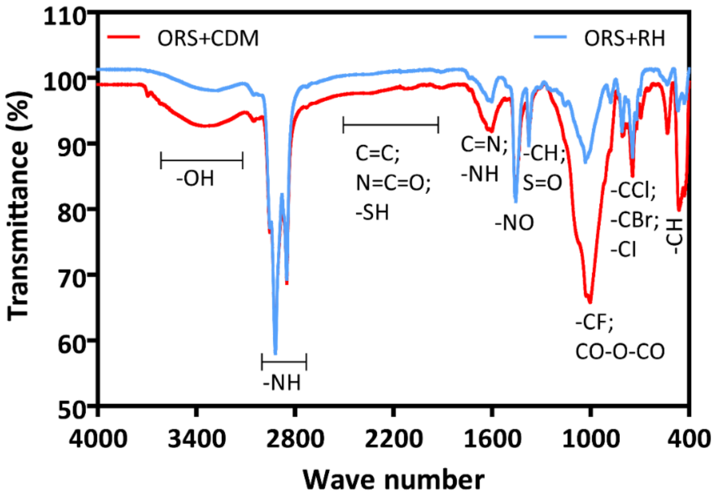

Figure 7. Functional groups present in ORS + RH and ORS + CDM (Thesis data published in the research paper: Nath, S., Das, S., 2025. Exploring the Reusability of Oil Refinery Sludge Post Blending With Natural Bulking Agents: Comparing the Suitability of Rice Husk and Cow Dung Manure. Environ. Qual. Manag. 35, e70203.)

4.1.6. Chemical footprint of the blended ORS samples and pollution potential

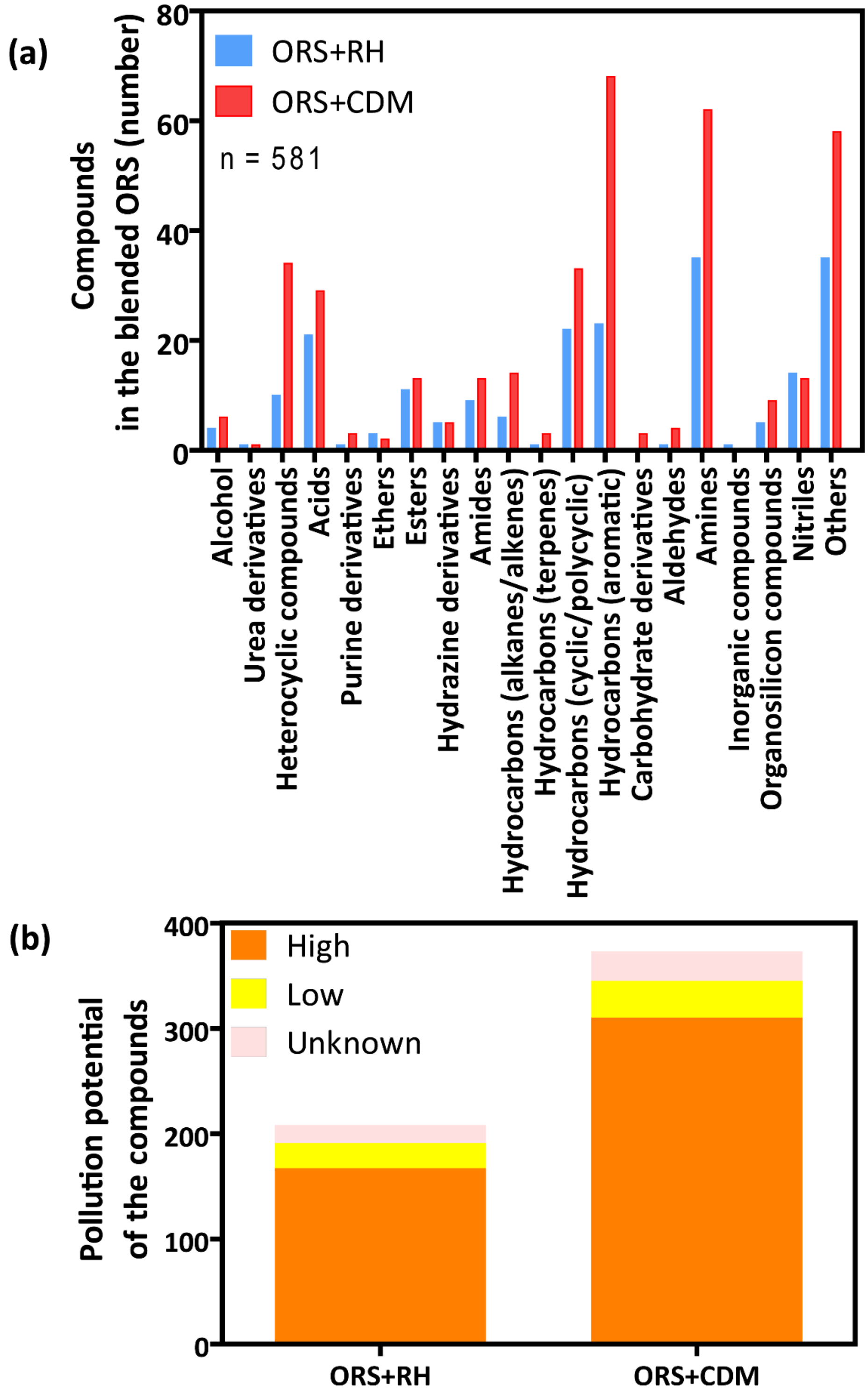

Figure 8. Chemical signatured of the blended ORS samples and pollution potential (Thesis data published in the research paper: Nath, S., Das, S., 2025. Exploring the Reusability of Oil Refinery Sludge Post Blending With Natural Bulking Agents: Comparing the Suitability of Rice Husk and Cow Dung Manure. Environ. Qual. Manag. 35, e70203.)

In total, 581 compounds were characterized in samples (Figure 8a; Appendix 1), with 56% common to both. ORS + CDM contained greater number of compounds (373) than ORS + RH (208), including 23% compounds specific to ORS + CDM than ORS + RH (11%). Hydrocarbons were the most abundant class (0.20-fold), followed by amines (0.16-fold), acids and esters (0.12-fold), and heterocyclic compounds (0.07-fold). Aromatic hydrocarbons were predominant (15%), with their cyclic/polycyclic derivatives accounting for 9%. Also, hydrocarbon availability was 1.2 times greater in ORS + CDM (Figure 8a). This difference could be due to the larger humic content in cow dung manure, which enhances hydrocarbon adsorption from ORS (Linkevich et al., 2021; Nath and Das, 2025).

Among the 581 compounds detected in the samples, the pollution risk ranged from low to high (Figure 8b; Appendix 1). The proportion of compounds with pollution potential was nearly twice in ORS + CDM (53%) as in ORS + RH (28%). This is due to the higher organic matter and microbial activity in CDM, which increase its affinity and reactivity toward the toxic constituents in ORS (Gupta et al., 2016). Petroleum hydrocarbons detected in ORS + CDM show the highest environmental and health risk due to their established cancer inducing and gene-altering properties (Y. Li et al., 2020; Nath and Das, 2025).

4.2. Phase II - Bioconversion experiment

4.2.1. Physicochemical parameters of the composting systems and treatments

The initial pH was slightly acidic in nature in the composting systems (Figure 9; Appendix 2). The presence of earthworms led to a 0.35-fold decrease in pH compared to a 0.06-fold decrease in the absence of earthworms. The *Eisenia*-system showed 38% reduction in pH, followed by 32% in *Eudrilus*-system. The EE_1 from the *Eudrilus*-system showed the highest decrease in pH by 39%. The reason could be the organic acids and anions that earthworms and their gut microbes produce during composting (Nath and Das, 2024). The EC of the compost was significantly higher in the earthworm systems than in the system without earthworms. The lowest EC was observed in the treatment AC_3 (6275.33 ± 20.79 µS cm^{-1}). By processing organic matter, earthworms release more soluble and mobile mineral forms in the compost (Jadia and Fulekar, 2008). A 0.22-fold increase in WHC was observed in the composting systems over the incubation, with 0.29-fold increment with *E. fetida* and 0.26-fold with *E. eugeniae* (p (Technique) < 0.001). On the 90th day, the treatment EE_2 recorded the highest WHC of 89%, followed by EF_2 (87%). The BD of the earthworm-systems decreased by 0.31-fold, while BD reduced by 0.13-fold in the absence of earthworms (p (Technique) < 0.001). The better structure and water retention of the earthworm systems, especially in treatments EF_2 and EE_2, could be due to reduced particle size and the formation of organic complexes facilitated by the mechanical grinding of earthworms (Nath et al., 2025).

A substantial reduction in TOC was observed in the earthworm systems over the first 45 days of composting, with levels stabilizing by the 90th day. The TOC reduction in the *Eisenia* and *Eudrilus* systems was 0.70-fold greater without earthworms (Nath et al., 2025). On the 90th day, EE_2 recorded the lowest TOC content (11.52 ± 0.08 %) and AC_1 recorded the highest (13.70 ± 0.04 %) (Figure 9; Appendix 2). The respiratory processes of earthworms and their microbes facilitate greater mineralization of the organic substrates (Das et al., 2016). A significant increase in TKN, TP, and TK was observed in the composts. Among these, the *Eudrilus*-system was most effective, elevating NPK content by 1.1-fold. Particularly on the 90th day, the treatment EE_2 had the highest TKN content (1.04 ± 0.06 %), followed by EF_2 (1.03 ± 0.02 %) (Nath et al., 2025). The NPK increment with earthworms was 0.38-fold higher than without earthworms. This is likely attributable to the gut microbes, whose enzymatic activity mineralizes organically bound NPK. The conversion to inorganic forms increases the bioavailability of nutrients, enriching the compost's nutrient pool (Paul et al., 2018).

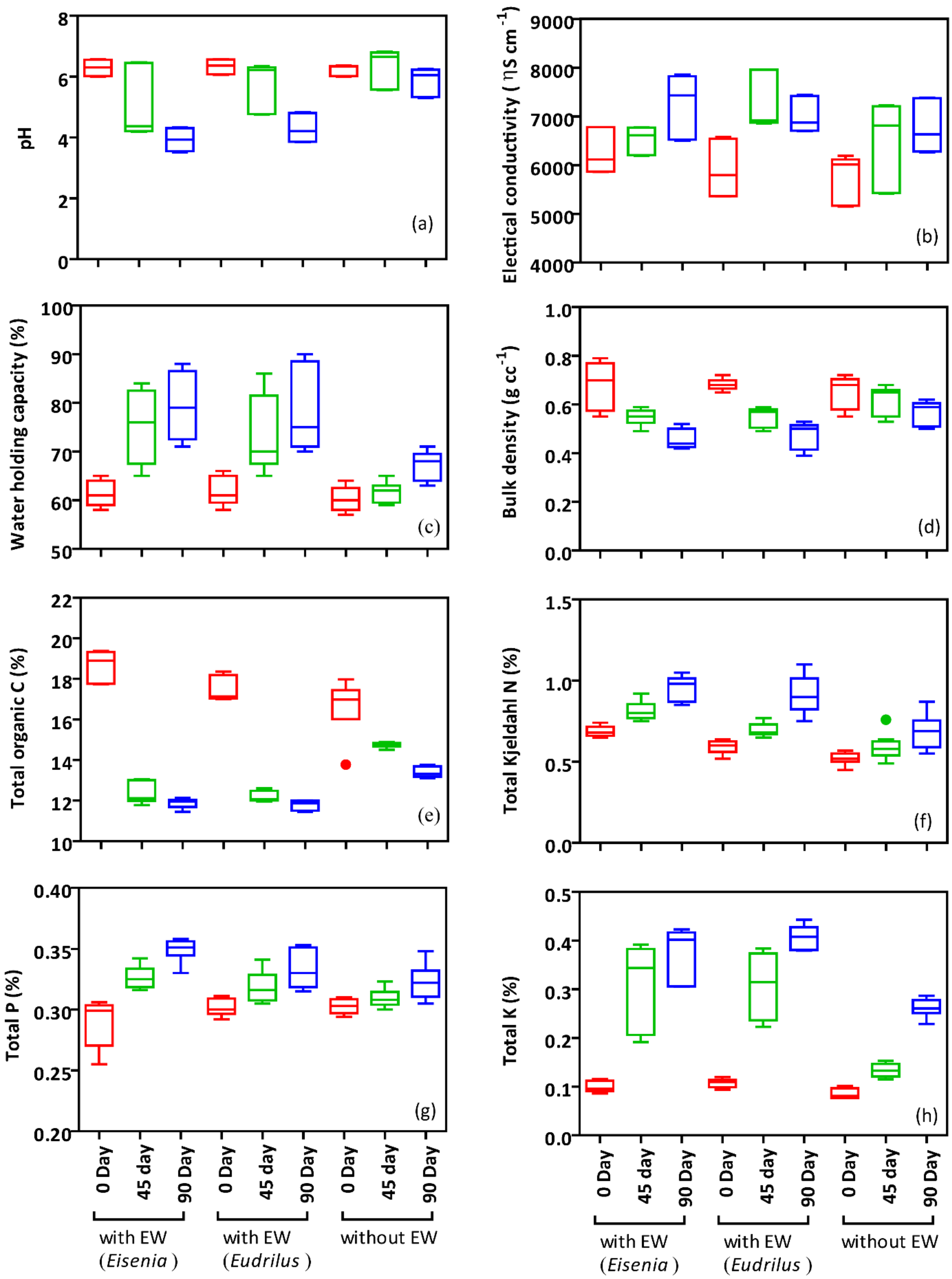

Figure 9. Physicochemical attributes of the composting systems during incubation (Thesis data published in the research paper: Nath, S., Dutta, U., Tangjang, S., Das, S., 2025. Assessing the compost-ability of oil refinery sludge in the presence or absence of earthworms: An eco-friendly approach of biodegradation. Int. Biodeterior. Biodegradation 198, 105987)

4.2.2. Heavy metal concentration of the composting systems and treatments

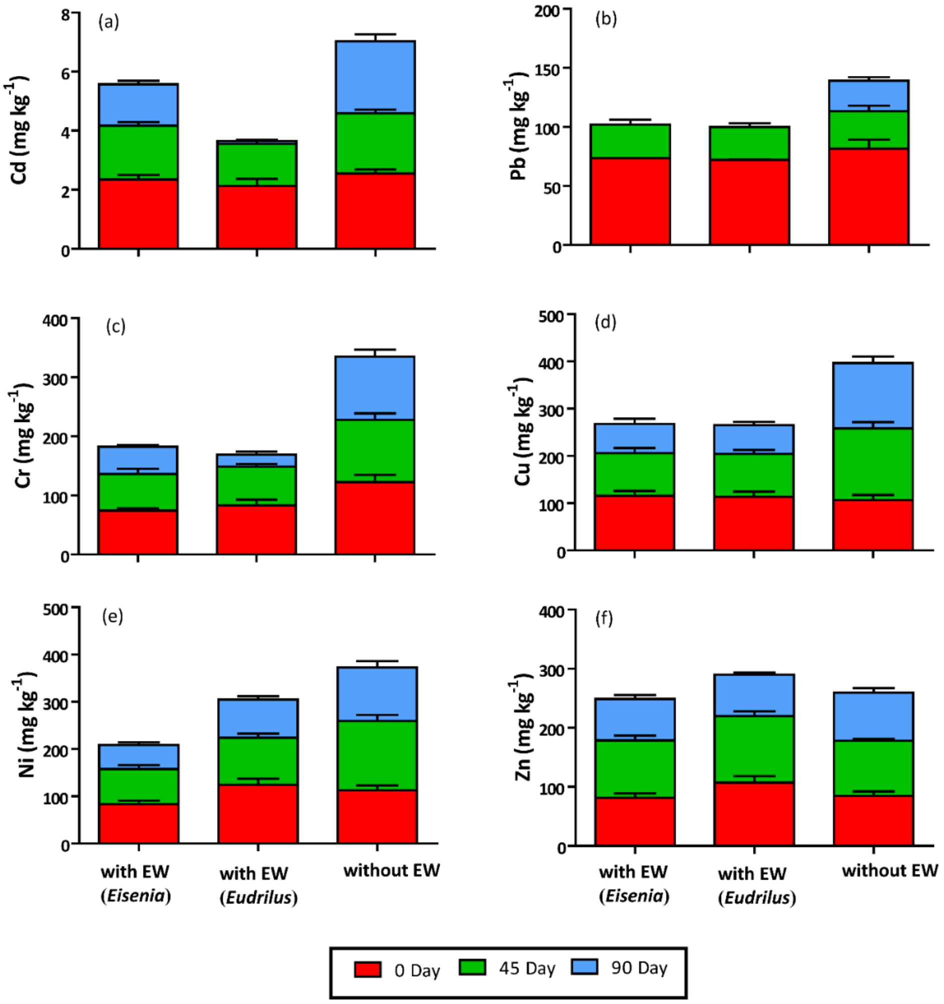

Figure 10. Heavy metal concentration of the composting systems during incubation (Thesis data published in the research paper: Nath, S., Dutta, U., Tangjang, S., Das, S., 2025. Assessing the compost-ability of oil refinery sludge in the presence or absence of earthworms: An eco-friendly approach of biodegradation. Int. Biodeterior. Biodegradation 198, 105987)

The heavy metal reduction with earthworms was 1.5 times higher than without earthworms. After 90 days, Cd was undetectable in the systems containing earthworms (Figure 10; Appendix 3). Also, Pb reduced by 0.98-fold in the *Eudrilus*-system, then the *Eisenia* system (0.97-fold), and the non-earthworm system (0.70-fold). The treatments EE_1, EE_2, EF_1, and EF_2 recorded Pb content below detection level at the end of the incubation. The very low bioavailability of Cd and Pb with earthworms could be attributed to the chelation of these metal ions by humic acids, resulting in stubborn metal-organic complexes (Boechat et al., 2016).

Furthermore, the *Eudrilus*-system had the highest decrease in Cr, Cu, and Ni concentrations (Cr by 0.72-fold, Cu by 0.54-fold, and Ni by 0.28-fold), followed by the *Eisenia*-system (Cr by 0.35-fold, Cu by 0.50-fold, and Ni by 0.28-fold). The lowest Cr and Cu concentration were observed in EE_2 (Cr = 20.13 ± 0.03 mg kg^{-1}; Cu = 60.65 ± 0.04 mg kg^{-1}) (Nath et al., 2025). The system without earthworms reduced Cr, Cu, and Ni by only 0.18-fold, 0.15-fold, and 0.08-fold, respectively. In Zn, EE_2 recorded the lowest Zn content (69.90 ± 0.03 mg kg^{-1}) on the 90^{th} day. The observed increases in the metal reduction within the earthworm systems may be attributed to the synthesis of metallothionein, a protein that procures metal ions within the chloragogenous tissues of earthworms (Nath et al., 2025).

4.2.3. Earthworm growth and proliferation in the composting systems

During the first week, the feedstocks containing greater ORS substrate had higher earthworm mortality rate (three to five earthworms per day) (Table 11). The low moisture in the substrates and heavy metal toxicity of ORS may have contributed to the initial death (Y. Li et al., 2020; Nath et al., 2025). But as the composting advanced, moisture levels increased and heavy metal mobility decreased in the substrates, which likely made it easier for the earthworms to survive. The process of cocoon formation began in week five and lasted until week thirteen. As evidenced, the amount of ORS (RH mixed) and FYM used had a significant impact on the earthworms' development. The feedstocks with higher percentages of FYM induced the largest gains in net weight, net earthworm count, net body length, and reproductive rate in earthworms (Nath et al., 2025). This implies that providing earthworms large amounts of C-rich substrates could promote their development and proliferation as these substrates provide easily accessible nutrients to improve earthworms' feeding ability to (Karwal and Kaushik, 2021). In the FYM-dense substrates, the net biomass gain was 286.67 ± 40.41 mg for *E. fetida* and 433.33 ± 110.15 for *E. eugeniae*. Additionally, *E. eugeniae* had the highest net proliferation (211%). *E. eugeniae* is typically significantly larger in size and a ravenous forager, which facilitate its growth. In addition, *E. eugeniae* is very productive in tropical locations because of its fast reproductive cycle, which helps it to mature faster in comparable conditions (Blakemore, 2015).

Table 11: Earthworm growth and health assessment during the composting experiment

(a) Biomass					
Treatments	**Feed mix [ORS (mixed with RH) +FYM=3kg]**	**Initial (@ 0 day)**	**After 45 days**	**After 90 days**	**Net biomass gain (mg)**
with EW	1.5+1.5	466.67 (15.28)	513.33 (32.15)	673.33 (23.09)	206.67 (37.86)
(*Eisenia*)	1.0+2.0	493.33 (15.28)	543.33 (30.55)	780.00 (26.46)	286.67 (40.41)
	2.0+1.0	473.33 (25.17)	596.67 (40.41)	640.00 (43.59)	166.67 (66.58)
with EW	1.5+1.5	790.00 (10.00)	916.67 (50.33)	1043.33 (20.82)	253.33 (28.87)
(*Eudrilus*)	1.0+2.0	790.00 (90.00)	1060.00 (45.83)	1223.33 (20.82)	433.33 (110.15)
	2.0+1.0	806.67 (40.41)	866.67 (51.32)	970.00 (20.00)	163.33 (20.82)
(b) Cocoon count		**Initial (@ 0 day)**	**After 45 days**	**After 90 days**	**Reproductive rate (cocoon EW^{-1})**
with EW	1.5+1.5	0 (-)	13 (2)	20 (2)	0.28 (0.042)
(*Eisenia*)	1.0+2.0	0 (-)	16 (2)	22 (2)	0.25 (0.009)
	2.0+1.0	0 (-)	8 (2)	10 (1)	0.16 (0.014)
with EW	1.5+1.5	0 (-)	15 (2)	17 (2)	0.19 (0.024)
(*Eudrilus*)	1.0+2.0	0 (-)	21 (2)	25 (3)	0.26 (0.008)
	2.0+1.0	0 (-)	10 (1)	11 (2)	0.14 (0.020)
(c) Earthworm number		**Initial (@ 0 day)**	**After 45 days**	**After 90 days**	**Net Proliferation (%)**
with EW	1.5+1.5	30 (-)	52 (3)	72 (6)	138.89 (19.53)
(*Eisenia*)	1.0+2.0	30 (-)	63 (4)	85 (5)	184.44 (15.75)
	2.0+1.0	30 (-)	49 (2)	62 (2)	106.67 (6.67)
with EW	1.5+1.5	30 (-)	73 (2)	91 (1)	203.33 (3.33)
(*Eudrilus*)	1.0+2.0	30 (-)	85 (5)	93 (7)	211.11 (22.19
	2.0+1.0	30 (-)	66 (5)	80 (2)	167.78 (5.09)
(d) Body Elongation		**Initial (@ 0 day)**	**After 45 days**	**After 90 days**	**Net Elongation (%)**
with EW	1.5+1.5	2.67 (0.25)	3.47 (0.33)	4.63 (0.61)	75.95 (38.90)
(*Eisenia*)	1.0+2.0	2.53 (0.21)	3.29 (0.27)	5.10 (0.10)	102.31 (18.39)
	2.0+1.0	2.53 (0.25)	3.29 (0.33)	4.03 (0.65)	59.56 (24.75)

with EW	1.5+1.5	5.27 (0.38)	6.85 (0.49)	9.27 (0.20)	76.67 (15.28)
(*Eudrilus*)	1.0+2.0	5.33 (0.42)	6.93 (0.54)	11.52 (1.33)	115.67 (8.14)
	2.0+1.0	5.47 (0.50)	7.11 (0.65)	7.54 (0.58)	38.00 (2.65)

The mean values are shown in the individual rows with their respective standard deviation in parenthesis

Thesis data published in the research paper: Nath, S., Dutta, U., Tangjang, S., Das, S., 2025. Assessing the compost-ability of oil refinery sludge in the presence or absence of earthworms: An eco-friendly approach of biodegradation. Int. Biodeterior. Biodegradation 198, 105987

4.2.4. Microbial and enzymatic activity in the composting systems and treatments

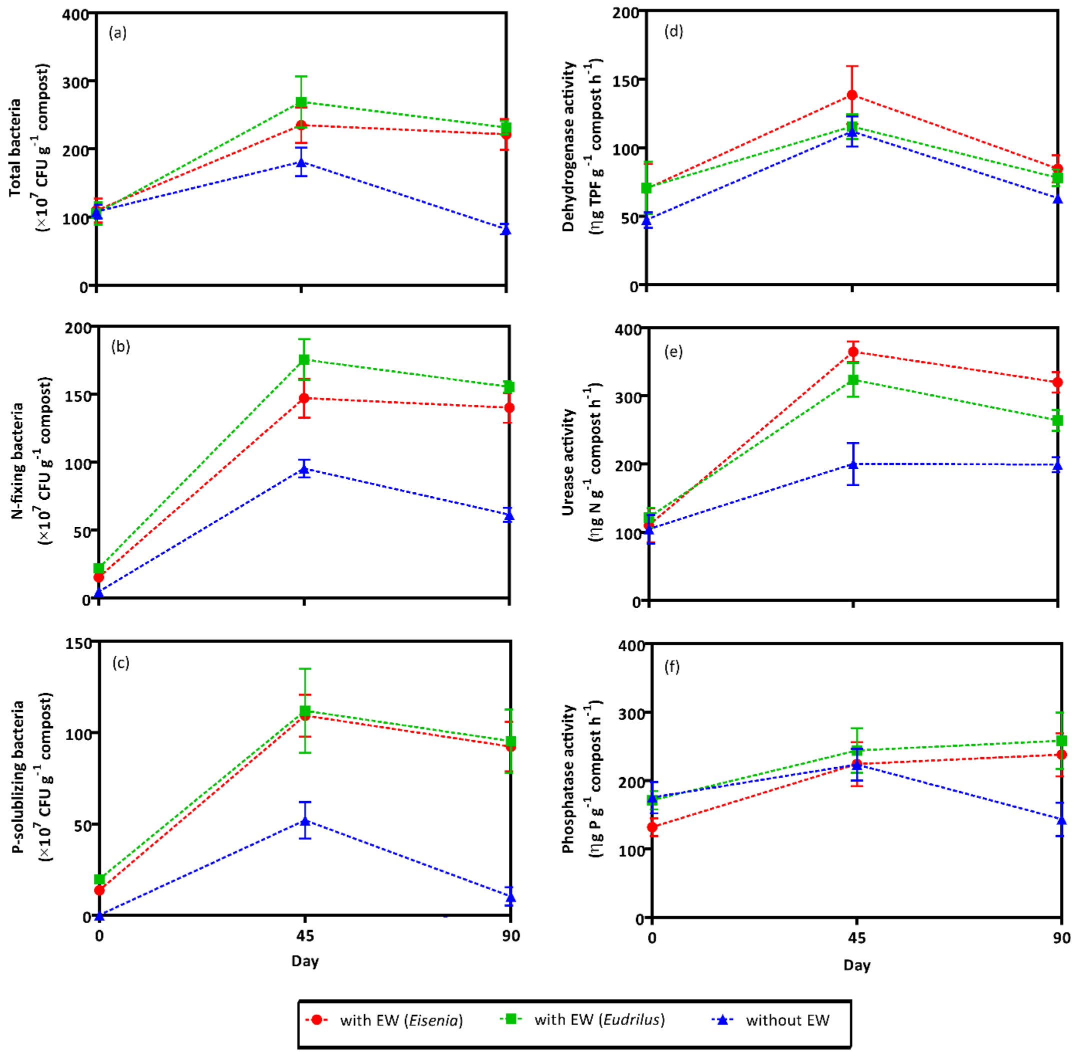

Figure 11. Microbial colony formation and enzymatic activity in the composting systems (Thesis data published in the research paper: Nath, S., Dutta, U., Tangjang, S., Das, S., 2025. Assessing the compost-ability of oil refinery sludge in the presence or absence of earthworms: An eco-friendly approach of biodegradation. Int. Biodeterior. Biodegradation 198, 105987)

On the 45th day, a significant rise was recorded in the bacterial population in the vermicomposting systems, which later decreased by the 90th day (Figure 11a; Appendix 4). The *Eudrilus*-system had the highest bacterial count on 45th day (239.22 ± 4.48 × 10^7 CFU g^{-1} compost), followed by *E. fetida*. The treatment EE_2 showed the best results in total bacterial growth with an overall increment of 25% (Nath et al., 2025). The earthworms' cast-mediated processes aided in the substrate's maturation and bacterial population turnover and could be responsible for a decreasing tendency in the overall bacterial population in the later stages (Aira et al., 2019). The total bacterial count with *E. eugeniae* increased by 3% compared to the *E. fetida*. This may be because *E. eugeniae* had a high rate of reproduction and proliferation (Table 11), which contributes to increased microbial stimulation. Without earthworms, a 0.20-fold overall decrease in the bacterial count was recorded. The low NPK level in the system suggested that the lack of earthworms may have slowed down the mineralization process. A 4.8-fold increase in the total number of N-fixing bacteria was recorded in the earthworm-based systems (Nath et al., 2025). In those systems, the total number of Phosphate-solubilizing bacteria was significant, particularly in the *Eisenia*-system, where Phosphate-solubilizing bacteria increased by 5-fold (Figure 11c; Appendix 4). The abundance of diazotrophic and phosphate-solubilizing bacteria in the vermicomposting systems may be due to the gut-mediated processes of earthworms, which give the microorganisms a suitable environment for growth with unrestrained inhibition (Aira et al., 2019). The urease activity was 0.95-fold higher in the earthworm-based composts than the non-earthworm counterpart. The *Eisenia*-system showed the highest increase in urease activity (1.8-fold), followed by the *E. eugeniae* (1.37-fold), whilst the system in the absence of earthworms recorded an increase of 0.81-fold. This improvement was probably caused by stable humic-enzyme complexes created by higher bacterial activity (Pramanik, 2010; Nath et al., 2025). *Eisenia* and *Eudrilus* composts had the highest levels of phosphatase and dehydrogenase activity. Earthworm gut microorganisms and related enzyme activity could have improved microbial metabolism and nutrition release in the systems consisting earthworms (Enebe and Erasmus, 2023a; Nath et al., 2025).

4.2.5. Quality assessment of the composting systems

The study observed greater CI (*Eudrilus*-compost = 4.73 and *Eisenia*-compost = 4.33) and FI values (3.20) (p (Technique) < 0.01) in the vermicomposting systems compared to the non-earthworm system (CI = 2.82; FI = 2.67). The earthworm composts were classified as class B (CI > 4 and FI = 3.1-3.5), whereas the non-earthworm compost was classified as RU-1 (CI and FI < 3.1) (Nath et al., 2025). The bioavailability of heavy metals got substantially reduced in the earthworm systems due to their acquisition in humified substances. Furthermore, the available nutrient content significantly increased in the earthworm-based composts as a result of enhanced mineralization, and microbial and enzymatic activity (Sharma et al., 2019). This facilitated the production of cleaner compost in those systems (Nath et al., 2025).

Earthworm systems showed 0.40-fold more HI than the system without earthworms. With *E. eugeniae*, the highest HI (12.8) was recorded, followed by *E. fetida* and without earthworms (9.03). This greater humification likely resulted from enhanced lignin degradation and the formation of recalcitrant carbon fractions during composting (Nath et al., 2025). This increase can be attributed to robust earthworm growth and stimulated microbial and enzymatic activity, which accelerated lignin breakdown (Bharathiraja et al., 2017; Nath et al., 2025). The higher HI of the earthworm-based composts also suggests that they have attained maturity and are more stable due to the decomposition of macromolecular compounds like lignocellulose (Zhu et al., 2021; Nath et al., 2025).

A 0.60-fold higher RGI was observed in *V. radiata* using earthworm-based composts compared to non-earthworm composts. The RGI was as follows: with earthworms > without earthworms. The elevated RGI in the *Eudrilus*-system suggested greater concentration of plant-accessible nutrients, which may be attributed to the biomass production and reproductive rate in *E. eugeniae*, leading to more efficient nutrient assimilation (Nath et al., 2025). The RGI was associated with the SGR and RER, both of which were higher in the systems with earthworms. The increased SGR could be linked with enhanced enzymatic activity and the presence of diazotrophic and phosphate-solubilizing bacteria, while the higher RER may be due to increased humic acid, which facilitated root development (Nath et al., 2025).

The highest CQI was recorded for the *Eudrilus*-system (7.39), followed by the *Eisenia*-system (7.12). Both of these composts were categorized as very good (Saha et al., 2010). The CQI of the system without earthworms was lower (1.74) and was classified as poor. Enhanced macronutrient solubility, increased microbial proliferation, and improved germination rates in earthworm-sourced composts contributed to the overall CQI. Increased humification, hydrolytic enzyme activity, and gut-associated homogenization and mineralization in earthworm systems have been shown to enhance microbial populations and nutrient availability. Additionally, earthworm casts have been found to elevate beneficial rhizobacteria, thereby improving seed germination (Sinha et al., 2010; Nath et al., 2025).

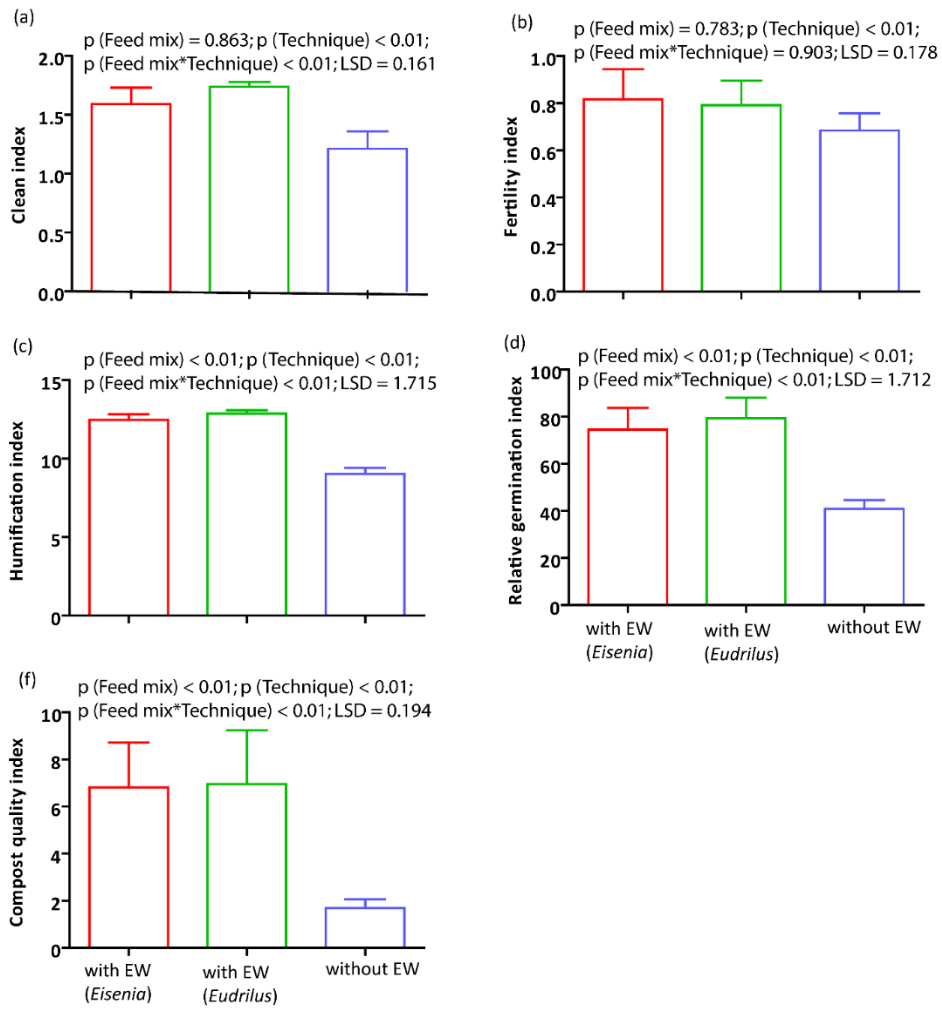

Fig 12. Quality assessment of the composting systems (Thesis data published in the research paper: Nath, S., Dutta, U., Tangjang, S., Das, S., 2025. Assessing the compost-ability of oil refinery sludge in the presence or absence of earthworms: An eco-friendly approach of biodegradation. Int. Biodeterior. Biodegradation 198, 105987)

4.2.6. Economic assessment of the composting systems

With earthworms, a net present value of 5.40-6.08 times higher was achieved than in systems without earthworms. This increased economic return could be linked to significantly faster waste biodegradation by earthworms, which allows for more waste-to-manure cycles per year (Chen et al., 2023). The benefit-cost ratio (BCR) showed that the *Eudrilus*-system was the most cost-effective, followed using *E. fetida* (Table 12). Although a BCR ≥ 1 typically indicates economic superiority, the present small-scale one-year pilot study recorded BCR values between 0.31 and 0.63 (Nath et al., 2025). Furthermore, the payback time (PBT) was shortest for the *Eudrilus* system (1.59 years), compared to the *Eisenia* system (1.83 years) and traditional composting (3.27 years). A shorter PBT means less time is needed to recover the initial investment (De Boni et al., 2022). In summary, the system with *E. eugeniae* demonstrated the best overall economic performance for ORS valorization.

Table 12: Economic assessment of the composting systems

	with EW (*Eudrilus*)	with EW (*Eisenia*)	without EW
Yearly expense (US $)	377.76	401.52	258.97
Installation cost (US $)	59.40	59.40	59.40
Gross expense in a year (US $)	437.16	460.92	318.37
Yearly production (kg)	60	60	50
Selling price (US $ 11.9/kg)	712.76	712.76	415.78
Net cash flow in a year (total sale - cost) (US $)	275.60	251.84	97.41
Net Present Value (US $)	**203.08**	**180.45**	**33.38**
Benefit-Cost Ratio	**0.63**	**0.55**	**0.31**
Pay-back time (years)	**1.59**	**1.83**	**3.27**

(Currency conversion: 1 US $ = 84.18 IN ₹)

Thesis data published in the research paper: Nath, S., Dutta, U., Tangjang, S., Das, S., 2025. Assessing the compost-ability of oil refinery sludge in the presence or absence of earthworms: An eco-friendly approach of biodegradation. Int. Biodeterior. Biodegradation 198, 105987

4.2.7. Ecotoxicity and health risk assessment of ORS CTs

The lowest RM_c value was recorded in EE_2 (2.65 ± 0.0009), while the highest was observed in AC_3 (5.03 ± 0.0021) (Table 13). Lower RM_c values in vermicompost systems align with the reduction in heavy metal bioavailability compared to aerobic composting systems (Nath and Das, 2024). The CD for CTs was within the range of 8.65 ± 0.03 and 28.28 ± 0.02, with EE_2 and AC_3 showing the lowest and highest values, respectively. The vermicompost teas (EF_1, EF_2, EF_3, EE_1, EE_2, and EE_3) exhibited substantially lower CD values than AC_1, AC_2, and AC_3. This pattern could be attributed to mechanisms inherent to vermicomposting, such as cation adsorption via dermal and gut-mediated processes (Pereira et al., 2014). Additionally, humification during vermicomposting promotes metal immobilization via increasing residual metal fractions and fostering organo-metallic complexation (He et al., 2016). The EF-CTs showed significantly low EF_c values, with EF_3 recording the lowest (0.39 ± 0.0007), followed by EF2 (0.48 ± 0.0009). All CTs exhibited EF_c values below 2, suggesting low contamination risk (Nath and Das, 2024). Similarly, the PI remained well below the threshold, indicating a low environmental threat (Nath and Das, 2024). EE_2 showed the lowest PI value (0.056 ± 9.7E-06), followed by EE_1 and EF_2. Intercellular metal-chelating proteins in earthworm chloragocyte tissues are key facilitators of the efficient heavy metal speciation observed during bioconversion (L Goswami et al., 2014). All vermicompost teas showed PERI values < 300, indicating moderate ecological risk. EE_2 showed the lowest value (221.05 ± 0.79), marking it as the optimal CT (Table 13). Conversely, aerobic compost teas (AC_1 to AC_3) had PERI values of 300 to 600, indicating a greater ecological risk due to their heavy metal content (Weissmannová and Pavlovský, 2017; Nath and Das, 2024).

Table 13. Ecotoxicological assessment of the produced compost teas

Treatments	RM_c	CD	EF_c	PI	PERI
EF_1	2.99 ± 0.0003	9.63 ± 0.02	0.49 ± 0.0009	0.068 ± 5.8E-06	243.07 ± 0.51
EF_2	2.65 ± 0.0009	9.45 ± 0.02	0.48 ± 0.0009	0.063 ± 2.6E-05	240.32 ± 0.52
EF_3	3.16 ± 0.0012	9.90 ± 0.02	0.39 ± 0.0007	0.069 ± 6.5E-06	249.88 ± 0.51
EE_1	2.73 ± 0.0014	9.37 ± 0.03	0.86 ± 0.0024	0.063 ± 7.4E-06	238.02 ± 0.78
EE_2	2.28 ± 0.0007	8.65 ± 0.03	1.01 ± 0.0030	0.056 ± 9.7E-06	221.05 ± 0.79
EE_3	2.91 ± 0.0020	9.49 ± 0.03	0.74 ± 0.0020	0.066 ± 1.0E-05	240.17 ± 0.79
AC_1	4.72 ± 0.0051	21.0 ± 0.02	0.62 ± 0.0006	0.100 ± 1.3E-04	566.04 ± 0.53
AC_2	4.72 ± 0.0046	27.69 ± 0.02	0.99 ± 0.0008	0.095 ± 1.1E-04	769.15 ± 0.60
AC_3	5.03 ± 0.0021	28.28 ± 0.02	0.72 ± 0.0004	0.101 ± 1.4E-05	783.71 ± 0.51
	p (Tq) < 0.001	p (Tq) < 0.001	p (Tq) < 0.001	p (Tq) < 0.001	p (Tq) < 0.001
	p (Fm) < 0.001	p (Fm) < 0.001	p (Fm) < 0.001	p (Fm) < 0.001	p (Fm) < 0.001
	LSD = 0.00122	LSD = 0.01004	LSD = 0.00074	LSD = 0.00003	LSD = 0.29591

Tq Technique; *Fm* Feed mixture; *LSD* Least significant difference

Thesis data published in the research paper: Nath, S., Das, S., 2024. Aqueous extracts of composted oil refinery sludge and their possible environmental impacts. Water Sci. Technol. wst2024229.

The HI revealed a distinct trend, showing low values for all CT samples (Table 14). For adults, the HI ranges were: Cr (9.653E-06 to 1.803E-05), Pb (2.476E-03 to 5.988E-03), Cu (4.719E-04 to 6.478E-04), Cd (1.613E-03 to 5.793E-03), and Zn (3.002E-06 to 1.528E-05) (Nath and Das, 2024). Corresponding values for children were also found to be significantly under the threshold limit, with a maximum HI of 4.790E-02 (Pb) and a minimum of 1.222E-04 (Zn). Although all CTs were below the threat level, two notable trends were observed: i) HI values for heavy metals were consistently more for children than for adults and ii) all AC-CTs exhibited higher HI values (Nath and Das, 2024). Stein et al. (2002) identified two reasons why children are more vulnerable to heavy metal pollution: a higher body weight-to-food consumption ratio and increased dermal absorption in children. The CI index data further indicated a non-lethal contribution from CTs regarding cancer emergence. All CTs exhibited a CI value of less than 1 for heavy metals. Among these, Pb recorded the highest CI value in adults and children. The overall order of CI was Zn < Cr < Cu < Cd < Pb. The low CI values justified the non-lethal aspects of the CT samples (Nath and Das, 2024).

Table 14. Non-carcinogenic and carcinogenic risks of the compost teas

Metal	Treatment	Adult					Children				
		HQ ingestion	HQ inhalation	HQ dermal	HI	CI	HQ ingestion	HQ inhalation	HQ dermal	HI	CI
Cr	**EF_1**	1.241E-05	1.825E-09	1.238E-07	1.253E-05	7.663E-08	9.926E-05	2.773E-09	6.948E-07	9.995E-05	1.165E-07
	EF_2	1.232E-05	1.811E-09	1.229E-07	1.244E-05	7.608E-08	9.854E-05	2.753E-09	6.898E-07	9.923E-05	1.156E-07
	EF_3	1.249E-05	1.836E-09	1.245E-07	1.261E-05	7.712E-08	9.988E-05	2.791E-09	6.992E-07	1.006E-04	1.172E-07
	EE_1	1.115E-05	1.640E-09	1.112E-07	1.126E-05	6.888E-08	8.921E-05	2.493E-09	6.245E-07	8.984E-05	1.047E-07
	EE_2	9.556E-06	1.405E-09	9.532E-08	9.653E-06	5.902E-08	7.645E-05	2.136E-09	5.351E-07	7.698E-05	8.971E-08
	EE_3	1.207E-05	1.775E-09	1.204E-07	1.219E-05	7.456E-08	9.658E-05	2.698E-09	6.760E-07	9.725E-05	1.133E-07
	AC_1	**1.785E-05**	**2.625E-09**	**1.781E-07**	**1.803E-05**	**1.103E-07**	**1.428E-04**	**3.990E-09**	**9.997E-07**	**1.438E-04**	**1.676E-07**
	AC_2	1.372E-05	2.018E-09	1.369E-07	1.386E-05	8.474E-08	1.098E-04	3.067E-09	7.683E-07	1.105E-04	1.288E-07
	AC_3	1.689E-05	2.483E-09	1.684E-07	1.706E-05	1.043E-07	1.351E-04	3.774E-09	9.456E-07	1.360E-04	1.585E-07
Pb	**EF_1**	3.338E-03	4.909E-07	1.005E-08	3.338E-03	2.062E-05	2.670E-02	7.461E-07	5.643E-08	2.670E-02	3.134E-05
	EF_2	2.632E-03	3.871E-07	7.926E-09	2.633E-03	1.626E-05	2.106E-02	5.884E-07	4.450E-08	2.106E-02	2.471E-05
	EF_3	3.496E-03	5.140E-07	1.053E-08	3.496E-03	2.159E-05	2.796E-02	7.814E-07	5.909E-08	2.797E-02	3.282E-05
	EE_1	3.100E-03	4.559E-07	9.336E-09	3.101E-03	1.915E-05	2.480E-02	6.930E-07	5.242E-08	2.480E-02	2.911E-05
	EE_2	2.476E-03	3.641E-07	7.455E-09	2.476E-03	1.529E-05	1.980E-02	5.534E-07	4.185E-08	1.981E-02	2.324E-05
	EE_3	3.258E-03	4.791E-07	9.810E-09	3.258E-03	2.012E-05	2.606E-02	7.282E-07	5.507E-08	2.606E-02	3.058E-05
	AC_1	5.355E-03	7.876E-07	1.613E-08	5.356E-03	3.308E-05	4.284E-02	1.197E-06	9.054E-08	4.285E-02	5.028E-05
	AC_2	5.726E-03	8.421E-07	1.724E-08	5.727E-03	3.537E-05	4.581E-02	1.280E-06	9.681E-08	4.581E-02	5.376E-05
	AC_3	**5.987E-03**	**8.805E-07**	**1.803E-08**	**5.988E-03**	**3.698E-05**	**4.790E-02**	**1.338E-06**	**1.012E-07**	**4.790E-02**	**5.621E-05**
Cu	**EF_1**	4.886E-04	7.185E-08	6.498E-10	4.886E-04	3.018E-06	3.908E-03	1.092E-07	3.648E-09	3.909E-03	4.587E-06
	EF_2	4.857E-04	7.142E-08	6.459E-10	4.857E-04	3.000E-06	3.885E-03	1.086E-07	3.626E-09	3.885E-03	4.559E-06
	EF_3	4.963E-04	7.298E-08	6.601E-10	4.964E-04	3.065E-06	3.970E-03	1.109E-07	3.706E-09	3.970E-03	4.659E-06
	EE_1	4.809E-04	7.071E-08	6.395E-10	4.809E-04	2.970E-06	3.847E-03	1.075E-07	3.590E-09	3.847E-03	4.514E-06
	EE_2	4.718E-04	6.938E-08	6.275E-10	4.719E-04	2.914E-06	3.774E-03	1.055E-07	3.523E-09	3.774E-03	4.429E-06

	EE_3	4.748E-04	6.983E-08	6.315E-10	4.749E-04	2.933E-06	3.799E-03	1.061E-07	3.546E-09	3.799E-03	4.458E-06
	AC_1	**6.477E-04**	**9.525E-08**	**8.614E-10**	**6.478E-04**	**4.000E-06**	**5.181E-03**	**1.448E-07**	**4.836E-09**	**5.182E-03**	**6.081E-06**
	AC_2	6.467E-04	9.510E-08	8.600E-10	6.467E-04	3.994E-06	5.173E-03	1.445E-07	4.828E-09	5.173E-03	6.071E-06
	AC_3	5.989E-04	8.807E-08	7.965E-10	5.990E-04	3.699E-06	4.791E-03	1.339E-07	4.472E-09	4.791E-03	5.622E-06
Cd	**EF_1**	1.772E-03	2.606E-07	7.070E-08	1.772E-03	1.095E-05	1.418E-02	3.961E-07	3.969E-07	1.418E-02	1.664E-05
	EF_2	1.753E-03	2.578E-07	6.994E-08	1.753E-03	1.083E-05	1.402E-02	3.918E-07	3.926E-07	1.402E-02	1.646E-05
	EF_3	1.822E-03	2.679E-07	7.269E-08	1.822E-03	1.125E-05	1.458E-02	4.073E-07	4.081E-07	1.458E-02	1.710E-05
	EE_1	1.736E-03	2.553E-07	6.928E-08	1.737E-03	1.072E-05	1.389E-02	3.881E-07	3.889E-07	1.389E-02	1.630E-05
	EE_2	1.612E-03	2.371E-07	6.433E-08	1.613E-03	9.958E-06	1.290E-02	3.604E-07	3.611E-07	1.290E-02	1.514E-05
	EE_3	1.752E-03	2.576E-07	6.989E-08	1.752E-03	1.082E-05	1.401E-02	3.915E-07	3.924E-07	1.401E-02	1.644E-05
	AC_1	4.165E-03	6.126E-07	1.662E-07	4.166E-03	2.573E-05	3.332E-02	9.311E-07	9.331E-07	3.333E-02	3.911E-05
	AC_2	5.683E-03	8.358E-07	2.268E-07	5.684E-03	3.510E-05	4.546E-02	1.270E-06	1.273E-06	4.547E-02	5.335E-05
	AC_3	**5.792E-03**	**8.517E-07**	**2.311E-07**	**5.793E-03**	**3.577E-05**	**4.633E-02**	**1.295E-06**	**1.297E-06**	**4.634E-02**	**5.437E-05**
Zn	**EF_1**	8.528E-06	1.254E-09	1.701E-11	8.529E-06	5.267E-08	6.822E-05	1.906E-09	9.551E-11	6.822E-05	8.006E-08
	EF_2	4.948E-06	7.276E-10	9.871E-12	4.949E-06	3.056E-08	3.958E-05	1.106E-09	5.542E-11	3.958E-05	4.645E-08
	EF_3	1.082E-05	1.592E-09	2.160E-11	1.083E-05	6.686E-08	8.660E-05	2.420E-09	1.212E-10	8.660E-05	1.016E-07
	EE_1	5.949E-06	8.749E-10	1.187E-11	5.950E-06	3.675E-08	4.760E-05	1.330E-09	6.663E-11	4.760E-05	5.585E-08
	EE_2	3.002E-06	4.414E-10	5.988E-12	3.002E-06	1.854E-08	2.401E-05	6.710E-10	3.362E-11	2.401E-05	2.818E-08
	EE_3	8.345E-06	1.227E-09	1.665E-11	8.346E-06	5.154E-08	6.676E-05	1.865E-09	9.346E-11	6.676E-05	7.834E-08
	AC_1	1.466E-05	2.157E-09	2.926E-11	1.467E-05	9.058E-08	1.173E-04	3.278E-09	1.642E-10	1.173E-04	1.377E-07
	AC_2	1.145E-05	1.684E-09	2.285E-11	1.145E-05	7.073E-08	9.161E-05	2.560E-09	1.283E-10	9.161E-05	1.075E-07
	AC_3	**1.527E-05**	**2.246E-09**	**3.047E-11**	**1.528E-05**	**9.434E-08**	**1.222E-04**	**3.414E-09**	**1.711E-10**	**1.222E-04**	**1.434E-07**

Thesis data published in the research paper: Nath, S., Das, S., 2024. Aqueous extracts of composted oil refinery sludge and their possible environmental impacts. Water Sci. Technol. wst2024229.

4.2.8. Multivariate analyses through correlation and PCA

To determine the key parameters influencing CQI, Pearson correlation analysis was conducted. The results revealed significant positive correlations between CQI and several variables: total organic carbon ($r = 0.689$; $p < 0.001$), water holding capacity ($r = 0.924$; $p < 0.001$), earthworm population ($r = 0.850$; $p < 0.001$), total nitrogen ($r = 0.897$; $p < 0.001$), phosphatase activity ($r = 0.632$; $p < 0.001$), and nitrogen-fixing bacteria ($r = 0.526$; $p < 0.001$) (Figure 13a; Appendix 5). Earthworms are known to enhance compost's physicochemical properties by fragmenting larger particles, which promotes moisture retention, nutrient availability, microbial activity, and carbon pools (Ahmed and Al-Mutairi, 2022). Conversely, significant negative correlations were observed between CQI and the heavy metals, as well as bulk density. These findings imply that detoxification of toxic metals and optimization of physical properties were the important contributors in producing high-quality compost. Comparable findings have been reported in earlier studies (Hanc et al., 2020; Nath et al., 2025).

PCA was employed to minimize the multidimensional nature of the dataset and to identify the principal factors influencing CQI, as visualized in Figure 13b. The suitability of the data was confirmed by Kaiser-Meyer-Olkin's (KMO) sampling adequacy (0.857) and significant Bartlett's sphericity test ($p < 0.001$). Examination of the scree plot revealed three distinct varimax factors (VF1, VF2, and VF3) with eigenvalues exceeding 1. The VF1 aggregated the most closely associated variables with CQI, including water-holding capacity, total organic carbon, total Kjeldahl nitrogen, total phosphorus, total potassium, as well as earthworm count and body weight. The VF2 encompassed various bacterial and enzymatic parameters. The VF3 comprised bulk density, heavy metals, and pH, exhibiting negative relationship with CQI. The loading plots accounted for 97.5% of the overall variance, with PC1 explaining 76.6% and PC2 explaining 20.9% (Figure 13b). In conclusion, PCA established VF1 as the most significant contributor to CQI, whereas VF3 demonstrated the least association (Reimann et al., 2011; Nath et al., 2025).

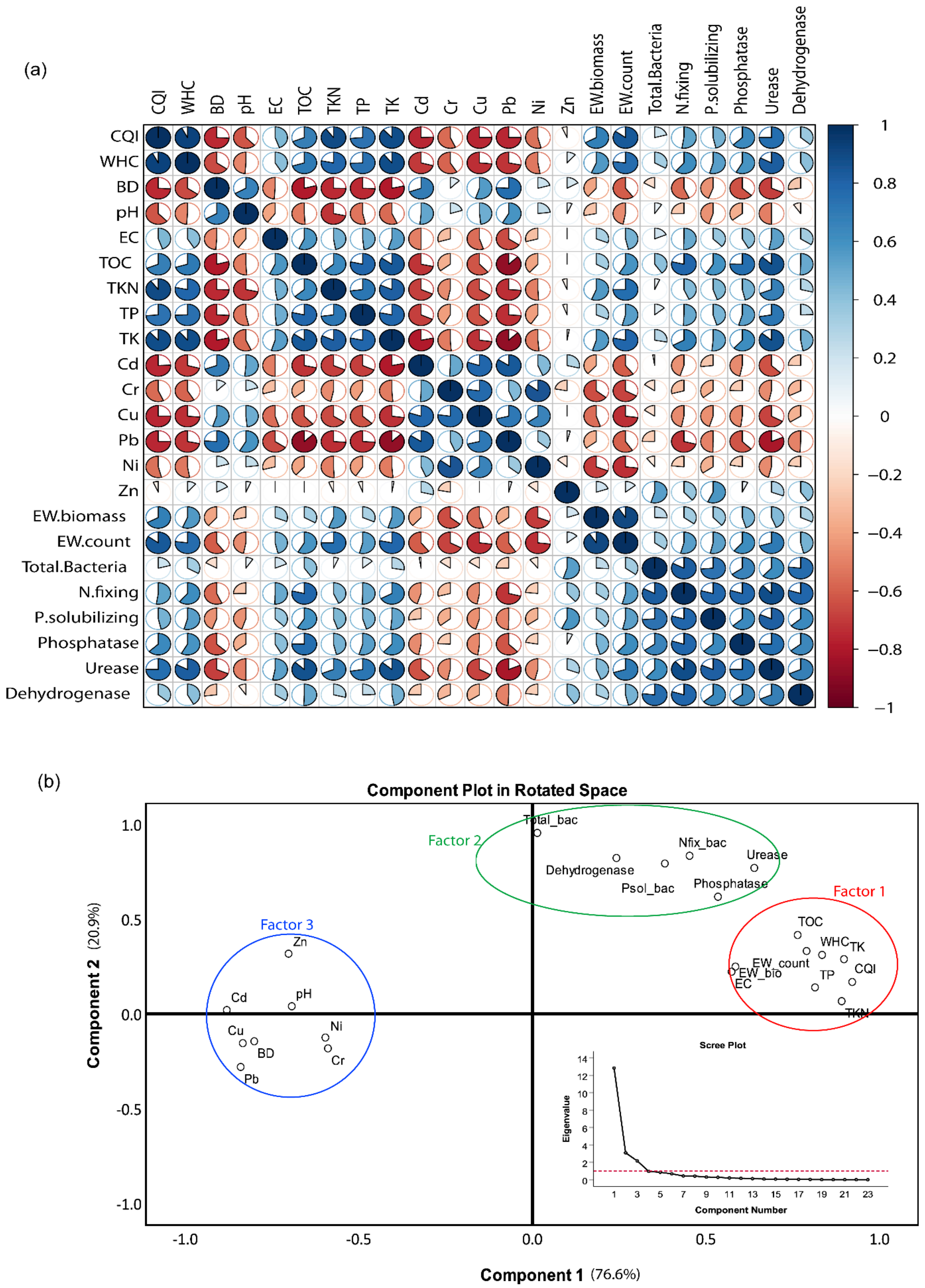

Figure 13. Relationship of CQI with various physico-chemical and biological parameters through Pearson's correlogram and PCA (Thesis data published in the research paper: Nath, S., Dutta, U., Tangjang, S., Das, S., 2025. Assessing the compost-ability of oil refinery sludge in the presence or absence of earthworms: An eco-friendly approach of biodegradation. Int. Biodeterior. Biodegradation 198, 105987)

4.3. Phase III - Large-scale composting experiment

4.3.1. Physicochemical characteristics of the two ORS vermicomposts

Both EF and EE samples exhibited a significant decrease in pH by the 90th day, with values of 5.60 and 5.62, respectively (Table 15). The activity of earthworms likely triggered the production of organic acids, anions, and other humified materials (Qian et al., 2024; Nath and Das, 2026). At the same time, a 27% and 48% elevation in electrical conductivity was recorded in EF and EE, respectively. Dume et al. (2023) also demonstrated that the EC was higher in vermicomposts than in conventional compost. There was a significant decrease in BD with incubation period and an increase in WHC (Nath and Das, 2026). As per Domínguez (2018), *E. eugeniae* helps in the formation of porous structures in the substrate, due to differences in burrowing behavior and tissue fragmentation, therefore facilitating physical properties that allow water infiltration and air to move freely. In EF and EE, the TOC reduced by 0.62-fold and 0.38-fold respectively throughout the incubation period (90 days). The increased TOC reduction by *E. fetida* may be an indication of metabolic changes due to the influence of metal stress, in which this species increases its respiration rate to meet the increased energy requirements towards homeostasis, thus oxidizing a significant portion of carbon to CO_2 (Hou et al., 2023; Nath and Das, 2026). Nitrogen dynamics showed that EE contained a more significant quantity of TN (7% higher than EF) and available N (Table 15). The microbiome of *E. eugeniae* could have increase the fixation of nitrogenous compounds into humic compounds, consequently decreasing NH_4^+ emissions (H. Li et al., 2025; Nath and Das, 2026).

Table 15. Physicochemical characteristics of the two ORS vermicomposts

	EF		EE		Two way-ANOVA			
Parameters	**0th Day**	**90th Day**	**0th Day**	**90th Day**	**p-value (Tq)**	**p-value (Tm)**	**p-value (Tq*Tm)**	**LSD**
pH	6.14 ± 0.02	5.60 ± 0.17	6.15 ± 0.01	5.62 ± 0.03	0.741	0.000	0.894	0.049
EC (µS cm^{-1})	2959.00 ± 15.52	3761.00 ± 3.61	2390.33 ± 5.51	3560 ± 2.00	0.000	0.000	0.000	4.902
WHC (%)	64.00 ± 3.00	75.00 ± 4.00	56.00 ± 3.00	78.00 ± 3.00	0.397	0.000	0.002	1.491
BD (g cm^{-3})	1.03 ± 0.02	0.64 ± 0.04	0.96 ± 0.02	0.53 ± 0.02	0.001	0.000	0.126	0.015
TOC (%)	14.50 ± 0.25	5.40 ± 0.04	10.57 ± 0.32	6.45 ± 0.02	0.000	0.000	0.000	0.117
TKN (%)	0.53 ± 0.32	0.94 ± 0.04	0.51 ± 0.01	1.02 ± 0.02	0.044	0.000	0.005	0.013

Available N (mg kg^{-1})	689.60 ± 4.15	1120.50 ± 4.90	435.15 ± 3.15	1089.30 ± 3.10	0.000	0.000	0.000	2.250
Available P (mg kg^{-1})	114.75 ± 0.25	240.03 ± 1.98	89.50 ± 1.00	280.33 ± 1.48	0.000	0.000	0.000	0.773
Available K (mg kg^{-1})	264.17 ± 0.67	635.71 ± 0.02	262.36 ± 0.19	578.57 ± 1.60	0.000	0.000	0.000	0.503

**EF - Vermicomposting with E. fetida; EE - Vermicomposting with E. eugeniae; Tq - Technique; Tm - Time; LSD - Least significant difference*

Thesis data published in the research paper: Nath, S., Das, S., 2026. Species-specific benefits in bioremediation of oil refinery sludge via large-scale vermicomposting process: a detailed comparison between *Eisenia fetida* and *Eudrilus eugeniae*. Chemosphere 394, 144782.

4.3.2. Heavy metal speciation of the two ORS vermicomposts

For Cd, EF showed a decrease in concentration across fractions. The most substantial reductions occurred in F2 (0.30-fold) and F4 (0.24-fold) fractions (Figure 14a-14g; Appendix 6). This likely resulted from the transcriptional upregulation of phytochelatin synthase (PCS). under Cd stress. PCS produces phytochelatins, which bind to bioavailable Cd to form stable complexes. These are subsequently transported into cellular vacuoles, reducing bioavailability (Chai et al., 2020). Research has shown *E. fetida* could convert labile Cd into stable forms in contaminated soils (Garau et al., 2022). EE compost demonstrated a greater reduction in the F4 (0.58-fold) and F5 (0.53-fold) fractions (p (Technique × Time) < 0.001). *E. eugeniae* primarily employs glutathione-mediated detoxification pathway for Cd. Exposure to Cd induces the upregulation of γ-glutamyl cysteine synthetase (γ-GCS), thereby enhancing the synthesis of glutathione (GSH). Subsequently, glutathione S-transferase (GST) catalyses the conjugation of Cd with GSH. This reaction produces Cd-GSH complexes, which are ultimately transported from cells via membrane transporters (Doherty et al., 2019; Nath and Das, 2026).

Regarding Cr, all fractions except the F6 declined in EF compost by 90^{th} day, with the most substantial decrease in the F4 fraction (0.28-fold) (p (Technique × Time) < 0.001) (Figure 14b-14h; Appendix 6). In *E. fetida*, chromium-resistant gut microbiome drives the upregulation of chromate reductases, enzymes that detoxify chromium by transforming it into less bioavailable species (Liu et al., 2023; Nath and Das, 2026). EE compost also showed a substantial reduction in the F4 fraction (0.15-fold) (p (Technique × Time) < 0.001) The F6 fraction decreased by 0.13-fold in EE, a reduction 70% greater than in EF. In *E. eugeniae*, this reduction of Cr is catalysed by oxidoreductase enzymes through specific metabolic pathways (Arumugaperumal et al., 2022; Nath and Das, 2026).

For Pb, the fraction order was F2 < F1 < F3 < F4 < F5 < F6 (Figure 14c-14i; Appendix 6). In EF, digestive enzymes such as acid and alkaline phosphatase liberate phosphate ions. These ions then precipitate soluble Pb into stable Pb-phosphate complexes (Liu et al., 2025; Nath and Das, 2026). In contrast, EE showed reductions in the F1 (0.03-fold), F3 (0.18-fold), and F6 (0.11-fold) fractions, indicating an enhanced mobilization of stable Pb forms. *E. eugeniae* relies on the GST pathway for Pb detoxification, where GST conjugates glutathione to Pb, thereby increasing solubility to promote elimination and reduce cellular uptake (Tiwari et al., 2016; Nath and Das, 2026).

In Cu, the F5 fraction in EF compost decreased most significantly (0.65-fold), followed by the F4 (0.32-fold) and F3 (0.35-fold) fractions (Figure 14d-14j; Appendix 6). EE compost showed a similar trend, with particular reductions in the residual fraction. The Cu tolerance of *E. fetida* is enhanced by its gut microbiota, particularly by the phyla *Proteobacteria* and *Firmicutes*, through encoding multicopper oxidases (CueO) and copper chaperones, which converts soluble Cu into less harmful oxidized forms (Zhang et al., 2024; Nath and Das, 2026). The substantial reduction in the F6 observed in EE indicates that *E. eugeniae* may enhance long-term copper uptake, potentially through the action of gut-associated enzymes. The detoxification of Cu in *E. eugeniae* may also be mediated by the synthesis of GST enzymes under conditions of metal stress (Julius et al., 2015; Nath and Das, 2026).

Ni followed the order F1 < F2 < F3 < F4 < F5 < F6 in the systems on the 90th day (Figure 14e-14k; Appendix 6). In EF, *Actinobacteria* contributed to Ni transformation via upregulated antibodies and metabolites that bind toxic Ni ions (Velásquez-Chávez et al., 2025; Nath and Das, 2026). In EE, substantial decreases occurred in the F1 (0.55-fold) and F6 (0.39-fold) fractions, along with reductions in the F3 (0.21-fold) and F5 (0.05-fold) fractions. This pattern suggests *E. eugeniae* employs more comprehensive metal mobilization mechanisms. Gut-associated *Pseudomonas* may catalyse Ni oxidation to less soluble forms or Ni could be precipitated as less bioavailable sulfides through the action of sulfate-reducing bacteria (Owagboriaye et al., 2021; Nath and Das, 2026).

For Zn, EF showed a 15.9% reduction in the organic-bound (F5) fraction, followed by the residual (F6) and exchangeable (F2) fractions (Figure 14f-14l; Appendix 6). Zn-induced stress triggers an enhancement (0.3-0.4-fold) in the cellulose-degrading enzymatic activity within *E. fetida*, potentially leading to faster decomposition of organic matter and the release of soluble Zn (Gupta and Yadav, 2014). In EE compost, F6 fraction decreased by 0.46-fold, alongside reductions in the F5 (0.20-fold) and F4 (0.28-fold) fractions, indicating effective disruption of oxide-associated Zn. The diverse gut microbiome of *E. eugeniae*, rich in *Proteobacteria*, *Actinobacteria*, and *Firmicutes*, may reduce Zn ions enzymatically or produce siderophores that produce Zn complexes (Thakur et al., 2022; Nath and Das, 2026).

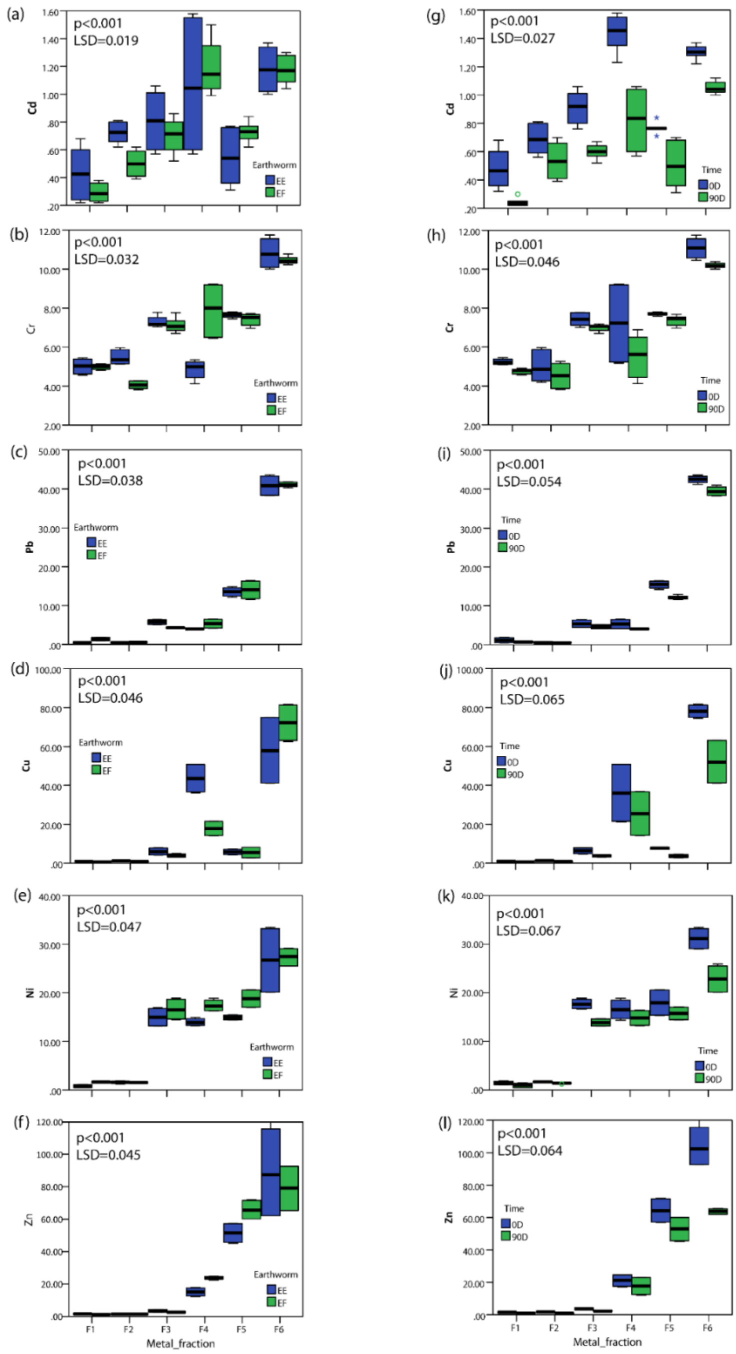

Figure 14. Speciation of heavy metals in the ORS vermicomposts (Thesis data published in the research paper: Nath, S., Das, S., 2026. Species-specific benefits in bioremediation of oil refinery sludge via large-scale vermicomposting process: a detailed comparison between *Eisenia fetida* and *Eudrilus eugeniae*. Chemosphere 394, 144782.)

4.3.3. Carbon fractionation of the two ORS vermicomposts

During the 90-day experiment, carbon fraction dynamics indicated substantial shifts in the composition of organic matter within both EF and EE systems (Figure 15; Appendix 7). Exchangeable C decreased substantially, with the highest decline in EE (2.7%), followed by EF (2.4%). This efficient reduction could be attributed to the decomposition processes driven by microbial activity and digestion of readily available organic material (W. Wang et al., 2021), *E. eugeniae* was found to process labile carbon more efficiently, showing a 12.5% higher rate. The outcomes are consistent with research by Balachandar et al. (2020) which showed that *E. eugeniae* effectively decreased labile carbon when processing pressmud. The physiology of the gut and the composition of microbial ecosystem differ across species which may explain this difference. *E.eugeniae* exhibits enhanced cellulose degradation, supported by robust activity of cellulase enzymes (Boruah and Deka, 2023).

Both systems led to a substantial augmentation of the FAC fraction during the 90-day incubation period (EF: 3.70% to 5.72%; EE: 4.83% to 5.73%). This increase reflects the enzymatic degradation of recalcitrant organic polymers mediated by hydrolytic enzymes (Bharathiraja et al., 2017). Significantly higher initial FAC levels were seen in EE, suggesting that the rapid initiation of the humification process by *E. eugeniae* is potentially linked to its high enzymatic output, specifically hemicellulases. These enzymes are key to the degradation of lignocellulosic substrates (Wang et al., 2024; Nath and Das, 2026).

A distinct trend was observed for the HAC fraction, wherein EF showed a 1.82% increase and an increase of 1.95% was exhibited by EE. The combined biochemical and microbial activity in *E. eugeniae*, driven by both its gut and its casts, could have accelerated the formation of humus. The secretory products from these processes act as nucleation sites, intensifying microbial metabolism and supporting the formation of HAC (Iordache, 2023). Conversely, the slow humification by *Eisenia fetida* may have resulted as a stress-induced change in the underlying biological mechanism that promoted the catabolic processing of carbon, culminating in its release as carbon dioxide (Gudeta et al., 2023; Wu et al., 2025). This interpretation was supported by the decrease in TOC observed in the EF system. Moreover, Additionally, the buildup of humic fractions in EE indicates that *E. eugeniae* could be efficient at fostering the development of stable humic materials (Jakubus and Michalak-Oparowska, 2022), indicating higher maturity and stability (Nath and Das, 2026).

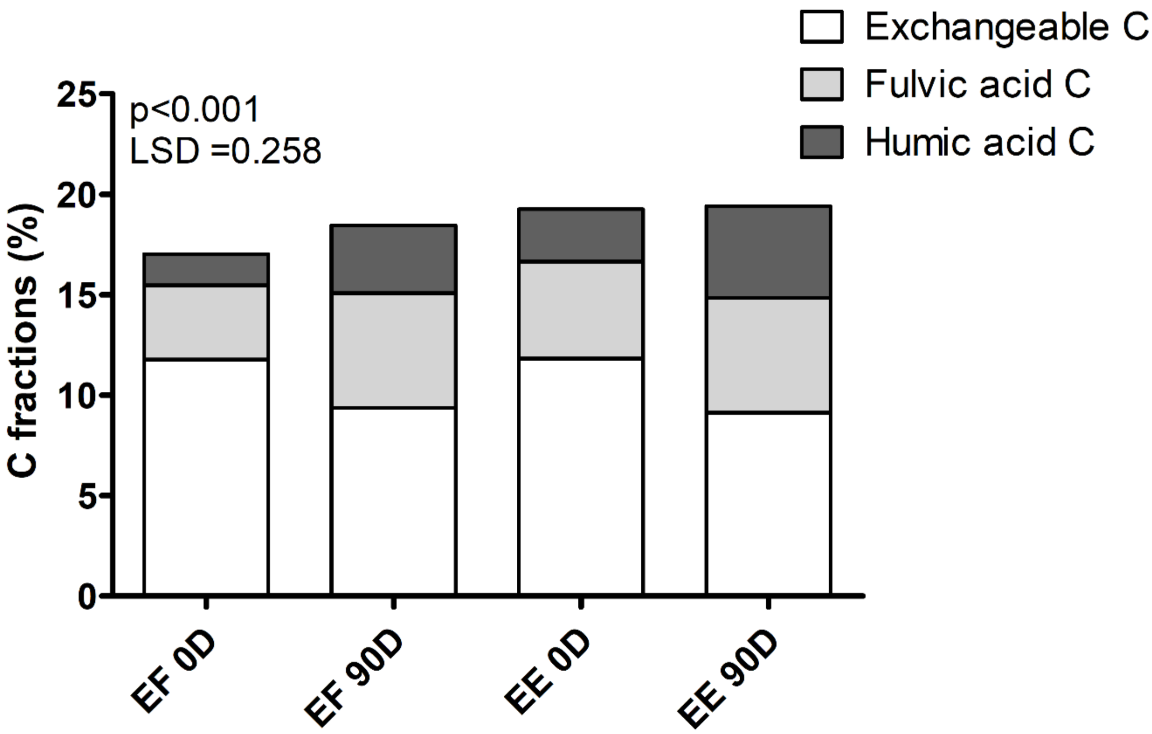

Figure 15. C fractionation of the two vermicomposting systems (Thesis data published in the research paper: Nath, S., Das, S., 2026. Species-specific benefits in bioremediation of oil refinery sludge via large-scale vermicomposting process: a detailed comparison between *Eisenia fetida* and *Eudrilus eugeniae*. Chemosphere 394, 144782.)

4.3.4. Earthworm growth and proliferation in the composting systems

Although both earthworms showed significant biomass gains, a greater net gain was observed for EE (Table 16). This enhanced growth in *E. eugeniae* may be attributed to its larger initial size, which could provide superior resource capacity or stronger competitive position (Soobhany et al., 2015). Population composition further demonstrated the superior proliferation rate of *E. eugeniae* (35.7%) over *E. fetida* (31%), with earthworm (EW) counts reaching 407 and 393 individuals, respectively. The enhanced resilience of *E. eugeniae* in ORS compost appears could be connected to the activation of anti-oxidant enzymes, including superoxide dismutase (SOD), glutathione peroxidase (GPx), and catalase (CAT). The primary role of these enzymes is to counter the oxidative stress by detoxifying the overabundance of reactive oxygen species (ROS) (Paul et al., 2022). Cocoon production was recorded from the 6^{th} to the 13^{th} week of incubation (Table 16). Also, *E. eugeniae* had the most favourable reproductive outcomes, with a cocoon count of 85 ± 7 and reproductive rate of 0.21 ± 0.02 cocoons EW^{-1}. Morphological changes also showed greater body elongation in *E. eugeniae*

(13.49 ± 2.10%) compared to *E. fetida* (10.16 ± 7.46%), indicating differences in the growth patterns of the species (Begum et al., 2025; Nath and Das, 2026).

Table 16. Growth and proliferation of *E. fetida* and *E. eugeniae* during vermicomposting

Parameters	***Eisenia fetida***			***Eudrilus eugeniae***				
	Initial (@ 0 day)	**After 90 days**	**Biomass gain (mg)**	**Initial (@ 0 day)**	**After 90 days**	**Biomass gain (mg)**	**p-value**	**t-value**
Biomass (mg)	716.67 ± 104.08	1150.00 ± 100.00	433.33 ± 160.72	1203.33 ± 45.09	1656.67 ± 70.24	453.33 ± 68.06	0.001	11.149
	Initial (@ 0 day)	**After 90 days**	**Net proliferation (%)**	**Initial (@ 0 day)**	**After 90 days**	**Net proliferation (%)**	**p-value**	**t-value**
EW count (no.)	300 ± 0	393 ± 4	31.00 ± 1.20	300 ± 0	407 ± 3	35.78 ± 0.84	0.940	2.066
	Initial (@ 0 day)	**After 90 days**	**Reproductive rate (cocoon EW^{-1})**	**Initial (@ 0 day)**	**After 90 days**	**Reproductive rate (cocoon EW^{-1})**	**p-value**	**t-value**
Cocoon count (no.)	0.00	78 ± 4	0.20 ± 0.01	0.00	85 ± 7	0.21 ± 0.02	0.206	1.453
	Initial (@ 0 day)	**After 90 days**	**Net elongation (%)**	**Initial (@ 0 day)**	**After 90 days**	**Net elongation (%)**	**p-value**	**t-value**
Body elongation (cm)	6.42 ± 0.39	7.05 ± 0.05	10.16 ± 7.46	8.73 ± 0.15	9.91 ± 0.03	13.49 ± 2.10	0.001	13.947

Thesis data published in the research paper: Nath, S., Das, S., 2026. Species-specific benefits in bioremediation of oil refinery sludge via large-scale vermicomposting process: a detailed comparison between *Eisenia fetida* and *Eudrilus eugeniae*. Chemosphere 394, 144782.

4.3.5. Bioaccumulation of heavy metals by earthworms

On the 90th day, greater Cd concentration was measured in the gut of *E. eugeniae* (1.30 ± 0.06 mg kg^{-1}) compared to *E. fetida* (1.01 ± 0.06 mg kg^{-1}), indicating a greater bioaccumulation capacity in *E. eugeniae*. This enhanced ability could be connected to a more effective toxin-removal process involving glutathione (GSH) synthesis and a unique gut microbiota capable of producing gluconic acid, siderophores, and EPS with carboxyl and amine species (Yuvaraj et al., 2020). The Cd detoxification potential of *E. eugeniae* was previously corroborated by Ekperusi and Aigbodion (2015) in petroleum-contaminated soils. In contrast, intestinal uptake of Cr was found to be significantly higher in *E. fetida* than in *E. eugeniae*. The observed variation could be linked to the unique biological characteristics of *E. fetida*, such as high tissue concentrations of lipids and proteins, which promote Cr uptake (Tang et al., 2019). However, for the other metals studied, intestinal accumulation was observed to be 0.20 to 0.42-fold more in *E. eugeniae*. Physiological adaptations in *E. eugeniae* including modified protein band profiles and heightened antioxidant enzyme activity to stress support its metal accumulation capacity. For instance, under pesticide stress, *E. eugeniae* demonstrated activation of SOD, CAT, and proteases, along with peroxidase (POD) activity throughout its complete lifespan (Kumar et al., 2024; Nath and Das, 2026). Also, in *E. eugenia*, a metal-binding protein Cytochrome Oxidase 1 (COX1) has been identified (Suvedha et al., 2024).

Precisely, the order of BAF was Cr < Zn < Pb < Cu < Ni < Cd for EE and Zn < Pb < Cr < Ni < Cu < Cd for EF. This process was facilitated by drilodefensins, which are surface-active metabolites secreted in the earthworm gut to help counter harmful oxidative substances like heavy metals and prevents proteins from damage, assisting in detoxifying metals (Gudeta et al., 2023). Further, MT production facilitates the deposition of metal cations in chloragogenous cells, promoting higher gut metal accumulation (Suvedha et al., 2024). The higher BAF observed in EE indicates that *E. eugeniae* is particularly efficient at metal bioremediation. This may be associated with genetic stability in *E. eugeniae*, which may be facilitated by DNA-methyltransferase activity and reflects a resilient epigenetic control system (Paul et al., 2022). Additionally, this species relies on an immune strategy centered on coelomocytes, whereby these specialized cells engulf metal particulates through phagocytosis (Höckner et al., 2020). This greater detoxification potential of *E. eugeniae* has been similarly observed for toxic metals in sediments and coal fly ash (Aladesida et al., 2024; Nath and Das, 2026).

Table 17. Gut metal accumulation and BAF in *E. fetida* and *E. eugeniae*

	EF			**EE**			**Two way-ANOVA**			
Heavy metals	**0D**	**90D**	**BAF**	**0D**	**90D**	**BAF**	**p-value (Tq)**	**p-value (Tm)**	**p-value (Tq*Tm)**	**LSD**
Cd (mg kg^{-1})	0.07 ± 0.02	1.01 ± 0.06	0.251 ± 0.015	0.09 ± 0.03	1.30 ± 0.06	0.372 ± 0.019	0.000	0.000	0.001	0.027
Cr (mg kg^{-1})	0.39 ± 0.03	2.75 ± 0.09	0.069 ± 0.002	0.40 ± 0.09	2.18 ± 0.09	0.056 ± 0.002	0.000	0.000	0.000	0.046
Cu (mg kg^{-1})	0.43 ± 0.06	10.15 ± 0.18	0.120 ± 0.002	0.43 ± 0.05	13.29 ± 0.11	0.151 ± 0.002	0.000	0.000	0.000	0.065

Pb (mg kg^{-1})	0.45 ± 0.06	3.20 ± 0.11	0.051 ± 0.002	0.43 ± 0.02	4.01 ± 0.14	0.066 ± 0.003	0.000	0.000	0.000	0.054
Ni (mg kg^{-1})	0.46 ± 0.05	6.96 ± 0.19	0.091 ± 0.002	0.59 ± 0.05	9.09 ± 0.12	0.144 ± 0.002	0.000	0.000	0.000	0.067
Zn (mg kg^{-1})	0.46 ± 0.05	5.25 ± 0.11	0.034 ± 0.001	0.49 ± 0.05	8.18 ± 0.18	0.065 ± 0.001	0.000	0.000	0.000	0.064

**EF - Vermicomposting with Eisenia fetida; EE - Vermicomposting with Eudrilus eugeniae; BAF - Bioaccumulation factor; Tq - Technique; Tm - Time; LSD - Least significant difference*

Thesis data published in the research paper: Nath, S., Das, S., 2026. Species-specific benefits in bioremediation of oil refinery sludge via large-scale vermicomposting process: a detailed comparison between *Eisenia fetida* and *Eudrilus eugeniae*. Chemosphere 394, 144782.

4.3.6. Benefit assessment of the two earthworm species

A higher VBI value was observed for EE (1.68) compared to EF (1.45) indicating better remediation potential of this species (Figure 16). This improved performance may stem from a stronger microbial ecosystem or efficient gut-microbe relationships, involving nitrogen-fixing *Azotobacter* and nutrient-mobilizing microbes like *Bacillus* and *Pseudomonas*, which solubilize phosphorus and potassium. Alternatively, optimal moisture, pH, and nutrient balance within the compost matrix of EE may have facilitated enhanced mineralization and stabilization processes (Nath and Das, 2026). Furthermore, optimal growth and reproduction rates are maintained by *E. eugeniae* indicating its ability to process substantial metal loads without major energetic trade-offs (Yadav et al., 2023). Higher levels of metallothionein which allows for the binding and removal of heavy metals have also been reported in *E. eugeniae* (Usmani et al., 2017). In contrast, EF's low VBI implies less aggressive remediation, a difference that can be attributed to variations in its microbial profile (Wonnapinij et al., 2022). Moreover, smaller size and biomass of *E. fetida* limit its ability to mix soil, reducing its effectiveness in dispersing nutrients and breaking down contaminants (Kharmawphlang et al., 2024).

The high BR in pH recorded in EE (0.088) suggests a faster rate of sludge decomposition, which is a process in which acidic micro-environments are usually formed as a by-product of microbial respiration (Das et al., 2016). Conversely, EF exhibited high BR in WHC (0.62) (Figure 16). High water-laden substrates have the ability to store moisture in their microporous structures and hence serve as reservoirs to provide water and nutrients to plants whenever the need arises (Bondì et al., 2022; Nath and Das, 2026). The increase of BR in TOC by 0.37-fold in EE suggests that EE has a better capacity to convert the lignin-rich material into the stable humus, which improves the structure and fertility of soil. EE also registered greater BRs in available N and P (Figure 15), which confirm its active nutrient mineralization potential (Pundee et al., 2023). These divergent capabilities prove that EE is an efficient fast-decomposing compost system and EF is more effective in moisture preservation and slow decomposition of the lignin-dense materials (Nath and Das, 2026).

The RE varied significantly with EE illustrating superior remediation potential (Figure 16). EE showed significantly higher RE for Cd (0.42), Cu (0.39), Zn (0.30), and Ni (0.24). This improvement in efficiency stems directly from EE's unique physiological adaptations. Its bigger body and slower digestion process extend the time that metals are exposed to digestive fluids. This allows for better formation of soluble metal complexes (Sabina et al., 2025). In contrast, both species demonstrated low RE for Cr and Pb, due to the strong affinity of these metals with organic materials, which reduces their availability for biological uptake (Mongchu et al., 2024). EE's superior RE also reflects a stronger excretory system. This includes a large coiled holonephridia beginning at segment 4, important for excreting excess metals and enhancing detoxification (Blakemore, 2015; Nath and Das, 2026).

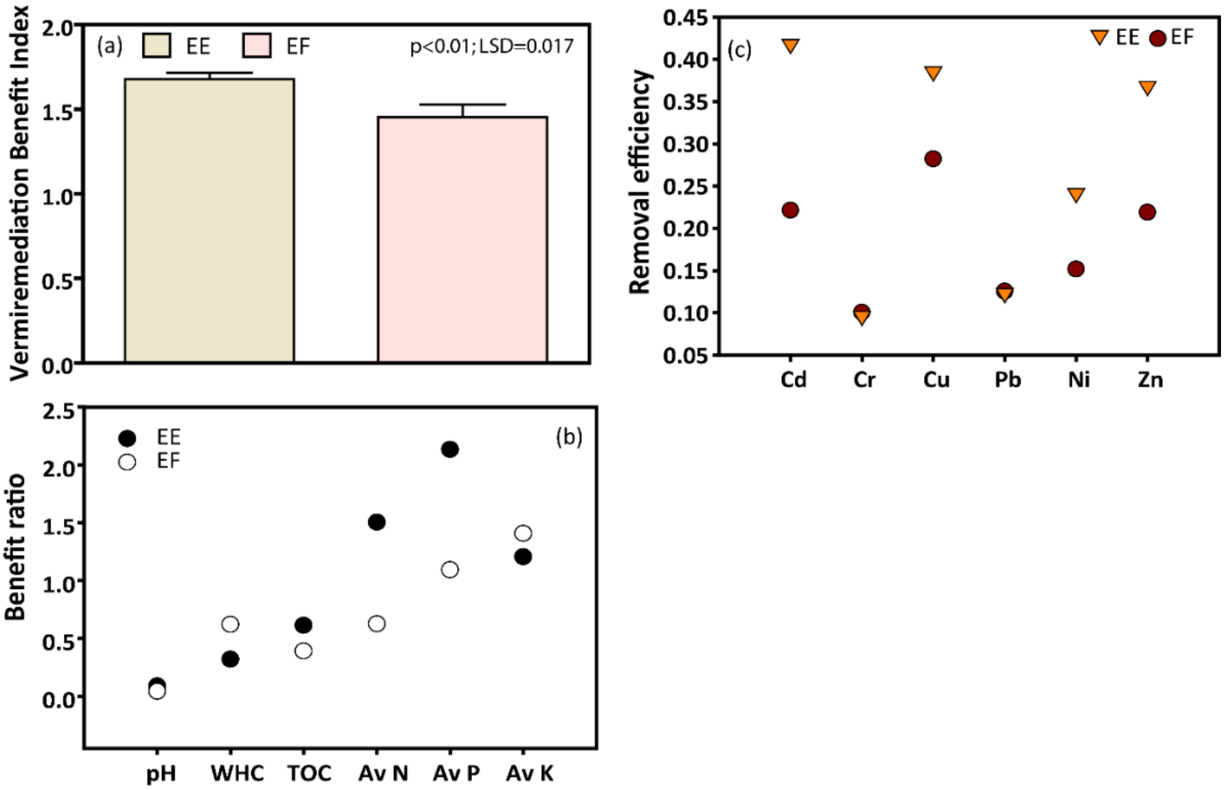

Figure 16. Benefit assessment of the two earthworm species (Thesis data published in the research paper: Nath, S., Das, S., 2026. Species-specific benefits in bioremediation of oil refinery sludge via large-scale vermicomposting process: a detailed comparison between *Eisenia fetida* and *Eudrilus eugeniae*. Chemosphere 394, 144782.)

4.3.7. Multivariate analyses through correlation and PCA

To identify key factors affecting VBI in *E. eugeniae* and *E. fetida*, a Pearson's correlation analysis was performed (Fig. 17a–b; Appendix 8). For *E. eugeniae*, VBI correlated strongly with nutrients (TOC, N, P, and K), reflecting high waste conversion efficiency driven by respiratory activity and gut-microbiome synergy (Mongchu et al., 2024). VBI was also linked to metal detoxification, particularly reduction of Cu and Zn and bioaccumulation of Cr, Cu, and Pb, facilitated by enzymatic responses and metal sequestration (Aladesida et al., 2024). Morphological and biological traits of earthworms (biomass, body length, and population) further correlated with VBI, underscoring EE's physiological robustness in waste bioconversion (Nath and Das, 2026). In contrast, *E. fetida* exhibited no significant correlation of VBI with nutrients, suggesting slower mineralization. Instead, VBI aligned closely with gut bioaccumulation of Cr, Cu, and Zn, indicating metabolic trade-offs between detoxification and nutrient cycling (Yadav et al., 2023). EF's VBI also positively correlated with water-holding capacity, highlighting its role in improving compost structure through burrowing and cast formation (Usta and Guven, 2024). Metal speciation analysis confirmed the metal detoxification differences of the two species (Figure 14). For instance, EE reduced bioavailable metal fractions more effectively, while EF's compost contained higher residual fractions. EE also showed 24% greater overall metal removal than EF. These findings suggest that species selection can be tailored to specific compost outcomes. For example, *E. eugeniae* favoured rapid stabilization and nutrient-rich compost suitable as fertilizer, whereas *E. fetida* enhanced porosity and moisture retention, making it an ideal soil conditioner (Nath and Das, 2026).

PCA was employed to reduce data dimensionality and visualize the principal factors influencing earthworm's vermiremediation efficiency (Fig. 17c-17d). Before analysis, Bartlett's sphericity test ($p < 0.001$) and the Kaiser-Meyer-Olkin's adequacy measure (8.08) confirmed the suitability of the data for PCA. Scree plots derived from *E. eugeniae* (EE) and *E. fetida* (EF) datasets indicated two varimax-rotated factors with eigenvalues exceeding 1 (Appendix 9). For *E. eugeniae*, Factor 1 integrated the most consistently correlated variables with the VBI, including total organic carbon, reductions in Cd, Cu, and Zn, and accumulations of Cr, Cu, Pb, and Ni, as well as earthworm counts, biomass, and body length. Factor 2 encompassed electrical conductivity, water-holding capacity, and available nitrogen, phosphorus, and potassium. The loadings plot accounted for 99.97% of the total variance, with component 1 and component 2 contributing 58.07% and 41.9%, respectively. In contrast, for *E. fetida*, Factor 1 combined water-holding capacity, total organic carbon, reductions in Cr, Cu, and Pb, accumulation of Cr and Cu, along with earthworm count and biomass. Factor 2 included electrical conductivity, available phosphorus and potassium, Zn reduction, and Cd and Pb accumulation. The loading plots explained 89.9% of the variance, with 54.2% in component 1 and 35.7% in component 2 (Fig. 17d). Collectively, PCA identified earthworm biomass and population density, metal accumulation, total organic carbon, and substrate moisture content as the most significant parameters associated with improved VBI in the two earthworm systems (Reimann et al., 2011; Nath and Das, 2026).

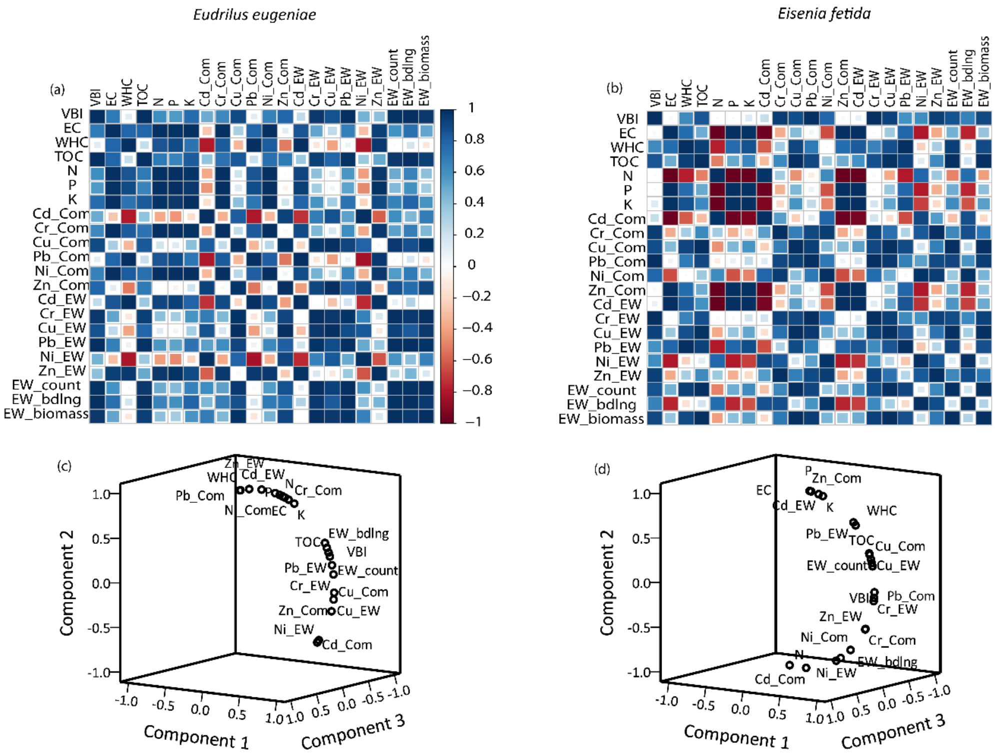

Figure 17. Influence of various ORS compost characteristics on the VBI of *E. eugeniae* and *E. fetida* through Pearson's correlation and PCA (Thesis data published in the research paper: Nath, S., Das, S., 2026. Species-specific benefits in bioremediation of oil refinery sludge via large-scale vermicomposting process: a detailed comparison between *Eisenia fetida* and *Eudrilus eugeniae*. Chemosphere 394, 144782.)

4.4. Phase IV - Field experiment

4.4.1. Physicochemical characteristics of soil during cultivation

The pH of soil (control) was slightly acidic in nature (6.76-6.78) (Table 18), which is in conformity with the agricultural soils of Assam (Gogoi et al., 2024). A substantial decrease in soil pH was observed from the initial to post-harvest stage across all treatments. The highest decrease in pH occurred in the EE_{100} treatment, with an 0.18-fold decrease (5.08) and a 0.16-

fold decrease (5.15) (p (treatment × time) < 0.001) during cabbage and tomato cultivation, respectively. The NPK_{100} treatment also showed significant acidification at the post-harvest stage. This decline in soil pH could be attributed to the release of H^+ ions due to the nitrification of ammonium-based fertilizers (Ayiti and Babalola, 2022), and an enhanced mineralization of organic materials in the ORS-vermicompost (Sánchez-Rosales et al., 2025). The findings coincide with the Tian et al. (2024) who revealed reduction of soil pH with the application of vermicompost. The corresponding EC increased across all treatments, suggesting an increment in the soluble mineral concentration during plant growth. The EC was highest in EE_{100} treatment with an increment of 0.38 to 0.61-fold during crop cultivation, followed by the EE_{50} and EF_{100} treatments. Application of higher concentration of vermicomposted ORS could have increased soil ionic strength in a similar level with chemical fertilizers due to the release of soluble ions (NO_3^-, PO_4^{3-}, Ca^{2+}, and Mg^{2+}). Similar findings of Toor et al. (2024) reported a 2-fold increment in soil EC by vermicompost during lettuce cultivation. In tomato cultivation, the WHC increased in all the treatments, with the highest WHC in EE_{50} (0.76-fold) and EF_{50} (0.73.-fold) treated soils. The corresponding BD was also much lower in the vermicompost treatments, with the most significant decrease observed in EF_{100} (0.55-0.62 g cm^{-3}) and EE_{100} (0.62-0.66 g cm^{-3}) (p (treatment × time) < 0.001). This improvement in water retention and pore volume in soils treated with vermicompost could be attributed to the enhanced input of organic matter through ORS vermicompost, since organic matter increases the binding properties of soil aggregates and thus facilitating a porous soil structure (Castellini et al., 2024). This is in agreement with Parihar et al. (2024) who showed improvements in the porosity of alluvial soils with vermicompost application.

The post-harvest TOC content in the vermi-treatments was significantly higher (8.02-9.85%) than in the control (~ 2.31%) and NPK_{100} (3.61-4.34%) (Table 18). This is because application of vermicompost significantly raises soil organic carbon by adding abundant organic matter, which in turn strengthens the long-term carbon storage within the soil. (Ganapathy et al., 2025). However, a decrease in TOC was observed across all the treatments post-cultivation, which could be attributed to an enhanced mineralization due to microbial respiration. Our findings are in agreement with the study of Goswami et al. (2017) which showed that application of vermicompost reduced soil organic C and increased humic acid C (10.59-12.97%) during tomato and cabbage cultivation. The TN substantially increased from the initial to post-harvest stage in all treatments, with the highest TN observed in the EE_{100} (0.65%) in tomato soil. This increment was 0.14-fold higher than NPK_{100} treatment. The increased microbial and enzymatic activity within vermicompost likely promotes the conversion of organic nitrogen into plant-accessible NH_4^+ and NO_3^- in the soil (Enebe and Erasmus, 2023b; Zhou et al., 2025). The concentrations of available P and K increased significantly post-harvest in the vermi-treatments in both the crop cultivation. The EE_{100} showed the highest available P content in cabbage soils (185.85 mg kg^{-1}), while the EF_{100} treatment showed the highest K in tomato soils (484.90 mg kg^{-1}). Vermicompost application significantly enhances the growth and diversity of P and K-solubilizing microbial communities, resulting in the release of various exogenous and endogenous enzymes in soil (Goswami et al., 2024). Guo et al. (2026) also showed that the root zone application of vermicompost increased P bioavailability in saline soils. Overall, vermicompost was more effective at enriching soil nutrients than the control group or commercial inorganic fertilizer (Table 18).

Table 18. Attributes of soil under inorganic fertilizer and ORS-vermicompost amendments during crop cultivation

Tomato cultivation	**Soil**	**pH**	**EC (mS cm^{-1})**	**WHC (%)**	**BD (g cm^{-3})**	**TOC (%)**	**TN (%)**	**Av. N (mg kg^{-1})**	**Av. P (mg kg^{-1})**	**Av. K (mg kg^{-1})**
Control	Initial	6.78 ± 0.05	303.05 ± 1.06	51.13 ± 1.70	1.02 ± 0.02	3.60 ± 0.26	0.21 ± 0.01	535.39 ± 3.14	31.26 ± 1.00	105.53 ± 1.67
	Post harvest	6.63 ± 0.04	446.34 ± 2.07	65.54 ± 3.54	0.90 ± 0.03	2.30 ± 0.35	0.33 ± 0.01	703.49 ± 1.62	72.55 ± 1.12	229.57 ± 4.31
NPK_{100}	Initial	6.25 ± 0.04	432.56 ± 2.76	53.47 ± 3.73	1.18 ± 0.06	5.55 ± 0.33	0.37 ± 0.01	885.21 ± 2.73	79.41 ± 1.76	183.72 ± 1.88
	Post harvest	5.35 ± 0.03	756.71 ± 2.14	68.26 ± 4.31	1.01 ± 0.02	3.61 ± 0.49	0.57 ± 0.02	1190.74 ± 7.32	137.36 ± 1.76	387.56 ± 5.80
EF_{25}	Initial	6.75 ± 0.04	446.06 ± 0.97	54.65 ± 3.58	1.06 ± 0.09	11.61 ± 0.84	0.31 ± 0.02	786.22 ± 3.55	62.46 ± 1.76	177.57 ± 3.20
	Post harvest	5.83 ± 0.02	727.78 ± 2.42	72.57 ± 2.24	0.66 ± 0.04	8.97 ± 0.18	0.45 ± 0.01	1096.36 ± 1.09	170.60 ± 0.60	305.02 ± 1.65
EF_{50}	Initial	6.64 ± 0.03	432.18 ± 1.94	57.14 ± 2.70	0.97 ± 0.03	12.72 ± 0.20	0.33 ± 0.01	724.41 ± 3.54	64.80 ± 1.53	154.28 ± 1.64
	Post harvest	5.40 ± 0.03	735.00 ± 3.78	73.64 ± 2.13	0.63 ± 0.09	8.85 ± 0.50	0.47 ± 0.02	1108.26 ± 4.29	166.85 ± 2.46	318.23 ± 3.64
EF_{100}	Initial	6.31 ± 0.02	444.82 ± 2.22	58.22 ± 1.58	0.88 ± 0.05	13.23 ± 0.15	0.29 ± 0.01	703.41 ± 1.05	65.83 ± 1.18	186.76 ± 3.13
	Post harvest	5.343 ± 0.05	745.67 ± 1.95	73.57 ± 3.46	0.55 ± 0.07	9.85 ± 0.27	0.54 ± 0.01	1125.47 ± 3.70	163.98 ± 3.00	484.90 ± 2.23

EE_{25}	Initial	6.46 ± 0.07	454.16 ± 4.15	52.35 ± 0.71	1.03 ± 0.03	12.21 ± 0.23	0.30 ± 0.01	892.36 ± 1.09	62.85 ± 0.60	186.15 ± 3.50
	Post harvest	5.75 ± 0.05	745.23 ± 4.05	69.78 ± 3.65	0.77 ± 0.07	8.55 ± 0.27	0.60 ± 0.01	1110.41 ± 2.73	164.75 ± 2.46	427.05 ± 3.28
EE_{50}	Initial	6.51 ± 0.04	453.44 ± 5.03	51.85 ± 3.84	0.96 ± 0.04	12.86 ± 0.25	0.34 ± 0.01	866.27 ± 1.62	64.80 ± 0.60	170.97 ± 1.88
	Post harvest	5.60 ± 0.05	851.78 ± 2.19	76.79 ± 3.85	0.62 ± 0.05	8.46 ± 0.25	0.50 ± 0.01	1093.87 ± 1.62	166.46 ± 5.27	444.09 ± 5.01
EE_{100}	Initial	6.12 ± 0.04	529.90 ± 1.73	55.05 ± 3.83	0.88 ± 0.04	13.76 ± 0.25	0.33 ± 0.02	745.34 ± 3.55	79.76 ± 1.05	184.24 ± 5.01
	Post harvest	5.15 ± 0.04	854.68 ± 3.22	74.89 ± 1.98	0.62 ± 0.07	8.76 ± 0.17	0.65 ± 0.02	1201.47 ± 2.57	173.45 ± 4.11	429.57 ± 1.67
Two-way ANOVA	**p value**	0.001	0.001	0.011	0.001	0.001	0.001	0.001	0.001	0.001
	LSD	0.026	1.634	1.792	0.031	0.205	0.007	1.860	1.317	1.944

Cabbage cultivation Soil		**pH**	**EC (mS cm^{-1})**	**WHC (%)**	**BD (g cm^{-3})**	**TOC (%)**	**TN (%)**	**Av. N (mg kg^{-1})**	**Av. P (mg kg^{-1})**	**Av. K (mg kg^{-1})**
Control	Initial	6.76 ± 0.04	349.64 ± 3.62	48.21 ± 4.27	1.05 ± 0.08	3.21 ± 0.17	0.19 ± 0.01	643.94 ± 2.17	35.16 ± 2.00	113.24 ± 2.23
	Post harvest	6.29 ± 0.03	447.82 ± 1.61	61.38 ± 4.27	0.84 ± 0.10	2.31 ± 0.18	0.39 ± 0.02	795.80 ± 3.55	65.31 ± 3.11	275.83 ± 4.70
NPK_{100}	Initial	6.27 ± 0.04	453.85 ± 3.80	49.99 ± 3.88	1.09 ± 0.05	5.25 ± 0.09	0.39 ± 0.01	876.84 ± 5.59	74.85 ± 0.60	117.20 ± 4.70
	Post harvest	5.60 ± 0.04	735.89 ± 3.90	64.58 ± 3.69	0.95 ± 0.04	4.34 ± 0.43	0.61 ± 0.01	1178.41 ± 4.29	139.80 ± 1.57	347.75 ± 2.23
EF_{25}	Initial	6.51 ± 0.05	411.59 ± 4.27	48.89 ± 3.84	0.97 ± 0.03	12.11 ± 0.26	0.30 ± 0.07	754.51 ± 1.09	64.41 ± 1.00	113.24 ± 2.23
	Post harvest	5.59 ± 0.03	645.11 ± 3.45	75.90 ± 3.20	0.71 ± 0.05	8.93 ± 0.25	0.50 ± 0.01	1183.21 ± 2.73	161.80 ± 0.60	336.46 ± 1.88
EF_{50}	Initial	6.29 ± 0.04	433.82 ± 3.61	52.13 ± 3.84	0.90 ± 0.05	12.91 ± 0.17	0.29 ± 0.01	727.56 ± 4.44	65.31 ± 1.00	125.58 ± 1.88
	Post harvest	5.23 ± 0.03	711.33 ± 4.30	73.95 ± 3.71	0.66 ± 0.06	9.47 ± 0.24	0.49 ± 0.07	1241.54 ± 2.39	155.52 ± 0.06	346.21 ± 2.23
EF_{100}	Initial	6.90 ± 0.02	450.49 ± 3.78	53.81 ± 4.72	0.92 ± 0.11	13.00 ± 0.28	0.35 ± 0.03	718.97 ± 1.62	72.89 ± 1.49	126.42 ± 7.15

	Post harvest	5.72 ± 0.06	754.01 ± 5.12	72.30 ± 4.18	0.64 ± 0.05	8.92 ± 0.23	0.58 ± 0.01	1264.77 ± 3.30	151.67 ± 0.67	373.51 ± 1.67
EE_{25}	Initial	6.77 ± 0.05	438.87 ± 4.04	57.66 ± 3.36	1.01 ± 0.02	13.15 ± 0.27	0.28 ± 0.01	703.47 ± 2.15	66.95 ± 2.46	180.32 ± 3.20
	Post harvest	5.23 ± 0.04	735.10 ± 3.21	79.02 ± 2.70	0.74 ± 0.05	8.62 ± 0.27	0.48 ± 0.07	1252.02 ± 5.71	174.80 ± 3.11	356.81 ± 2.66
EE_{50}	Initial	6.54 ± 0.04	452.16 ± 3.40	58.84 ± 3.76	0.96 ± 0.02	12.89 ± 0.21	0.29 ± 0.03	758.07 ± 1.62	72.21 ± 2.05	105.87 ± 3.50
	Post harvest	5.31 ± 0.03	722.15 ± 3.44	78.74 ± 4.01	0.67 ± 0.04	8.23 ± 0.21	0.43 ± 0.03	1332.89 ± 4.08	169.51 ± 5.24	386.32 ± 3.00
EE_{100}	Initial	6.23 ± 0.03	551.80 ± 3.65	61.34 ± 1.86	0.91 ± 0.02	13.55 ± 0.12	0.28 ± 0.02	733.74 ± 1.62	77.44 ± 1.95	186.15 ± 3.50
	Post harvest	5.08 ± 0.02	765.94 ± 0.72	77.93 ± 3.86	0.62 ± 0.04	8.02 ± 0.21	0.53 ± 0.01	1352.11 ± 3.05	185.85 ± 3.00	368.00 ± 2.12
Two-way ANOVA	**p value**	0.001	0.001	0.073	0.001	0.001	0.001	0.001	0.001	0.001
	LSD	0.024	2.098	2.168	0.032	0.136	0.019	1.952	1.304	1.937

4.4.2. Metal concentrations of soil and metal uptake in crops during cultivation

A significant decrease in the concentration of heavy metals was observed in the soils from the initial to the post-harvest stage across all treatments (Table 19). For Cd, the following trend was observed: EE_{50} > NPK_{100} > control > EE_{25} > EF_{100} > EE_{100} > EF_{50} > EF_{25} (in tomato) (p (treatment × time) < 0.001) and NPK_{100} > EE_{25} > EE_{50} = control > EF_{25} > EE_{100} > EF_{100} > EF_{50} (in cabbage) (p (treatment × time) < 0.001). The better performance of ORS-vermicompost treated soils in reducing Cd bioavailability could be associated with the inherent humic acid content in vermicompost, which forms stable complexes with metal ions (Nath et al., 2025). Moreover, the large surface area, high cation exchange capacity (CEC), and functional groups (carboxyl and hydroxyl) present in vermicompost contribute as in-situ sorbent for Cd ions (Iqbal et al., 2024). Vermicompost application has shown peak absorption rates of 170.65 mg/g for Cd^{2+} in soil (Zhu et al., 2017). Post-harvest, all the treatments showed Cd levels below 1.0 mg kg^{-1}, which was below the permissible threshold limits of EU (1.00-3.00 mg kg^{-1}). In Cr, the following trend was recorded: control > NPK_{100} > EE_{25} > EF_{25} > EF_{50} > EE_{50} > EF_{100} > EE_{100} (in tomato) (p (treatment × time) < 0.05) and control > NPK_{100} > EE_{25} > EF_{25} > EF_{100} > EF_{50} > EE_{50} > EE_{100} (in cabbage) (p (treatment × time) < 0.05). The increased bioavailability of Cr observed with the NPK_{100} treatment likely resulted from the associated rise in soil acidity. Under acidic conditions, Cr (VI) exhibits greater solubility and reduced tendency to adsorb to soil particles (Khedr et al., 2023). Pb levels in EF_{100} and EE_{100} were the lowest, which may indicate an increase in Pb immobilization in the soil induced by vermicompost. Vermicompost triggers the catalytic activity of enzymes like acid phosphatase and alkaline phosphatase in the soil that precipitates the soluble Pb species into stable Pb-phosphate species (Liu et al., 2025). Ni concentrations were also lowest in EE_{100} (tomato soil = 28.78 mg kg^{-1}; cabbage soil = 28.99 mg kg^{-1}) and EF_{25} (tomato soil = 31.24 mg kg^{-1}; cabbage soil = 31.46 mg kg^{-1}), indicating a dose-dependent reduction effect. Ni may have reduced to less bioavailable Ni-sulfide precipitates in soil through the reductive processes mediated by sulfate-reducing bacteria (SRBs) present in vermicompost (Owagboriaye et al., 2021). In soils treated with EF and EE, the observed decrease in metal bioavailability may be linked to the diverse microbial community within ORS-vermicompost. This community facilitates heavy metal immobilization through three key mechanisms: altering metal solubility via redox changes, forming stable compounds through bio-precipitation, and binding or accumulating metals on cell walls or internally (Hu and Chen, 2023).

The lowest metal uptake by the crops was observed in the treatments that had the lowest metal concentrations in soil, especially in EF_{100} and EE_{100}. The Cd uptake was lowest in EE_{100} for both tomato (0.00833 mg kg^{-1}) and cabbage (0.00967 mg kg^{-1}), which was significantly below the FAO/WHO safe limits of 0.3 mg kg^{-1} (Table 3). Cr concentration was also lowest in tomato (0.21167 mg kg^{-1}) and cabbage leaves (0.26667 mg kg^{-1}) in EE_{100} treatment (Table 19). Similar trends were observed in the uptake of Cu and Pb in both the crops: Cu = $NPK_{100} > EE_{25} > EF_{25} >$ control $> EE_{50} > EF_{100} > EF_{50} > EE_{100}$ (p (treatment) < 0.001) and Pb = $EE_{25} > EE_{50} > NPK_{100} > EE_{100} > EF_{25} >$ Control $> EF_{50} > EF_{100}$ (p (treatment) $<$ 0.001). This phenomenon may be attributed to the greater biomass resulting from plant invigoration by vermicompost, which causes a dilution of metal content within the plant tissues (Blouin et al., 2019). For instance, 10-20% vermicompost amendment rate in soils reduced Pb concentration in plant leaves and roots by 0.65-fold (Landorfa-Svalbe et al., 2022). The EE_{100} treatment minimized nickel uptake in tomato and cabbage leaves more effectively than the other treatments, and EF_{100} showed the lowest levels of Zn. The activity of free metal ions in the soil was reduced as a result of enhanced metal complexation and adsorption promoted by vermicompost. (Nath and Das, 2026), thus their availability to plant roots. In addition, vermicompost boosts the innate defence mechanism of the plants as it activates antioxidant enzymes like SOD, POD, and CAT. Such physiological hardiness helps the plants to endure metal stress and can affect roots exudates, which eventually decrease the metal uptake (Iqbal et al., 2024). The higher metal uptake observed in cabbage leaves relative to tomato leaves (Table 19) stems from physiological differences in their root systems. Cabbages possess a fibrous root architecture that promotes hyperaccumulation by effectively moving metals from the soil into the foliar biomass (Zhang et al., 2016; Mi et al., 2019).

Table 19. Metal concentrations of soil under different treatments and metal uptake in crops

Tomato cultivation	**Sample**	**Cd (mg kg^{-1})**	**Cr (mg kg^{-1})**	**Cu (mg kg^{-1})**	**Pb (mg kg^{-1})**	**Ni (mg kg^{-1})**	**Zn (mg kg^{-1})**
Control	Initial (in soil)	0.97 ± 0.02	23.63 ± 0.56	43.67 ± 0.49	33.00 ± 0.97	38.67 ± 0.60	78.59 ± 0.66
	Post harvest (in soil)	0.47 ± 0.02	20.47 ± 0.02	40.80 ± 0.59	29.80 ± 0.60	33.77 ± 1.97	67.58 ± 1.09
	Crop (leaves)	0.01033 ± 0.00015	0.23427 ± 0.00256	0.12550 ± 0.00502	0.80983 ± 0.00099	0.14187 ± 0.00254	1.46363 ± 0.00651
NPK_{100}	Initial (in soil)	1.04 ± 0.03	20.39 ± 0.59	47.05 ± 0.99	34.05 ± 1.72	39.72 ± 1.52	80.30 ± 1.72
	Post harvest (in soil)	0.55 ± 0.03	18.21 ± 0.58	42.55 ± 2.62	30.85 ± 1.52	33.82 ± 1.73	69.96 ± 2.07
	Crop (leaves)	0.00960 ± 0.00010	0.24627 ± 0.00577	0.13627 ± 0.00586	0.81627 ± 0.00577	0.15627 ± 0.00569	1.40960 ± 0.09995
EF_{25}	Initial (in soil)	1.14 ± 0.03	21.48 ± 0.55	44.14 ± 4.36	31.81 ± 0.55	36.48 ± 1.54	75.39 ± 3.63
	Post harvest (in soil)	0.18 ± 0.03	17.51 ± 0.58	40.51 ± 0.58	28.61 ± 0.58	31.24 ± 1.54	65.39 ± 2.54
	Crop (leaves)	0.00920 ± 0.00010	0.22587 ± 0.00577	0.12920 ± 0.00010	0.80587 ± 0.00586	0.14253 ± 0.00586	1.34253 ± 0.05782
EF_{50}	Initial (in soil)	1.12 ± 0.02	20.11 ± 0.01	43.78 ± 1.16	32.78 ± 0.57	38.45 ± 1.15	78.36 ± 1.00
	Post harvest (in soil)	0.22 ± 0.02	16.88 ± 0.56	39.22 ± 1.02	29.58 ± 1.15	32.88 ± 1.73	66.69 ± 2.64
	Crop (leaves)	0.00877 ± 0.00012	0.22210 ± 0.00572	0.12210 ± 0.00589	0.78543 ± 0.00583	0.13210 ± 0.00572	1.17543 ± 0.05779
EF_{100}	Initial (in soil)	1.56 ± 0.11	19.51 ± 0.06	42.85 ± 0.59	30.85 ± 0.52	37.18 ± 0.54	77.10 ± 0.59
	Post harvest (in soil)	0.33 ± 0.04	16.66 ± 0.61	36.66 ± 0.61	27.64 ± 0.96	31.28 ± 0.96	65.42 ± 1.14
	Crop (leaves)	0.00857 ± 0.00012	0.21557 ± 0.00613	0.12190 ± 0.00589	0.77523 ± 0.00583	0.12523 ± 0.00583	1.07523 ± 0.05779
EE_{25}	Initial (in soil)	1.42 ± 0.03	20.74 ± 0.57	45.07 ± 1.55	32.41 ± 1.70	38.07 ± 1.12	77.66 ± 0.04

	Post harvest (in soil)	0.42 ± 0.04	18.08 ± 0.60	39.08 ± 0.59	29.20 ± 1.12	31.51 ± 1.19	65.98 ± 1.76
	Crop (leaves)	0.00950 ± 0.00010	0.24250 ± 0.00617	0.13617 ± 0.00586	0.83283 ± 0.00569	0.14283 ± 0.00569	1.22377 ± 0.01597
EE_{50}	Initial (in soil)	1.25 ± 0.06	21.57 ± 0.55	44.90 ± 0.61	31.90 ± 2.04	36.24 ± 0.95	76.49 ± 0.95
	Post harvest (in soil)	0.72 ± 0.63	17.06 ± 0.53	37.06 ± 0.53	28.70 ± 1.48	31.34 ± 1.09	65.15 ± 1.52
	Crop (leaves)	0.00853 ± 0.00015	0.23187 ± 0.00566	0.12520 ± 0.00589	0.82520 ± 0.00563	0.12520 ± 0.00580	1.14187 ± 0.05788
EE_{100}	Initial (in soil)	1.35 ± 0.02	18.34 ± 0.05	44.01 ± 1.20	31.68 ± 1.11	34.68 ± 3.21	73.93 ± 1.51
	Post harvest (in soil)	0.25 ± 0.04	15.59 ± 0.58	35.59 ± 0.58	28.47 ± 0.98	28.78 ± 3.79	62.25 ± 0.54
	Crop (leaves)	0.00833 ± 0.00015	0.21167 ± 0.00592	0.11500 ± 0.00563	0.80500 ± 0.00563	0.10900 ± 0.00130	1.07578 ± 0.05854

Cabbage cultivation Sample		**Cd (mg kg^{-1})**	**Cr (mg kg^{-1})**	**Cu (mg kg^{-1})**	**Pb (mg kg^{-1})**	**Ni (mg kg^{-1})**	**Zn (mg kg^{-1})**
Control	Initial (in soil)	0.86 ± 0.04	22.19 ± 0.60	41.34 ± 0.57	32.48 ± 0.97	37.12 ± 0.66	75.52 ± 0.60
	Post harvest (in soil)	0.27 ± 0.02	19.60 ± 0.59	38.14 ± 1.52	27.93 ± 0.60	32.32 ± 1.09	65.40 ± 0.09
	Crop (leaves)	0.01517 ± 0.00006	0.28927 ± 0.00256	0.19440 ± 0.00502	0.91003 ± 0.00099	0.19457 ± 0.00254	1.81963 ± 0.00651
NPK100	Initial (in soil)	1.12 ± 0.03	20.79 ± 0.55	41.72 ± 1.15	33.53 ± 1.72	38.17 ± 1.14	77.24 ± 2.07
	Post harvest (in soil)	0.44 ± 0.04	19.44 ± 0.04	39.88 ± 0.55	29.65 ± 2.07	33.70 ± 1.14	66.79 ± 1.52
	Crop (leaves)	0.01257 ± 0.00015	0.30127 ± 0.00577	0.20517 ± 0.00586	0.91647 ± 0.00577	0.20897 ± 0.00569	1.76560 ± 0.09995
EF25	Initial (in soil)	1.14 ± 0.04	21.14 ± 0.04	43.48 ± 0.60	31.29 ± 0.55	35.59 ± 1.16	70.99 ± 3.62
	Post harvest (in soil)	0.16 ± 0.03	18.49 ± 0.60	37.51 ± 0.60	26.74 ± 0.55	31.46 ± 0.99	61.54 ± 2.68
	Crop (leaves)	0.01057 ± 0.00012	0.28087 ± 0.00577	0.19810 ± 0.00010	0.90607 ± 0.00586	0.19523 ± 0.00586	1.69853 ± 0.05782
EF50	Initial (in soil)	1.08 ± 0.03	20.74 ± 0.60	44.11 ± 0.99	32.26 ± 0.57	37.56 ± 0.57	73.30 ± 2.07
	Post harvest (in soil)	0.13 ± 0.04	17.46 ± 0.55	36.88 ± 0.59	27.37 ± 1.73	32.43 ± 1.73	64.85 ± 2.08
	Crop (leaves)	0.01023 ± 0.00015	0.27710 ± 0.00572	0.19100 ± 0.00589	0.88563 ± 0.00583	0.18480 ± 0.00572	1.53143 ± 0.05779
EF100	Initial (in soil)	1.44 ± 0.04	20.77 ± 0.54	43.51 ± 1.79	30.33 ± 0.52	35.63 ± 0.52	73.03 ± 0.57

	Post harvest (in soil)	0.20 ± 0.06	17.54 ± 0.62	36.00 ± 1.19	25.77 ± 0.95	31.50 ± 0.54	63.58 ± 1.50
	Crop (leaves)	0.00983 ± 0.00015	0.27057 ± 0.00613	0.19080 ± 0.00589	0.87543 ± 0.00583	0.17793 ± 0.00583	1.43123 ± 0.05779
EE25	Initial (in soil)	1.40 ± 0.02	21.06 ± 0.59	42.41 ± 1.70	31.89 ± 1.70	36.19 ± 1.96	73.92 ± 0.61
	Post harvest (in soil)	0.36 ± 0.03	19.02 ± 0.56	36.08 ± 1.13	27.00 ± 0.55	31.39 ± 1.49	64.14 ± 1.12
	Crop (leaves)	0.01087 ± 0.00015	0.29750 ± 0.00617	0.20507 ± 0.00586	0.93303 ± 0.00569	0.19553 ± 0.00569	1.57977 ± 0.01597
EE50	Initial (in soil)	1.22 ± 0.02	19.55 ± 0.57	42.57 ± 0.55	31.38 ± 2.04	34.68 ± 1.12	72.75 ± 1.12
	Post harvest (in soil)	0.27 ± 0.07	16.60 ± 0.55	35.06 ± 0.53	25.83 ± 0.55	29.89 ± 1.52	63.30 ± 1.12
	Crop (leaves)	0.01020 ± 0.00026	0.28687 ± 0.00566	0.19410 ± 0.00589	0.92540 ± 0.00563	0.17790 ± 0.00580	1.49787 ± 0.05788
EE100	Initial (in soil)	1.24 ± 0.03	19.57 ± 0.60	41.01 ± 1.20	31.16 ± 1.11	33.79 ± 3.04	70.98 ± 1.54
	Post harvest (in soil)	0.15 ± 0.05	15.48 ± 0.62	34.59 ± 1.16	25.94 ± 1.54	28.99 ± 3.21	60.74 ± 1.73
	Crop (leaves)	0.00967 ± 0.00025	0.26667 ± 0.00592	0.18390 ± 0.00563	0.90520 ± 0.00563	0.16170 ± 0.00130	1.43178 ± 0.05854
Permissible limits							
Agricultural soil	EU 86/278/EEC	1.00-3.00	_	50-140	50-300	30-75	150-300
Crop	FAO/WHO (JECFA)	0.30	0.10	_	1.00	0.10	2.00

4.4.3. Health assessment of soil under different treatments

The soil health under the various amendments was determined by two quality indices: i) Soil Quality Index (SQI) and ii) Degradation Index (DI) (Figure 18). Control (0.46) and NPK_{100} soils (0.48) had the lowest SQI in comparison to the vermicompost-treated soils. This shows that chemical fertilizers do not lead to system-wide changes that are required to enhance the quality of the soil. The physicochemical attributes corroborated that the NPK_{100} treatment increased the acidification of soil along with lower soil organic carbon and moisture retention (Table 18). The application of inorganic fertilizers has been reported to degrade soil structure, decrease the soil's ability to retain nutrients, and lower the energy sources for microorganisms (Xing et al., 2025). In a cacao agroforestry study conducted over a long period, it was found that the SOC stocks (42.8 to 49.6 Mg C ha^{-1}) of soils under chemical fertilization were considerably lower than those of organically managed (60.2-69.8 Mg C ha^{-1}) (Eduah et al., 2025). ORS-vermicompost application also had relatively better effects on the physical properties of soils, wherein WHC increased up to 0.79-fold and BD reduced down to 0.55 g cm^{-3}. The TOC were also maintained at higher levels (8.02-9.85%). These enhancements in the organic matter content, soil structure, and water retention were the main drivers of the 0.30 to 0.50-fold higher SQI values (0.60-0.69). Also, EE_{100} was more effective in comparison to EF_{100} among the vermicompost-treated soils. This could be attributed to the differences in active microbial community between the two ORS-vermicompost (Wonnapinij et al., 2022). The reduction in the heavy metal content also showed that the use of vermicompost leads to an overall better soil quality (Goswami et al., 2017).

The NPK_{100} had the highest DI (0.81), as it rapidly increased the soil fertility through higher inputs of available NPK. The high DI in NPK_{100} also suggests a degradative trend induced by acidification and an imbalanced rate of nutrients, leading to unhealthy short-term productivity. This is consistent with studies which suggest that traditional chemical fertilization induce considerable negative effects on the soil health compared to less intensively managed soils (Zahedifar, 2023). Conversely, EF and EE-based ORS compost led to a moderate DI (0.38-0.61). The EF_{100} and EE_{100} treatments had significantly lower DI compared to NPK_{100}, indicating multifunctional soil restoration. A seven-year investigation in drought and salinized areas in Bangladesh revealed that the use of vermicompost decreased the salinity level of the soil and enhanced the nutrient status of the coastal region (Hossain et al., 2025). A similar study showed that the use of vermicompost enhanced the aggregate stability, improved the organic carbon (84.8%), and minimized the level of erosion (55.4%) in semi-arid parts of Iran (Safadoust et al., 2025). Vermicompost amended soils, therefore, can induce better improvements in soil degradation through balanced physical, chemical, and biological changes that provides a more viable route of long-term management relative to NPK_{100}.

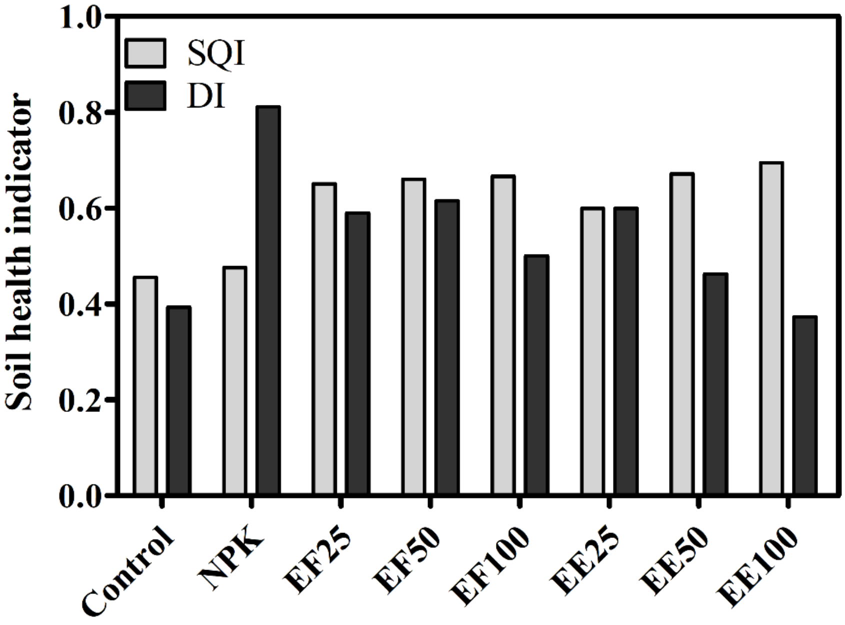

Figure 18. Assessment of soil health under the different amendments

4.4.4. Morphological characteristics of crops – tomato and cabbage

The implementation of various amendments showed positive impacts on the growth, morphology and post-harvest quality of tomato and cabbage (Table 20). All treatments (p (treatment) < 0.001) had a significant influence on the head diameter and the weight of both crops, with all fertilized plots performing better than the control. Among tomato plants, the EE_{25} treatment produced the largest head diameter (9.87 cm). The NPK_{100} treatment (9.29 cm) yielded results similar to those of the other organic vermicompost applications. For cabbage, the largest head diameters were measured in the EF_{100} (17.95 cm) and EE_{100} (17.59 cm) treatments, both exceeding the diameter achieved with NPK_{100} (17.25 cm). Vermicompost delivers a balanced spectrum of macronutrients and essential micronutrients, which supports steady plant development and the formation of larger produce (Yang et al., 2015). Wu et al. (2023) further showed that vermicompost could alleviate soil salinity stress and enhance carbohydrate translocation within tomato plants. Tomato biomass followed the order: EE_{100} > EF_{100} > EF_{50} > EE_{50} > EF_{25} = EE_{25} > NPK_{100} > control. Likewise, cabbage weight was highest under the EE_{100} (760.33 g) and EF_{100} (750.33 g) treatments, compared to NPK_{100} (713.00 g). This increase in biomass may be attributed to plant growth-stimulating hormones like auxin and cytokinin present in vermicompost, which function as natural biostimulants (Rehman et al., 2023). Additionally, a consistent supply of nutrients enhances cell expansion and photosynthetic activity, leading to the development of larger fruits (Belay et al., 2025). The humic substances in vermicompost also improve rhizospheric health, sustaining plant growth throughout the season. These findings align with Wang et al. (2017) who observed a 0.74-fold increase in tomato yield with vermicompost application.

Analysis of crop dimensions revealed that length and width were not significantly influenced by fertilizer type (p (treatment × crop) > 0.05). For tomatoes, the highest length occurred with EF_{100} and EE_{100} treatments, whereas for cabbages, EE_{50} and EE_{100} treatments produced the longest crops. Cabbage width displayed the following order in treatments: EE_{100} > EE_{25} > EE_{50} > EF_{25} > EF_{100} > EF_{50} > NPK_{100} > control (Table 20). These findings imply that while organic vermicompost enhances overall plant vigor and biomass, specific dimensional traits such as length and width may be more strongly determined by genetic and cultivar-specific factors (Zannat et al., 2023). Moreover, vermicompost application positively influenced post-harvest longevity (shelf-life). Tomato shelf-life extended from 10 days in control plots to a maximum of 13 days under EE_{100}, while cabbage shelf-life increased from 19 days to 24 days under the same treatment. This enhancement is likely due to an improved mineral nutrition of Ca and P, which strengthened cell wall structure. Also, reduced uptake of senescence-accelerating heavy metals and increased production of antioxidant compounds in plants could have facilitated the process. Altogether, these effects delayed physiological breakdown and microbial decay in crops (Al Jaouni et al., 2019; Iqbal et al., 2024)

Table 20. Morphometric characteristics of tomato and cabbage under different amendment

Tomato	**Treatments**	**Head Diameter (cm)**	**Length (cm)**	**Width (cm)**	**Weight (g)**	**Shelf life (days)**
	Control	8.18 ± 0.08	4.67 ± 0.46	4.16 ± 0.06	113.00 ± 3.61	10 ± 1
	NPK_{100}	9.29 ± 0.09	5.45 ± 0.41	5.63 ± 2.39	129.67 ± 5.03	11 ± 1
	EF_{25}	8.77 ± 0.10	4.77 ± 0.06	4.74 ± 0.12	138.67 ± 7.37	11 ± 1
	EF_{50}	9.60 ± 0.33	5.57 ± 0.30	4.53 ± 0.32	144.00 ± 4.36	12 ± 1
	EF_{100}	9.33 ± 0.30	6.59 ± 2.08	4.33 ± 0.30	154.33 ± 4.51	12 ± 1
	EE_{25}	9.87 ± 0.12	5.10 ± 0.55	4.15 ± 0.44	138.67 ± 7.09	12 ± 1
	EE_{50}	9.29 ± 0.28	5.58 ± 0.31	4.47 ± 0.24	142.67 ± 7.77	12 ± 1
	EE_{100}	9.23 ± 0.23	6.21 ± 0.25	4.22 ± 0.29	160.33 ± 4.51	13 ± 1
Two-way	**p value**	0.001	0.11	0.51	0.001	0.001
ANOVA	**LSD**	0.17494	0.66304	0.72135	4.68152	0.4714
Cabbage	**Treatments**	**Head Diameter (cm)**	**Length (cm)**	**Width (cm)**	**Weight (g)**	**Shelf life (days)**
	Control	14.90 ± 0.72	12.25 ± 0.18	11.30 ± 0.22	614.33 ± 2.52	19 ± 1
	NPK_{100}	17.25 ± 0.25	12.65 ± 0.56	11.32 ± 0.20	713.00 ± 7.21	21 ± 1
	EF_{25}	16.46 ± 0.36	12.58 ± 0.49	11.78 ± 0.48	699.33 ± 3.06	22 ± 1
	EF_{50}	17.42 ± 0.37	13.56 ± 0.27	11.46 ± 0.35	735.33 ± 5.51	23 ± 1

	EF_{100}	17.95 ± 0.07	13.59 ± 0.45	12.27 ± 0.09	750.33 ± 12.66	23 ± 1
	EE_{25}	15.99 ± 0.37	14.26 ± 0.07	13.42 ± 0.31	729.67 ± 4.16	23 ± 2
	EE_{50}	17.35 ± 0.10	14.37 ± 0.12	13.18 ± 0.55	744.67 ± 4.51	23 ± 1
	EE_{100}	17.59 ± 0.31	14.33 ± 0.21	17.59 ± 0.31	760.33 ± 6.81	24 ± 1
Two-way	**p value**	0.001	0.11	0.51	0.001	0.001
ANOVA	**LSD**	0.30205	0.27769	0.27927	5.34114	0.78174

4.4.5. Phytochemical composition of crops – tomato and cabbage

The use of fertilizers had a considerable positive effect on the photosynthetic pigments of the two crops (Figure 17). In tomato, chlorophyll-A increased substantially in EF_{100} (6.93 mg g^{-1}) and EE_{100} (5.51 mg g^{-1}), which was 1.5 to 2.2-fold higher than control (2.13 mg g^{-1}) (Figure 19a; Appendix 10). In cabbage, chlorophyll-A was highest in EE_{100} (1.33 mg g^{-1}), showing a 45% increase over control (0.92 mg g^{-1}) (p (treatment × crop) < 0.001; LSD = 0.084) (Figure 19a). In terms of chlorophyll-B, the following trends were observed in tomato: $EE_{50} > EE_{100} > EF_{50} > EE_{25} > EF_{10} > EF_{25} > NPK_{100}$ > control and in cabbage: $EF_{100} > EF_{50} = EF_{25} > EE_{100} > NPK_{100} > EE_{50} > EE_{25}$ > control (p (treatment × crop) < 0.001; LSD = 0.016) (Figure 19b). The total chlorophyll content also exhibited a similar trend with tomato and cabbage recording the highest values under EF_{100} (8.75 mg g^{-1}) and EE_{100} (1.69 mg g^{-1}), respectively (p (treatment × crop) < 0.001; LSD = 0.082) (Figure 19c). Soils treated with vermicompost have been reported to perform better than NPK_{100} in the enhancement of photosynthetic pigments, particularly in tomato leaves. For instance, the net photosynthetic rate (Pn), PSII photochemical efficiency (Fv/Fm), and light energy absorption/trapping were enhanced with vermicompost application (Liu et al., 2022). Another study has also established that vermicompost treatments led to the better consonance of chlorophyll in tomato leaves relative to the control and chemically cultivated plants (Nithya et al., 2024). Similarly, carotenoid content in tomato increased from 1.74 mg g^{-1} (in control) to 2.43 mg g^{-1} (in EF_{100}) and 2.44 mg g^{-1} (in EE_{100}) (Figure 19d). The presence of beneficial microorganisms in the soil rhizosphere such as *Enterobacteriaceae*, *Pseudomonadaceae* and *Flavobacteriaceae* also contribute to the activation of plant growth hormones, which improves the production of plant pigments (Jiang et al., 2023).

The concentrations of antioxidant compounds exhibited significant increases under vermicompost-treated soils, indicating an enhancement in the nutritional and functional quality of the produce. β-carotene, a vital provitamin A compound, increased in both the crops, with cabbage showing an increase from 0.015 mg g^{-1} (control) to 0.022 mg g^{-1} under EE_{100} (Figure 19e; Appendix 10). The total flavonoid content in tomato increased from 12.51 mg g^{-1} (in control) to 15.40 mg g^{-1} under EF_{50} and 15.42 mg g^{-1} under EE_{50}. In cabbage, total flavonoid showed a clear dose-dependent increase, with EE_{100} recording a 23% increase than control (p (treatment × crop) < 0.001; LSD = 0.463) (Figure 19f; Appendix 10). The total phenolic content in tomato also increased 20% under EE_{50} compared to the control. We observed the following trend in the phenolic content of cabbage: EE_{100} > EF_{100} > EE_{50} > EF_{50} > NPK_{100} > control > EF_{25} > EE_{25} (p (treatment × crop) < 0.001; LSD = 0.155) (Figure 17g). The total lycopene content also increased from 1.06 mg g^{-1} in the control to 1.35 mg g^{-1} under both EF_{100} and EE_{100}, outperforming the recommended NPK_{100} (1.08 mg g^{-1}) (Figure 19h; Appendix 10). The increase in these secondary metabolites is a plant response to the mild stress often associated with organic growing conditions, as well as the improved availability of micronutrients and precursors from vermicompost that serve as cofactors in phenolic, flavonoid, and lycopene pathways (Teshome et al., 2025).

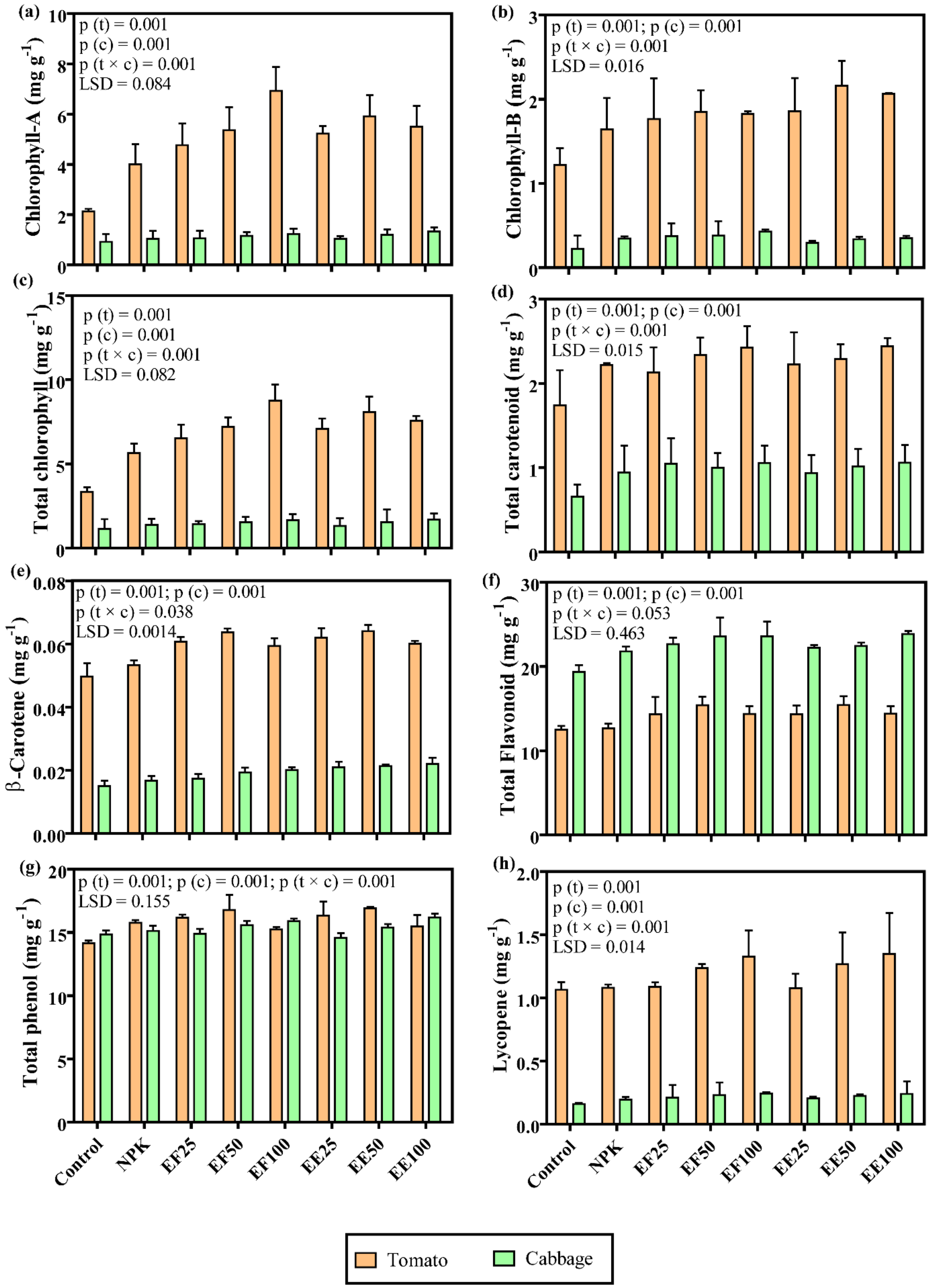

Figure 19. Phytochemical composition in tomato and cabbage under different treatments

4.4.6. Multivariate analyses and structured equation modelling

Principal component analysis was conducted to minimize the multidimensionality of the dataset and determine the most significant variables that influence the SQI and DI of the soils under the different amendments (Figure 20). The PCA adequacy was validated as Kaiser-Meyer-Olkin sampling-adequacy statistic (KMO = 0.792) and Bartlett test of sphericity ($p = 0.000$) were acceptable. The three principal components (PC1, PC2, PC3) obtained by the analysis explained 82.01% of the total variance. The PC1 explained 38.91% variance and loaded SQI and DI with physicochemical parameters such as pH, EC, WHC, TOC, N, P and K. The PC 2 was able to predict 33.74% of the variance and included BD alongside heavy metals (Cd, Cr, Cu, Pb, Ni, and Zn). The PC 3 was able to explain 9.35% of the variance, and most of it loaded plant phytochemical constituents. These outcomes prove that primary soil chemical properties, macronutrients, and heavy metals (PC1 and PC2) are the most influential parameters associated with the overall soil health (Kahsay et al., 2025). The relatively lower variance explained by the PC3 shows that plant photosynthetic and antioxidant compounds are weak drivers of soil quality and are instead outcomes of the existing soil environment induced by the amendments. Our results align with the findings of Ogundola et al. (2022).

Pearson's correlation analysis was employed to identify the important parameters associated with the SQI of the soils under the different fertilizer regimes (inorganic fertilizer and ORS vermicompost) (Figure 20). The SQI showed high positive correlation with its aggregate nutrients, such as TOC ($r = 0.820$, $p < 0.001$), available N ($r = 0.700$, $p < 0.001$), P ($r = 0.760$, $p < 0.001$), and K ($r = 0.409$, $p < 0.05$). In addition, the SQI was found to be significantly correlated with WHC ($r = 0.724$, $p < 0.001$) and EC ($r = 0.509$, $p < 0.001$). The addition of vermicompost in soils has been reported to significantly increase organic matter, soil aggregation, and microbial activities, thereby enhancing the retention of nutrients (Pan et al., 2025). Conversely, SQI showed strong negative association with pH ($r = -0.632$, $p < 0.001$) and BD ($r = -0.757$, $p < 0.001$), and metal concentrations of Cr ($r = -0.758$), Pb ($r = -0.651$), Cu ($r = -0.635$), Zn ($r = -0.620$), Ni ($r = -0.570$), and Cd ($r = -0.409$) (all $p < 0.001$). The negative relationship of SQI with BD could be attributed to the soil-loosening effect of vermicompost that reduces compaction in soils (N. Li et al., 2025). Furthermore, the mineralization of organic matter led to the production of organic acids in ORS-vermicompost treated soils, resulting in lower pH. In addition, heavy metals have also shown to reduce the activity of vital enzymes in soils, including β-glucosidase and urease, and affect the microbearthropod communities, thus deteriorating the biological integrity of soils. Interestingly, the SQI had weak and non-significant correlation with the DI and most of the plant phytochemical attributes (all $p > 0.05$), except for total phenol ($r = 0.416$, $p < 0.05$) and total flavonoid ($r = 0.375$, $p < 0.05$). The weak correlation between SQI and the plant phytochemical composition indicates that although organic amendments improve soil ecology that enhances plant growth attributes (yield and biomass) as evident (Table 4), the changes in the phytochemical content in crops may be mediated by other factors such as genetic variation and cultivar type (Cuiyun et al., 2023; Zannat et al., 2023).

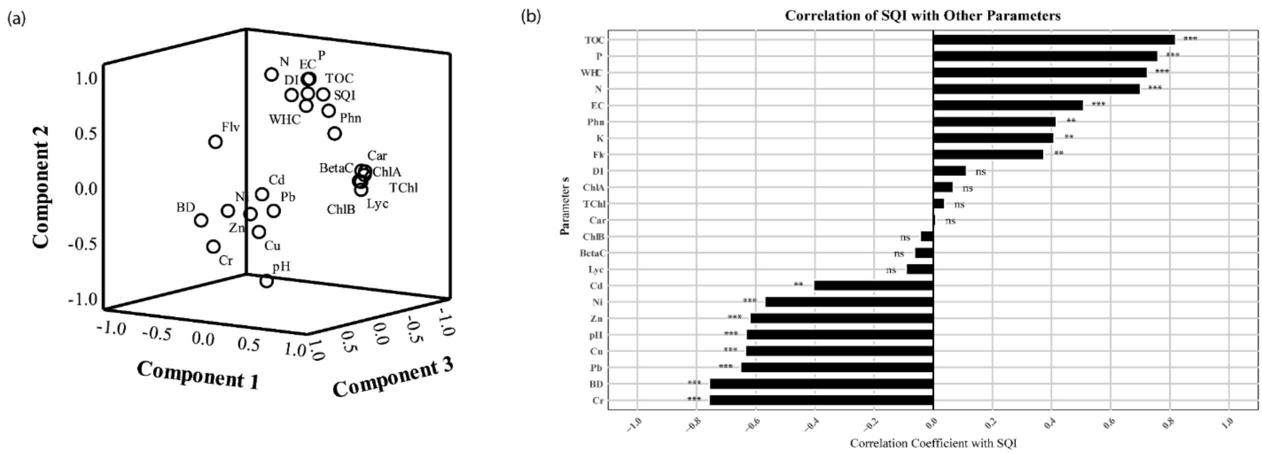

Figure 20. Relationship of SQI with the different soil physicochemical and heavy metal attributes, and plant phytochemical composition through PCA and Pearson's correlation

The relationships between SQI and DI and primary soil physicochemical properties, heavy-metal concentrations, and plant phytochemicals were further explained by a structural equation model (Figure 21). The models had acceptable fit to the observed data. In case of SQI, the chi-square test was significant ($\chi^2 = 185.212$, df = 165, p value = 0.012). The model had the validity value of comparative fit index (CFI = 0.951) and Tucker Lewis Index (TLI = 0.942), both close to the standard value of 0.95 for an excellent fit. The root mean square error of approximation (RMSEA) was 0.037 which is less than the 0.05 level of close approximation fit, and the standardized root mean square residual (SRMR) stood at 0.044 (Kang and Ahn, 2021). Standardized path coefficients indicated that physicochemical parameters in the soils had a strong direct positive impact on SQI ($\beta = 0.39$; $p < 0.01$) (Figure 21). The heavy metal concentration had a significant negative effect on SQI ($\beta = -0.66$; $p < 0.01$). The strong positive effect of soil physicochemical properties on SQI confirms their role in soil health and function. On the contrary, the significant negative between heavy metals and SQI highlights heavy metals as critical stressors directly affecting the functioning of the soil (Kandziora-Ciupa et al., 2021). For DI, the chi-square test was significant ($\chi^2 = 168.745$, df = 155, $p = 0.022$), confirmed through the CFI (0.938) and TLI (0.928). The RMSEA was 0.028 and the SRMR was 0.051. The availability of heavy metals had a positive impact on DI ($\beta = 0.77$, $p < 0.01$) (Figure 21), which highlights their contribution to soil degradation. However, soil physicochemical parameters showed a significant negative effect on DI ($\beta = -0.41$, $p < 0.01$), confirming that better soil conditions mitigate degradation (Lal, 2015).

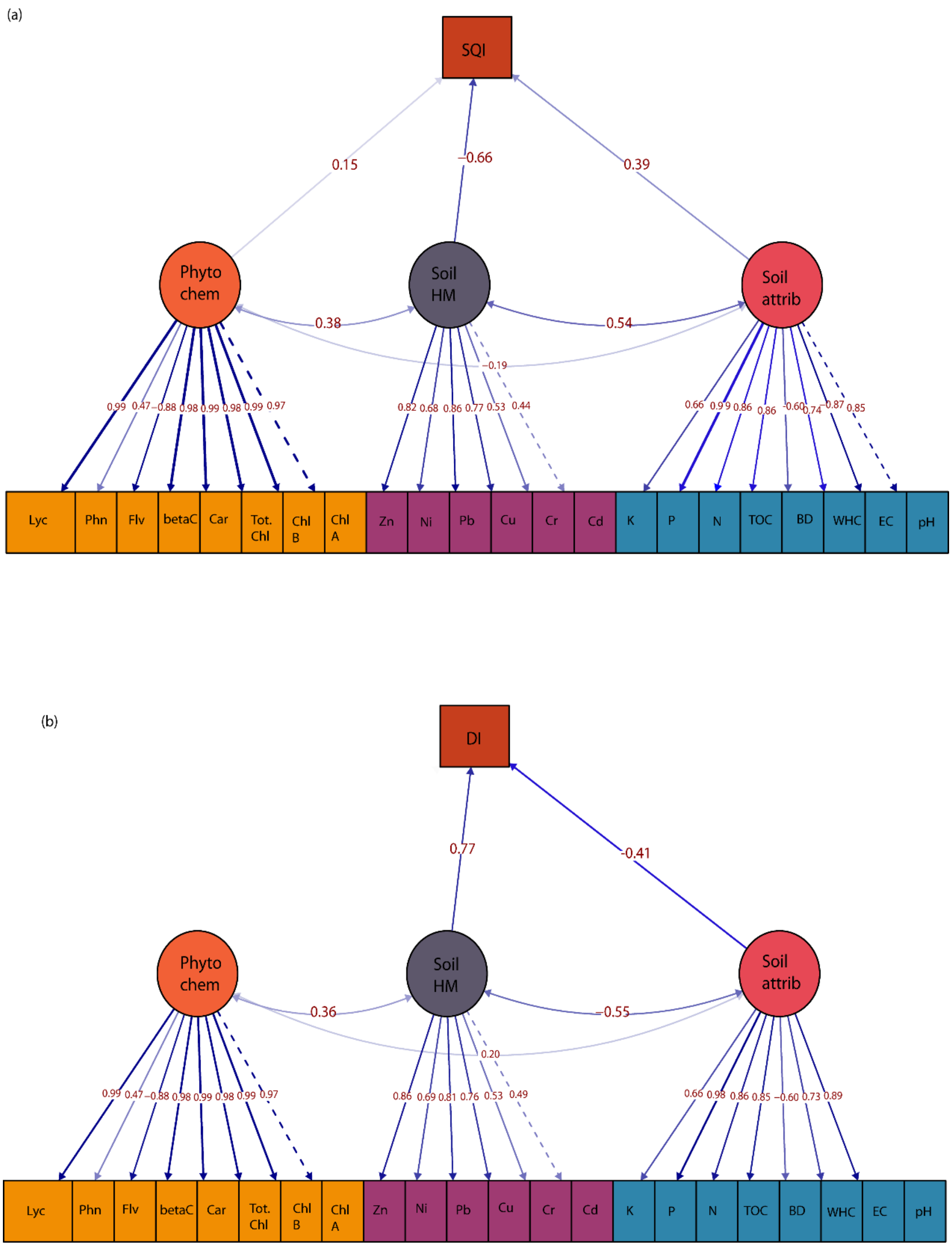

Figure 21. Structured equation modelling (SEM) of Soil Quality Index (SQI) and Degradation Index (DI) with the soil physicochemical attributes, heavy metals, and plant phytochemicals

CHAPTER 5

SUMMARY AND CONCLUSIONS

CHAPTER 5

5. SUMMARY AND CONCLUSIONS

5.1. Phase I – Characterization experiment

In the characterization experiment (Phase I), the two blended samples ORS + RH and ORS + CDM were empirically assessed for their physicochemical and heavy metal characteristics, their structural and morphological makeup, along with their elemental and overall chemical composition. The results revealed that ORS + RH was more acidic in nature along with corresponding higher EC (Table 9), suggesting better mineralization in this sample. The WHC and BD of this sample were in the appropriate range, suggesting that this sample was a better potting media for composting compared to its counterpart ORS + CDM. The availability of C, H, and N were also significant in ORS + RH compared to CDM, showing better elemental retention by the former sample (Table 9).

The structural and morphological intactness of ORS + RH was also confirmed by the SEM analysis as demonstrated by the rugged and rutted nature of the outer surfaces of this sample (Figure 4). This structural trait of ORS + RH was mainly facilitated by the presence of SiO_2 in the sample as confirmed by the EDX analysis. The EDX analysis also demonstrated that ORS + RH sample had higher C, O, K and Si proportions than ORS + CDM. Structurally, ORS + RH was more resilient to chemical interactions as compared to ORS + CDM. This indicated the structural and morphological superiority of the sample over ORS + CDM.

The thermal degradation of ORS + RH was more efficient than ORS + CDM as corroborated by the TGA-DTG analysis. ORS + RH exhibited a greater thermal susceptibility profile in which it lost 87% of its initial mass compared to ORS + CDM (Figure 5). The comprehensive combustion index (CCI) confirmed these findings wherein ORS + RH demonstrated a higher CCI than ORS + CDM (Table 10). It implies that ORS + RH could be potentially incinerated or pyrolyzed into ORS ash or ORS char for reutilization. Moreover, van Krevelen plots of the samples showed their transformation from the petrogenic region to the biomass region (Figure 6), indicating their inherent characteristic change at atomic level. Overall, ORS + RH was a better material for thermal degradation than ORS + CDM.

Chemically, both the samples demonstrated the presence of various functional groups as confirmed by the FTIR analysis. However, the presence of these functional groups was more significant in ORS + CDM than ORS + RH (Figure 7). The FTIR analysis attributed the presence of alcohols, thiols, isocyanates, hydrocarbons, and halogenated compounds more prominently in ORS + CDM. This was attributed to the presence of organic matter and microbial diversity in cow dung manure which facilitated adsorption of these compounds from ORS in the sample. The GCMS analysis also revealed that a total of 581 compounds were collectively present in samples of which 139 compounds were specific to ORS + CDM. The proportion of hydrocarbons in ORS + CDM was 120% higher than ORS + RH, indicating the susceptibility of the former sample to interact with the harmful compounds of ORS. The pollution potential as estimated by PubChem and ASTDR databases revealed that ORS + CDM was potentially more toxic than ORS + RH (Figure 8).

Based on the results of the characterization experiment, ORS + RH was selected as the most appropriate substrate for composting in the bioconversion experiment (Phase II), owing to its better physicochemical properties, structural and morphological attributes, and less toxic chemical composition compared to its counterpart ORS + CDM.

5.2. Phase II – Bioconversion experiment

The bioconversion experiment was conducted in-vitro with ORS + RH as the primary substrate. To facilitate the composting process, ORS + RH was mixed with farmyard manure (FYM) in three different ratios: 1:1, 1:2, and 2:1 of their weight.

The physicochemical results revealed that both the earthworm systems showed higher reduction of pH and increment in their EC during the incubation. This was linked to the efficient processing of organic matter by the earthworms, releasing more soluble and mobile mineral forms in the compost matrix. The WHC and BD was also optimal for the earthworm systems, with EF_2 and EE_2 outperforming the other treatments (Figure 9). The reduction of TOC and the augmentation of N, P, and K were also high in both the earthworm systems compared to the system without earthworms. Also, the two treatments EF_2 and EE_2 consistently performed better than the remaining treatments in terms of overall NPK pool (Appendix 2).

In terms of heavy metal reduction, the two earthworm systems overshadowed the non-earthworm system, with Cd and Pb concentrations measured below detection level during the incubation. The presence of earthworms facilitated better detoxification of the substrates mainly due to the production of stable metal-humic complexes in the system. Also, the production of MT proteins by earthworms further advanced the metal detoxification in those two systems. Among the treatments, EF_2 and EE_2 showed the lowest metal concentrations, while the treatments AC_1, AC_2, and AC_3 showed higher metal load (Appendix 3).

Earthworm health and growth assessment revealed better performance of *E. eugeniae* over *E. fetida*, with a net biomass gain of 433.33 ± 110.15 in *E. eugeniae*. Also, *E. eugeniae* showed the highest net proliferation rate (211%) than *E. fetida* (Table 11). *E. eugeniae*'s significantly larger size and a voracious feeding facilitated its growth over *E. fetida*. Also, *E. eugeniae* is more productive in tropical climate because of its fast reproductive cycle. The results showed that *E. eugeniae* was more adaptable to the ORS composting environment, indicating its potential in ORS bioconversion.

The results also revealed that the augmentation of microbes (total bacteria, N-fixing, and P-solubilizing and enzymes (urease, dehydrogenase, and phosphatase) was higher in the two earthworm systems compared to the non-earthworm system (Figure 11). The treatment EE_2 showed the best results in total bacterial growth with an overall increment of 25% (Appendix 4). This was attributed to the gut-associated processes and cast-associated processes induced by earthworms which facilitated better proliferation of microbes and upregulation of their associated enzymes in the substrates. The results implied that the overall microbial and enzymatic activity was better in the two earthworm systems compared to the non-earthworm system. Also, EF_2 and EE_2 consistently performed better in this aspect.

The overall quality assessment estimated through CI, FI, HI, RGI, and CQI also showed the superiority of the earthworm systems over non-earthworm system in producing cleaner and safer composts (Figure 12). The proliferation of earthworms contributed to the formation of humic substances, augmentation of beneficial microbes, and enzymes in the systems contributed to the overall quality of the composts. In addition, the economic assessment revealed the superiority of EE over the other two systems in terms of NPV, BCR, and PBT (Table 12), signifying its marketable prospects in the ORS bioconversion process.

The ecological and health risk assessments of the compost teas (CTs) produced from the composts showed prominent results, with CTs of the earthworm systems showing the lowest ecological risks compared to the CTs of the non-earthworm system (Table 13). These results were consistent with the carcinogenic and non-carcinogenic assessment of the CTs, with CTs of the earthworm systems outperforming the non-earthworm system CTs. Among the various CTs, EF_2 and EE_2 showed the best results in terms of minimized ecological risks and health hazards, whereas AC_1, AC_2, and AC_3 demonstrated higher risks (Table 14).

From the results of the bioconversion experiment, it was revealed that the two earthworm systems performed better than the non-earthworm system in terms of overall nutrient accretion, metal reduction, microbial and enzymatic stimulation, compost quality, economic viability, and minimizing environmental and health risks. This was synergistically brought about by the earthworm activity and their associated gut microbes. Bases on the results from the various aspects, the treatments EF_2 and EE_2 were selected as the two best treatments for the large-scale composting experiment under Phase III.

5.3. Phase III – Large-scale composting experiment

The large-scale composting experiment was a continuation of the bioconversion experiment with the two best treatments EF_2 i.e., EF and EE_2 i.e., EE. This experiment was conducted on a systematic scale for 90 days to comprehensively compare the performance of *E. fetida* and *E. eugeniae* in ORS vermicomposting. Moreover, the vermicomposts produced from this experiment were utilized in the Phase IV (Field experiment).

The physicochemical assessment of the two vermicomposts revealed comparable results. However, the composts of *E. eugeniae* showed better WHC and BD compared to the composts of *E. fetida* (Table 15). In addition, the accretion of available nutrients, especially N and P, were higher in EE compared to EF. The results revealed differences in the physiological adaptations of the two species which contributed to the varying results. In terms of heavy metal speciation, the results revealed that *E. eugeniae* was more efficient in reducing the bioavailable fractions of heavy metals compared to *E. fetida*, with EE showing a 24% greater metal removal than EF (Appendix 6).

In terms of carbon fractionation, the HAC fractions were more significant in EE compared to EF (Figure 15), signifying that the composts were more mature. This was brought about by the robust microbiota of *E. eugeniae* which facilitated the production of humified compounds. Overall, the composts of EE were more mature and stable than EF.

Earthworm health assessment consistently revealed *E. eugeniae* to be the better performing species in ORS vermicomposting. This was corroborated by the higher proliferation rate, body elongation, body mass, and reproductive rate of the species in the ORS composting environment (Table 16). This was attributed to the physiological differences of the species and habitat adaptability. Moreover, *E eugeniae* is further facilitated by a resilient defence system characterized by SOD, CAT, POD, which helps this species in sustaining its health in a toxic environment more efficiently than *E. fetida*.

Gut bioaccumulation of heavy metals as well as bioaccumulation factor were also high in *E. eugeniae* than *E. fetida*. The BAF was in the order Cr < Zn < Pb < Cu < Ni < Cd for EE and Zn < Pb < Cr < Ni < Cu < Cd for EF. *E. eugeniae* demonstrated 20-42% higher bioaccumulation of heavy metals in its gut tissues (Table 17), attributed to its larger size, extensive feeding, and better stress-induced physiological adaptations than *E. fetida*. From the results, it is suggestive that *E. eugeniae* was more efficient in accumulating heavy metals, underlying its potential in ORS detoxification in future ORS vermicomposting operations.

The benefit assessment of the earthworms showed promising trends, with EE demonstrating higher VBI than EF (Figure 16). This suggested that *E. eugeniae* was a slightly better species than *E. fetida* in the ORS vermicomposting process. The higher VBI was brought about by various factors such as enhanced nutrient increment, metal reduction, metal accumulation, and better proliferation of *E. eugeniae*, indicating its superiority over *E. fetida*. In addition, EE showed better BR for most key parameter including TOC, N, and P and better RE for most heavy metals. The results suggest that *E. eugeniae* can be tailored for ORS vermicomposting process that require high nutritional output and metal detoxification.

From the results of the large-scale composting experiment, it can be concluded that both the species were comparable in performance in terms of ORS vermicomposting. However, the physiological adaptations of *E. eugeniae* make it more advantageous in adapting to the toxic composting environment of ORS, making it the preferable species in ORS bioconversion.

5.4. Phase IV – Field experiment

The field experiment was carried out to understand the effects of the two ORS vermicomposts produced from the large-scale composting experiment (Phase III) on the soil system and on two morphologically different crops i.e., tomato and cabbage.

The physicochemical attributes of soil during cultivation revealed that soil pH decreased substantially from the initial to post-harvest stage across all treatments. The highest decrease in pH occurred in the EE_{100} treatment, attributed to the production of organic acids during cultivation. The WHC of the soils increased considerably in the ORS vermicompost treated soils, especially in EF_{100} and EE_{100}. Also, the overall carbon retention as well as nutrient aggregation was high in the vermicompost treated soils compared to the positive control (NPK_{100}) and negative control (soil) (Table 18). This suggested that ORS vermicomposts can enhance the structural quality and nutrients of soil more efficiently than inorganic fertilizers.

In terms of metal concentration of soils, the ORS vermicompost treated soils showed lower content in most heavy metals compared to NPK_{100}, especially at higher concentrations (Table 19). This was attributed to the better metal chelation and adsorption capabilities of vermicompost that facilitated in its lower metal bioavailability and mobility. This was also reflected in the metal uptake in both the crop specimens, wherein the crops grown under the ORS vermicompost treatment (EF and EE) showed lesser metal content than the crops grown under the negative control (soil) and positive control (NPK_{100}) treatments. Notably, the metal concentrations in crops were under the permissible limits of WHO and FAO.

The soil health assessment through SQI and DI revealed that the application of ORS vermicomposts promoted a balanced resilient soil system compared to NPK_{100} (Figure 18). This was brought about by the slow release of nutrients by ORS vermicompost, preventing leaching and loss of the essential nutrients in the soil system. It was further facilitated by the better metal chelation of ORS vermicomposts, which reduced the overall metal bioavailability in soils. The results indicated the potential of ORS vermicomposts in promoting long-term sustainability of the soil system compared to inorganic fertilizer (NPK_{100}).

The morphological characteristics of the crops grown under the different treatments were comparable. However, the crops grown under the ORS vermicompost treatments showed slightly better results than the crops grown under NPK_{100} (Table 20). A similar trend was also observed in the phytochemical composition of the crops, wherein ORS vermicomposts consistently outperformed the NPK100 and negative control (soil) (Figure 19). The presence of humified compounds in ORS vermicomposts facilitated better nutrient uptake of the crops, as well as the presence of PGPRs in vermicomposts enhanced the phytochemical synthesis of the crops. Overall, the phytochemical synthesis was 16% higher in the crops grown under ORS vermicompost (Appendix 10).

From the results of the field experiment, it can be concluded that ORS vermicomposts produced by *E. fetida* and *E. eugeniae* can potentially substitute inorganic fertilizer in terms of nutritional inputs, metal reduction, and maintaining overall soil health. Moreover, the application of ORS vermicomposts has shown positive outcomes in the yield of tomato and cabbage, signifying its role as an organic amendment. However, further research should be carried out to assess the long-term feasibility of the ORS vermicomposts in agriculture and assess their ecological and health risks in ORS valorization.

APPENDICES

APPENDIX 1. Chemical compounds detected in ORS + RH and ORS + CDM with their CAS number, area/height (A/H) ratio, m/z values, classification, and pollution potential

Retention Time	ORS + RH	ORS + CDM	CAS	A/H	m/z	Class	Pollution Potential
5.325	–	Urea	57-13-6	5.84	17.15	Amides	High
5.510	–	Ethanedial, dioxime	557-30-2	5.94	18.15	Others	High
5.560	Meglumine	–	141-83-3	4.15	19.15	Alcohol	Low
5.676	–	Urea, (aminoiminomethyl)-	107-16-4	5.43	19.15	Urea derivatives	Low
5.910	–	Acetonitrile, hydroxy-	107-16-4	1.87	28.10	Nitriles	High
6.324	Acetonitrile, hydroxy-	–	107-16-4	4.90	28.10	Nitriles	High
7.242	–	Acetonitrile, hydroxy-	107-16-4	2.67	18.15	Nitriles	High
7.445	3-Amino-1,2-propanediol	–	616-30-8	1.53	17.15	Amines	High
7.519	–	Acetonitrile, hydroxy-	708-42-9	1.93	28.10	Nitriles	High
7.761	–	Acetonitrile, hydroxy-	79-14-1	4.71	19.15	Nitriles	High
7.941	Manganese, acetylpentacarbonyl-, (OC-6-21)-	–	107-16-4	3.84	28.10	Organometallic Compound	High
8.645	–	3-Amino-1,2-propanediol	7803-49-8	1.98	19.15	Amines	High
8.884	Acetonitrile, hydroxy-	–	298-12-4	0.83	17.15	Nitriles	High
8.925	5-Aminobarbituric acid	–	56-41-7	1.15	17.15	Acids	Low
8.972	–	3-(n-Propylamino)-2,1-benzisothiazole	76-05-1	1.24	17.15	Heterocyclic compounds	High
9.181	–	Acetic acid, hydroxy-	79-17-4	3.42	17.15	Acids	High
9.340	Urea	–	556-52-5	2.39	17.15	Amides	High
9.426	–	Acetonitrile, hydroxy-	753-90-2	1.16	18.15	Nitriles	High
9.600	–	Hydroxylamine	99-16-1	1.94	19.15	Hydrazine derivatives	High
9.759	Ammonia	–	302-01-2	2.66	17.15	Inorganic	High
9.845	Hydrazinecarboxylic acid, ethyl ester	–	627-03-2	0.97	28.10	Esters	High
10.119	Acetonitrile, hydroxy-	–	57-13-6	3.86	28.10	Nitriles	High
10.130	–	Acetic acid, oxo-	627-03-2	4.83	19.15	Acids	High

10.195	–	Alanine	79-14-1	1.02	19.15	Acids	Low
11.065	–	Trifluoroacetic acid	515-96-8	3.75	19.15	Acids	High
11.124	Glycyl-D-asparagine	–	107-16-4	2.49	18.15	Carbohydrates	Low
11.200	–	Aminoguanidine	32064-67-8	3.58	18.15	Amides	Unknown
11.286	–	Glycidol	99-16-1	1.03	19.15	Alcohol	High
11.375	–	Allantoic acid	7803-49-8	3.26	19.15	Purine derivatives	High
11.375	–	2,2,2-Trifluoroethylamine	1111-78-0	1.07	19.15	Amines	High
11.680	Allantoic acid	–	56-41-7	0.90	19.15	Purine derivatives	High
11.765	1,2-Hydrazinedicarboxaldehyde	–	67-56-1	2.24	18.15	Hydrazine derivatives	High
12.266	–	Hydrazine	692-45-5	1.14	32.10	Hydrazine derivatives	High
12.310	–	Acetic acid, ethoxy-	107-16-4	3.91	19.15	Esters	High
12.696	Trimethylene oxide	–	79-05-0	6.82	28.10	Ethers	High
12.715	–	Urea, (aminoiminomethyl)-	107-16-4	2.03	17.15	Urea derivatives	Low
12.785	Acetonitrile, hydroxy-	–	1111-78-0	6.98	19.15	Nitriles	High
12.942	–	Acetic acid, ethoxy-	1120-21-4	2.07	19.15	Esters	High
13.155	–	Acetic acid, hydroxy-	0-00-0	0.92	19.15	Acids	High
13.220	–	Semioxamazide	98236-55-6	1.63	19.15	Others	High
13.417	N,N,N',N'-Tetramethylsulfonamide	–	107-16-4	4.83	18.15	Amides	High
13.482	Hydrazine	–	20235-19-2	1.87	32.10	Hydrazine derivatives	High
13.646	Acetic acid, oxo-	–	98236-55-6	1.21	18.15	Acids	High
13.876	Acetonitrile, hydroxy-	–	80655-44-3	4.87	18.15	Nitriles	High
14.054	4(4-Chlorphenyl)-3-morpholinopyrrol-2-carboxylic acid, methyl ester	–	3891-98-3	2.83	18.15	Heterocyclic compounds	High
14.512	–	Acetonitrile, hydroxy-	708-42-9	0.93	17.15	Nitriles	High
14.705	–	Hydrazine, (1,1-dimethylethyl)-	36052-28-5	1.62	32.10	Hydrazine derivatives	High
15.031	Glycyl-D-asparagine	–	629-59-4	2.94	18.15	Acids	Low
15.084	–	Allantoic acid	708-42-9	1.62	19.15	Purine derivatives	High
15.225	–	Hydroxylamine	13992-25-1	3.96	18.15	Hydrazine derivatives	High

15.706	–	Carbamic acid, monoammonium salt	7803-49-8	1.11	18.15	Acids	High
15.751	–	Alanine	708-42-9	1.62	19.15	Acids	Low
16.127	–	Methyl Alcohol	569-41-5	3.21	17.15	Alcohol	High
16.192	–	Formic acid, ethenyl ester	571-61-9	3.34	28.10	Esters	High
17.015	1,2-Hydrazinedicarboxaldehyde	–	0-00-0	1.34	18.15	Hydrazine derivatives	High
17.170	–	Acetonitrile, hydroxy-	98-01-1	4.05	18.15	Nitriles	High
17.418	N,N,N',N'-Tetramethylsulfonamide	–	7664-41-7	2.93	18.15	Amides	High
17.650	–	Propanamide	708-42-9	5.57	19.15	Amides	High
17.820	–	Acetonitrile, hydroxy-	708-42-9	0.68	28.10	Nitriles	High
18.030	Acetonitrile, hydroxy-	–	575-37-1	2.85	18.15	Nitriles	High
18.062	–	Carbamic acid, monoammonium salt	24667-21-8	1.47	18.15	Acids	High
18.194	–	Undecane	118-78-5	2.98	18.15	Hydrocarbon (alkane)	Low
18.456	–	1,3,4,6-Tetrabromopentacyclo [9.3.1.1(6,10).0(3,11).0(4,10)] hexadecane	708-42-9	1.85	18.15	Hydrocarbon (cyclic/polycyclic)	High
18.691	–	4(4-Chlorphenyl)-3-morpholinopyrrol-2-carboxylic acid, methyl ester	3891-99-4	3.08	17.15	Heterocyclic compounds	High
19.394	–	Acetonitrile, hydroxy-	57387-76-5	2.18	18.15	Nitriles	High
19.490	–	DL-Arabinose	288586-33-4	3.54	19.15	Alcohol	Low
19.545	Aminoguanidine	–	24667-21-8	2.09	18.15	Amides	Unknown
19.625	Nickel tetracarbonyl	–	0-00-0	1.13	28.10	Inorganic	High
19.749	2H-1,4-Benzoxazin-3(4H)-one, 4-(.beta.-D-glucopyranosyloxy)-2-hydroxy-7-methoxy-	–	629-92-5	3.09	28.10	Flavonoid Glycoside	Low
20.154	–	4(4-Chlorphenyl)-3-morpholinopyrrol-2-carboxylic acid, methyl ester	121-57-3	3.67	18.15	Heterocyclic compounds	High
20.159	3-(n-Propylamino)-2,1-benzisothiazole	–	0-00-0	4.98	18.15	Amines	High
20.215	–	Decahydro-1,1,4a,5,6-pentamethylnaphthalene	0-00-0	2.10	18.15	Hydrocarbon (cyclic/polycyclic)	High
20.309	Hexadecane	–	24667-21-8	0.92	28.10	Hydrocarbon (alkane)	High
20.310	–	Dodecane, 2,6,10-trimethyl-	16204-67-4	4.87	57.15	Hydrocarbon (alkane)	High
20.379	1,3,4,6-Tetrabromopentacyclo [9.3.1.1(6,10).0(3,11).0(4,10)] hexadecane	–	0-00-0	2.59	18.15	Hydrocarbon (cyclic/polycyclic)	High

20.492	–	3-(n-Propylamino)-2,1-benzisothiazole	829-26-5	5.99	18.15	Amines	High
20.635	4-Phenylsemicarbazide	–	57-13-6	1.74	32.10	Aromatic compounds	High
20.744	Acetonitrile, hydroxy-	–	98236-55-6	0.78	18.15	Nitriles	High
20.834	4(4-Chlorphenyl)-3-morpholinopyrrol-2-carboxylic acid, methyl ester	–	0-00-0	3.74	18.15	Heterocyclic compounds	High
20.846	–	1-Naphthalenemethanol, 1,2,3,4-tetrahydro-8-methyl	98236-55-6	2.60	18.15	Alcohol	High
20.956	–	Tetradecane	829-26-5	2.73	57.15	Hydrocarbon (alkane)	High
20.958	Hexadecane	–	33666-64-7	1.99	57.15	Hydrocarbon (alkane)	High
21.053	5-Aminobarbituric acid	–	0-00-0	3.38	18.15	Acids	Low
21.135	–	3-(n-Propylamino)-2,1-benzisothiazole	0-00-0	2.13	19.15	Amines	High
21.249	–	. beta. -D-Glucopyranosyl azide, 2,3,4,6-tetraacetate	98236-55-6	1.65	28.10	Carbohydrates	Low
21.275	–	Hydroxylamine	7664-41-7	2.09	19.15	Hydrazine derivatives	High
21.346	Acetonitrile, hydroxy-	–	0-00-0	2.42	28.10	Nitriles	High
21.372	–	3-(n-Propylamino)-2,1-benzisothiazole	708-42-9	2.01	18.15	Amines	High
21.545	3-(n-Propylamino)-2,1-benzisothiazole	–	941-81-1	2.95	18.15	Amines	High
21.584	–	Naphthalene, 1,8-dimethyl-	38701-09-6	1.09	156.20	Hydrocarbon (aromatic)	High
21.670	–	Naphthalene, 1,5-dimethyl-	56-41-7	2.38	141.20	Hydrocarbon (aromatic)	High
21.715	–	1,3,4,6-Tetrabromopentacyclo [9.3.1.1(6,10).0(3,11).0(4,10)] hexadecane	629-94-7	2.61	18.15	Hydrocarbon (cyclic/polycyclic)	High
21.780	–	Furfural	574-42-5	3.25	19.15	Aldehydes	High
21.844	–	Ammonia	57-13-6	5.02	17.15	Inorganic	High
22.029	–	3-(n-Propylamino)-2,1-benzisothiazole	24667-21-8	2.10	19.15	Amines	High
22.060	–	3-(n-Propylamino)-2,1-benzisothiazole	0-00-0	3.07	19.15	Amines	High
22.079	Stearic acid hydrazide	–	0-00-0	3.09	17.15	Acids	Unknown
22.120	–	Naphthalene, 1,7-dimethyl-	560-27-0	7.69	18.15	Hydrocarbon (aromatic)	High
22.165	3-Pentanol, 3-ethyl-	–	1921-70-6	3.69	17.15	Alcohol	Low
22.410	3-Oxobutan-2-yl 2-methylbutanoate	–	98236-55-6	2.10	19.15	Others	Low

22.427	–	Glycyl-D-asparagine	134-58-7	1.57	18.15	Acids	Low
22.500	–	5-Aminobarbituric acid	40710-32-5	3.22	17.15	Acids	Low
22.530	–	3-(n-Propylamino)-2,1-benzisothiazole	36052-28-5	0.96	18.15	Amines	High
22.578	2,6,10-Trimethyltridecane	–	339006-39-2	0.91	71.20	Hydrocarbon (alkane)	Unknown
22.583	–	2,6,10-Trimethyltridecane	54972-18-8	1.00	71.20	Hydrocarbon (alkane)	Unknown
22.655	–	Borinic acid, diethyl-, 3,3,5-trimethyl-1-cyclohexen-1-yl ester	490-65-3	3.20	19.15	Esters	High
22.740	–	Hexafluorobutane-2,3-diimine	483-78-3	3.75	19.15	Imines	High
23.120	–	Glycyl-D-asparagine	832-62-2	1.40	18.15	Hydrocarbon (cyclic/polycyclic)	High
23.222	–	1,3,4,6-Tetrabromopentacyclo [9.3.1.1(6,10).0(3,11).0(4,10)] hexadecane	529-05-5	2.91	18.15	Hydrocarbon (cyclic/polycyclic)	High
23.380	Naphthalene, 1,2,3,4-tetrahydro-2,2,5,7-tetramethyl-	–	629-94-7	3.18	132.20	Hydrocarbon (cyclic/polycyclic)	High
23.460	Butanal, 3-hydroxy-	–	1921-70-6	3.62	19.15	Aldehydes	High
23.562	Nonadecane	–	98236-55-6	2.88	57.15	Hydrocarbon (alkane)	High
23.568	–	Nonadecane	0-00-0	1.67	57.15	Hydrocarbon (alkane)	High
23.680	–	Benzenesulfonic acid, 4-amino-	116-31-4	3.50	19.15	Aromatic compounds	High
23.698	3-(n-Propylamino)-2,1-benzisothiazole	–	23140-98-9	1.53	18.15	Amines	High
23.808	–	3-(2-Methyl-propenyl)-1H-indene	80812-36-8	2.48	155.20	Indene derivative	High
24.055	–	1,3,4,6-Tetrabromopentacyclo [9.3.1.1(6,10).0(3,11).0(4,10)] hexadecane	107-16-4	1.54	18.15	Hydrocarbon (cyclic/polycyclic)	High
24.121	1,3,4,6-Tetrabromopentacyclo [9.3.1.1(6,10).0(3,11).0(4,10)] hexadecane	–	4695-13-0	3.31	18.15	Hydrocarbon (cyclic/polycyclic)	High
24.150	–	Glycyl-D-asparagine	118-78-5	1.61	17.15	Hydrocarbon (cyclic/polycyclic)	High
24.220	–	1,1,4,5,6-Pentamethyl-2,3-dihydro-1H-indene	13601-24-6	1.88	173.25	Hydrocarbon (cyclic/polycyclic)	High
24.357	–	1,3,4,6-Tetrabromopentacyclo [9.3.1.1(6,10).0(3,11).0(4,10)] hexadecane	708-42-9	1.10	18.15	Hydrocarbon (cyclic/polycyclic)	High
24.485	–	Naphthalene, 2,3,6-trimethyl-	612-75-9	2.96	170.20	Hydrocarbon (aromatic)	High
24.494	Naphthalene, 2,3,6-trimethyl-	–	41002-74-8	4.40	155.20	Hydrocarbon (aromatic)	High

24.540	O,O-Diethyl S-eththionylmethyl phosphorothioate	–	708-42-9	2.02	17.15	Organophosphorus compound	High
24.565	–	Urea	58163-61-4	1.68	17.15	Amides	High
24.590	–	4(4-Chlorphenyl)-3-morpholinopyrrol-2-carboxylic acid, methyl ester	611-08-5	1.46	18.15	Heterocyclic compounds	High
24.681	Acetic acid, ethoxy-	–	98236-55-6	3.50	18.15	Esters	High
24.695	–	1,3,4,6-Tetrabromopentacyclo [9.3.1.1(6,10).0(3,11).0(4,10)] hexadecane	55334-72-0	4.04	18.15	Hydrocarbon (cyclic/polycyclic)	High
24.780	–	4(4-Chlorphenyl)-3-morpholinopyrrol-2-carboxylic acid, methyl ester	98236-55-6	4.85	18.15	Heterocyclic compounds	High
24.876	Naphthalene, 2,3,6-trimethyl-	–	4425-82-5	5.17	155.15	Hydrocarbon (aromatic)	High
24.879	–	Naphthalene, 2,3,6-trimethyl-	629-94-7	4.40	155.20	Hydrocarbon (aromatic)	High
25.021	1,3,4,6-Tetrabromopentacyclo [9.3.1.1(6,10).0(3,11).0(4,10)] hexadecane	–	3891-99-4	5.11	18.15	Hydrocarbon (cyclic/polycyclic)	High
25.270	–	1,10-Decanedione, 1,10-di-1-naphthyl-	708-42-9	1.65	18.15	Naphthalene derivative	High
25.275	3-(2-Methyl-propenyl)-1H-indene	–	708-42-9	5.18	155.20	Indene derivative	High
25.301	–	1,3,4,6-Tetrabromopentacyclo [9.3.1.1(6,10).0(3,11).0(4,10)] hexadecane	107-16-4	2.64	18.15	Hydrocarbon (cyclic/polycyclic)	High
25.380	–	1,3,4,6-Tetrabromopentacyclo [9.3.1.1(6,10).0(3,11).0(4,10)] hexadecane	708-42-9	2.42	18.15	Hydrocarbon (cyclic/polycyclic)	High
25.405	–	4(4-Chlorphenyl)-3-morpholinopyrrol-2-carboxylic acid, methyl ester	618-71-3	1.18	18.15	Heterocyclic compounds	High
25.460	. psi.,. psi. -Carotene, 7,7',8,8',11,11',12,12'-octahydro-	–	77536-58-4	1.71	40.10	Carotenoid	Low
25.465	–	Ammonia	708-42-9	1.58	17.15	Inorganic	High
25.527	Glutaric acid, isobutyl 1-phenyl-2-(3-cyclohexenyl) ethyl ester	–	54972-18-8	2.30	19.15	Esters	Low
25.535	–	1,3,4,6-Tetrabromopentacyclo [9.3.1.1(6,10).0(3,11).0(4,10)] hexadecane	04-05-5627	1.13	18.15	Hydrocarbon (cyclic/polycyclic)	High
25.580	–	3-(n-Propylamino)-2,1-benzisothiazole	0-00-0	1.68	18.15	Amines	High
25.670	3-(n-Propylamino)-2,1-benzisothiazole	–	0-00-0	2.45	18.15	Amines	High
25.916	–	4,6,8-Trimethylazulene	4130-54-5	1.87	155.20	Hydrocarbon (cyclic/polycyclic)	High
25.924	1,10-Decanedione, 1,10-di-1-naphthyl-	–	708-42-9	3.86	18.15	Naphthalene derivative	High
25.945	–	2,3-Pentadienoic acid, 2-ethyl-4-phenyl-, ethyl ester	708-42-9	1.70	17.15	Esters	High

25.975	–	Alanine	17619-97-5	1.78	19.15	Acids	Low
26.042	–	Heneicosane	40710-32-5	3.30	57.15	Hydrocarbon (alkane)	High
26.045	Heptadecane	–	13475-75-7	3.36	57.15	Hydrocarbon (alkane)	High
26.100	Naphthalene, 1-(2-propenyl)-	–	0-00-0	1.64	168.15	Hydrocarbon (aromatic)	High
26.130	–	Benzene, 1,1',1'',1'''-(oxydimethylidyne)tetrakis-	23140-98-9	2.52	19.15	Hydrocarbon (aromatic)	High
26.300	2-Chloro-6-fluorobenzyl alcohol, acetate	–	832-69-9	2.64	19.15	Aromatic compounds	High
26.555	–	Urea	26963-43-9	1.27	17.15	Amides	High
26.603	1,3,4,6-Tetrabromopentacyclo [9.3.1.1(6,10).0(3,11).0(4,10)] hexadecane	–	779-02-2	3.07	19.20	Hydrocarbon (cyclic/polycyclic)	High
26.680	–	Glycyl-D-asparagine	1210-34-0	1.86	18.15	Hydrocarbon (cyclic/polycyclic)	High
26.718	–	2-Isopropyl-3-methylnaphthalene	708-42-9	1.21	18.15	Hydrocarbon (aromatic)	High
26.831	–	1,3,4,6-Tetrabromopentacyclo [9.3.1.1(6,10).0(3,11).0(4,10)] hexadecane	708-42-9	1.62	18.15	Hydrocarbon (cyclic/polycyclic)	High
27.050	–	Propanedioic acid, dihydroxy-	708-42-9	3.98	19.15	Acids	Low
27.196	–	Pentadecane, 2,6,10,14-tetramethyl-	708-42-9	1.61	57.15	Hydrocarbon (terpenes)	High
27.203	Octane, 2-bromo-	–	708-42-9	4.04	28.10	Hydrocarbon (alkane)	High
27.290	–	4(4-Chlorphenyl)-3-morpholinopyrrol-2-carboxylic acid, methyl ester	0-00-0	3.97	18.15	Heterocyclic compounds	High
27.340	–	8-Azaguanine	0-00-0	2.14	19.15	Purine derivatives	High
27.381	–	Nonahexacontanoic acid	18279-67-9	1.07	19.15	Acids	Unknown
27.621	–	1-Naphthalenemethanol, 1,2,3,4-tetrahydro-8-methyl-	832-64-4	5.66	17.15	Naphthylmethanol	Unknown
27.675	–	N-(2-Fluorophenethyl)-N'-(2-fluorophenyl) oxamide	0-00-0	4.42	16.20	Aromatic compounds	High
27.705	–	3,3-Bis(carbamino)diaziridine	102177-18-4	3.33	18.15	Heterocyclic compounds	High
27.755	2-Fluorobenzyl alcohol, TMS derivative	–	708-42-9	0.90	32.10	Aromatic compounds	High
27.880	–	Naphthalene, 1-methyl-7-(1-methylethyl)-	0-00-0	3.50	18.15	Hydrocarbon (aromatic)	High
28.045	Naphthalene, 1,6-dimethyl-4-(1-methylethyl)-	–	69340-71-2	1.57	183.20	Hydrocarbon (aromatic)	High

28.045	–	Naphthalene, 1,6-dimethyl-4-(1-methylethyl)-	288586-33-4	3.15	183.20	Hydrocarbon (aromatic)	High
28.085	tetra-n-Propoxymethane	–	0-00-0	1.30	19.15	Ethers	High
28.117	N-(Dibenzofuran-3-yl)-2-(2-pyridylthio) acetamide	–	708-42-9	0.99	18.15	Heterocyclic compounds	High
28.120	–	4,6,8-Trimethyl-1-azulenecarbaldehyde	3768-63-6	0.96	18.15	Aldehydes	High
28.256	–	Chamazulene	3891-99-4	2.02	169.20	Hydrocarbon (aromatic)	Low
28.267	1,3,4,6-Tetrabromopentacyclo [9.3.1.1(6,10).0(3,11).0(4,10)] hexadecane	–	4584-57-0	4.15	18.15	Hydrocarbon (cyclic/polycyclic)	High
28.386	Eicosane	–	708-42-9	2.50	57.15	Hydrocarbon (alkane)	Low
28.389	–	Heneicosane	52251-71-5	3.34	57.15	Hydrocarbon (alkane)	High
28.501	2,6,10-Trimethyltridecane	–	0-00-0	4.51	57.15	Hydrocarbon (alkane)	Unknown
28.506	–	Pentadecane, 2,6,10,14-tetramethyl-	3674-66-6	3.89	57.15	Hydrocarbon (terpenes)	High
28.675	–	4(4-Chlorphenyl)-3-morpholinopyrrol-2-carboxylic acid, methyl ester	0-00-0	3.39	18.15	Heterocyclic compounds	High
28.743	–	1,3,4,6-Tetrabromopentacyclo [9.3.1.1(6,10).0(3,11).0(4,10)] hexadecane	708-42-9	3.07	18.15	Hydrocarbon (cyclic/polycyclic)	High
28.744	(2-Methyl-3-biphenylyl) methanol	–	52251-71-5	3.19	165.20	Alcohol	High
28.770	–	Retinal	118-78-5	2.03	97.20	Aldehydes	Low
28.805	Acetonitrile, hydroxy-	–	131567-34-5	1.56	19.15	Nitriles	High
28.836	–	2H-1,4-Benzoxazin-3(4H)-one, 4- (. beta. -D-glucopyranosyloxy)-2-hydroxy-7-methoxy-	85440-62-6	1.91	28.10	Flavonoid Glycoside	Low
28.860	–	[1,2,4] Triazolo[1,5-a] pyrimidine, 7-chloro-2,5-dimethyl-	0-00-0	3.20	19.15	Heterocyclic compounds	Low
28.913	–	Acetonitrile, hydroxy-	3674-66-6	2.95	19.15	Nitriles	High
28.965	–	Benzene acetamide, alpha. -phenyl-	7664-41-7	2.33	18.15	Amides	High
29.020	–	5-Aminobarbituric acid	0-00-0	0.89	18.15	Acids	Low
29.080	–	Manganese, pentacarbonyl methyl-	206-44-0	2.86	18.15	Organometallic compound	High
29.145	–	3-(n-Propylamino)-2,1-benzisothiazole	838-88-0	2.76	17.15	Amines	High
29.160	1,2-Hydrazinedicarboxaldehyde	–	04-11-5702	3.16	18.15	Hydrazine derivatives	High
29.189	–	3,3'-Dimethylbiphenyl	112-60-7	1.12	19.15	Hydrocarbon (aromatic)	High

29.340	1H,2H,3H-Cyclopenta[a]naphthalen-5-ylmethane	–	98236-55-6	1.81	19.15	Hydrocarbon (aromatic)	High
29.370	–	1-Acenaphthylenol, 1,2-dihydro-1-methyl-	13287-24-6	4.20	169.20	Hydrocarbon (aromatic)	High
29.509	N, N’, N"-Methylidynetrisformamide	–	75045-09-9	4.33	28.10	Amides	High
29.565	1,1'-Biphenyl, 3-(1-methylethyl)-	–	37985-11-8	4.25	18.15	Hydrocarbon (aromatic)	High
29.667	1,3,4,6-Tetrabromopentacyclo [9.3.1.1(6,10).0(3,11).0(4,10)] hexadecane	–	0-00-0	2.44	18.15	Hydrocarbon (cyclic/polycyclic)	High
29.678	–	3-(n-Propylamino)-2,1-benzisothiazole	16983-74-7	3.13	18.15	Amines	High
29.980	–	Borinic acid, diethyl-, (2-ethyl-1,3,2-dioxaborinan-4-yl) methyl ester	708-42-9	0.71	28.10	Esters	High
29.994	4,6,8-Trimethyl-1-azulenecarbaldehyde	–	129-00-0	3.12	18.15	Aldehydes	High
30.025	–	2,4(1H,3H)-Pyrimidinedione, 5-nitro-	0-00-0	1.87	28.10	Heterocyclic compounds	High
30.124	–	4(4-Chlorphenyl)-3-morpholinopyrrol-2-carboxylic acid, methyl ester	58506-72-2	6.07	18.15	Heterocyclic compounds	High
30.245	–	Benzene, (2-decyldodecyl)-	708-42-9	1.97	28.10	Hydrocarbon (aromatic)	High
30.289	–	4(4-Chlorphenyl)-3-morpholinopyrrol-2-carboxylic acid, methyl ester	708-42-9	1.30	18.15	Heterocyclic compounds	High
30.380	1,3,4,6-Tetrabromopentacyclo [9.3.1.1(6,10).0(3,11).0(4,10)] hexadecane	–	0-00-0	1.30	18.15	Hydrocarbon (cyclic/polycyclic)	High
30.430	6-Aminohexanoic acid, 2-[(5-fluorenyl) methoxycarbonyl amino]-	–	37985-11-8	2.09	178.20	Acids	Low
30.455	–	9H-Fluorene, 9-methylene-	123-25-1	1.56	178.20	Hydrocarbon (aromatic)	High
30.535	3-(n-Propylamino)-2,1-benzisothiazole	–	15295-31-5	3.22	18.15	Amines	High
30.604	Nonahexacontanoic acid	–	4364-78-7	3.40	18.15	Acids	Unknown
30.613	–	Heneicosane	708-42-9	1.78	57.15	Hydrocarbon (alkane)	High
30.730	3-(n-Propylamino)-2,1-benzisothiazole	–	1498-80-2	3.45	19.15	Amines	High
30.803	–	2,6,10-Trimethyltridecane	77536-58-4	3.98	57.15	Hydrocarbon (alkane)	Unknown
30.910	–	3-(n-Propylamino)-2,1-benzisothiazole	26698-45-3	2.79	18.15	Amines	High
30.930	4(4-Chlorphenyl)-3-morpholinopyrrol-2-carboxylic acid, methyl ester	–	2199-60-2	2.43	18.15	Heterocyclic compounds	High
30.985	–	3-(n-Propylamino)-2,1-benzisothiazole	111530-37-1	2.58	18.15	Amines	High

31.060	–	Acetonitrile, hydroxy-	85440-62-6	1.44	19.15	Nitriles	High
31.163	N, N, N’, N'-Tetramethylsulfonamide	–	0-00-0	1.51	19.15	Amides	High
31.195	–	3-(n-Propylamino)-2,1-benzisothiazole	0-00-0	0.81	18.15	Amines	High
31.235	5-(2-Morpholino-1-thiophen-2-yl-vinyl)-1,2,4-thiadiazole	–	2029236-76-6	8.74	18.15	Aromatic compounds	High
31.255	–	Ethyl 3,5-dinitrobenzoate	708-42-9	1.26	19.15	Esters	High
31.295	–	4-Phenanthrenol, 1,2,3,4-tetrahydro-4-methyl-	708-42-9	1.52	18.15	Others	Unknown
31.310	1,3,4,6-Tetrabromopentacyclo [9.3.1.1(6,10).0(3,11).0(4,10)] hexadecane	–	75410-89-8	3.27	18.15	Hydrocarbon (cyclic/polycyclic)	High
31.442	–	3-(n-Propylamino)-2,1-benzisothiazole	5385-37-5	0.74	18.15	Amines	High
31.460	3-(n-Propylamino)-2,1-benzisothiazole	–	57169-35-4	0.78	19.15	Amines	High
31.514	–	3,3-Bis(carbamino)diaziridine	33543-31-6	3.45	19.15	Heterocyclic compounds	High
31.550	–	Uridine, 5,6-dihydro-	53545-70-3	1.28	19.15	Carbohydrates	Low
31.771	–	1,3,4,6-Tetrabromopentacyclo [9.3.1.1(6,10).0(3,11).0(4,10)] hexadecane	1023-91-2	1.45	18.15	Hydrocarbon (alkane)	High
31.780	4-Phenylsemicarbazide	–	56-41-7	3.00	32.10	Aromatic compounds	High
31.874	Acetonitrile, hydroxy-	–	243-17-4	1.65	18.15	Nitriles	High
31.900	–	1,3,4,6-Tetrabromopentacyclo [9.3.1.1(6,10).0(3,11).0(4,10)] hexadecane	708-42-9	1.68	18.15	Hydrocarbon (cyclic/polycyclic)	High
31.967	–	Stearic acid hydrazide	33543-31-6	2.27	18.15	Acids	High
32.050	–	3-(n-Propylamino)-2,1-benzisothiazole	96581-95-2	1.09	18.15	Amines	High
32.152	–	3-(n-Propylamino)-2,1-benzisothiazole	0-00-0	1.50	19.15	Amines	High
32.247	–	Oxirane, 2,3-diphenyl-	708-42-9	0.92	18.15	Hydrocarbon (aromatic)	High
32.338	1,3,4,6-Tetrabromopentacyclo [9.3.1.1(6,10).0(3,11).0(4,10)] hexadecane	–	95676-48-5	1.40	18.15	Hydrocarbon (cyclic/polycyclic)	High
32.400	5-Brom-2-cyclopropylbenzamide	–	0-00-0	3.68	19.15	Amides	High
32.561	–	Nonahexacontanoic acid	708-42-9	3.09	18.15	Acids	Unknown
32.739	–	Pentadecane, 8-hexyl-	3442-78-2	4.23	57.15	Hydrocarbon (alkane)	Low
32.800	–	4-Phenylbicyclo (3.2.2) nona-3,6-dien-2-one	0-00-0	2.10	18.15	Others	Unknown
32.840	–	2H-1,4-Benzoxazin-3(4H)-one, 4- (. beta. -D-glucopyranosyloxy)-2-hydroxy-7-methoxy-	16434-62-1	2.19	17.15	Flavonoid Glycoside	Low

32.890	Butane dioic acid, hydroxy-, diethyl ester, (. +/-.)-	–	3674-73-5	0.87	19.15	Acids	High
32.905	–	Phenanthrene, 1-methyl-	708-42-9	1.88	192.20	Hydrocarbon (aromatic)	High
32.930	3-(n-Propylamino)-2,1-benzisothiazole	–	118-78-5	4.34	18.15	Amines	High
32.940	–	2-Amino-4-methyl-6-(2-thienyl) pyrimidine	0-00-0	4.13	82.55	Heterocyclic compounds	Low
33.000	Silane, dichloromethylpentyl-	–	57-13-6	2.42	28.10	Organosilicon	High
33.020	–	Anthracene, 9-methyl-	0-00-0	1.87	18.15	Hydrocarbon (aromatic)	High
33.026	3-(n-Propylamino)-2,1-benzisothiazole	–	348579-19-1	1.75	18.15	Amines	High
33.050	–	5H-Dibenzo [a, d] cyclohepten-5-ol, 10,11-dihydro-	23140-98-9	2.28	19.15	Hydrocarbon (aromatic)	High
33.094	–	3-(n-Propylamino)-2,1-benzisothiazole	708-42-9	2.52	18.15	Amines	High
33.115	1,3,4,6-Tetrabromopentacyclo [9.3.1.1(6,10).0(3,11).0(4,10)] hexadecane	–	0-00-0	7.90	18.15	Hydrocarbon (cyclic/polycyclic)	High
33.120	–	3-(n-Propylamino)-2,1-benzisothiazole	64401-21-4	2.60	19.15	Amines	High
33.155	–	3-(n-Propylamino)-2,1-benzisothiazole	92-94-4	2.81	18.15	Amines	High
33.233	–	3-(n-Propylamino)-2,1-benzisothiazole	57652-74-1	1.36	18.15	Amines	High
33.300	–	3-(n-Propylamino)-2,1-benzisothiazole	2175-90-8	2.49	18.15	Amines	High
33.303	Pentanamide, 4-oxo-N-phenyl-	–	0-00-0	4.30	19.15	Amides	High
33.355	–	1,3,4,6-Tetrabromopentacyclo [9.3.1.1(6,10).0(3,11).0(4,10)] hexadecane	346612-18-8	2.12	18.15	Hydrocarbon (cyclic/polycyclic)	High
33.439	–	Halobolin	98236-55-6	2.12	19.15	Coumarin	High
33.445	10-Nitro-dibenz [b, f] azepin-5-carboxamide	–	2571-81-5	4.44	165.15	Heterocyclic compounds	High
33.470	–	Silane, (2-chloroethyl) triethoxy-	1059-14-9	0.60	19.15	Organosilicon	High
33.557	10-Nitro-dibenz [b, f] azepin-5-carboxamide	–	2097-60-1	1.38	165.20	Heterocyclic compounds	High
33.593	–	Phenanthrene, 4-methyl-	30248-06-7	2.60	17.15	Hydrocarbon (aromatic)	High
33.666	Thiourea, 1-[2-(2-benzylphenoxy) ethyl]-3-(O-tolyl)-	–	959-02-4	1.27	44.10	Aromatic compounds	High
33.694	–	1,3,4,6-Tetrabromopentacyclo [9.3.1.1(6,10).0(3,11).0(4,10)] hexadecane	239-35-0	4.06	18.15	Hydrocarbon (cyclic/polycyclic)	High
33.745	1,3-Diaminoguanidine	–	332-80-9	1.81	19.15	Amides	Unknown

33.775	–	EMDP	1023-91-2	1.73	29.10	Heterocyclic compounds	High
33.795	–	3-(n-Propylamino)-2,1-benzisothiazole	98236-55-6	2.44	18.15	Amines	High
33.864	–	1,3,4,6-Tetrabromopentacyclo [9.3.1.1(6,10).0(3,11).0(4,10)] hexadecane	55044-64-9	2.29	18.15	Hydrocarbon (cyclic/polycyclic)	High
33.915	–	1,8-Naphthyridine, 1,2,3,4,4a,5,6,7-octahydro-2,2,4a,7,7-pentamethyl-, 8-oxide	98236-55-6	4.47	19.15	Heterocyclic compounds	Low
33.975	3-(n-Propylamino)-2,1-benzisothiazole	–	0-00-0	2.22	18.15	Amines	High
34.105	–	Hexafluorobutane-2,3-diimine	56-41-7	3.83	32.10	Imines	High
34.175	–	4-Phenylbicyclo (3.2.2) nona-3,6-dien-2-one	708-42-9	2.03	19.15	Others	Unknown
34.282	3-(n-Propylamino)-2,1-benzisothiazole	–	708-42-9	2.61	18.15	Amines	High
34.375	–	3-(n-Propylamino)-2,1-benzisothiazole	98236-55-6	6.01	18.15	Amines	High
34.700	Glycyl-D-asparagine	–	708-42-9	5.64	18.15	Acids	Low
34.735	–	N, N, N', N'-Tetramethylsulfonamide	35187-44-1	3.20	19.15	Amides	High
34.763	–	2,6,10-Trimethyltridecane	56-55-3	5.17	71.20	Hydrocarbon (alkane)	Unknown
35.018	–	Benzenamine, N, N-dimethyl-4-[2-(4-nitrophenyl) ethenyl]-	107-16-4	2.38	17.15	Amines	High
35.024	2H-1,4-Benzoxazin-3(4H)-one, 4- (. beta. -D-glucopyranosyloxy)-2-hydroxy-7-methoxy-	–	218-01-9	6.27	17.15	Flavonoid Glycoside	Low
35.071	–	3-(n-Propylamino)-2,1-benzisothiazole	708-42-9	5.36	18.15	Amines	High
35.184	–	Anthracene, 2-ethyl-	67309-35-7	1.99	206.25	Hydrocarbon (aromatic)	High
35.270	–	4-Phenylbicyclo (3.2.2) nona-3,6-dien-2-one	537-47-3	3.06	19.15	Others	Unknown
35.381	–	Phenanthrene, 2,5-dimethyl-	98236-55-6	2.59	206.25	Hydrocarbon (aromatic)	High
35.434	–	1,3,4,6-Tetrabromopentacyclo [9.3.1.1(6,10).0(3,11).0(4,10)] hexadecane	708-42-9	1.04	18.15	Hydrocarbon (cyclic/polycyclic)	High
35.515	–	3-(n-Propylamino)-2,1-benzisothiazole	5323-57-9	2.38	18.15	Amines	High
35.715	3-(n-Propylamino)-2,1-benzisothiazole	–	0-00-0	5.79	18.15	Amines	High
35.728	–	Anthracene, 2-ethyl-	708-42-9	4.24	206.25	Hydrocarbon (aromatic)	High
35.741	Anthracene, 2-ethyl-	–	2498-76-2	5.08	206.25	Hydrocarbon (aromatic)	High
35.800	–	5-Aminobarbituric acid	98236-55-6	5.53	18.15	Acids	Low
35.825	Acetonitrile, hydroxy-	–	0-00-0	2.17	18.15	Nitriles	High

35.830	–	Anthracene, 9-(3-methoxypropyl)-	0-00-0	1.63	28.10	Hydrocarbon (aromatic)	High
35.860	Anthracene, 2-ethyl-	–	115026-73-8	1.74	18.15	Hydrocarbon (aromatic)	High
35.864	–	[14] Annulene, 1,6:7,12-bis(methanol)-, anti-	57289-37-9	2.12	18.15	Hydrocarbon (aromatic)	High
35.920	–	1,3,4,6-Tetrabromopentacyclo [9.3.1.1(6,10).0(3,11).0(4,10)] hexadecane	1705-85-7	5.11	18.15	Hydrocarbon (cyclic/polycyclic)	High
35.986	–	Phenanthrene, 2,5-dimethyl-	3697-24-3	6.24	206.25	Hydrocarbon (aromatic)	High
36.114	–	Ammonia	4076-39-5	3.76	17.15	Inorganic	High
36.124	Phenanthrene, 9-ethyl-	–	708-42-9	2.06	191.20	Hydrocarbon (aromatic)	High
36.135	–	1,3,4,6-Tetrabromopentacyclo [9.3.1.1(6,10).0(3,11).0(4,10)] hexadecane	2097-60-1	2.73	18.15	Hydrocarbon (cyclic/polycyclic)	High
36.150	1,3,4,6-Tetrabromopentacyclo [9.3.1.1(6,10).0(3,11).0(4,10)] hexadecane	–	17582-54-6	1.23	18.15	Hydrocarbon (cyclic/polycyclic)	High
36.291	–	Fluoranthene	2097-60-1	1.63	202.20	Hydrocarbon (aromatic)	High
36.426	–	Benzenamine, 4,4'-methylenebis [2-methyl-	2097-60-1	1.56	17.15	Amines	High
36.475	1,3,4,6-Tetrabromopentacyclo [9.3.1.1(6,10).0(3,11).0(4,10)] hexadecane	–	2097-60-1	1.07	18.15	Hydrocarbon (cyclic/polycyclic)	High
36.500	–	Silanamine, N-silyl-	2097-60-1	0.83	17.15	Organosilicon	High
36.530	–	Tetraethylene glycol	708-42-9	0.77	17.15	Alcohol	High
36.590	1,3,4,6-Tetrabromopentacyclo [9.3.1.1(6,10).0(3,11).0(4,10)] hexadecane	–	4325-74-0	3.19	18.15	Hydrocarbon (cyclic/polycyclic)	High
36.600	–	4(4-Chlorphenyl)-3-morpholinopyrrol-2-carboxylic acid, methyl ester	2097-60-1	2.26	18.15	Heterocyclic compounds	High
36.701	–	Nonadecane, 9-methyl-	708-42-9	1.69	57.20	Hydrocarbon (alkane)	Low
36.712	1,2,3,4-Tetrahydro-1-phenyl-1,2,3-methanonaphthalene	–	2097-60-1	1.52	17.15	Heterocyclic compounds	High
36.834	–	1,3,2-Dioxaphospholane, 2-chloro-4,5-bis(methoxycarbonyl)-, (E)-	708-42-9	2.67	19.15	Heterocyclic compounds	High
36.908	–	1-(4-Methylphenyl)-4-phenylbuta-1,3-diene	0-00-0	0.90	18.15	Hydrocarbon (cyclic/polycyclic)	High
36.940	Glycyl-dl-aspartic acid	–	298-12-4	1.47	17.15	Acids	Low
37.035	–	5-Acetyl-4-(2,2-dimethyl- [1,3] dioxolan-4-yl)-1-phenyl-4,5-dihydro-1H-pyrazol-3-carboxylic acid, ethyl esterqe287731	708-42-9	3.37	17.15	Heterocyclic compounds	High
37.210	–	Hydrazinecarboxamide, 2-(1,3-diphenyl-2-propenylidene)-	298-12-4	2.07	205.20	Hydrazine derivatives	High
37.230	–	3-(n-Propylamino)-2,1-benzisothiazole	107-16-4	3.86	18.15	Amines	High

37.311	Pyrene	–	103-60-6	1.84	202.20	Hydrocarbon (aromatic)	High
37.316	–	Pyrene	19904-90-6	1.69	202.20	Hydrocarbon (aromatic)	High
37.350	–	5-(2-Morpholino-1-thiophen-2-yl-vinyl)-1,2,4-thiadiazole	54833-70-4	1.51	32.10	Aromatic compounds	High
37.365	3-(n-Propylamino)-2,1-benzisothiazole	–	2097-60-1	0.50	18.15	Amines	High
37.405	–	2-Dimethylamino-3,3-bis(trifluoromethyl)-1,2-azirine	0-00-0	1.33	32.10	Heterocyclic compounds	High
37.415	Iridomyrmecin	–	16354-50-0	3.57	18.15	Hydrocarbon (terpenes)	Low
37.504	9-Octadecenoic acid, (E)-	–	0-00-0	2.07	55.15	Acids	Low
37.550	1,3,4,6-Tetrabromopentacyclo [9.3.1.1(6,10).0(3,11).0(4,10)] hexadecane	–	313-74-6	1.64	18.15	Hydrocarbon (cyclic/polycyclic)	High
37.610	1,3-Diaminoguanidine	–	708-42-9	0.87	18.15	Amides	Unknown
37.655	3-Bromo-5-methoxy-1-(methoxymethyl)-1,2,4-triazole	–	28622-84-6	3.15	18.15	Ethers	Unknown
37.709	–	3-(n-Propylamino)-2,1-benzisothiazole	79-17-4	0.83	18.15	Amines	High
37.798	–	3-(n-Propylamino)-2,1-benzisothiazole	20803-54-7	3.22	18.15	Amines	High
37.835	–	1,3,4,6-Tetrabromopentacyclo [9.3.1.1(6,10).0(3,11).0(4,10)] hexadecane	7664-41-7	1.61	18.15	Hydrocarbon (cyclic/polycyclic)	High
37.883	–	1-(4-Methylphenyl)-4-phenylbuta-1,3-diene	0-00-0	1.24	18.15	Hydrocarbon (cyclic/polycyclic)	High
37.914	–	Butanedioic acid, diethyl ester	118-78-5	3.20	19.15	Acids	High
38.005	–	1,3-Pentadiene, 1,1-diphenyl-, (Z)-	0-00-0	1.31	18.15	Aromatic compounds	High
38.065	–	1,3-Diaminoguanidine	0-00-0	3.59	19.15	Amides	Unknown
38.175	–	3-(n-Propylamino)-2,1-benzisothiazole	611-48-3	1.35	18.15	Amines	High
38.229	Phenanthrene, 2,3,5-trimethyl-	–	0-00-0	3.94	18.15	Hydrocarbon (aromatic)	High
38.255	–	Anthracene, 9-(1-methylethyl)-	198-55-0	4.93	19.15	Hydrocarbon (aromatic)	High
38.355	–	4-Phenanthrenol, 1,2,3,4-tetrahydro-4-methyl-	492-80-8	1.42	17.15	Others	Unknown
38.387	–	1-Phenanthrylene oxide	1089-80-1	0.98	28.10	Hydrocarbon (aromatic)	High
38.505	–	1H-Pyrrole-2,4-dicarboxylic acid, 5-formyl-3-methyl-, diethyl ester	74764-12-8	1.10	19.15	Esters	High
38.535	–	Di-n-decylsulfone	98236-55-6	1.61	57.15	Esters	High

38.610	5-(2-Morpholino-1-thiophen-2-yl-vinyl)-1,2,4-thiadiazole	–	0-00-0	1.27	18.15	Aromatic compounds	High
38.622	–	[14] Annulene, 1,6:7,12-bis(methano)-, anti-	4774-33-8	0.92	189.20	Hydrocarbon (aromatic)	High
38.665	–	Anthracene, 9,10-dihydro-9-(2-hydroxy-2-propyl)-9,10-dimethyl-	708-42-9	1.73	189.20	Hydrocarbon (aromatic)	High
38.670	1,1'-Biphenyl, 3-(1,1-dimethylethoxy)-	–	19211-90-6	3.64	32.10	Hydrocarbon (aromatic)	High
38.690	–	Anthracene, 9,10-dihydro-9-(2-hydroxy-2-propyl)-9,10-dimethyl-	98236-55-6	1.45	19.15	Hydrocarbon (aromatic)	High
38.725	1,3,4,6-Tetrabromopentacyclo [9.3.1.1(6,10).0(3,11).0(4,10)] hexadecane	–	1801-42-9	1.53	18.15	Hydrocarbon (cyclic/polycyclic)	High
38.795	–	1,1'-Biphenyl, 3-(1-pentyn-1-yl)-	24667-21-8	5.07	220.25	Hydrocarbon (aromatic)	High
38.880	–	3-(n-Propylamino)-2,1-benzisothiazole	0-00-0	0.91	18.15	Amines	High
38.907	–	3-(n-Propylamino)-2,1-benzisothiazole	528-16-5	1.84	18.15	Amines	High
38.946	Quinoline-4-carboxamide, 2-phenyl-N-n.-octyl-	–	18030-67-6	1.79	205.20	–	High
38.960	–	Benzo(c)phenanthrene-3-. alpha.,4-. beta. -diol, 1,2,3,4-tetrahydro-1-. beta.,2-. beta. -epoxy-, (. +/-.)-	708-42-9	2.93	189.10	Hydrocarbon (aromatic)	High
39.025	–	Pyrene, 1,2,3,3a,4,5-hexahydro-	23140-98-9	1.14	18.15	Hydrocarbon (aromatic)	High
39.086	–	3,4-Pentadien-2-ol, 2-methyl-5,5-diphenyl-	708-42-9	1.87	18.15	Amines	High
39.164	–	Fluoranthene, 2-methyl-	0-00-0	1.81	216.20	Hydrocarbon (aromatic)	High
39.181	1-(9-Anthryl)-2-propyn-1-ol	–	708-42-9	1.24	32.10	Alcohol	Unknown
39.240	–	Anthracene, 9,9'-(1,2-ethanediyl) bis [10-methyl-	98236-55-6	4.59	205.20	Hydrocarbon (aromatic)	High
39.262	–	1-Isobenzofuranol, 1,3-dihydro-3,3-dimethyl-1-phenyl-	708-42-9	6.69	28.10	Others	Unknown
39.350	–	Alanine	708-42-9	1.64	17.15	Acids	Low
39.460	Morphina-2,4-diol-6-one, N-methyl-	–	55887-58-6	4.31	19.15	Hydrocarbon (aromatic)	Low
39.516	–	11H-Benzo[b]fluorene	0-00-0	1.75	216.20	Hydrocarbon (aromatic)	High
39.523	Pyrene, 1,2,3,3a,4,5-hexahydro-	–	708-42-9	1.38	19.15	Hydrocarbon (aromatic)	High
39.555	4(4-Chlorphenyl)-3-morpholinopyrrol-2-carboxylic acid, methyl ester	–	2752-17-2	2.01	216.2	Heterocyclic compounds	High
39.555	–	3-(n-Propylamino)-2,1-benzisothiazole	0-00-0	2.41	18.15	Amines	High
39.587	11H-Benzo[b]fluorene	–	98236-55-6	4.46	18.15	Hydrocarbon (aromatic)	High

39.590	–	Fluoranthene, 2-methyl-	0-00-0	3.10	216.20	Hydrocarbon (aromatic)	High
39.611	3-(n-Propylamino)-2,1-benzisothiazole	–	3555-45-1	3.00	18.15	Amines	High
39.665	–	Cyclohexane, 1,4-bis(diphenylmethylene)-	31570-04-4	4.78	19.15	Hydrocarbon (aromatic)	High
39.735	–	Anthracene, 9,10-dihydro-9-(2-hydroxy-2-propyl)-9,10-dimethyl-	554-95-0	1.09	17.15	Hydrocarbon (aromatic)	High
39.760	–	3-(n-Propylamino)-2,1-benzisothiazole	708-42-9	2.19	18.15	Amines	High
39.790	–	Phenanthrene, 9,10-dihydro-1-methyl-	708-42-9	1.09	19.15	Hydrocarbon (aromatic)	High
39.805	3-(n-Propylamino)-2,1-benzisothiazole	–	0-00-0	2.26	18.15	Amines	High
39.819	–	1,3,4,6-Tetrabromopentacyclo [9.3.1.1(6,10).0(3,11).0(4,10)] hexadecane	995-82-4	1.06	18.15	Hydrocarbon (cyclic/polycyclic)	High
39.885	Ammonia	–	995-83-5	4.04	17.15	Inorganic	High
39.940	Retene	–	541-01-5	3.47	17.15	Hydrocarbon (aromatic)	High
39.946	–	3-(n-Propylamino)-2,1-benzisothiazole	107-52-8	1.50	18.15	Amines	High
40.011	Pyrene, 2-methyl-	–	6284-40-8	2.18	18.15	Hydrocarbon (aromatic)	High
40.011	–	Pyrene, 2-methyl-	107-16-4	3.70	18.15	Hydrocarbon (aromatic)	High
40.087	–	Anthracene, 9,10-dihydro-9-(2-hydroxy-2-propyl)-9,10-dimethyl-	616-30-8	1.25	101.15	Hydrocarbon (aromatic)	High
40.171	–	Benz[a]anthracene, 1,2,3,4,7,12-hexahydro-	13963-91-2	3.84	17.15	Hydrocarbon (aromatic)	High
40.204	–	Phenanthrene, 2,3,5-trimethyl-	107-16-4	6.04	17.15	Hydrocarbon (aromatic)	High
40.240	–	3-(n-Propylamino)-2,1-benzisothiazole	118-78-5	1.82	18.15	Amines	High
40.302	2-Furancarboxylic acid, 1-methylethyl ester	–	57-13-6	1.52	19.20	Esters	Low
40.350	–	5-Aminobarbituric acid	7664-41-7	2.06	18.15	Acids	Low
40.396	1,3,4,6-Tetrabromopentacyclo [9.3.1.1(6,10).0(3,11).0(4,10)] hexadecane	–	4114-31-2	3.00	17.15	Hydrocarbon (cyclic/polycyclic)	High
40.515	5,8-Diethoxy-1,2,3,4-tetrahydro-2,3-dioxoquinoxaline	–	107-16-4	2.10	17.15	–	High
40.593	–	1,3-dimethyl-2-phenyl-naphthalene	24667-21-8	1.46	19.15	–	High
40.634	Acetonitrile, hydroxy-	–	99-16-1	1.67	18.15	Nitriles	High
40.680	Ethanedial, dioxime	–	628-36-4	2.87	18.15	Others	High
40.685	–	Urea	503-30-0	2.48	17.15	Amides	High

40.770	–	3-Amino-4-cyano-5-methyl-cyclohexa-2,6-dien-1,2,4,5-tetracarboxylic acid, tetraethyl ester	107-16-4	6.74	18.15	–	Unknown
40.810	–	N-cyclopropyl-9-phenanthrenamine	3768-63-6	2.17	19.15	Hydrocarbon (aromatic)	High
40.876	–	2H-1,4-Benzoxazin-3(4H)-one, 4- (. beta. -D-glucopyranosyloxy)-2-hydroxy-7-methoxy-	302-01-2	2.78	17.15	Flavonoid Glycoside	Low
40.940	–	3-(n-Propylamino)-2,1-benzisothiazole	298-12-4	6.10	17.15	Amines	High
41.060	–	1,3,4,6-Tetrabromopentacyclo [9.3.1.1(6,10).0(3,11).0(4,10)] hexadecane	107-16-4	4.80	18.15	Hydrocarbon (cyclic/polycyclic)	High
41.270	N-Desmethylcyclobenzaprine, N-trifluoroacetyl-	–	98236-55-6	1.26	215.15	Organofluorine	Low
41.275	–	Pyrene, 1,3-dimethyl-	24667-21-8	3.31	18.15	Hydrocarbon (aromatic)	High
41.332	–	p-Terphenyl	628-36-4	1.03	18.15	Hydrocarbon (aromatic)	High
41.332	3-(n-Propylamino)-2,1-benzisothiazole	–	3768-63-6	1.65	18.15	Amines	High
41.375	–	3,4-Dihydro-benz(a)anthracene-1-(2H)-one	107-16-4	3.49	17.15	Hydrocarbon (aromatic)	High
41.402	–	6,6-Diphenylfulvene	79-17-4	4.24	18.15	Hydrocarbon (alkene)	High
41.585	–	Methyl (25RS)-3. alpha. -hydroxy-5. beta. -cholestan-26-oate, TMS derivative	13463-39-3	3.14	215.20	–	Low
41.642	–	Pyrimidine-2,4,6(1H,3H,5H)-trione, 5-(2-chlorophenylaminomethylidene)-1-[2-(4-fluorophenyl) ethy]-	23140-98-9	2.98	18.15	Heterocyclic compounds	High
41.719	–	4(4-Chlorphenyl)-3-morpholinopyrrol-2-carboxylic acid, methyl ester	708-42-9	1.45	18.15	Heterocyclic compounds	High
41.805	1H-Isoindole-1,3(2H)-dione, 2-butyl-4,5,6,7-tetrahydro-	–	544-76-3	1.63	17.15	–	Low
41.810	–	Azuleno[4,5-b] furan-2,9-dione, decahydro-6a-hydroxy-6,9a-dimethyl-3-methylene-, [3aS-(3a. alpha.,6. beta.,6a. alpha.,9a. beta.,9b. a	0-00-0	2.77	18.15	Hydrocarbon (aromatic)	Unknown
41.915	–	Taraxasterol	537-47-3	3.40	17.15	Terpenoid	Low
41.938	–	Stannane, triethylmethyl-	107-16-4	2.14	18.15	Organotin	High
41.998	–	Phenanthro[10,1-bc] pyran-5,11(1H,4H)-dione, 2,3,3a,6a. beta.,7,7a. alpha.,8,11a, 11b.alpha.,11c-decahydro-1. alpha.,3. beta.,3a. beta	98236-55-6	1.28	19.15	Hydrocarbon (aromatic)	High
42.030	–	Naphthacene, 5,12-dihydro-	544-76-3	2.54	18.15	Hydrocarbon (aromatic)	High
42.161	–	Benzo[b]naphtho[2,1-d] thiophene	118-78-5	3.42	234.20	Hydrocarbon (aromatic)	High
42.200	–	L-Histidine, 1-methyl-	107-16-4	7.55	17.15	Heterocyclic compounds	Low

42.245	–	1-Isobenzofuranol, 1,3-dihydro-3,3-dimethyl-1-phenyl-	708-42-9	1.11	18.15	Others	Unknown
42.304	–	4(4-Chlorphenyl)-3-morpholinopyrrol-2-carboxylic acid, methyl ester	4130-54-5	3.71	18.15	Heterocyclic compounds	High
42.350	–	Acetamide, N-(3-bromopropyl)-N-pentyl-	597-49-9	1.12	28.10	Acids	High
42.515	–	4(4-Chlorphenyl)-3-morpholinopyrrol-2-carboxylic acid, methyl ester	0-00-0	2.46	18.15	Heterocyclic compounds	High
42.600	–	1,8-Dimethyltetracyclo [6.6.2.0(2,7).0(9,14)] hexadeca-2,4,6,9,11,13,15-heptaene-15,16-dicarboxylic acid	3891-99-4	2.54	17.15	Acids	Unknown
42.640	–	Alanine	23342-25-8	4.54	19.15	Acids	Low
42.720	–	3-(n-Propylamino)-2,1-benzisothiazole	107-89-1	3.49	18.15	Amines	High
42.791	–	3-(n-Propylamino)-2,1-benzisothiazole	629-92-5	2.92	18.15	Amines	High
42.850	–	4(4-Chlorphenyl)-3-morpholinopyrrol-2-carboxylic acid, methyl ester	708-42-9	3.83	18.15	Heterocyclic compounds	High
42.965	–	3-(n-Propylamino)-2,1-benzisothiazole	0-00-0	2.82	18.15	Amines	High
43.156	–	7,12-Dihydro-2-methylbenz[a]anthracene	829-26-5	3.66	18.15	Hydrocarbon (aromatic)	High
43.265	Acetic acid	–	08-05-2588	1.84	19.15	Acids	High
43.348	–	Benz[a]anthracene	627-03-2	1.02	228.20	Hydrocarbon (aromatic)	High
43.363	Benz[a]anthracene	–	829-26-5	3.10	228.20	Hydrocarbon (aromatic)	High
43.420	Benzo[c]phenanthrene	–	0-00-0	4.89	28.10	Hydrocarbon (aromatic)	High
43.420	–	Acetonitrile, hydroxy-	0-00-0	6.89	19.15	Nitriles	High
43.525	–	Chrysene	540-04-5	1.82	18.15	Hydrocarbon (aromatic)	High
43.539	Chrysene	–	0-00-0	5.38	228.20	Hydrocarbon (aromatic)	High
43.682	3-(n-Propylamino)-2,1-benzisothiazole	–	708-42-9	6.24	18.15	Amines	High
43.740	Succinic acid, 2-chloro-6-fluorophenyl 2-fluoro-3-(trifluoromethyl)phenyl ester	–	33666-64-7	3.62	18.15	Esters	High
43.887	–	3-(n-Propylamino)-2,1-benzisothiazole	629-78-7	3.10	18.15	Amines	High
43.928	–	10-Hydroxyamitriptyline N-oxide	2489-86-3	6.02	18.15	Hydrocarbon (aromatic)	Low
43.995	–	4-Phenylsemicarbazide	0-00-0	4.62	18.15	Aromatic compounds	High
44.082	–	4(4-Chlorphenyl)-3-morpholinopyrrol-2-carboxylic acid, methyl ester	0-00-0	5.03	18.15	Heterocyclic compounds	High

44.120	–	3-(n-Propylamino)-2,1-benzisothiazole	557-35-7	2.40	18.15	Amines	High
44.160	–	2,4-Quinolinedicarboxylic acid	1227612-35-2	4.98	19.15	Acids	High
44.245	Acetic acid, oxo-	–	483-78-3	2.52	28.10	Acids	High
44.294	–	2-Methylbenzo[b]naphtho[2,1-d] thiophene	597-72-8	1.12	248.20	Organosulfur	High
44.385	–	3-(n-Propylamino)-2,1-benzisothiazole	332026-11-6	1.40	19.15	Amines	High
44.447	–	Benz[a]anthracene, 2-methyl-	0-00-0	2.66	242.20	Hydrocarbon (aromatic)	High
44.602	–	4(4-Chlorphenyl)-3-morpholinopyrrol-2-carboxylic acid, methyl ester	112-95-8	3.94	18.15	Heterocyclic compounds	High
44.640	3-(n-Propylamino)-2,1-benzisothiazole	–	3891-99-4	4.05	18.15	Amines	High
44.675	4(4-Chlorphenyl)-3-morpholinopyrrol-2-carboxylic acid, methyl ester	–	76350-90-8	4.18	18.15	Heterocyclic compounds	High
44.694	–	1,4-Thiazine, perhydro-1-benzoylimino-4-(3-chloro-5-trifluoromethyl-2-pyridyl)-	107-16-4	1.84	32.10	–	High
44.962	Acetonitrile, hydroxy-	–	628-36-4	2.89	28.10	Nitriles	High
44.970	–	3-Amino-4-cyano-5-methyl-cyclohexa-2,6-dien-1,2,4,5-tetracarboxylic acid, tetraethyl ester	1624-22-2	3.51	18.15	–	Unknown
45.011	–	N-Crotonyl-N-(4-methoxyphenyl)-aminomalonic acid, diethyl ester	4774-33-8	0.89	19.15	Esters	Unknown
45.132	–	3(2H)-Phenanthrenone, 7-ethenyl-1,4,4a,4b,5,6,7,8,10,10a-decahydro-1-(hydroxymethyl)-4a-methyl-, [1R-(1. alpha.,4ab,4b. alpha.,7.	20282-30-8	2.58	19.15	Hydrocarbon (aromatic)	High
45.228	–	Chrysene, 6-methyl-	0-00-0	3.17	242.20	Hydrocarbon (aromatic)	High
45.294	1,3,4,6-Tetrabromopentacyclo [9.3.1.1(6,10).0(3,11).0(4,10)] hexadecane	–	832-62-2	2.68	18.50	Hydrocarbon (cyclic/polycyclic)	High
45.446	–	Chrysene, 5-methyl-	0-00-0	1.84	242.20	Hydrocarbon (aromatic)	High
45.455	Chrysene, 6-methyl-	–	105047-45-8	7.27	242.20	Hydrocarbon (aromatic)	High
45.505	Diazene, bis(3,5-dimethylphenyl)-	–	708-42-9	3.24	17.15	Phosphorus compound	High
45.535	3-(n-Propylamino)-2,1-benzisothiazole	–	40710-32-5	2.67	18.15	Amines	High
45.600	9H-Tribenzo [a, c, e) cycloheptene	–	708-42-9	1.06	121.10	Hydrocarbon (aromatic)	High
45.600	–	Benzo[c]phenanthrene, 1-methyl-	98236-55-6	3.03	242.20	Hydrocarbon (aromatic)	High
45.630	–	3-(n-Propylamino)-2,1-benzisothiazole	3768-63-6	1.92	18.15	Amines	High

45.631	1-Phenanthrenecarboxylic acid, 7-ethenyl-1,2,3,4,4a,4b,5,6,7,9,10,10a-dodecahydro-1,4a,7-trimethyl-, ethyl ester, [1R-(1. alpha.	–	0-00-0	5.06	18.15	Esters	Unknown
45.675	4'-Hydroxybutyrophenone semicarbazone	–	0-00-0	6.51	19.15	–	High
45.685	–	Stannane, triethylmethyl-	708-42-9	2.73	18.15	Organotin	High
45.730	–	Stannane, cyclopropyltrimethyl-	537-47-3	2.65	18.15	Hydrides	High
45.760	3-(n-Propylamino)-2,1-benzisothiazole	–	107-16-4	2.14	19.15	Amines	High
45.770	–	Stannane, triethylmethyl-	0-00-0	7.46	18.15	Organotin	High
45.818	–	Stannane, triethylmethyl-	121146-17-6	1.54	119.60	Organotin	High
45.820	Chrysene, 6-methyl-	–	626-11-9	1.57	18.15	Hydrocarbon (aromatic)	High
45.830	–	Stannane, triethylmethyl-	708-42-9	1.46	28.10	Organotin	High
45.860	–	Stannane, triethylmethyl-	13682-99-0	0.52	119.35	Organotin	High
45.881	–	3-(n-Propylamino)-2,1-benzisothiazole	708-42-9	2.47	18.15	Amines	High
45.950	Aminoguanidine	–	0-00-0	3.71	17.15	Amides	Unknown
45.975	Diethyl 2,6-dimethyl-4-phenyl-3,5-pyridinedicarboxylate	–	23132-35-6	0.87	19.20	Acids	Unknown
45.976	–	1,2'-Binaphthalene	78880-64-5	5.33	18.15	Hydrocarbon (aromatic)	Unknown
46.010	4(4-Chlorphenyl)-3-morpholinopyrrol-2-carboxylic acid, methyl ester	–	78880-64-5	3.30	18.15	Heterocyclic compounds	High
46.030	–	Stannane, triethylmethyl-	0-00-0	3.04	18.15	Organotin	High
46.055	–	3-(n-Propylamino)-2,1-benzisothiazole	4364-78-7	4.61	18.15	Amines	High
46.090	Stannane, cyclopropyltris(1-methylethyl)-	–	708-42-9	1.93	28.10	Hydrides	High
46.100	–	Stannane, triethylmethyl-	708-42-9	3.34	17.15	Organotin	High
46.150	–	3-(n-Propylamino)-2,1-benzisothiazole	24667-21-8	2.63	18.15	Amines	High
46.260	Bis-(3-azido-4-methoxy-phenyl) methanone	–	23140-98-9	3.45	28.10	–	Low
46.333	1,2-Propanediol-1-phosphate, 3TMS derivative	–	708-42-9	1.57	18.15	Esters	Unknown
46.375	–	l-Methionine, N-(5-chlorovaleryl)-, methyl ester	52251-71-5	1.77	207.15	Esters	Unknown
46.429	–	Acetic acid, oxo-	107-16-4	3.66	19.15	Acids	High
46.540	–	3-(n-Propylamino)-2,1-benzisothiazole	52251-71-5	2.04	18.15	Amines	High

46.585	–	Acetic acid, oxo-	3674-75-7	1.64	19.15	Acids	High
46.665	–	Acetonitrile, hydroxy-	0-00-0	1.06	19.15	Nitriles	High
46.710	–	2-Phenoxyethyl isobutyrate	0-00-0	3.21	19.15	Ethers	Low
46.825	1,4-Dioxane-2,3-diol, bis(chlorodifluoroacetate)	–	0-00-0	2.05	17.15	Ethers	High
46.995	–	2,4-Dimethyl-N-(p-nitrobenzyl) aniline	138089-69-7	2.43	19.15	–	High
47.135	–	Stannane, dibutyl methyl(1-methylethyl)-	79731-35-4	5.14	19.15	–	High
47.140	3-(n-Propylamino)-2,1-benzisothiazole	–	129-00-0	2.95	18.15	Amines	High
47.171	–	Stannane, triethylmethyl-	708-42-9	1.27	193.20	Organotin	High
47.197	–	1H-Indole-2-carboxylic acid, 5-chloro-3-methyl-, ethyl ester	485-43-8	2.47	19.15	Esters	Unknown
47.229	(4-(4-Chlorphenyl)-3-morpholino-pyrrol-2-yl)-butenedioic acid, dimethyl ester	–	112-79-8	4.06	18.15	Esters	High
47.305	–	Benz(a)anthracene, 7-ethyl-12-methyl-	0-00-0	1.56	19.15	Hydrocarbon (aromatic)	High
47.365	–	2,2-Dimethyl-6-hexyl-7-hydroxY3,4-dihydro-2H-1-benzopyran	4364-78-7	2.12	18.15	Esters	High
47.445	–	Benz[a]anthracene, 1,12-dimethyl-	0-00-0	2.73	17.15	Hydrocarbon (aromatic)	High
47.445	Stannane, triethylmethyl-	–	3674-73-5	3.91	17.15	Organotin	High
47.475	–	3-(n-Propylamino)-2,1-benzisothiazole	0-00-0	3.09	19.15	Amines	High
47.488	Stannane, triethylmethyl-	–	55059-21-7	2.05	17.15	Organotin	High
47.515	Stannane, triethylmethyl-	–	0-00-0	2.39	135.30	Organotin	High
47.627	–	Benzo(a)pyrene, 4,5-dihydro-4,5-dihydroxy-	303134-30-7	5.83	18.15	Hydrocarbon (aromatic)	High
47.665	–	Aminoguanidine	31067-61-5	1.25	18.15	Amides	Unknown
47.735	–	4'-Hydroxylaurophenone semicarbazone	0-00-0	1.55	28.10	Imines	High
47.791	–	Ammonia	5385-37-5	0.97	19.15	Inorganic	High
47.830	–	1,3,4,6-Tetrabromopentacyclo [9.3.1.1(6,10).0(3,11).0(4,10)] hexadecane	98236-55-6	1.18	18.15	Hydrocarbon (cyclic/polycyclic)	High
47.920	–	5-Aminobarbituric acid	243-17-4	1.58	18.15	Acids	Low
47.982	–	5-(2-Morpholino-1-thiophen-2-yl-vinyl)-1,2,4-thiadiazole	708-42-9	1.82	18.15	Aromatic compounds	High
48.045	–	8a-Hydroxy-1-(2-hydroxyethyl)-1,2,5,5-tetramethyldecalin(1R,2R,4as,8as)	708-42-9	4.07	19.15	Acids	Unknown
48.179	1,3,4,6-Tetrabromopentacyclo [9.3.1.1(6,10).0(3,11).0(4,10)] hexadecane	–	7664-41-7	1.31	18.15	Hydrocarbon (cyclic/polycyclic)	High

48.190	–	Naphthalene, 1-(2-naphthalenylmethyl)-	483-65-8	1.91	32.10	Hydrocarbon (aromatic)	High
48.225	–	Trichloroacetic acid, 4-isopropylphenyl ester	3442-78-2	1.98	28.10	Esters	High
48.376	3-(n-Propylamino)-2,1-benzisothiazole	–	6270-34-4	2.51	18.15	Amines	High
48.397	–	Perylene	0-00-0	2.67	252.20	Hydrocarbon (aromatic)	High
48.460	–	Auramine	92959-72-3	1.19	17.15	Imines	High
48.562	–	Estra-1,3,5(10),9(11)-tetraen-17-one, 3-hydroxy-	107-16-4	0.96	17.15	–	High
48.595	–	Manganese, dicarbonyl (2,3-diazabicyclo [2.2.1] hept-2-ene-N2, N3) [(1,2,3,4, 5-.eta.)-1-methyl-2,4-cyclopentadien-1-yl]-	557-30-2	1.92	19.15	–	High
48.790	3-(n-Propylamino)-2,1-benzisothiazole	–	0-00-0	2.62	18.15	Amines	High
48.855	–	4(4-Chlorphenyl)-3-morpholinopyrrol-2-carboxylic acid, methyl ester	708-42-9	1.89	18.15	Heterocyclic compounds	High
48.895	–	3-Ethoxy-6-(5-methyl-1-trimethylsiloxy-4-hexenyl)-2-cyclohexen-1-one	54934-85-9	0.96	18.15	–	Unknown
48.930	–	N, N’, N"-Methylidynetrisformamide	64-19-7	1.90	19.15	Amides	High
49.162	1,3,4,6-Tetrabromopentacyclo [9.3.1.1(6,10).0(3,11).0(4,10)] hexadecane	–	56-55-3	4.73	18.15	Hydrocarbon (cyclic/polycyclic)	High
49.279	–	3-(n-Propylamino)-2,1-benzisothiazole	195-19-7	1.70	19.15	Amines	High
49.295	Acetonitrile, hydroxy-	–	218-01-9	5.97	18.15	Nitriles	High
49.430	1,3,4,6-Tetrabromopentacyclo [9.3.1.1(6,10).0(3,11).0(4,10)] hexadecane	–	708-42-9	3.94	18.15	Hydrocarbon (cyclic/polycyclic)	High
49.531	–	9-Cycloheptatrienylidene-9,10-dihydro-10-oxoanthracene	0-00-0	1.59	282.20	Hydrocarbon (aromatic)	High
49.590	3-(n-Propylamino)-2,1-benzisothiazole	–	298-12-4	6.70	17.15	Amines	High
49.650	3-(n-Propylamino)-2,1-benzisothiazole	–	708-42-9	1.53	17.15	Amines	High
49.659	–	4(4-Chlorphenyl)-3-morpholinopyrrol-2-carboxylic acid, methyl ester	98236-55-6	0.96	18.15	Heterocyclic compounds	High
49.716	–	1H-Inden-1-one, 2,3-diphenyl-	107-16-4	1.22	18.15	Stilbenoid	High
49.730	.mu. <3>-Phenylmethylidyne-tricobalt nonacarbonyl	–	0-00-0	1.35	28.10	–	High
49.744	–	Glycyl-D-asparagine	1705-85-7	5.15	18.15	Acids	Low
49.762	3-(n-Propylamino)-2,1-benzisothiazole	–	77611-71-3	1.73	18.15	Amines	High
49.810	6.beta.-Hydroxymethandienone, 2TMS derivative	–	708-42-9	1.85	18.15	–	High
49.880	–	Silane, diethylbutoxy(3-phenylpropoxy)-	213-10-5	2.22	19.15	Organosilicon	High
49.915	1-Cyclopentene-1-carboxylic acid	–	57274-58-5	1.82	19.15	Acids	Unknown

49.957	3-(n-Propylamino)-2,1-benzisothiazole	–	0-00-0	0.98	18.15	Amines	High
49.970	–	D-Glucopyranuronic acid	708-42-9	2.14	18.15	Acids	High
50.025	–	3-Ethoxy-1,1,1,5,5,5-hexamethyl-3-(trimethylsiloxy)trisiloxane	1705-85-7	4.65	17.15	Organosilicon	High
50.095	–	3-(n-Propylamino)-2,1-benzisothiazole	79-17-4	1.02	18.15	Amines	High
50.198	Ethanedial, dioxime	–	1539-44-2	1.22	18.15	Others	High
50.275	–	2H-1,4-Benzoxazin-3(4H)-one, 4- (. beta. -D-glucopyranosyloxy)-2-hydroxy-7-methoxy-	98236-55-6	1.85	17.15	Flavonoid Glycoside	Low
50.298	–	3-(n-Propylamino)-2,1-benzisothiazole	35825-29-7	2.44	18.15	Amines	High
50.445	–	4-Chloro-8-methoxy-N, N-dimethyl-5-nitroquinolin-2-amine	0-00-0	3.98	28.10	Amines	High
50.476	–	3-(n-Propylamino)-2,1-benzisothiazole	0-00-0	1.30	18.15	Amines	High
50.524	4'-Hydroxyvalerophenone, TMS derivative	–	0-00-0	1.68	18.15	–	Unknown
50.637	–	4(4-Chlorphenyl)-3-morpholinopyrrol-2-carboxylic acid, methyl ester	708-42-9	2.85	18.15	Heterocyclic compounds	High
50.788	–	3-(n-Propylamino)-2,1-benzisothiazole	164221-37-8	1.49	19.15	Amines	High
50.989	–	3-(n-Propylamino)-2,1-benzisothiazole	2097-60-1	6.59	18.15	Amines	High
51.030	Silicic acid, diethyl bis(trimethylsilyl) ester	–	2097-60-1	1.43	207.15	Organosilicon	High
51.145	–	Salicylamide, 2TMS derivative	2097-60-1	0.47	266.20	Alcohol	Unknown
51.158	Methyl (1R,2R,8aS)-2-(methoxycarbonyl)-2-hydroxy-5,5,8a-trimethyl-trans-decalin-1-acetate	–	0-00-0	3.37	32.10	–	Unknown
51.235	–	5-(2-Morpholino-1-thiophen-2-yl-vinyl)-1,2,4-thiadiazole	708-42-9	3.46	18.15	Aromatic compounds	High
51.267	–	3-(n-Propylamino)-2,1-benzisothiazole	708-42-9	3.96	18.15	Amines	High
51.465	–	Ethanamine, 2,2'-oxybis-	0-00-0	4.00	18.15	Acids	High
51.495	–	16,17-Epoxy--pregna-5,7-diene-3,20-dione	107-16-4	3.89	19.15	–	High
51.549	3-(n-Propylamino)-2,1-benzisothiazole	–	0-00-0	1.05	18.15	Amines	High
51.625	–	4(4-Chlorphenyl)-3-morpholinopyrrol-2-carboxylic acid, methyl ester	708-42-9	6.86	18.15	Heterocyclic compounds	High
51.630	3-(n-Propylamino)-2,1-benzisothiazole	–	708-42-9	2.89	18.15	Amines	High
51.695	–	1,3,4,6-Tetrabromopentacyclo [9.3.1.1(6,10).0(3,11).0(4,10)] hexadecane	13682-03-6	4.09	18.15	Hydrocarbon (cyclic/polycyclic)	High
51.735	3-(n-Propylamino)-2,1-benzisothiazole	–	708-42-9	1.89	18.15	Amines	High
51.790	–	Silicic acid, diethyl bis(trimethylsilyl) ester	67896-65-5	1.64	207.15	Organosilicon	High
51.845	Phenol, 2,4-bis(1,1-dimethylethyl)-, phosphite (3:1)	–	1560-11-8	1.45	441.40	Acids	High

51.856	–	Phenol, 2,4-bis(1,1-dimethylethyl)-, phosphite (3:1)	708-42-9	1.31	441.45	Acids	High
51.910	Silane, diphenyl-bis-[2-(1,3,5,5,7,7-heptamethyl-2,4,6,8-tetraoxy-1,3,5,7-tetrasilacyclooctyl) ethyl]	–	557-30-2	1.01	281.15	Organosilicon	High
51.920	–	1,3,5-Benzenetricarboxylic acid	33342-92-6	2.89	18.15	Acids	High
51.955	3-(n-Propylamino)-2,1-benzisothiazole	–	3555-45-1	7.05	18.15	Amines	High
51.984	1,2-Propanediol-1-phosphate, 3TMS derivative	–	106933-14-6	2.63	18.15	Others	Unknown
51.986	–	3-(n-Propylamino)-2,1-benzisothiazole	708-42-9	4.03	18.15	Amines	High
52.264	3-(n-Propylamino)-2,1-benzisothiazole	–	708-42-9	4.93	18.15	Amines	High
52.295	–	3-(n-Propylamino)-2,1-benzisothiazole	708-42-9	1.56	18.15	Amines	High
52.375	Ethyl 4-benzoyl-3,5-dimethylbenzoate	–	31570-04-4	4.75	207.15	Esters	Low
52.455	3-(n-Propylamino)-2,1-benzisothiazole	–	331839-19-1	1.45	18.15	Amines	High
52.526	N-Cinnamoyl-N-(4-methoxyphenyl)-aminomalonic acid, diethyl ester	–	708-42-9	1.19	18.15	Esters	High
52.540	–	Iminostilbene-10,11-dihydrodiol,2TMS derivative	0-00-0	6.33	19.15	–	High
52.566	–	Hexasiloxane, 1,1,3,3,5,5,7,7,9,9,11,11-dodecamethyl-	708-42-9	2.23	18.15	Organosilicon	Unknown
52.660	Pentasiloxane, 1,1,3,3,5,5,7,7,9,9-decamethyl-	–	0-00-0	2.63	281.15	Organosilicon	High
52.669	–	Pentasiloxane, 1,1,3,3,5,5,7,7,9,9-decamethyl-	708-42-9	1.75	18.15	Organosilicon	High
52.690	3-Ethoxy-1,1,1,5,5,5-hexamethyl-3-(trimethylsiloxy)trisiloxane	–	0-00-0	2.43	281.15	Organosilicon	High
52.730	7-Acetoxy-3-methylflavanone	–	995-83-5	1.09	18.15	Heterocyclic compounds	High
52.770	3-(n-Propylamino)-2,1-benzisothiazole	–	18030-67-6	1.37	18.15	Amines	High
52.780	–	Heptasiloxane, hexadecamethyl-	0-00-0	1.75	18.15	Organosilicon	High
52.827	–	Hexasiloxane, tetradecamethyl-	708-42-9	1.06	18.15	Organosilicon	High
52.895	4-(Acridin-9-ylamino)-butyric acid	–	194362-64-6	1.96	207.15	Acids	Low

APPENDIX 2. Temporal changes in the physicochemical attributes of the composts (values represent Mean ± SD)

Treatment	WHC (%)			BD (g cm^{-3})			pH			EC (µS cm^{-1})		
	0D	45D	90D	0D	45D	90D	0D	45D	90D	0D	45D	90D
EF$_1$	61 ± 2	76 ± 1	79 ± 1	0.70 ± 0.01	0.58 ± 0.01	0.51 ± 0.02	6.30 ± 0.01	4.36 ± 0.02	3.54 ± 0.03	6781.33 ± 1.15	6198.67 ± 7.77	7833.00 ± 19.16
EF$_2$	64 ± 1	83 ± 1	87 ± 1	0.78 ± 0.02	0.55 ± 0.02	0.43 ± 0.02	6.56 ± 0.01	6.46 ± 0.02	4.32 ± 0.02	6115.67 ± 2.08	6611.67 ± 11.50	6514.33 ± 11.59
EF$_3$	59 ± 1	67 ± 2	72 ± 1	0.57 ± 0.02	0.51 ± 0.03	0.43 ± 0.01	6.01 ± 0.01	4.20 ± 0.02	3.92 ± 0.02	5863.00 ± 1.00	6771.00 ± 1.00	7433.00 ± 20.66
EE$_1$	61 ± 1	70 ± 1	74 ± 3	0.68 ± 0.01	0.57 ± 0.02	0.51 ± 0.01	6.36 ± 0.01	4.76 ± 0.02	3.86 ± 0.01	5793.67 ± 1.15	6917.67 ± 3.21	7426.00 ± 16.37
EE$_2$	65 ± 1	83 ± 3	89 ± 1	0.71 ± 0.02	0.50 ± 0.01	0.41 ± 0.02	6.57 ± 0.01	6.22 ± 0.02	4.22 ± 0.02	6552.00 ± 35.16	6865.00 ± 23.39	6865.67 ± 13.58
EE$_3$	59 ± 1	67 ± 2	71 ± 1	0.66 ± 0.02	0.58 ± 0.01	0.50 ± 0.03	6.07 ± 0.01	6.32 ± 0.03	4.81 ± 0.02	5364.00 ± 4.36	7962.67 ± 1.53	6703.00 ± 7.94
AC$_1$	60 ± 2	62 ± 1	68 ± 2	0.68 ± 0.02	0.62 ± 0.02	0.59 ± 0.02	6.35 ± 0.01	6.65 ± 0.01	6.24 ± 0.01	6032.00 ± 30.35	7211.67 ± 18.93	6621.33 ± 17.62
AC$_2$	62 ± 2	63 ± 2	70 ± 2	0.71 ± 0.02	0.67 ± 0.02	0.61 ± 0.02	6.33 ± 0.02	6.80 ± 0.02	6.07 ± 0.07	5163.00 ± 13.75	5421.00 ± 8.54	7377.33 ± 10.02
AC$_3$	58 ± 1	59 ± 1	64 ± 1	0.57 ± 0.02	0.54 ± 0.02	0.51 ± 0.01	6.01 ± 0.01	5.57 ± 0.02	5.32 ± 0.02	6140.00 ± 43.49	6810.33 ± 10.50	6275.33 ± 20.79
	p (Fm) < 0.001 p (Tq) < 0.001 p (Tm) < 0.001 p (Fm*Tq*Tm) < 0.001 LSD = 0.38845			p (Fm) < 0.001 p (Tq) < 0.001 p (Tm) < 0.001 p (Fm*Tq*Tm) < 0.001 LSD = 0.00415			p (Fm) < 0.001 p (Tq) < 0.001 p (Tm) < 0.001 p (Fm*Tq*Tm) < 0.001 LSD = 0.00556			p (Fm) < 0.001 p (Tq) < 0.001 p (Tm) < 0.001 p (Fm*Tq*Tm) < 0.001 LSD = 4.63945		

Treatment	TOC (%)			TKN (%)			TP (%)			TK (%)		
	0D	45D	90D	0D	45D	90D	0D	45D	90D	0D	45D	90D
EF$_1$	18.89 ± 0.02	13.02 ± 0.03	12.06 ± 0.08	0.67 ± 0.01	0.82 ± 0.06	0.97 ± 0.01	0.299 ± 0.007	0.325 ± 0.008	0.349 ± 0.003	0.114 ± 0.003	0.340 ± 0.011	0.409 ± 0.014
EF$_2$	19.34 ± 0.04	12.09 ± 0.08	11.67 ± 0.23	0.66 ± 0.01	0.85 ± 0.06	1.03± 0.02	0.266 ± 0.0010	0.335 ± 0.007	0.352 ± 0.007	0.089 ± 0.004	0.386 ± 0.007	0.412 ± 0.011
EF$_3$	17.76 ± 0.02	11.92 ± 0.12	11.89 ± 0.14	0.72 ± 0.02	0.78 ± 0.03	0.86 ± 0.02	0.302 ± 0.004	0.320 ± 0.003	0.346 ± 0.014	0.096 ± 0.000	0.201 ± 0.009	0.306 ± 0.000
EE$_1$	17.16 ± 0.04	12.06 ± 0.04	11.99 ± 0.01	0.62 ± 0.02	0.68 ± 0.02	0.90 ± 0.03	0.297 ± 0.004	0.309 ± 0.004	0.318 ± 0.004	0.106 ± 0.011	0.315 ± 0.008	0.409 ± 0.005

EE_2	18.24 ± 0.10	12.53 ± 0.09	11.52 ± 0.08	0.55 ± 0.03	0.70 ± 0.05	1.04 ± 0.06	0.301 ± 0.008	0.331 ± 0.010	0.348 ± 0.006	0.111 ± 0.009	0.377 ± 0.010	0.433 ± 0.009
EE_3	17.02 ± 0.03	11.99 ± 0.03	11.76 ± 0.22	0.61 ± 0.03	0.71 ± 0.06	0.80 ± 0.04	0.307 ± 0.004	0.316 ± 0.011	0.334 ± 0.017	0.107 ± 0.010	0.232 ± 0.008	0.381 ± 0.001
AC_1	15.59 ± 1.64	14.81 ± 0.13	13.70 ± 0.04	0.49 ± 0.03	0.55 ± 0.08	0.61 ± 0.09	0.308 ± 0.003	0.316 ± 0.006	0.323 ± 0.007	0.080 ± 0.003	0.143 ± 0.009	0.258 ± 0.006
AC_2	16.36 ± 0.55	14.67 ± 0.15	13.15 ± 0.05	0.52 ± 0.02	0.57 ± 0.03	0.72 ± 0.14	0.303 ± 0.005	0.309 ± 0.004	0.331 ± 0.018	0.077 ± 0.000	0.137 ± 0.015	0.247 ± 0.016
AC_3	17.62 ± 0.53	14.73 ± 0.04	13.29 ± 0.08	0.56 ± 0.02	0.65 ± 0.10	0.72 ± 0.07	0.297 ± 0.003	0.303 ± 0.004	0.313 ± 0.009	0.098 ± 0.003	0.119 ± 0.003	0.281 ± 0.007
		p (Fm) = 0.170			p (Fm) < 0.05			p (Fm) = 0.145			p (Fm) < 0.001	
		p (Tq) < 0.001			p (Tq) < 0.001			p (Tq) < 0.001			p (Tq) < 0.001	
		p (Tm) < 0.001			p (Tm) < 0.001			p (Tm) < 0.001			p (Tm) < 0.001	
		p (Fm*Tq*Tm) < 0.001			p (Fm*Tq*Tm) = 0.056			p (Fm*Tq*Tm) < 0.05			p (Fm*Tq*Tm) < 0.001	
		LSD = 0.09816			LSD = 0.01402			LSD = 0.00222			LSD = 0.00229	

0D, 45D, 90D = 0-90 days' compost; WHC= Water holding capacity; BD = Bulk Density; EC= Electrical conductivity; TOC= Total organic C; TKN= Total Kjeldahl N; TP = Total Phosphorus; TK = Total Potassium; Fm = Feed mixture; Tq = Technique; Tm = Time; LSD = Least significant difference

APPENDIX 3. Effects of different treatments on the concentration of heavy metals in the composts (values represent Mean ± SD)

Treatment	Cd (mg kg^{-1})			Cr (mg kg^{-1})			Cu (mg kg^{-1})		
	0D	**45D**	**90D**	**0D**	**45D**	**90D**	**0D**	**45D**	**90D**
EF$_1$	2.35 ± 0.05	1.82 ± 0.02	1.40 ± 0.02	64.57 ± 0.03	52.89 ± 0.02	50.84 ± 0.05	144.52 ± 0.03	114.13± 0.05	64.67 ± 0.02
EF$_2$	2.53 ± 0.08	1.65 ± 0.03	BDL	74.46 ± 0.04	61.86 ± 0.03	46.23 ± 0.04	115.73 ± 0.03	90.25 ± 0.03	61.65 ± 0.04
EF$_3$	2.88 ± 0.07	1.92 ± 0.02	BDL	115.18 ± 0.03	92.94 ± 0.56	60.68 ± 0.02	118.65 ± 0.03	96.13 ± 0.02	62.67 ± 0.02
EE$_1$	2.13 ± 0.04	1.43 ± 0.03	0.09 ± 0.02	80.35 ± 0.05	64.34 ± 0.03	23.86 ± 0.03	126.22 ± 0.02	103.80 ± 0.56	63.68 ± 0.03
EE$_2$	2.61 ± 0.04	1.54 ± 0.03	BDL	83.15 ± 0.03	65.72 ± 0.03	20.13 ± 0.03	113.64 ± 0.03	90.93 ± 0.03	60.65 ± 0.04
EE$_3$	3.88 ± 0.03	2.30 ± 0.02	BDL	104.66 ± 0.08	88.94 ± 0.03	33.04 ± 0.04	187.27 ± 0.02	117.96 ± 0.03	65.68 ± 0.02
AC$_1$	2.75 ± 0.03	2.02 ± 0.02	1.24 ± 0.03	96.34 ± 0.05	88.01 ± 0.04	74.06 ± 0.02	126.13 ± 0.02	95.84 ± 0.03	86.65 ± 0.03
AC$_2$	2.27 ± 0.04	1.75 ± 0.02	1.19 ± 0.02	122.53 ± 0.08	105.38 ± 0.02	107.04 ± 0.03	151.67 ± 0.03	135.02 ± 0.03	137.66 ± 0.04
AC$_3$	2.55 ± 0.04	2.04 ± 0.02	2.44 ± 0.03	276.55 ± 0.05	232.27 ± 0.02	223.45 ± 0.03	177.04 ± 0.05	161.07 ± 0.03	168.64 ± 0.04
	p (Fm) < 0.001 *p* (Tq) < 0.001 *p* (Tm) < 0.001 *p* (Fm*Tq*Tm) < 0.001 LSD = 0.00970			*p* (Fm) < 0.001 *p* (Tq) < 0.001 *p* (Tm) < 0.001 *p* (Fm*Tq*Tm) < 0.001 LSD = 0.03091			*p* (Fm) < 0.001 *p* (Tq) < 0.001 *p* (Tm) < 0.001 *p* (Fm*Tq*Tm) < 0.001 LSD = 0.03037		

Treatment	Ni (mg kg^{-1})			Pb (mg kg^{-1})			Zn (mg kg^{-1})		
	0D	**45D**	**90D**	**0D**	**45D**	**90D**	**0D**	**45D**	**90D**
EF$_1$	83.54 ± 0.02	79.57 ± 0.02	76.84 ± 0.02	56.52 ± 0.02	21.84 ± 0.03	BDL	93.30 ± 0.02	110.05 ± 0.04	90.92 ± 0.02
EF$_2$	83.55 ± 0.02	74.35 ± 0.03	50.54 ± 0.03	73.54 ± 0.02	28.44 ± 0.03	BDL	81.55 ± 0.02	97.05 ± 0.02	70.33 ± 0.02
EF$_3$	112.37 ± 0.01	85.44 ± 0.03	70.46 ± 0.02	77.95 ± 0.03	28.74 ± 0.03	8.05 ± 0.03	93.85 ± 0.02	109.83 ± 0.03	70.32 ± 0.04
EE$_1$	88.07 ± 0.02	66.03 ± 0.03	74.74 ± 0.04	58.40 ± 0.02	22.65 ± 0.03	BDL	80.85 ± 0.03	92.22 ± 0.02	72.13 ± 0.02
EE$_2$	124.41 ± 0.04	99.54 ± 0.03	80.82 ± 0.02	72.14 ± 0.03	27.83 ± 0.03	BDL	107.25 ± 0.02	112.57 ± 0.03	69.90 ± 0.03
EE$_3$	80.23 ± 0.02	60.96 ± 0.03	51.64 ± 0.05	84.88 ± 0.03	31.95 ± 0.03	6.05 ± 0.04	84.23 ± 0.03	95.17 ± 0.04	71.72 ± 0.06
AC$_1$	105.82 ± 0.02	132.37 ± 0.01	81.48 ± 0.01	82.06 ± 0.02	31.85 ± 0.03	24.25 ± 0.03	64.76 ± 0.04	77.73 ± 0.03	87.66 ± 0.03
AC$_2$	112.86 ± 0.03	146.53 ± 0.01	113.42 ± 0.03	81.66 ± 0.03	31.53 ± 0.02	25.93 ± 0.02	84.88 ± 0.01	93.36 ± 0.04	81.36 ± 0.03

AC_3	173.03 ± 0.03	183.39 ± 0.03	170.06 ± 0.04	83.75 ± 0.03	31.43 ± 0.03	23.84 ± 0.03	65.06 ± 0.02	72.88 ± 0.01	79.15 ± 0.03
	p (Fm) < 0.001 p (Tq) < 0.001 p (Tm) < 0.001 p (Fm*Tq*Tm) < 0.001 LSD = 0.00706			p (Fm) < 0.001 p (Tq) < 0.001 p (Tm) < 0.001 p (Fm*Tq*Tm) < 0.001 LSD = 0.00722			p (Fm) < 0.001 p (Tq) < 0.001 p (Tm) < 0.001 p (Fm*Tq*Tm) < 0.001 LSD = 0.00783		

0D, 45D, 90D = 0-90 days' compost; BDL = Below detection level; Fm = Feed mixture; Tq = Technique; Tm = Time; LSD = Least significant difference

APPENDIX 4. Changes in the bacterial composition and enzymatic activity of the composts (values represent Mean ± SD)

Treatment	Total Bacteria (10^7 CFU g^{-1} soil)			N-fixing bacteria (10^7 CFU g^{-1} soil)			P-solubilizing bacteria (10^7 CFU g^{-1} soil)		
	0D	45D	90D	0D	45D	90D	0D	45D	90D
EF_1	103.00 ± 6.24	208.67 ± 1.53	109.00 ± 1.00	11.00 ± 2.00	128.67 ± 7.51	77.00 ± 2.00	13.00 ± 1.00	131.67 ± 2.52	94.67 ± 4.04
EF_2	109.67 ± 7.51	235.00 ± 6.00	121.33 ± 2.52	15.33 ± 1.53	147.00 ± 4.36	89.00 ± 1.00	13.67 ± 1.53	109.33 ± 1.53	42.33 ± 3.51
EF_3	97.67 ± 9.02	194.67 ± 4.51	103.33 ± 6.81	15.67 ± 4.16	134.33 ± 5.03	81.00 ± 1.00	11.33 ± 1.53	146.33 ± 4.04	99.33 ± 2.52
EE_1	108.33 ± 6.81	241.67 ± 1.53	122.00 ± 1.00	12.33 ± 2.08	157.33 ± 5.03	96.00 ± 2.65	20.33 ± 3.06	92.00 ± 3.61	19.67 ± 1.53
EE_2	105.33 ± 6.51	269.00 ± 7.55	131.33 ± 10.02	22.00 ± 3.61	175.33 ± 5.03	105.33 ± 4.16	19.67 ± 1.53	112.00 ± 3.00	59.33 ± 7.37
EE_3	106.33 ± 14.36	207.00 ± 4.36	99.00 ± 11.14	19.33 ± 2.52	125.67 ± 8.14	75.33 ± 3.21	11.00 ± 1.00	67.33 ± 4.73	12.67 ± 2.08
AC_1	111.00 ± 11.79	167.67 ± 2.08	90.00 ± 1.00	5.67 ± 4.04	101.67 ± 11.02	64.33 ± 4.04	0.00 ± 0.00	44.00 ± 4.00	7.33 ± 4.73
AC_2	108.00 ± 10.15	181.00 ± 1.00	82.33 ± 7.64	4.67 ± 3.21	95.33 ± 6.51	61.33 ± 5.13	0.00 ± 0.00	52.00 ± 1.00	10.33 ± 5.03
AC_3	103.00 ± 10.58	177.00 ± 2.00	86.33 ± 8.74	7.33 ± 4.73	104.33 ± 8.33	65.00 ± 5.29	0.00 ± 0.00	28.33 ± 4.73	8.33 ± 3.79
	p (Fm) < 0.001 p (Tq) < 0.001 p (Tm) < 0.001 p (Fm*Tq*Tm) < 0.001 LSD = 1.95046			p (Fm) < 0.001 p (Tq) < 0.001 p (Tm) < 0.001 p (Fm*Tq*Tm) < 0.001 LSD = 1.34392			p (Fm) < 0.001 p (Tq) < 0.001 p (Tm) < 0.001 p (Fm*Tq*Tm) < 0.001 LSD = 0.88425		

Treatment	Urease (µg N g^{-1} h^{-1})			Dehydrogenase (µg TPF g^{-1} h^{-1})			Alkaline-Phosphatase (µg P g^{-1} h^{-1})		
	0D	45D	90D	0D	45D	90D	0D	45D	90D
EF_1	102.33 ± 8.66	330.00 ± 8.66	306.00 ± 5.29	71.23 ± 2.46	120.26 ± 17.25	84.28 ± 15.46	112.46 ± 3.81	219.47 ± 2.93	234.74 ± 8.27
EF_2	110.00 ± 5.03	364.67 ± 5.03	320.00 ± 5.00	70.33 ± 18.15	138.48 ± 21.14	84.80 ± 10.01	131.93 ± 2.70	224.09 ± 32.16	237.89 ± 1.39
EF_3	101.67 ± 5.86	296.67 ± 5.86	254.67 ± 4.51	69.71 ± 23.75	89.29 ± 4.49	79.43 ± 8.72	152.28 ± 2.19	217.72 ± 3.81	216.49 ± 9.88
EE_1	104.33 ± 4.58	274.00 ± 4.58	242.33 ± 2.08	66.41 ± 8.13	121.31 ± 8.05	116.71 ± 9.19	158.42 ± 1.58	255.44 ± 2.90	225.61 ± 2.70
EE_2	121.33 ± 4.73	323.67 ± 4.73	264.00 ± 5.29	70.70 ± 19.11	115.45 ± 8.95	78.03 ± 6.06	171.40 ± 3.38	244.04 ± 2.49	258.25 ± 1.10
EE_3	97.33 ± 2.52	252.33 ± 2.52	255.67 ± 4.04	69.55 ± 10.35	111.75 ± 12.09	76.29 ± 10.01	181.23 ± 0.30	259.82 ± 1.10	211.05 ± 4.82
AC_1	101.00 ± 1.00	190.00 ± 1.00	180.00 ± 5.00	59.48 ± 9.30	95.64 ± 12.29	70.80 ± 7.78	171.05 ± 1.82	218.95 ± 2.73	153.16 ± 2.29
AC_2	104.33 ± 1.00	200.00 ± 1.00	199.00 ± 1.00	42.27 ± 5.70	111.86 ± 10.96	63.28 ± 3.48	175.26 ± 2.93	223.33 ± 3.08	143.51 ± 4.29
AC_3	97.33 ± 1.00	176.00 ± 1.00	170.00 ± 2.00	47.10 ± 5.44	102.05 ± 5.82	67.47 ± 5.31	179.82 ± 1.32	229.12 ± 7.18	168.77 ± 6.05

p (Fm) < 0.001 *p* (Tq) < 0.001 *p* (Tm) < 0.001 *p* (Fm*Tq*Tm) < 0.001 LSD = 1.08192	*p* (Fm) < 0.001 *p* (Tq) < 0.001 *p* (Tm) < 0.001 *p* (Fm*Tq*Tm) < 0.001 LSD = 3.17956	*p* (Fm) < 0.001 *p* (Tq) < 0.001 *p* (Tm) < 0.001 *p* (Fm*Tq*Tm) < 0.001 LSD = 1.99432

0D, 45D, 90D = 0-90 days' compost; Fm = Feed mixture; Tq = Technique; Tm = Time; LSD = Least significant difference

APPENDIX 5. Pearson's correlation between compost quality index (CQI) and the different parameters

		pH	EC	WHC	BD	TOC	TKN	TP	TK
CQI	Pearson Correlation	-0.624**	0.444**	0.924**	-0.741**	0.689**	0.897**	0.738**	0.882**
	Sig. (2-tailed)	.000	.000	.000	.000	.000	.000	.000	.000
	N	81	81	81	81	81	81	81	81
		Cd	**Pb**	**Cu**	**Cr**	**Ni**	**Zn**	**EW Biomass**	**EW count**
CQI	Pearson Correlation	-0.757**	-0.751**	-0.753**	-0.569**	-0.541**	-0.067^{ns}	0.671**	0.850**
	Sig. (2-tailed)	.000	.000	.000	.000	.000	.555	.000	.000
	N	81	81	81	81	81	81	81	81
		Total Bacteria	**N-fixing bacteria**	**P-solubilizing bacteria**	**Urease**	**Dehydrogenase**	**Alkaline-Phosphatase**		
CQI	Pearson Correlation	0.209^{ns}	0.526**	0.463**	0.751**	0.361**	0.632**		
	Sig. (2-tailed)	0.061	.000	.000	.000	.000	.000		
	N	81	81	81	81	81	81		

*** = Correlation is significant at the 0.01 level (2-tailed).*
** = Correlation is significant at the 0.05 level (2-tailed).*
ns = non-significant
WHC= Water holding capacity; BD = Bulk Density; EC= Electrical conductivity; TOC= Total organic C; TKN= Total Kjeldahl N; TP = Total Phosphorus; TK = Total Potassium

APPENDIX 6. Temporal changes in the heavy metal fractions (mg kg^{-1}) of the two ORS vermicomposts

Treatments	Water soluble (F1)	Exchangeable (F2)	Carbonate bound (F3)	Fe-Mn bound (F4)	Organic bound (F5)	Residual fraction (F6)
Cd						
EF 0th Day	0.35 ± 0.03	0.59 ± 0.03	0.81 ± 0.05	1.36 ± 0.14	0.79 ± 0.04	1.27 ± 0.04
EF 90th Day	0.23 ± 0.02	0.41 ± 0.03	0.60 ± 0.08	1.03 ± 0.04	0.67 ± 0.04	1.08 ± 0.04
EE 0th Day	0.61 ± 0.07	0.79 ± 0.03	1.02 ± 0.04	1.51 ± 0.09	0.75 ± 0.03	1.34 ± 0.03
EE 90th Day	0.25 ± 0.04	0.66 ± 0.04	0.60 ± 0.04	0.62 ± 0.06	0.35 ± 0.03	1.02 ± 0.02
	p (Tm) < 0.001; p (Tq) < 0.001; p (Tm ×Tq) < 0.001; LSD (Tq) and (Tm) = 0.019; LSD (Tm ×Tq) = 0.027					
Cr						
EF 0th Day	5.11 ± 0.04	4.24 ± 0.05	7.37 ± 0.38	9.18 ± 0.07	7.66 ± 0.07	10.60 ± 0.17
EF 90th Day	4.86 ± 0.05	3.87 ± 0.06	6.89 ± 0.20	6.61 ± 0.24	7.18 ± 0.25	10.31 ± 0.08
EE 0th Day	5.37 ± 0.08	5.76 ± 0.28	7.47 ± 0.33	5.25 ± 0.09	7.74 ± 0.08	11.58 ± 0.16
EE 90th Day	4.66 ± 0.12	5.18 ± 0.07	7.11 ± 0.08	4.45 ± 0.34	7.56 ± 0.12	10.07 ± 0.05
	p (Tm) < 0.001; p (Tq) < 0.001; p (Tm ×Tq) < 0.001; LSD (Tq) and (Tm) = 0.032; LSD (Tm ×Tq) = 0.046					
Cu						
EF 0th Day	0.87 ± 0.05	1.06 ± 0.07	4.84± 0.14	21.38 ± 0.25	8.09 ± 0.03	81.38 ± 0.35
EF 90th Day	0.44 ± 0.05	0.75± 0.12	3.13 ± 0.04	14.34 ± 0.30	2.82 ± 0.07	62.95 ± 0.44
EE 0th Day	1.07 ± 0.03	1.61 ± 0.06	7.79 ± 0.11	50.69 ± 0.22	7.18 ± 0.08	74.79 ± 0.31
EE 90th Day	0.78 ± 0.04	0.86 ± 0.06	4.19 ± 0.05	36.53 ± 0.33	4.39 ± 0.14	41.21 ± 0.08
	p (Tm) < 0.001; p (Tq) < 0.001; p (Tm ×Tq) < 0.001; LSD (Tq) and (Tm) = 0.046; LSD (Tm ×Tq) = 0.065					
Pb						

EF 0th Day	1.81 ± 0.06	0.60 ± 0.04	4.47 ± 0.04	6.47 ± 0.06	16.29 ± 0.17	41.58 ± 0.31
EF 90th Day	0.96 ± 0.04	0.55 ± 0.03	4.17 ± 0.11	4.24 ± 0.08	11.77 ± 0.22	40.60 ± 0.36
EE 0th Day	0.51 ± 0.04	0.52 ± 0.04	6.35 ± 0.11	4.12 ± 0.04	14.57 ± 0.34	43.38 ± 0.21
EE 90th Day	0.49 ± 0.04	0.50 ± 0.05	5.15 ± 0.05	3.88 ± 0.09	12.53 ± 0.40	38.36 ± 0.08
	p (Tm) < 0.001; p (Tq) < 0.001; p (Tm ×Tq) < 0.001; LSD (Tq) and (Tm) = 0.038; LSD (Tm ×Tq) = 0.054					
Ni						
EF 0th Day	1.81 ± 0.05	1.59 ± 0.06	18.61 ± 0.30	18.48 ± 0.38	20.54 ± 0.10	29.08 ± 0.08
EF 90th Day	1.43 ± 0.04	1.46 ± 0.05	14.58 ± 0.11	16.34 ± 0.10	17.03 ± 0.06	25.61 ± 0.23
EE 0th Day	1.11 ± 0.05	1.81 ± 0.06	16.79 ± 0.14	14.66 ± 0.30	15.38 ± 0.09	33.27 ± 0.19
EE 90th Day	0.49 ± 0.03	1.36 ± 0.10	13.18 ± 0.08	13.32 ± 0.13	14.47 ± 0.07	20.17 ± 0.08
	p (Tm) < 0.001; p (Tq) < 0.001; p (Tm ×Tq) < 0.001; LSD (Tq) and (Tm) = 0.047; LSD (Tm ×Tq) = 0.067					
Zn						
EF 0th Day	1.36 ± 0.06	1.92 ± 0.03	3.01 ± 0.04	24.62 ± 0.16	71.48 ± 0.48	92.67 ± 0.09
EF 90th Day	0.90 ± 0.04	0.83 ± 0.05	2.19 ± 0.06	22.84 ± 0.34	60.15 ± 0.08	65.45 ± 0.22
EE 0th Day	1.82 ± 0.06	1.66 ± 0.12	4.23 ± 0.11	17.56 ± 0.33	57.19 ± 0.18	115.90 ± 3.96
EE 90th Day	1.16 ± 0.06	1.18 ± 0.04	2.56 ± 0.11	12.57 ± 0.43	45.61 ± 0.44	62.24 ± 0.27
	p (Tm) < 0.001; p (Tq) < 0.001; p (Tm ×Tq) < 0.001; LSD (Tq) and (Tm) = 0.045; LSD (Tm ×Tq) = 0.064					

**EF - Vermicomposting with E. fetida; EE - Vermicomposting with E. eugeniae; Tq - Technique; Tm - Time; LSD - Least significant difference*

APPENDIX 7. Temporal changes in the C fractions of the two ORS vermicomposts

Treatments	Exchangeable (%)	Fulvic acid C (%)	Humic acid C (%)
EF 0th Day	11.77 ± 0.58	3.70 ± 0.57	1.54 ± 0.52
EF 90th Day	9.35 ± 0.65	5.72 ± 0.58	3.36 ± 0.46
EE 0th Day	11.82 ± 0.57	4.83 ± 0.71	2.61 ± 0.52
EE 90th Day	9.12 ± 1.01	5.73 ± 0.57	4.56 ± 0.69
p (Tm) < 0.001; p (Tq) < 0.001; p (Tm ×Tq) < 0.001; LSD (Tq) and (Tm) = 0.149; LSD (Tm ×Tq) = 0.258			

**EF - Vermicomposting with E. fetida; EE - Vermicomposting with E. eugeniae; Tq - Technique; Tm - Time; LSD - Least significant difference*

APPENDIX 8. Pearson's correlation between vermiremediation benefit index (VBI) and the different parameters of the earthworm systems EF and EE

EF		EC	WHC	TOC	N	P	K	$Cd_{Compost}$	$Cr_{Compost}$	$Cu_{Compost}$	$Pb_{Compost}$	$Ni_{Compost}$
VBI	Pearson Correlation	.034^{ns}	.629**	.858**	.011^{ns}	.013^{ns}	.149^{ns}	.233^{ns}	.942**	.890**	.995**	.784**
	Sig. (2-tailed)	.103	.000	.000	.113	.192	.086	.059	.000	.000	.000	.000

VBI	Pearson Correlation	$Zn_{Compost}$	Cd_EW	Cr_EW	Cu_EW	Pb_EW	Ni_EW	Zn_EW	EW_count	EW_length	EW_biomass
	Sig. (2-tailed)	.031^{ns}	.091^{ns}	.999**	.924**	.596**	.615**	.939**	.866**	.668**	.910**
	N	.077	.062	.000	.000	.000	.000	.000	.000	.000	.000

EE		EC	WHC	TOC	N	P	K	$Cd_{Compost}$	$Cr_{Compost}$	$Cu_{Compost}$	$Pb_{Compost}$	$Ni_{Compost}$
VBI	Pearson Correlation	.708**	.125^{ns}	.993**	.614**	.563**	.766**	.497*	.647**	.900**	.116^{ns}	.668**
	Sig. (2-tailed)	.000	.080	.000	.000	.000	.000	.000	.000	.000	.075	.000

VBI		$Zn_{Compost}$	Cd_EW	Cr_EW	Cu_EW	Pb_EW	Ni_EW	Zn_EW	EW_count	EW_length	EW_biomass
	Pearson Correlation	.786**	.242^{ns}	.970**	.863**	.999**	.466*	.402*	.990**	.998**	.970**
	Sig. (2-tailed)	.000	.058	.000	.000	.000	.000	.000	.000	.000	.000

*** = Correlation is significant at the 0.01 level (2-tailed); * = Correlation is significant at the 0.05 level (2-tailed).; ns = non-significant*

**EF - Vermicomposting with E. fetida; EE - Vermicomposting with E. eugeniae; EC – electrical conductivity; WHC – water holding capacity; TOC – total organic C*

**Compost – reduction of metal concentration in compost sample*

**EW – accumulation of metal in earthworm gut*

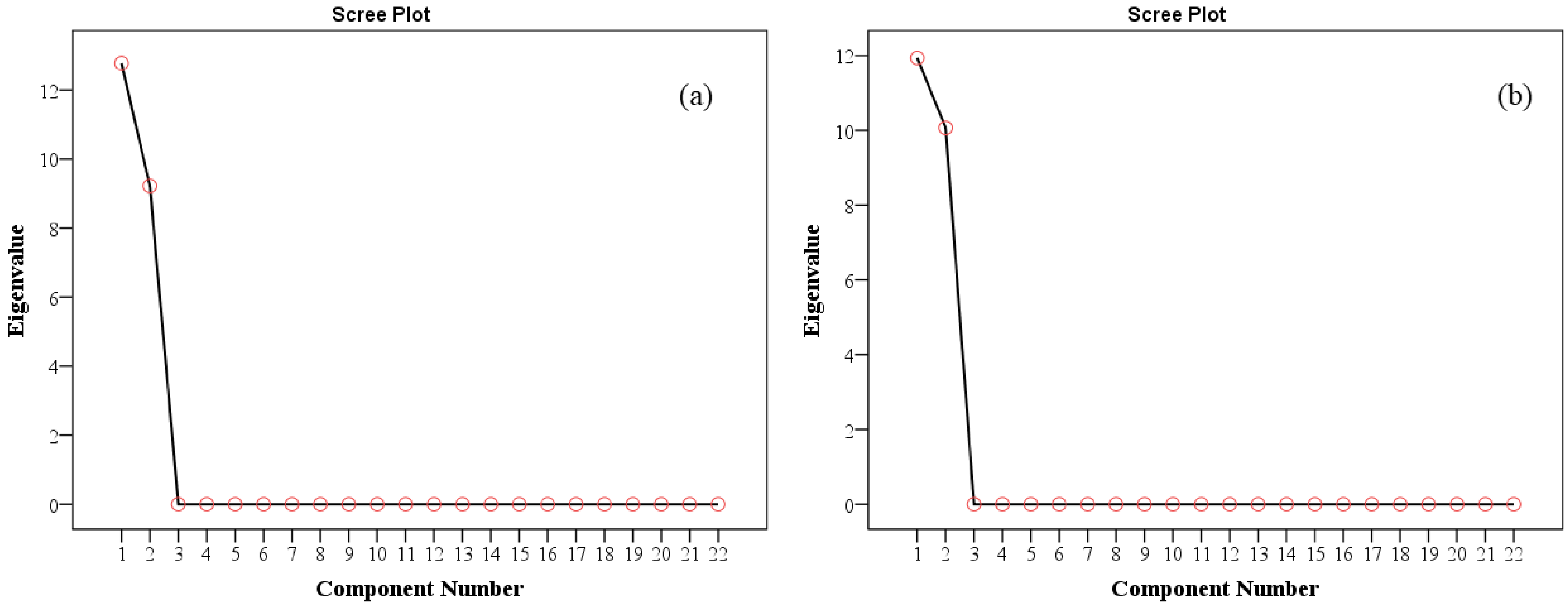

APPENDIX 9. Scree plots depicting the component numbers with respect to the datasets of (a) *Eudrilus eugeniae* and (b) *Eisenia fetida* vermicomposting systems

APPENDIX 10. Phytochemical composition of tomato and cabbage under the different treatments (mean and SD)

Treatments	Chlorophyll a (mg/g)		Chlorophyll b (mg/g)		Chlorophyll Total (mg/g)		Carotenoids (mg/g)		B-carotene (mg/g)		Flavonoid (mg/g)		Phenol (mg/g)		Lycopene (mg/g)	
Tomato	**Mean**	**SD**	**Mean**	**SD**	**Mean**	**SD**	**Mean**	**SD**	**Mean**	**SD**	**Mean**	**SD**	**Mea n**	**SD**	**Mean**	**SD**
Control	2.13	0.01	1.22	0.02	3.35	0.03	1.74	0.04	0.050	0.004	12.51	0.44	14.15	0.22	1.06	0.06
NPK_{100}	4.01	0.58	1.64	0.04	5.65	0.55	2.22	0.02	0.053	0.002	12.66	0.57	15.77	0.22	1.08	0.03
EF_{25}	4.77	0.04	1.77	0.05	6.53	0.08	2.13	0.03	0.061	0.002	14.36	0.02	16.17	0.24	1.09	0.04
EF_{50}	5.35	0.01	1.85	0.03	7.20	0.02	2.34	0.02	0.064	0.001	15.40	0.02	16.78	0.20	1.24	0.03
EF_{100}	6.93	0.04	1.83	0.03	8.75	0.07	2.43	0.03	0.059	0.003	14.37	0.02	15.24	0.21	1.33	0.02
EE_{25}	5.22	0.03	1.86	0.04	7.08	0.03	2.23	0.04	0.062	0.003	14.35	0.02	16.35	0.09	1.08	0.01
EE_{50}	5.91	0.04	2.16	0.03	8.07	0.02	2.29	0.02	0.064	0.002	15.42	0.03	16.93	0.12	1.27	0.03
EE_{100}	5.51	0.02	2.06	0.01	7.57	0.03	2.44	0.01	0.060	0.001	14.39	0.02	15.48	0.12	1.35	0.03
Cabbage																
Control	0.92	0.02	0.23	0.02	1.14	0.01	0.66	0.04	0.015	0.002	19.37	0.81	14.83	0.31	0.16	0.01
NPK_{100}	1.04	0.01	0.35	0.03	1.38	0.04	0.94	0.03	0.017	0.002	21.80	0.56	15.13	0.40	0.20	0.02
EF_{25}	1.05	0.01	0.38	0.02	1.43	0.02	1.05	0.03	0.017	0.002	22.67	0.74	14.90	0.40	0.21	0.01
EF_{50}	1.15	0.02	0.38	0.02	1.53	0.03	1.00	0.02	0.019	0.002	23.57	2.23	15.57	0.35	0.23	0.01
EF_{100}	1.23	0.01	0.43	0.03	1.66	0.04	1.06	0.02	0.020	0.001	23.60	1.71	15.90	0.20	0.24	0.01
EE_{25}	1.03	0.02	0.29	0.03	1.32	0.05	0.94	0.02	0.021	0.002	22.23	0.32	14.57	0.38	0.20	0.02
EE_{50}	1.21	0.02	0.34	0.03	1.55	0.04	1.02	0.02	0.021	0.001	22.43	0.40	15.40	0.26	0.22	0.01
EE_{100}	1.33	0.02	0.35	0.03	1.69	0.04	1.06	0.01	0.022	0.002	23.87	0.35	16.20	0.30	0.24	0.01

Plate 8. EF_1, EF_2, and EF_3 treatments of the *Eisenia*-system

Plate 9. EE_1, EE_2, and EE_3 treatments of the *Eudrilus*-system

Plate 10. AC_1, AC_2, and AC_3 treatments of the non-earthworm system

Plate 11. Land preparation for the cultivation of tomato and cabbage

Plate 12. Plantation of tomato under different treatments

Plate 12. Plantation of cabbage under different treatments

Plate 12. Growth of tomato under different treatments

Plate 12. Growth of cabbage under different treatments

REFERENCES

AAU, A.A.U., DOA, D. of A., 2015. Package of Practices for Rabi crops of Assam 1–105.

Abdullah, N., Chin, N.L., Mokhtar, M.N., Taip, F.S., 2013. Effects of bulking agents, load size or starter cultures in kitchen-waste composting. Int. J. Recycl. Org. Waste Agric. 2, 1–10.

Abdulqader, M.A., Syed-Hassan, S.S.A., Jawad, A.H., Abed, O., 2021. Characterization study of oily sludge produced from North Refineries Company Baiji to determine the suitability for conversion into solid fuel.

Adhikari, B.K., Barrington, S., Martinez, J., King, S., 2008. Characterization of food waste and bulking agents for composting. Waste Manag. 28, 795–804. https://doi.org/https://doi.org/10.1016/j.wasman.2007.08.018

Aguelmous, A., Lahsaini, S., ElFels, L., Souabi, S., Zamama, M., Hafidi, M., 2016. Assessment of organo-mineral fraction during storage of oil refinery sludge. Moroccan J. Chem. 4, J-Chem.

Ahmed, N., Al-Mutairi, K.A., 2022. Earthworms effect on microbial population and soil fertility as well as their interaction with agriculture practices. Sustainability 14, 7803.

Ahmed, R., Deka, H., 2022. Vermicomposting of patchouli bagasse—A byproduct of essential oil industries employing Eisenia fetida. Environ. Technol. Innov. 25, 102232. https://doi.org/https://doi.org/10.1016/j.eti.2021.102232

Aira, M., Pérez-Losada, M., Domínguez, J., 2019. Microbiome dynamics during cast ageing in the earthworm Aporrectodea caliginosa. Appl. Soil Ecol. 139, 56–63.

Aksakal, E.L., Sari, S., Angin, I., 2016. Effects of vermicompost application on soil aggregation and certain physical properties. L. Degrad. Dev. 27, 983–995.

Al-Hazmi, H.E., Mohammadi, A., Hejna, A., Majtacz, J., Esmaeili, A., Habibzadeh, S., Saeb, M.R., Badawi, M., Lima, E.C., Mąkinia, J., 2023. Wastewater reuse in agriculture: Prospects and challenges. Environ. Res. 236, 116711. https://doi.org/https://doi.org/10.1016/j.envres.2023.116711

Al-Mutairi, N., Bufarsan, A., Al-Rukaibi, F., 2008. Ecorisk evaluation and treatability potential of soils contaminated with petroleum hydrocarbon-based fuels. Chemosphere

74, 142–148. https://doi.org/10.1016/j.chemosphere.2008.08.020

Al Jaouni, S., Selim, S., Hassan, S.H., Mohamad, H.S.H., Wadaan, M.A.M., Hozzein, W.N., Asard, H., AbdElgawad, H., 2019. Vermicompost supply modifies chemical composition and improves nutritive and medicinal properties of date palm fruits from Saudi Arabia. Front. Plant Sci. 10, 424.

Aladesida, A.A., Kehinde, F.O., D Umoren, O., Ariwoola, N.O., 2024. Heavy metals concentrations in earthworms (Eudrilus eugeniae) exposed to water and sediments from Ogun river. J. Nat. Sci. Eng. Technol. 23, 83–90.

Alburquerque, J.A., Gonzálvez, J., García, D., Cegarra, J., 2006. Effects of bulking agent on the composting of “alperujo”, the solid by-product of the two-phase centrifugation method for olive oil extraction. Process Biochem. 41, 127–132.

Alexandrovich, D.R., Sergeevich, M.S., 2018. Innovations aimed at the secondary use of waste of PJSC RN-Komsomolsk Oil Refinery, in: Scientific and Technical Conference of Students of the 10 Th and 11 Th Grades of ROSNEFT.

Ananthavalli, R., Ramadas, V., John Paul, J.A., Karunai Selvi, B., Karmegam, N., 2019. Seaweeds as bioresources for vermicompost production using the earthworm, Perionyx excavatus (Perrier). Bioresour. Technol. 275, 394–401. https://doi.org/https://doi.org/10.1016/j.biortech.2018.12.091

Armstrong, F.A.J., 1963. Determination of Nitrate in Water Ultraviolet Spectrophotometry. Anal. Chem. 35, 1292–1294.

Arockiam JeyaSundar, P.G.S., Ali, A., Guo, di, Zhang, Z., 2020. Waste treatment approaches for environmental sustainability, Microorganisms for Sustainable Environment and Health. INC. https://doi.org/10.1016/B978-0-12-819001-2.00006-1

Arumugaperumal, A., Sudalaimani, D.K., Arumugaswami, V., Sivasubramaniam, S., 2022. Draft Genome Sequence of the Earthworm Eudrilus eugeniae. Curr. Genomics 23, 118–125.

Aydın Temel, F., 2023. Evaluation of the influence of rice husk amendment on compost quality in the composting of sewage sludge. Bioresour. Technol. 373, 128748. https://doi.org/https://doi.org/10.1016/j.biortech.2023.128748

Ayiti, O.E., Babalola, O.O., 2022. Factors influencing soil nitrification process and the effect on environment and health. Front. Sustain. Food Syst. 6, 821994.

Azizi, A.B., Lim, M.P.M., Noor, Z.M., Abdullah, N., 2013. Vermiremoval of heavy metal in sewage sludge by utilising Lumbricus rubellus. Ecotoxicol. Environ. Saf. 90, 13–20.

Bai, X., Lu, W., Xu, J., Li, Q., Xue, Z., Wang, X.-X., 2025. Effects of cattle manure and sludge vermicompost on nutrient dynamics and yield in strawberry cultivation with distinct continuous cropping histories in a greenhouse. Front. Plant Sci. 15, 1514675.

Balachandar, R., Baskaran, L., Yuvaraj, A., Thangaraj, R., Subbaiya, R., Ravindran, B., Chang, S.W., Karmegam, N., 2020. Enriched pressmud vermicompost production with green manure plants using Eudrilus eugeniae. Bioresour. Technol. 299, 122578. https://doi.org/https://doi.org/10.1016/j.biortech.2019.122578

Banu, R.J., Yeom, I.T., Esakkiraj, K.N., Lee, Y.W., Vallinayagam, S., 2008. Biomanagement of sago-sludge using an earthworm, Lampito mauritii. J. Environ. Biol. 29, 753–757.

Bashat, H., 2002. Managing Waste in Exploration and Production Activities of the Petroleum Industry. Environ. Advis. SENV 37.

Begum, K.S., Kashem, M.A., Sarker, M.M.H., 2025. Seasonal effects on growth and reproduction of Eisenia fetida and Eudrilus eugeniae. Eurasian J. Soil Sci. 14, 178–188.

Belay, T., Tassie, N., Tilahun, G., Ejigu, D., Girmay, S., Seid, A., Assefa, W.W., Wondie, A., Kassa, Y., Fetene, B., 2025. Effect of water hyacinth (Pontederia crassipes) vermicompost on tomato (Solanum lycopersicum L.) growth and yield in the vicinity of lake Tana, Northwest Ethiopia. Discov. Food 5, 362.

Bera, R., Datta, A., Bose, S., Dolui, A.K., Chatterjee, A.K., Dey, G.C., Barik, A.K., Sarkar, R.K., Majumdar, D., Seal, A., 2013. Comparative evaluation of compost quality, process convenience and cost under different composting methods to assess their large scale adoptability potential as also complemented by compost quality index. Int. J. Sci. Res. Publ. 3, 406–417.

Bergmann, M., Gutow, L., Klages, M., 2015. Marine anthropogenic litter. Mar. Anthropog. Litter 1–447. https://doi.org/10.1007/978-3-319-16510-3

Bharathiraja, S., Suriya, J., Krishnan, M., Manivasagan, P., Kim, S.-K., 2017. Production of enzymes from agricultural wastes and their potential industrial applications, in: Advances in Food and Nutrition Research. Elsevier, pp. 125–148.

Bhardwaj, P., Sharma, R.K., 2015. Vermicomposting efficiency of earthworm species from eastern Haryana. J. Entomol. Zool. Stud. 3, 191–195.

Bhat, S.A., Singh, J., Vig, A.P., 2018a. Earthworms as Organic Waste Managers and Biofertilizer Producers. Waste and Biomass Valorization 9, 1073–1086. https://doi.org/10.1007/s12649-017-9899-8

Bhat, S.A., Singh, J., Vig, A.P., 2017. Instrumental characterization of organic wastes for evaluation of vermicompost maturity. J. Anal. Sci. Technol. 8, 1–12.

Bhat, S.A., Singh, J., Vig, A.P., 2016. Effect on growth of earthworm and chemical parameters during vermicomposting of pressmud sludge mixed with cattle dung mixture. Procedia Environ. Sci. 35, 425–434.

Bhat, S.A., Singh, J., Vig, A.P., 2013. Vermiremediation of dyeing sludge from textile mill with the help of exotic earthworm Eisenia fetida Savigny. Environ. Sci. Pollut. Res. 20, 5975–5982. https://doi.org/10.1007/s11356-013-1612-2

Bhat, S.A., Singh, S., Singh, J., Kumar, S., Bhawana, Vig, A.P., 2018b. Bioremediation and detoxification of industrial wastes by earthworms: Vermicompost as powerful crop nutrient in sustainable agriculture. Bioresour. Technol. 252, 172–179. https://doi.org/10.1016/j.biortech.2018.01.003

Bhattacharyya, J.K., Shekdar, A. V, 2003. Treatment and disposal of refinery sludges: Indian scenario. Waste Manag. Res. 21, 249–261.

Bhuiyan, M.A.H., Parvez, L., Islam, M.A., Dampare, S.B., Suzuki, S., 2010. Heavy metal pollution of coal mine-affected agricultural soils in the northern part of Bangladesh. J. Hazard. Mater. 173, 384–392.

Bilal, M., Iqbal, H.M.N., 2020. Microbial bioremediation as a robust process to mitigate pollutants of environmental concern. Case Stud. Chem. Environ. Eng. 2, 100011. https://doi.org/https://doi.org/10.1016/j.cscee.2020.100011

Biruntha, M., Karmegam, N., Archana, J., Selvi, B.K., Paul, J.A.J., Balamuralikrishnan, B., Chang, S.W., Ravindran, B., 2020. Vermiconversion of biowastes with low-to-high C/N ratio into value added vermicompost. Bioresour. Technol. 297, 122398.

Biswas, J.K., Banerjee, A., Sarkar, B., Sarkar, D., Sarkar, S.K., Rai, M., Vithanage, M., 2020. Exploration of an extracellular polymeric substance from earthworm gut bacterium

(Bacillus licheniformis) for bioflocculation and heavy metal removal potential. Appl. Sci. 10, 349.

Blakemore, R.J., 2015. Eco-taxonomic profile of an iconic vermicomposter-the'African Nightcrawler'earthworm, Eudrilus eugeniae (Kinberg, 1867). African Invertebr. 56, 527–548.

Blouin, M., Barrere, J., Meyer, N., Lartigue, S., Barot, S., Mathieu, J., 2019. Vermicompost significantly affects plant growth. A meta-analysis. Agron. Sustain. Dev. 39, 34.

Boechat, C.L., Pistóia, V.C., Ludtke, A.C., Gianello, C., Camargo, F.A. de O., 2016. Solubility of heavy metals/metalloid on multi-metal contaminated soil samples from a gold ore processing area: effects of humic substances. Rev. Bras. Ciência do Solo 40, e0150383.

Bondì, C., Castellini, M., Iovino, M., 2022. Compost amendment impact on soil physical quality estimated from hysteretic water retention curve. Water 14, 1002.

Borah, R.C., 2015. Remediation of Guwahati refinery waste sludge by pyrolysis. Int. J. Eng. Res. Manag. Technol. 2, 65–73.

Boruah, T., Barman, A., Kalita, P., Lahkar, J., Deka, H., 2019. Vermicomposting of citronella bagasse and paper mill sludge mixture employing Eisenia fetida. Bioresour. Technol. 294, 122147. https://doi.org/https://doi.org/10.1016/j.biortech.2019.122147

Boruah, T., Deka, H., 2023. Comparative investigation on synergistic changes in enzyme activities during vermicomposting of cereal grain processing industry sludge employing three epigeic earthworm species. Environ. Sci. Pollut. Res. 30, 123324–123334.

Bryman, A., Cramer, D., 2009. Quantitative data analysis with SPSS 14, 15 & 16: A guide for social scientists. Routledge/Taylor & Francis Group.

Busato, J.G., Papa, G., Canellas, L.P., Adani, F., de Oliveira, A.L., Leão, T.P., 2016. Phosphatase activity and its relationship with physical and chemical parameters during vermicomposting of filter cake and cattle manure. J. Sci. Food Agric. 96, 1223–1230.

Casida Jr, L.E., Klein, D.A., Santoro, T., 1964. Soil dehydrogenase activity. Soil Sci. 98, 371–376.

Castellini, M., Bondì, C., Giglio, L., Iovino, M., 2024. Impact of vermicompost addition on water availability of differently textured soils. Heliyon 10.

Chabukdhara, M., Nema, A.K., 2013. Heavy metals assessment in urban soil around industrial clusters in Ghaziabad, India: probabilistic health risk approach. Ecotoxicol. Environ. Saf. 87, 57–64.

Chai, L., Yang, Y., Yang, H., Zhao, Y., Wang, H., 2020. Transcriptome analysis of genes expressed in the earthworm Eisenia fetida in response to cadmium exposure. Chemosphere 240, 124902.

Chang, J.I., Chen, Y.J., 2010. Effects of bulking agents on food waste composting. Bioresour. Technol. 101, 5917–5924.

Channgam, K., Premalatha, M., Abbasi, S.A., 2015. Use of manure worm (Eisenia andrei) in direct vermicomposting of an aquatic weed salvinia (Salvinia molesta Mitchell) by applying the concept of high-rate vermicomposting: a reconnoitery study. Int. J. Curr. Sci. 18, 59–63.

Chatterjee, R., Debnath, A., Mishra, S., 2020. Vermicompost and Soil Health, in: Soil Health. pp. 69–88. https://doi.org/10.1007/978-3-030-44364-1_4

Chaudhary, P., Garg, S., George, T., Shabin, M., Saha, S., Subodh, S., Sinha, B., 2021. Underreporting and open burning – the two largest challenges for sustainable waste management in India. Resour. Conserv. Recycl. 175, 105865. https://doi.org/https://doi.org/10.1016/j.resconrec.2021.105865

Chen, G., Lock Yue, P., Mujumdar, A.S., 2002. SLUDGE DEWATERING AND DRYING, Drying Technology. An Int. J. 20, 883–916.

Chen, H., Wang, X., Liang, H., Chen, B., Liu, Y., Ma, Z., Wang, Z., 2024. Characterization and treatment of oily sludge: A systematic review. Environ. Pollut. 344, 123245. https://doi.org/https://doi.org/10.1016/j.envpol.2023.123245

Chen, J., Jin, C., Sun, S., Yang, D., He, Y., Gan, P., Nalume, W.G., Ma, Y., He, W., Li, G., 2023. Recognizing the challenges of composting: Critical strategies for control, recycling, and valorization of nitrogen loss. Resour. Conserv. Recycl. 198, 107172. https://doi.org/https://doi.org/10.1016/j.resconrec.2023.107172

Chinakwe, E.C., Ibekwe, V.I., Ofoh, M.C., Nwogwugwu, N.U., Adeleye, S.A., Chinakwe, P.O., Nwachukwu, I.N., Ihejirika, C.E., 2019. Effect of temperature changes on the bacterial and fungal succession patterns during composting of some organic wastes in greenhouse. J. Adv. Microbiol. 15, 1–10.

Choudhary, K., Vivekanand, V., Pareek, N., 2022. Chapter 14 - Recent advancements in microbial bioremediation of industrial effluents: challenges and future outlook, in: Das, S., Dash, H.R.B.T.-M.B. and B. (Second E. (Eds.), . Elsevier, pp. 293–303. https://doi.org/https://doi.org/10.1016/B978-0-323-85455-9.00022-9

Colacevich, A., Sierra, M.J., Borghini, F., Millán, R., Sanchez-Hernandez, J.C., 2011. Oxidative stress in earthworms short- and long-term exposed to highly Hg-contaminated soils. J. Hazard. Mater. 194, 135–143. https://doi.org/https://doi.org/10.1016/j.jhazmat.2011.07.091

Corrochano, N., de Tuesta, J.L.D., de Mora, A., Pariente, M.I., Segura, Y., Molina, R., Martínez, F., 2025. Valorization of refinery sludges by hydrothermal carbonization towards circular economy. Waste Manag. 204, 114949. https://doi.org/https://doi.org/10.1016/j.wasman.2025.114949

Costa, O.Y.A., Raaijmakers, J.M., Kuramae, E.E., 2018. Microbial extracellular polymeric substances: ecological function and impact on soil aggregation. Front. Microbiol. 9, 1636.

Cuiyun, Y., Yihang, L., Jing, Y., Hongyou, Z., Zhaoyou, D., Deying, T., Oo, A.K., Lixia, Z., 2023. Correlation between soil environment and yield and quality of Sharen (Amomi Fructus) under different planting patterns. Digit. Chinese Med. 6, 221–233. https://doi.org/https://doi.org/10.1016/j.dcmed.2023.07.011

Cunha, A.H.N., Brasil, E.P.F., Ferreira, R.B., Vieira, J.A., AraÃºjo, C.S.T., Silva, S.M.C., 2016. Vermicompost of tannery sludge and sewage as conditioners soil with grown tomato. African J. Agric. Res. 11, 4086–4091.

Dal Mas, F., Zeng, X., Huang, Q., Li, J., 2021. Quantifying material flow of oily sludge in China and its implications. J. Environ. Manage. 287, 112115. https://doi.org/https://doi.org/10.1016/j.jenvman.2021.112115

Das, D., Bhattacharyya, P., Ghosh, B.C., Banik, P., 2012. Effect of vermicomposting on calcium, sulphur and some heavy metal content of different biodegradable organic wastes under liming and microbial inoculation. J. Environ. Sci. Heal. - Part B Pestic.

Food Contam. Agric. Wastes 47, 205–211. https://doi.org/10.1080/03601234.2012.634346

Das, S., Deka, P., Goswami, L., Sahariah, B., Hussain, N., Bhattacharya, S.S., 2016. Vermiremediation of toxic jute mill waste employing Metaphire posthuma. Environ. Sci. Pollut. Res. 23, 15418–15431.

Das, S., Goswami, L., Bhattacharya, S.S., 2020. Vermicomposting: earthworms as potent bioresources for biomass conversion, in: Current Developments in Biotechnology and Bioengineering. Elsevier, pp. 79–102.

De Boni, A., Melucci, F.M., Acciani, C., Roma, R., 2022. Community composting: A multidisciplinary evaluation of an inclusive, participative, and eco-friendly approach to biowaste management. Clean. Environ. Syst. 6, 100092.

Deng, S., Wang, X., Tan, H., Mikulčić, H., Yang, F., Li, Z., Duić, N., 2016. Thermogravimetric study on the Co-combustion characteristics of oily sludge with plant biomass. Thermochim. Acta 633, 69–76. https://doi.org/10.1016/j.tca.2016.03.006

Dias, B.O., Silva, C.A., Higashikawa, F.S., Roig, A., Sánchez-Monedero, M.A., 2010. Use of biochar as bulking agent for the composting of poultry manure: Effect on organic matter degradation and humification. Bioresour. Technol. 101, 1239–1246. https://doi.org/https://doi.org/10.1016/j.biortech.2009.09.024

Doherty, F. V, Aneyo, I., Otitoloju, A.A., 2019. Histopathological and biochemical alterations in Eudrilus eugeniae (Kinberg 1867) as biomarkers of exposure to monocyclic aromatic hydrocarbons in oil impacted site. J. Basic Appl. Zool. 80, 63.

Domínguez, J., 2018. Earthworms and vermicomposting. IntechOpen London (UK).

Douglas, R.K., Araka, P.P., Fou, A., Hart, A., 2024. Evaluation of the potential of agricultural wastes-cattle manure and poultry manure for bioremediation of crude oil-contaminated soil. Bioremediat. J. 1–8. https://doi.org/10.1080/10889868.2024.2322471

Duan, M., Wang, X., Fang, S., Zhao, B., Li, C., Xiong, Y., 2018. Treatment of Daqing oily sludge by thermochemical cleaning method. Colloids Surfaces A Physicochem. Eng. Asp. 554, 272–278. https://doi.org/10.1016/j.colsurfa.2018.06.046

Dume, B., Hanc, A., Svehla, P., Michal, P., Chane, A.D., Nigussie, A., 2023. Composting and vermicomposting of sewage sludge at various C/N ratios: technological feasibility and end-product quality. Ecotoxicol. Environ. Saf. 263, 115255.

Eduah, J.O., Arthur, A., Amoako-Attah, I., Manso, E.F., Quaye, A.K., Dogbatse, J.A., Padi, F.K., 2025. Differential impacts of organic and chemical fertilization on soil organic carbon pools and stability, and soil quality in cacao agroforestry. Soil Environ. Heal. 3, 100147.

Edwards, C.A., Lofty, J.R., 1977. Biology of Earthworms, Chapman and Hall. London, UK.

Ekperusi, O.A., Aigbodion, I.F., 2015. Bioremediation of heavy metals and petroleum hydrocarbons in diesel contaminated soil with the earthworm: Eudrilus eugeniae. Springerplus 4, 1–13.

Elvira, C., Sampedro, L., Benítez, E., Nogales, R., 1998. Vermicomposting of sludges from paper mill and dairy industries with Eisena andrei: A pilot-scale study. Bioresour. Technol. 63, 205–211. https://doi.org/10.1016/S0960-8524(97)00145-4

Enebe, M.C., Erasmus, M., 2023a. Vermicomposting technology - A perspective on vermicompost production technologies, limitations and prospects. J. Environ. Manage. 345, 118585. https://doi.org/https://doi.org/10.1016/j.jenvman.2023.118585

Enebe, M.C., Erasmus, M., 2023b. Mediators of biomass transformation – A focus on the enzyme composition of the vermicomposting process. Environ. Challenges 12, 100732. https://doi.org/https://doi.org/10.1016/j.envc.2023.100732

Equeenuddin, S.M., Tripathy, S., Sahoo, P.K., Panigrahi, M.K., 2013. Metal behavior in sediment associated with acid mine drainage stream: role of pH. J. Geochemical Explor. 124, 230–237.

Ferrarese, E., Andreottola, G., Oprea, I.A., 2008. Remediation of PAH-contaminated sediments by chemical oxidation. J. Hazard. Mater. 152, 128–139. https://doi.org/https://doi.org/10.1016/j.jhazmat.2007.06.080

Gajalakshmi, S., Ramasamy, E. V, Abbasi, S.A., 2002. High-rate composting–vermicomposting of water hyacinth (Eichhornia crassipes, Mart. Solms). Bioresour. Technol. 83, 235–239.

Ganapathy, N.R.V., Elango, A.C., Balaji, G., Sankaranarayanan, M., Sharma, M., 2025. A comprehensive review of earthworm-derived vermiproducts and their role in sustainable agriculture. Discov. Appl. Sci. 7, 995.

Garau, M., Sizmur, T., Coole, S., Castaldi, P., Garau, G., 2022. Impact of Eisenia fetida earthworms and biochar on potentially toxic element mobility and health of a contaminated soil. Sci. Total Environ. 806, 151255. https://doi.org/https://doi.org/10.1016/j.scitotenv.2021.151255

Garg, V.K., Gupta, R., 2011a. Optimization of cow dung spiked pre-consumer processing vegetable waste for vermicomposting using Eisenia fetida. Ecotoxicol. Environ. Saf. 74, 19–24.

Garg, V.K., Gupta, R., 2011b. Effect of temperature variations on vermicomposting of household solid waste and fecundity of Eisenia fetida. Bioremediat. J. 15, 165–172.

Garg, V.K., Kaushik, P., 2005. Vermistabilization of textile mill sludge spiked with poultry droppings by an epigeic earthworm Eisenia foetida. Bioresour. Technol. 96, 1063–1071.

Gaur, V.K., Sharma, P., Sirohi, R., Awasthi, M.K., Dussap, C.G., Pandey, A., 2020. Assessing the impact of industrial waste on environment and mitigation strategies: A comprehensive review. J. Hazard. Mater. 398, 123019. https://doi.org/10.1016/j.jhazmat.2020.123019

Gebresamuel, G., Singh, B.R., Dick, Ø., 2010. Land-use changes and their impacts on soil degradation and surface runoff of two catchments of Northern Ethiopia. Acta Agric. Scand. Sect. B–Soil Plant Sci. 60, 211–226.

Gieguzynska, A., 1998. Studies on humic acids in eroded soils of Western Pomerania. 1. Differentiation of some chemical as well as optical properties of humic acids along the eroded slope.

Gogoi, N., Sarma, A., Choudhury, M., Samanta, P., Faizan, M., Sadhak, S., 2024. Soil heavy metal pollution and ecological risk assessment in disturbed and undisturbed soil of Morigaon, Assam. Discov. Environ. 2, 13.

Gomez-Brandon, M., Aira, M., Lores, M., Domínguez, J., 2011. Epigeic earthworms exert a bottleneck effect on microbial communities through gut associated processes. PLoS One 6, e24786.

Gong, L., Qiu, D., Yao, X., Yang, G., 2020. Determination of heavy metals in the plant sample pretreatment methods, in: Journal of Physics: Conference Series. IOP Publishing, p. 22008.

Gopal, M., Gupta, A., Thomas, G. V, 2004. Optimum weather conditions for efficient vermicomposting of coconut leaves by Eudrilus sp. in coastal tract of Kerala.

Goswami, L., Ekblad, A., Choudhury, R., Bhattacharya, S.S., 2024. Vermi-converted Tea Industry Coal Ash efficiently substitutes chemical fertilization for growth and yield of cabbage (Brassica oleracea var. capitata) in an alluvial soil: A field-based study on soil quality, nutrient translocation, and metal-risk remedia. Sci. Total Environ. 907, 168088.

Goswami, L., Nath, A., Sutradhar, S., Bhattacharya, S.S., Kalamdhad, A., Vellingiri, K., Kim, K.-H., 2017. Application of drum compost and vermicompost to improve soil health, growth, and yield parameters for tomato and cabbage plants. J. Environ. Manage. 200, 243–252.

Goswami, L., Pratihar, S., Dasgupta, S., Bhattacharyya, P., Mudoi, P., Bora, J., Bhattacharya, S.S., Kim, K.H., 2016. Exploring metal detoxification and accumulation potential during vermicomposting of Tea factory coal ash: sequential extraction and fluorescence probe analysis. Sci. Rep. 6, 1–13.

Goswami, L., Sarkar, S., Mukherjee, S., Das, S., Barman, S., Raul, P., Bhattacharyya, P., Mandal, N.C., Bhattacharya, S., Bhattacharya, S.S., 2014. Vermicomposting of Tea Factory Coal Ash: Metal accumulation and metallothionein response in Eisenia fetida (Savigny) and Lampito mauritii (Kinberg). Bioresour. Technol. 166, 96–102. https://doi.org/10.1016/j.biortech.2014.05.032

Goswami, L, Sarkar, S., Mukherjee, S., Das, S., Barman, S., Raul, P., Bhattacharyya, P., Mandal, N.C., Bhattacharya, S., Bhattacharya, S.S., 2014. Vermicomposting of Tea Factory Coal Ash: Metal accumulation and metallothionein response in Eisenia fetida (Savigny) and Lampito mauritii (Kinberg). Bioresour. Technol. 166, 96–102. https://doi.org/https://doi.org/10.1016/j.biortech.2014.05.032

Goyal, S., Dhull, S.K., Kapoor, K.K., 2005. Chemical and biological changes during composting of different organic wastes and assessment of compost maturity. Bioresour. Technol. 96, 1584–1591.

Gudeta, K., Kumar, V., Bhagat, A., Julka, J.M., Bhat, S.A., Ameen, F., Qadri, H., Singh, S., Amarowicz, R., 2023. Ecological adaptation of earthworms for coping with plant polyphenols, heavy metals, and microplastics in the soil: A review. Heliyon 9. https://doi.org/10.1016/j.heliyon.2023.e14572

Guo, M., Wang, C., Wu, W., 2026. Root-zone application of vermicompost to enhance phosphorus mineralization in saline soil. Soil Ecol. Lett. 8, 1–11.

Gupta, K.K., Aneja, K.R., Rana, D., 2016. Current status of cow dung as a bioresource for sustainable development. Bioresour. Bioprocess. 3, 28. https://doi.org/10.1186/s40643-016-0105-9

Gupta, S., Yadav, S., 2014. Bioaccumulation of ZnO-NPs in earthworm Eisenia fetida (Savigny). J Bioremediat Biodegrad 5, 250.

Haider, K.M., Focsa, C., Decuq, C., Esnault, B., Lafouge, F., Loubet, B., Petitprez, D., Ciuraru, R., 2024. Chemical characterization of volatile organic compounds emitted by animal manure. J. Environ. Manage. 364, 121453.

Hait, S., Tare, V., 2012. Transformation and availability of nutrients and heavy metals during integrated composting–vermicomposting of sewage sludges. Ecotoxicol. Environ. Saf. 79, 214–224.

Hakanson, L., 1980. An ecological risk index for aquatic pollution control. A sedimentological approach. Water Res. 14, 975–1001.

Hamman, A., Momo, F.R., Duhour, A., Falco, L., Sagario, M.C., Cuadrado, M.E., 2003. Effect of UV radiation on Eisenia fetida populations: The 7th international symposium on earthworm ecology · Cardiff · Wales · 2002. Pedobiologia (Jena). 47, 842–845. https://doi.org/https://doi.org/10.1078/0031-4056-00269

Hanc, A., Chadimova, Z., 2014. Nutrient recovery from apple pomace waste by vermicomposting technology. Bioresour. Technol. 168, 240–244.

Hanc, A., Dreslova, M., 2016. Effect of composting and vermicomposting on properties of particle size fractions. Bioresour. Technol. 217, 186–189.

Hanc, A., Hrebeckova, T., Pliva, P., Cajthaml, T., 2020. Vermicomposting of sludge from a malt house. Waste Manag. 118, 232–240.

Harper, E.H., 1905. Reactions to light and mechanical stimuli in the earthworm Perichaeta bermudensis (Beddard). Biol. Bull. 10, 17–34.

Hasan, A.M.A., Kamal, R.S., Farag, R.K., Abdel-Raouf, M.E., 2024. Petroleum sludge formation and its treatment methodologies: a review. Environ. Sci. Pollut. Res. 31, 8369–8386.

He, X., Zhang, Y., Shen, M., Zeng, G., Zhou, M., Li, M., 2016. Effect of vermicomposting on concentration and speciation of heavy metals in sewage sludge with additive materials. Bioresour. Technol. 218, 867–873.

Hendrix, P.F., 1995. Earthworm ecology and biogeography in North America. CRC press.

Höckner, M., Piechnik, C.A., Fiechtner, B., Weinberger, B., Tomanek, L., 2020. Cadmium-related effects on cellular immunity comprises altered metabolism in earthworm coelomocytes. Int. J. Mol. Sci. 21, 599.

Homa, J., Stürzenbaum, S.R., Kolaczkowska, E., 2016. Metallothionein 2 and heat shock protein 72 protect Allolobophora chlorotica from cadmium but not nickel or copper exposure: body malformation and coelomocyte functioning. Arch. Environ. Contam. Toxicol. 71, 267–277.

Hossain, M.L., Shapna, K.J., Li, J., Kabir, M.H., Siddika, F., Khandker, S., Beierkuhnlein, C., 2025. Transforming agriculture with vermicompost: 7-year empirical evidence from drought-prone and salinization-affected regions of Bangladesh. J. Clean. Prod. 508, 145595. https://doi.org/https://doi.org/10.1016/j.jclepro.2025.145595

Hossen, M.S., Khan, M.R.I., Azad, M.A.K., Hashem, M.A., Bhuiyan, M.K.J., Rahman, M.M., 2022. Effects of moisture content on the quality of vermicompost produced from cattle manure. Bangladesh J. Anim. Sci. 51, 40–46.

Hou, Z., Mo, F., Zhou, Q., 2023. Elucidating response mechanisms at the metabolic scale of Eisenia fetida in typical oil pollution sites: A native driver in influencing carbon flow. Environ. Pollut. 337, 122545. https://doi.org/https://doi.org/10.1016/j.envpol.2023.122545

Hu, G., Feng, H., He, P., Li, J., Hewage, K., Sadiq, R., 2020. Comparative life-cycle assessment of traditional and emerging oily sludge treatment approaches. J. Clean. Prod. 251, 119594. https://doi.org/10.1016/j.jclepro.2019.119594

Hu, G., Li, J., Zeng, G., 2013. Recent development in the treatment of oily sludge from petroleum industry: A review, Journal of Hazardous Materials. Elsevier B.V. https://doi.org/10.1016/j.jhazmat.2013.07.069

Hu, X., Chen, H., 2023. Phosphate solubilizing microorganism: a green measure to effectively control and regulate heavy metal pollution in agricultural soils. Front. Microbiol. 14, 1193670.

Huang, K., Xia, H., Li, F., Wei, Y., Cui, G., Fu, X., Chen, X., 2016. Optimal growth condition of earthworms and their vermicompost features during recycling of five different fresh fruit and vegetable wastes. Environ. Sci. Pollut. Res. 23, 13569–13575.

Hussain, N., Chatterjee, S.K., Maiti, T.K., Goswami, L., Das, S., Deb, U., Bhattacharya, S.S., 2021. Metal induced non-metallothionein protein in earthworm: A new pathway for cadmium detoxification in chloragogenous tissue. J. Hazard. Mater. 401, 123357. https://doi.org/https://doi.org/10.1016/j.jhazmat.2020.123357

Iordache, M., 2023. Chemical composition of earthworm casts as a tool in understanding the earthworm contribution to ecosystem sustainability–a review. Plant, Soil Environ. 69, 247.

Iqbal, A., Khan, R., Hussain, Q., Imran, M., Mo, Z., Hua, T., Adnan, M., Abid, I., Rizwana, H., Soliman Elshikh, M., 2024. Vermicompost application enhances soil health and plant physiological and antioxidant defense to conferring heavy metals tolerance in fragrant rice. Front. Sustain. Food Syst. 8, 1418554.

Jadia, C.D., Fulekar, M.H., 2008. Vermicomposting of vegetable waste: A biophysicochemical process based on hydro-operating bioreactor. African J. Biotechnol. 7.

Jafarinejad, S., 2017. Pollutions and Wastes From the Petroleum Industry, Petroleum Waste Treatment and Pollution Control. https://doi.org/10.1016/b978-0-12-809243-9.00002-x

Jakubus, M., Michalak-Oparowska, W., 2022. Valorization of quality of vermicomposts and composts using various parameters. Agriculture 12, 293.

Jariyal, M., Yadav, M., Singh, N.K., Yadav, S., Sharma, I., Dahiya, S., Thanki, A., 2020. Microbial remediation progress and future prospects, in: Bioremediation of Pollutants. Elsevier, pp. 187–214.

Jasmine, J., Mukherji, S., 2015. Characterization of oily sludge from a refinery and biodegradability assessment using various hydrocarbon degrading strains and reconstituted consortia. J. Environ. Manage. 149, 118–125. https://doi.org/10.1016/j.jenvman.2014.10.007

Jasrotia, S., Kansal, A., Mehra, A., 2017. Performance of aquatic plant species for phytoremediation of arsenic-contaminated water. Appl. Water Sci. 7, 889–896. https://doi.org/10.1007/s13201-015-0300-4

Jayakumar, M., Emana, A.N., Subbaiya, R., Ponraj, M., Ashok Kumar, K.K., Muthusamy, G., Kim, W., Karmegam, N., 2022. Detoxification of coir pith through refined vermicomposting engaging Eudrilus eugeniae. Chemosphere 291, 132675. https://doi.org/https://doi.org/10.1016/j.chemosphere.2021.132675

Jerez, S., Ventura, M., Molina, R., Pariente, M.I., Martínez, F., Melero, J.A., 2021. Comprehensive characterization of an oily sludge from a petrol refinery: A step forward for its valorization within the circular economy strategy. J. Environ. Manage. 285, 112124. https://doi.org/https://doi.org/10.1016/j.jenvman.2021.112124

Jiang, X., Lu, C., Hu, R., Shi, W., Zhou, L., Wen, P., Jiang, Y., Lo, Y.M., 2023. Nutritional and microbiological effects of vermicompost tea in hydroponic cultivation of maple peas (Pisum sativum var. arvense L.). Food Sci. Nutr. 11, 3184–3202.

Johnson, O.A., Affam, A.C., 2019. Petroleum sludge treatment and disposal: A review. Environ. Eng. Res. 24, 191–201. https://doi.org/10.4491/EER.2018.134

Julius, A., Adewunmi, B., Kehinde, O., Oluseyi, A., Adeyemi, A., 2015. Heavy metal accumulation and biochemical evaluation of earthworms from sawmills in Abeokuta, South-Western Nigeria. Rev. Biol. Trop. 63, 1213–1221.

Kahsay, A., Haile, M., Gebresamuel, G., Mohammed, M., 2025. Developing soil quality indices to investigate degradation impacts of different land use types in Northern Ethiopia. Heliyon 11, e41185. https://doi.org/https://doi.org/10.1016/j.heliyon.2024.e41185

Kandaswamy, K., Vadivelu, K., Christyraj, J.D.S., Chelladurai, K.S., Rajagopalan, K., Das, P., Chandrasekar, M., Balamurugan, N., Subramanian, V., Christyraj, J.R.S.S., 2024. An improved protocol for inducing the gut cleaning process in earthworm for various experiments. Anim. Biol. 74, 255–269.

Kandziora-Ciupa, M., Nadgórska-Socha, A., Barczyk, G., 2021. The influence of heavy metals on biological soil quality assessments in the Vaccinium myrtillus L. rhizosphere under different field conditions. Ecotoxicology 30, 292–310.

Kang, H., Ahn, J.-W., 2021. Model Setting and Interpretation of Results in Research Using Structural Equation Modeling: A Checklist with Guiding Questions for Reporting. Asian Nurs. Res. (Korean. Soc. Nurs. Sci). 15, 157–162. https://doi.org/https://doi.org/10.1016/j.anr.2021.06.001

Karwal, M., Kaushik, A., 2021. Bioconversion of lawn waste amended with kitchen waste and buffalo dung in to value-added vermicompost using Eisenia foetida to alleviate landfill burden. J. Mater. Cycles Waste Manag. 23, 358–370.

Karwal, M., Kaushik, A., 2020. Co-composting and vermicomposting of coal fly-ash with press mud: changes in nutrients, micro-nutrients and enzyme activities. Environ. Technol. Innov. 18, 100708.

Kaushik, P., Garg, V.K., 2003. Vermicomposting of mixed solid textile mill sludge and cow dung with the epigeic earthworm Eisenia foetida. Bioresour. Technol. 90, 311–316.

Khalifa, T.H., Mariey, S.A., Ghareeb, Z.E., Khatab, I.A., Alyamani, A., 2022. Effect of organic amendments and nano-zinc foliar application on alleviation of water stress in some soil properties and water productivity of barley yield. Agronomy 12, 585.

Khan, M.B., Cui, X., Jilani, G., Lazzat, U., Zehra, A., Hamid, Y., Hussain, B., Tang, L., Yang, X., He, Z., 2019. Eisenia fetida and biochar synergistically alleviate the heavy metals content during valorization of biosolids via enhancing vermicompost quality. Sci. Total Environ. 684, 597–609. https://doi.org/https://doi.org/10.1016/j.scitotenv.2019.05.370

Kharmawphlang, I.M., Deka, H., Hussain, N., 2024. Unravelling the detoxification trail of potential toxic heavy metals: an insight into heavy metal auditing and ecological health upon valorisation by Lampito mauritii and Eudrilus eugeniae. Environ. Sci. Pollut. Res. 31, 64007–64022.

Khedr, M., Emran, M., Gispert, M., Rashad, M., 2023. Immobilization of Cr3+, Cd2+, and Pb2+ added to calcareous soil amended with composted agro-industrial residues. Sci. Rep. 13, 8197.

Kotecha, J.L., Ram, V.R., 2023. Extraction and Spectrophotometric Determination of Chlorophyll Content and Carotenoids from Cocos nucifera L. Leaf using Various Solvents in Saurashtra Region. Int. J. PLANT Environ. 9, 364–368.

Krishnan, S., Zulkapli, N.S., Kamyab, H., Taib, S.M., Din, M.F.B.M., Majid, Z.A., Chaiprapat, S., Kenzo, I., Ichikawa, Y., Nasrullah, M., Chelliapan, S., Othman, N., 2021. Current technologies for recovery of metals from industrial wastes: An overview. Environ. Technol. Innov. 22, 101525. https://doi.org/https://doi.org/10.1016/j.eti.2021.101525

Kumar, A., Prakash, C.H.B., Brar, N.S., Kumar, B., 2018. Potential of vermicompost for sustainable crop production and soil health improvement in different cropping systems. Int. J. Curr. Microbiol. Appl. Sci. 7, 1042–1055.

Kumar Badhwar, V., Singh, S., Singh, B., 2020. Biotransformation of paper mill sludge and tea waste with cow dung using vermicomposting. Bioresour. Technol. 318, 124097. https://doi.org/https://doi.org/10.1016/j.biortech.2020.124097

Kumar, D., Jamwal, A., Madaan, R., Kumar, S., 2014. Estimation of Total Phenols and Flavonoids in Selected Indian Traditional Plants. J. Pharm. Technol. Res. Manag. 2, 77–86. https://doi.org/10.15415/jptrm.2014.21006

Kumar, M., Patel, S., 2014. The Characteristics and Power Generation Energetics of Coal, Cattle Dung, Rice Husk, and Their Blends. Energy Sources 36. https://doi.org/10.1080/15567036.2010.545798

Kumar, M., Upadhyay, S.N., Mishra, P.K., 2019. A comparative study of thermochemical characteristics of lignocellulosic biomasses. Bioresour. Technol. Reports 8, 100186.

Kumar, P., Nandi, B.K., 2022. Effect of rice husk blending on combustion characteristics of high ash Indian coal analyzed in TGA. Int. J. Coal Prep. Util. 42, 3698–3711.

Kumar, R., Yadav, R., Gupta, R.K., Pal, A., Yodha, K., Kumar, A., 2024. Antioxidant enzyme activities and markers of oxidative stress in the life cycle of different Earthworm species: Antioxidant activities and markers of oxidative stress in Earthworms. Indian J. Exp. Biol. 62, 578–583.

Lal, R., 2015. Restoring soil quality to mitigate soil degradation. Sustainability 7, 5875–5895.

Lalander, C.H., Komakech, A.J., Vinnerås, B., 2015. Vermicomposting as manure management strategy for urban small-holder animal farms–Kampala case study. Waste Manag. 39, 96–103.

Lamichhane, J., 2017. Vermicompost and its Role in Plant Growth Promotion. Int. J. Res. 4.

Landorfa-Svalbe, Z., Vikmane, M., Ievinsh, G., 2022. Vermicompost amendment in soil affects growth and physiology of Zea mays plants and decreases Pb accumulation in tissues. Agriculture 12, 2098.

Laurelta, T.-A., Ernest, A., 2020. Toxicological Effects of Petroleum Refinery Sludge on the Terrestial Environment Using Bacteria and Earthworm as Bio Indicators. J. Adv. Microbiol. 30–40. https://doi.org/10.9734/jamb/2020/v20i430234

Li, H., Wu, G., Li, M., Duan, C., Liu, C., 2025. C/N-Driven Synergies: Earthworms optimize CO2/N2O mitigation and soil quality in floral waste recycling. Environ. Res. 286, 122712. https://doi.org/https://doi.org/10.1016/j.envres.2025.122712

Li, L., Wu, J., Tian, G., Xu, Z., 2009. Effect of the transit through the gut of earthworm (Eisenia fetida) on fractionation of Cu and Zn in pig manure. J. Hazard. Mater. 167, 634–640.

Li, N., Chen, S., Yue, W., Yan, A., 2025. Effects of Combined Application of Vermicompost and Mineral Fertilizers on Melon Quality and Soil Environmental Quality. Agronomy 15, 2428.

Li, X., Zhang, F., Guan, B., Sun, J., Liao, G., 2020. Review on oily sludge treatment technology. IOP Conf. Ser. Earth Environ. Sci. 467. https://doi.org/10.1088/1755-1315/467/1/012173

Li, Y., Wang, X., Sun, Z., 2020. Ecotoxicological effects of petroleum-contaminated soil on the earthworm Eisenia fetida. J. Hazard. Mater. 393, 122384.

Li, Z., Zheng, Z., Li, H., Xu, D., Li, X., Xiang, L., Tu, S., 2023. Review on rice husk biochar as an adsorbent for soil and water remediation. Plants 12, 1524.

Liang, J., Zhao, L., Du, N., Li, H., Hou, W., 2014. Solid effect in solvent extraction treatment of pre-treated oily sludge. Sep. Purif. Technol. 130, 28–33.

Liang, J., Zhao, L., Hou, W., 2017. Solid effect in chemical cleaning treatment of oily sludge. Colloids Surfaces A Physicochem. Eng. Asp. 522, 38–42. https://doi.org/https://doi.org/10.1016/j.colsurfa.2017.02.038

Liang, Y., Yang, C., Dong, H., Li, W., Hu, H., Xiao, Y., Zheng, M., Liu, Y., 2017. Facile synthesis of highly porous carbon from rice husk. ACS Sustain. Chem. Eng. 5, 7111–7117.

Lin, J., Liu, Z., Xing, H., Luo, S., Yuan, Q., Cao, H., 2018. Earthworm photophobic movement under different light conditions and quantitative analysis of mechanical separating vermicompost parameters. Trans. Chinese Soc. Agric. Eng. 34, 235–241.

Linkevich, E. V, Yudina, N. V, Savel'eva, A. V, 2021. Role of humic acids in the detoxification of petroleum hydrocarbons in soil. Solid Fuel Chem. 55, 332–337.

Liu, M., Wang, M., Fu, X., Song, F., Zhou, F., Li, T., Wang, J., 2025. Metabolomic-Based Assessment of Earthworm (Eisenia fetida) Exposure to Different Petroleum Fractions in Soils. Metabolites 15, 97.

Liu, N., Lou, X., Li, X., Shuai, Z., Liu, H., Jiang, Z., Wei, S., 2021a. Rhizosphere dissolved organic matter and iron plaque modified by organic amendments and its relations to cadmium bioavailability and accumulation in rice. Sci. Total Environ. 792, 148216.

Liu, N., Wei, Z., Wei, H., 2021b. Colorimetric detection of nitrogen, phosphorus, and potassium contents and integration into field irrigation decision technology, in: IOP Conference Series: Earth and Environmental Science. IOP Publishing, p. 42044.

Liu, P., Song, Y., Wei, J., Mao, W., Ju, J., Zheng, S., Zhao, H., 2023. Synergistic effects of earthworms and plants on chromium removal from acidic and alkaline soils: biological responses and implications. Biology (Basel). 12, 831.

Liu, X., Yao, T., Lai, R., Xiu, J., Huang, L., Sun, S., Luo, Y., Song, Z., Zhang, Z., 2019. Recovery of crude oil from oily sludge in an oilfield by sophorolipid. Pet. Sci. Technol. 37, 1582–1588.

Liu, X., Zhang, J., Wang, Q., Chang, T., Shaghaleh, H., Hamoud, Y.A., 2022. Improvement of photosynthesis by biochar and vermicompost to enhance tomato (Solanum lycopersicum L.) yield under greenhouse conditions. Plants 11, 3214.

Machín-Ramírez, C., Okoh, A.I., Morales, D., Mayolo-Deloisa, K., Quintero, R., Trejo-Hernández, M.R., 2008. Slurry-phase biodegradation of weathered oily sludge waste. Chemosphere 70, 737–744. https://doi.org/10.1016/j.chemosphere.2007.06.017

Madejón, E., Díaz, M.J., López, R., Cabrera, F., 2001. Co-composting of sugarbeet vinasse: influence of the organic matter nature of the bulking agents used. Bioresour. Technol. 76, 275–278.

Maity, S., Padhy, P.K., Chaudhury, S., 2008. The role of earthworm Lampito mauritii

(Kinberg) in amending lead and zinc treated soil. Bioresour. Technol. 99, 7291–7298. https://doi.org/https://doi.org/10.1016/j.biortech.2007.12.079

Malal, H., Romero, V.S., Horwath, W.R., Dore, S., Beckett, P., Ait Hamza, M., Lakhtar, H., Lazcano, C., 2024. Vermifiltration and sustainable agriculture: unveiling the soil health-boosting potential of liquid waste vermicompost. Front. Sustain. Food Syst. 8, 1383715.

Malińska, K., Zabochnicka-Świątek, M., Cáceres, R., Marfà, O., 2016. The effect of precomposted sewage sludge mixture amended with biochar on the growth and reproduction of Eisenia fetida during laboratory vermicomposting. Ecol. Eng. 90, 35–41.

Manish, B., Richa, G., Archana, T., 2013. Implementation of bulking agents in composting: a review. J. Bioremediation Biodegrad. 4.

Marin, J.A., Hernandez, T., Garcia, C., 2005. Bioremediation of oil refinery sludge by landfarming in semiarid conditions: Influence on soil microbial activity. Environ. Res. 98, 185–195. https://doi.org/10.1016/j.envres.2004.06.005

Martin, N.A., 1976. Effect of four insecticides on the pasture ecosystem: V. Earthworms (Oligochaeta: Lumbricidae) and arthropoda extracted by wet sieving and salt flotation. New Zeal. J. Agric. Res. 19, 111–115.

Martínez González, A., Silva Lora, E.E., Escobar Palacio, J.C., 2019. Syngas production from oil sludge gasification and its potential use in power generation systems: An energy and exergy analysis. Energy 169, 1175–1190. https://doi.org/10.1016/j.energy.2018.11.087

Massoud, R., Hadiani, M.R., Hamzehlou, P., Khosravi-Darani, K., 2019. Bioremediation of heavy metals in food industry: Application of Saccharomyces cerevisiae. Electron. J. Biotechnol. 37, 56–60. https://doi.org/https://doi.org/10.1016/j.ejbt.2018.11.003

Meretin, R.N., 2021. Nikiforova TE Investigation of the reactivity of the surface of a carbon-containing silicate sorbent of plant origin. ChemChemTech [Izv. Vyss. Uchebn. Zaved. Khim. Khim. Tekhnol.] 64, 147–155.

Mi, B., Liu, F., Xie, L., Zhou, H., Wu, F., Dai, X., 2019. Evaluation of the uptake capacities of heavy metals in Chinese cabbage. Ecotoxicol. Environ. Saf. 171, 511–517. https://doi.org/https://doi.org/10.1016/j.ecoenv.2019.01.022

Milotić, T., Hoffmann, M., 2016. Reduced germination success of temperate grassland seeds sown in dung: consequences for post-dispersal seed fate. Plant Biol. 18, 1038–1047.

Minelgaitė, A., Liobikienė, G., 2019. Waste problem in European Union and its influence on waste management behaviours. Sci. Total Environ. 667, 86–93. https://doi.org/10.1016/j.scitotenv.2019.02.313

Mokhtar, N.M., Omar, R., Salleh, M.M., Idris, A., 2011. Characterization of sludge from the wastewater-treatment plant of a refinery. Int. J. Eng. Technol. 8, 48–56.

Mondal, A., Das, S., Sah, R.K., Bhattacharyya, P., Bhattacharya, S.S., 2017. Environmental footprints of brick kiln bottom ashes: Geostatistical approach for assessment of metal toxicity. Sci. Total Environ. 609, 215–224.

Mongchu, C., Iwai, C.B., Noller, B.N., 2024. Enhancing the potential of Eisenia foetida and Eudrillus eugeniae species and their valorization in tannery leather industry sludge management via vermicomposting with bamboo biochar amendment. Case Stud. Chem. Environ. Eng. 10, 100986. https://doi.org/https://doi.org/10.1016/j.cscee.2024.100986

Mousavi, S.M., Bahmanyar, M.A., Pirdashti, H., 2010. Lead and cadmium availability and uptake by rice plant in response to different biosolids and inorganic fertilizers. Am. J. Agric. Biol. Sci. 5, 25–31.

Mulatu, G., Bayata, A., 2024. Vermicompost as Organic Amendment: Effects on Some Soil Physical, Biological Properties and Crops Performance on Acidic Soil: A Review. Front. Environ. Microbiol. 10, 66–73. https://doi.org/10.11648/j.fem.20241004.11

Munnoli, P.M., Arora, J.K., Sharma, S.K., 2000. Organic waste management through vermiculture: A case study of Pepsi Foods Channoo Punjab. Waste Resour. Recycl. Dev. World, Sapana Print. Work. Kolkatta 203–208.

Mupambwa, H.A., Ravindran, B., Mnkeni, P.N.S., 2016. Potential of effective micro-organisms and Eisenia fetida in enhancing vermi-degradation and nutrient release of fly ash incorporated into cow dung–paper waste mixture. Waste Manag. 48, 165–173.

Naimpally, G., Nayak, R., 1978. EFFECT OF COLOURED LIGHT ON EARTHWORMS. Curr. Sci. 47, 116–118.

Nannoni, F., Protano, G., Riccobono, F., 2011. Fractionation and geochemical mobility of heavy elements in soils of a mining area in northern Kosovo. Geoderma 161, 63–73. https://doi.org/https://doi.org/10.1016/j.geoderma.2010.12.008

Nath, S., Das, S., 2026. Species-specific benefits in bioremediation of oil refinery sludge via large-scale vermicomposting process: a detailed comparison between Eisenia fetida and Eudrilus eugeniae. Chemosphere 394, 144782.

Nath, S., Das, S., 2025. Exploring the Reusability of Oil Refinery Sludge Post Blending With Natural Bulking Agents: Comparing the Suitability of Rice Husk and Cow Dung Manure. Environ. Qual. Manag. 35, e70203.

Nath, S., Das, S., 2024. Aqueous extracts of composted oil refinery sludge and their possible environmental impacts. Water Sci. Technol. wst2024229.

Nath, S., Dutta, U., Tangjang, S., Das, S., 2025. Assessing the compost-ability of oil refinery sludge in the presence or absence of earthworms: An eco-friendly approach of biodegradation. Int. Biodeterior. Biodegradation 198, 105987.

Nath, S., Qureshi, A., Das, S., 2023. Role of bulking agents, process optimization, and different earthworm species in the vermiremediation process of industrial wastes: A review. Not. Sci. Biol. 15, 11490.

Nath, S., Singh, K.K., Tangjang, S., Das, S., 2024. Industrial Solid Wastes and Environment: An Overview on Global Generation, Implications, and Available Management Options. Tech. Landfills Waste Manag. Vol. 1 Landfill Impacts, Charact. Valoris. 221–246.

Ndegwa, P.M., Thompson, S.A., 2001. Integrating composting and vermicomposting in the treatment. Bioresour. Technol. 76, 107–112.

Nithya, S., Sethuraman, O.S., Sasikumar, K., 2024. Effect of vermicompost and organic fertilizer on improved growth, productivity and quality of tomato (Solanum lycopersicum) plant. Indian J. Sci. Technol 17, 142–148.

Niu, A., Sun, X., Lin, C., 2022. Trend in research on characterization, environmental impacts and treatment of oily sludge: A systematic review. Molecules 27, 7795.

Nonthapa, A., Iwai, C.B., Chankaew, S., Falab, S., 2024. Dual-Purpose Vermicompost for the Growth Promotion and Suppression of Damping-Off Disease on Potted Vegetable Soybean. Plants 13, 1607.

Ogundola, A.F., Bvenura, C., Ehigie, A.F., Afolayan, A.J., 2022. Effects of soil types on phytochemical constituents and antioxidant properties of Solanum nigrum. South African J. Bot. 151, 325–333. https://doi.org/https://doi.org/10.1016/j.sajb.2022.09.048

Oleszczuk, P., 2006. Influence of different bulking agents on the disappearance of polycyclic aromatic hydrocarbons (PAHs) during sewage sludge composting. Water. Air. Soil Pollut. 175, 15–32.

Oliveira, H., Pinheiro, I., Ramos, A., Venturini, O., Mariano, A., Santiago, Y., 2024. Influence of Physicochemical Properties of Oil Sludge on Syngas Production for Energy Applications. Resources 14, 8.

Olougou, M.N.E., Kungang, N.A., Ndzeshala, S.T., Ngone, M.A., Ngosong, C., 2025. Exploring the fertilizer value of vermicompost and poultry manure to enhance soil health and yield of sweet bitter-leaf Vernonia hymenolepis. Discov. Soil 2, 42.

Osibuamhe, M.O., Popoola, L.T., Asmara, Y.P., Taura, U., Aderibigbe, T.A., 2024. Self-ignition behaviour of corn cob, wheat bran and rice husk residues in ambient air from biomass gasification. Heliyon 10, e36875. https://doi.org/https://doi.org/10.1016/j.heliyon.2024.e36875

Oviedo-Ocaña, R., Marmolejo-Rebellón, L.F., Torres-Lozada, P., Daza, M., Andrade, M., Torres-López, W.A., Abonia-Gonzalez, R., 2015. Effect of adding bulking materials over the composting process of municipal solid biowastes. Chil. J. Agric. Res. 75, 472–480.

Owa, S.O., Peters, S., Dedeke, G.A., Aladesida, A., 2008. Effects of light colour and oscillator frequency on earthworm bioactivity. African J. Agric. Res. 3, 29–36.

Owagboriaye, F., Mesnage, R., Dedeke, G., Adegboyega, T., Aladesida, A., Adeleke, M., Owa, S., Antoniou, M.N., 2021. Impacts of a glyphosate-based herbicide on the gut microbiome of three earthworm species (Alma millsoni, Eudrilus eugeniae and Libyodrilus violaceus): A pilot study. Toxicol. Reports 8, 753–758.

Oyege, I., Balaji Bhaskar, M.S., 2023. Effects of vermicompost on soil and plant health and promoting sustainable agriculture. Soil Syst. 7, 101.

Özer, M.Ö., Kar, H., Doğru, S.M., Bekar, N.K., 2021. Morphological characterization of some hybrid red head cabbage (Brassica oleracea L. var. capitata subvar. rubra) varieties. Tekirdağ Ziraat Fakültesi Derg. 18, 428–435.

Ozyazici, G., Turan, N., 2021. Effect of vermicompost application on mineral nutrient composition of grains of buckwheat (Fagopyrum esculentum M.). Sustainability 13, 6004.

Page, A.L., Miller, R., Keeney, D., 1982. Methods of soil analysis. Part 2. Chemical and microbiological properties.

Palsania, J., Sharma, R., Srivastava, J.K., Sharma, D., 2008. Effect of moisture content variation over kinetic reaction rate during vermicomposting process. Appl. Ecol. Environ. Res. 6, 49–61.

Pan, F., Zhang, J., Tang, J., Chen, B., 2025. Soil aggregate and organic nitrogen distributions as influenced by vermicompost application in vegetable greenhouse. Sci. Rep. 15, 22407.

Pandit, L., Sethi, D., Pattanayak, S.K., Nayak, Y., 2020. Bioconversion of lignocellulosic organic wastes into nutrient rich vermicompost by Eudrilus eugeniae. Bioresour. Technol. Reports 12, 100580. https://doi.org/https://doi.org/10.1016/j.biteb.2020.100580

Paredes, C., Bernal, M.P., Roig, A., Cegarra, J., Sánchez-Monedero, M.A., 1996. Influence of the bulking agent on the degradation of olive-mill wastewater sludge during composting. Int. Biodeterior. Biodegradation 38, 205–210. https://doi.org/https://doi.org/10.1016/S0964-8305(96)00052-2

Parihar, S.S., Singh, N., Tomar, B., Patle, T., Gupta, S., 2024. Elucidating Potential Application of Vermicompost on Alluvial Soil (Entisols) Physico-chemical Properties of Gwalior District, Madhya Pradesh. Ecol. Environ. Conserv. 30, 70–74.

Paul Choudhury, S., Kalamdhad, A.S., 2021. Optimization of electrokinetic pretreatment for enhanced methane production and toxicity reduction from petroleum refinery sludge. J. Environ. Manage. 298, 113469. https://doi.org/10.1016/j.jenvman.2021.113469

Paul, S., Das, S., Raul, P., Bhattacharya, S.S., 2018. Vermi-sanitization of toxic silk industry waste employing Eisenia fetida and Eudrilus eugeniae: substrate compatibility, nutrient enrichment and metal accumulation dynamics. Bioresour. Technol. 266, 267–274.

Paul, S., Goswami, L., Pegu, R., Chatterjee, S.K., Bhattacharya, S.S., 2022. Epigenetic regulations enhance adaptability and valorization efficiency in Eisenia fetida and Eudrilus eugeniae during vermicomposting of textile sludge: Insights on repair mechanisms of metal-induced genetic damage and oxidative stress. Bioresour. Technol. 345, 126493.

Paul, S., Goswami, L., Pegu, R., Sundar Bhattacharya, S., 2020. Vermiremediation of cotton textile sludge by Eudrilus eugeniae: Insight into metal budgeting, chromium speciation, and humic substance interactions. Bioresour. Technol. 314, 123753. https://doi.org/https://doi.org/10.1016/j.biortech.2020.123753

Pavan, G., Jyothi, V., 2019. The Flame photometric determination of Na + and K + from selected some citrus fruits and their antioxidant capacity in vitro method 7, 56–63.

Pegu, R., Prakash, A., Borah, P., Paul, S., Bhattacharya, S.S., 2024. Unveiling the earthworm-associated preferential remediation of emerging organic pollutants and heavy metals in MSW-based vermicomposting systems: Insights through the lens of multivariate techniques and novel empirical models. Chemosphere 363, 142782. https://doi.org/https://doi.org/10.1016/j.chemosphere.2024.142782

Pereira, M. de G., Cardoso de Souza Neta, L., Fontes, M.P.F., Souza, A.N., Carvalho Matos, T., de Lima Sachdev, R., dos Santos, A.V., Oliveira da Guarda Souza, M., de Andrade, M.V.A.S., Marinho Maciel Paulo, G., 2014. An overview of the environmental applicability of vermicompost: From wastewater treatment to the development of sensitive analytical methods. Sci. World J. 2014.

Pérez-Patricio, M., Camas-Anzueto, J.L., Sanchez-Alegría, A., Aguilar-González, A., Gutiérrez-Miceli, F., Escobar-Gómez, E., Voisin, Y., Rios-Rojas, C., Grajales-Coutiño, R., 2018. Optical method for estimating the chlorophyll contents in plant leaves. Sensors 18, 650.

Pinos, N.Q., Louro Berbara, R.L., Elias, S.S., van Tol de Castro, T.A., García, A.C., 2019. Combination of humic substances and arbuscular mycorrhizal fungi affecting corn plant growth. J. Environ. Qual. 48, 1594–1604.

Polak, J., Bartoszek, M., Sułkowski, W.W., 2009. Comparison of some spectroscopic and physico-chemical properties of humic acids extracted from sewage sludge and bottom sediments. J. Mol. Struct. 924, 309–312.

Pradhan, S., Pokhrel, M.R., 2013. Spectrophotometric determination of phosphate in sugarcane juice, fertilizer, detergent and water samples by molybdenum blue method. Sci. world 11, 58–62.

Pramanik, P., 2010. Changes in enzymatic activities and microbial properties in vermicompost of water hyacinth as affected by pre-composting and fungal inoculation: A comparative study of ergosterol and chitin for estimating fungal biomass. Waste Manag. 30, 1472–1476.

Prashija, K. V, Ameer Basha, S., Parthasarathi, K., 2017. Lampito mauritii (Kinberg)–A potential indigenous earthworm for vermicomposting lingocellulosic waste resources. Int. J. Mod. Res. Rev. 5, 1639–1646.

Procházková, P., Hanč, A., Dvořák, J., Roubalová, R., Drešlová, M., Částková, T., Šustr, V., Škanta, F., Pacheco, N.I.N., Bilej, M., 2018. Contribution of Eisenia andrei earthworms in pathogen reduction during vermicomposting. Environ. Sci. Pollut. Res. 25, 26267–26278.

Przemieniecki, S.W., Zapałowska, A., Skwiercz, A., Damszel, M., Telesiński, A., Sierota, Z., Gorczyca, A., 2021. An evaluation of selected chemical, biochemical, and biological parameters of soil enriched with vermicompost. Environ. Sci. Pollut. Res. 28, 8117–8127.

Pundee, K., Akeprathumchai, S., Tripetchkul, S., Salaipeth, L., 2023. Unveiling the microbial dynamics in vermicomposting with coir pith as earthworm substrate. Heliyon 9.

Qian, F., Lu, F., Yang, L., Li, T., 2024. Cultivation of earthworms and analysis of associated bacterial communities during earthworms' growth using two types of agricultural wastes. Bioresour. Bioprocess. 11, 66.

Quintern, M., Morley, M., Seaton, B., Hamilton, R., 2016. How we transform industrial organic waste into vermicompost and champion environmental sustainability. WIT Trans. Ecol. Environ. 202, 147–159.

Rajadurai, M., Karmegam, N., Kannan, S., Yuvaraj, A., Thangaraj, R., 2022. Vermiremediation of engine oil contaminated soil employing indigenous earthworms, Drawida modesta and Lampito mauritii. J. Environ. Manage. 301, 113849. https://doi.org/https://doi.org/10.1016/j.jenvman.2021.113849

Ramírez-García, R., Gohil, N., Singh, V., 2019. Chapter 21 - Recent Advances, Challenges, and Opportunities in Bioremediation of Hazardous Materials, in: Pandey, V.C., Bauddh, K.B.T.-P. of P.S. (Eds.), . Elsevier, pp. 517–568. https://doi.org/https://doi.org/10.1016/B978-0-12-813912-7.00021-1

Ramnarain, Y.I., Ansari, A.A., Ori, L., 2019. Vermicomposting of different organic materials using the epigeic earthworm Eisenia foetida. Int. J. Recycl. Org. Waste Agric. 8, 23–36.

Ravindran, B., Contreras-Ramos, S.M., Sekaran, G., 2015. Changes in earthworm gut associated enzymes and microbial diversity on the treatment of fermented tannery waste using epigeic earthworm Eudrilus eugeniae. Ecol. Eng. 74, 394–401.

Ravindran, B., Wong, J.W.C., Selvam, A., Sekaran, G., 2016. Influence of microbial diversity and plant growth hormones in compost and vermicompost from fermented tannery waste. Bioresour. Technol. 217, 200–204.

Rehman, S. ur, De Castro, F., Aprile, A., Benedetti, M., Fanizzi, F.P., 2023. Vermicompost: Enhancing plant growth and combating abiotic and biotic stress. Agronomy 13, 1134.

Reimann, C., Filzmoser, P., Garrett, R., Dutter, R., 2011. Statistical data analysis explained: applied environmental statistics with R. John Wiley & Sons.

Robertson, S.J., McGill, W.B., Massicotte, H.B., Rutherford, P.M., 2007. Petroleum hydrocarbon contamination in boreal forest soils: A mycorrhizal ecosystems perspective. Biol. Rev. 82, 213–240. https://doi.org/10.1111/j.1469-185X.2007.00012.x

Rorat, A., Vandenbulcke, F., 2019. Earthworms converting domestic and food industry wastes into biofertilizer, Industrial and Municipal Sludge: Emerging Concerns and Scope for Resource Recovery. Elsevier Inc. https://doi.org/10.1016/B978-0-12-815907-1.00005-2

Rostami, R., Nabaey, A., Eslami, A., 2009. Survey of optimal temperature and moisture for worms growth and operating vermicompost production of food wastes. Iran. J. Heal. Environ. 1, 105–112.

Roy, A., Dutta, A., Pal, S., Gupta, A., Sarkar, J., Chatterjee, A., Saha, A., Sarkar, P., Sar, P., Kazy, S.K., 2018. Biostimulation and bioaugmentation of native microbial community accelerated bioremediation of oil refinery sludge. Bioresour. Technol. 253, 22–32. https://doi.org/10.1016/j.biortech.2018.01.004

Rupani, P.F., Embrandiri, A., Ibrahim, M.H., Shahadat, M., Hansen, S.B., Mansor, N.N.A., 2017. Bioremediation of palm industry wastes using vermicomposting technology: its environmental application as green fertilizer. 3 Biotech 7, 155.

Saba, S., Zara, G., Bianco, A., Garau, M., Bononi, M., Deroma, M., Pais, A., Budroni, M.,

2019. Comparative analysis of vermicompost quality produced from brewers' spent grain and cow manure by the red earthworm Eisenia fetida. Bioresour. Technol. 293, 122019. https://doi.org/https://doi.org/10.1016/j.biortech.2019.122019

Sabina, R., Dey, R., Ghosh, S., Bhattacharya, P., Bhattacharya, S.S., Hussain, N., 2025. Unlocking the potential of Eudrilus eugeniae in mitigating the pollution risk of pesticides and heavy metals: Fostering machine learning tactics to optimize environmental health. Sci. Total Environ. 971, 179039. https://doi.org/https://doi.org/10.1016/j.scitotenv.2025.179039

Safadoust, A., Azimi, S.B., Dehghan, M.B., 2025. Restoring soil functionality in drylands: Soil texture-specific impacts of vermicompost as an organic waste-based amendment. J. Arid Environ. 231, 105446. https://doi.org/https://doi.org/10.1016/j.jaridenv.2025.105446

Saha, J.K., Panwar, N., Singh, M. V, 2010. An assessment of municipal solid waste compost quality produced in different cities of India in the perspective of developing quality control indices. Waste Manag. 30, 192–201.

Sahariah, B., Goswami, L., Farooqui, I.U., Raul, P., Bhattacharyya, P., Bhattacharya, S., 2015a. Solubility, hydrogeochemical impact, and health assessment of toxic metals in municipal wastes of two differently populated cities. J. Geochemical Explor. 157, 100–109.

Sahariah, B., Goswami, L., Kim, K.-H., Bhattacharyya, P., Bhattacharya, S.S., 2015b. Metal remediation and biodegradation potential of earthworm species on municipal solid waste: A parallel analysis between Metaphire posthuma and Eisenia fetida. Bioresour. Technol. 180, 230–236. https://doi.org/https://doi.org/10.1016/j.biortech.2014.12.062

Said, O. Ben, Cravo-Laureau, C., Armougom, F., Cipullo, S., Khelil, M. Ben, Yahiya, M.B.H., Douihech, A., Beyrem, H., Coulon, F., Duran, R., 2021. Enhanced pilot bioremediation of oily sludge from petroleum refinery disposal under hot-summer Mediterranean climate. Environ. Technol. Innov. 24, 102037. https://doi.org/10.1016/j.eti.2021.102037

Saleh, H.M., Aglan, R.F., Mahmoud, H.H., 2019. Ludwigia stolonifera for remediation of toxic metals from simulated wastewater. Chem. Ecol. 35, 164–178. https://doi.org/10.1080/02757540.2018.1546296

Saleh, H.M., Bayoumi, T.A., Mahmoud, H.H., Aglan, R.F., 2017. Uptake of cesium and cobalt radionuclides from simulated radioactive wastewater by Ludwigia stolonifera aquatic plant. Nucl. Eng. Des. 315, 194–199. https://doi.org/10.1016/j.nucengdes.2017.02.018

Sánchez-Rosales, R., Hernández-Rodríguez, O.A., Ojeda-Barrios, D.L., Quezada, G.D.Á., 2025. Mineralization and humification of organic matter in controlled transformation systems. Int. J. Recycl. Org. Waste Agric. 14.

Sandberg, M., Klockars, K., Wilén, K., 2019. Green growth or degrowth? Assessing the normative justifications for environmental sustainability and economic growth through critical social theory. J. Clean. Prod. 206, 133–141. https://doi.org/10.1016/j.jclepro.2018.09.175

Santos, J.L.A., Busato, J.G., Pittarello, M., da Silva, J., Horák-Terra, I., Evaristo, A.B., Dobbss, L.B., 2022. Alkaline extract from vermicompost reduced the stress promoted by As on maize plants and increase their phytoextraction capacity. Environ. Sci. Pollut. Res. 29, 20864–20877.

Sengupta, S., Bhattacharyya, K., Mandal, J., Bhattacharya, P., Halder, S., Pari, A., 2021. Deficit irrigation and organic amendments can reduce dietary arsenic risk from rice: Introducing machine learning-based prediction models from field data. Agric. Ecosyst. Environ. 319, 107516.

Setyorini, D., Sugito, Y., Aini, N., Tyasmoro, S.Y., 2018. Lycopene, beta-carotene and productivity of tomato varieties at different shade levels under medium land of Indonesia. J. Appl. Hortic. 20, 92–96.

Shagoti, U.M., Amoji, S.D., Biradar, V.A., Biradar, P.M., 2001. Effect of temperature on growth and reproduction of the epigeic earthworm, Eudrilus Eugeniae (Kinberg). J. Environ. Biol. 22, 213–217.

Shah, R.U., Abid, M., Qayyum, M.F., Ullah, R., 2015. Dynamics of chemical changes through production of various composts/vermicompost such as farm manure and sugar industry wastes. Int. J. Recycl. Org. Waste Agric. 4, 39–51.

Shahbazi, S., Kurdve, M., Bjelkemyr, M., Jönsson, C., Wiktorsson, M., 2013. Industrial Waste Management Within Manufacturing: a Comparative Study of Tools, Policies, Visions and Concepts. 11th Int. Conf. Manuf. Res. 637–642.

Sharma, A., Ganguly, R., Gupta, A.K., 2019. Spectral characterization and quality assessment of organic compost for agricultural purposes. Int. J. Recycl. Org. waste Agric. 8, 197–213.

Shen, Z., Yu, Z., Xu, L., Zhao, Y., Yi, S., Shen, C., Wang, Y., Li, Y., Zuo, W., Gu, C., 2022. Effects of vermicompost application on growth and heavy metal uptake of barley grown in mudflat salt-affected soils. Agronomy 12, 1007.

Sinex, S.A., Helz, G.R., 1981. Regional geochemistry of trace elements in Chesapeake Bay sediments. Environ. Geol. 3, 315–323.

Singh, B., Kumar, P., 2020. Physicochemical characteristics of hazardous sludge from effluent treatment plant of petroleum refinery as feedstock for thermochemical processes. J. Environ. Chem. Eng. 8, 103817.

Singh, J., Kalamdhad, A.S., 2012. Concentration and speciation of heavy metals during water hyacinth composting. Bioresour. Technol. 124, 169–179.

Singh, J., Kaur, A., Vig, A.P., Rup, P.J., 2010. Role of Eisenia fetida in rapid recycling of nutrients from bio sludge of beverage industry. Ecotoxicol. Environ. Saf. 73, 430–435. https://doi.org/10.1016/j.ecoenv.2009.08.019

Singh, S., Misal, N.B., 2022. Effect of different levels of organic and inorganic fertilizers on maize (Zea mays L.). Indian J. Agric. Res. 56, 562–566.

Singha, W.J., Deka, H., 2024. Ecological and human health risk associated with heavy metals (HMs) contaminant sourced from petroleum refinery oily sludge. J. Hazard. Mater. 476, 135077.

Sinha, R.K., Agarwal, S., Chauhan, K., Valani, D., 2010. The wonders of earthworms & its vermicompost in farm production: Charles Darwin's 'friends of farmers', with potential to replace destructive chemical fertilizers. Agric. Sci. 1, 76.

Sivakumar, S., Prabha, D., Barathi, S., Nityanandi, D., Subbhuraam, C. V, Lakshmipriya, T., Kamala-Kannan, S., Jang, S.H., Yi, P.I., 2015. The influence of the earthworm Lampito mauritii (Kinberg) on the activity of selected soil enzymes in cadmium-amended soil. Environ. Monit. Assess. 187, 1–8.

Sivaperumal, P., Kamala, K., Rajaram, R., 2017. Chapter Eight - Bioremediation of Industrial Waste Through Enzyme Producing Marine Microorganisms, in: Kim, S.-K., Toldrá, F.B.T.-A. in F. and N.R. (Eds.), Marine Enzymes Biotechnology: Production and Industrial Applications, Part III - Application of Marine Enzymes. Academic Press, pp. 165–179. https://doi.org/https://doi.org/10.1016/bs.afnr.2016.10.006

Soliman, N.K., Moustafa, A.F., 2020. Industrial solid waste for heavy metals adsorption features and challenges; a review. J. Mater. Res. Technol. 9, 10235–10253. https://doi.org/10.1016/j.jmrt.2020.07.045

Song, Q., Zhao, H., Jia, J., Zhang, F., Wang, Z., Lv, W., Yang, L., Zhang, W., Zhang, Y., Shu, X., 2019. Characterization of the products obtained by pyrolysis of oil sludge with steel slag in a continuous pyrolysis-magnetic separation reactor. Fuel 255, 115711. https://doi.org/https://doi.org/10.1016/j.fuel.2019.115711

Song, Y., Liang, H., Ma, J., Wang, X., Li, Z., You, J., Wang, S., 2022. Probing the separation mechanism of solid–liquid components in oily sludge and sludge containing polymers for a harmless treatment process of sludge. RSC Adv. 12, 29543–29553.

Soobhany, N., Gunasee, S., Rago, Y.P., Joyram, H., Raghoo, P., Mohee, R., Garg, V.K., 2017. Spectroscopic, thermogravimetric and structural characterization analyses for comparing Municipal Solid Waste composts and vermicomposts stability and maturity. Bioresour. Technol. 236, 11–19.

Soobhany, N., Mohee, R., Garg, V.K., 2015. Comparative assessment of heavy metals content during the composting and vermicomposting of Municipal Solid Waste employing Eudrilus eugeniae. Waste Manag. 39, 130–145. https://doi.org/https://doi.org/10.1016/j.wasman.2015.02.003

Spinosa, L., Molinari, L., 2023. Standardization: A Necessary Support for the Utilization of Sludge/Biosolids in Agriculture. Standards 3, 385–399.

Srivastava, R., Kumar, D., Gupta, S.K., 2005. Bioremediation of municipal sludge by vermitechnology and toxicity assessment by Allium cepa. Bioresour. Technol. 96, 1867–1871. https://doi.org/10.1016/j.biortech.2005.01.029

Su, M., Kong, L., Liao, C., Chen, D., Shih, K., 2019. Stabilization of cadmium in industrial sludge—Generation of crystalline products, in: Industrial and Municipal Sludge.

Elsevier, pp. 503–524.

Suleimanov, R.R., Gabbasova, I.M., Sitdikov, R.N., 2005. Changes in the properties of oily gray forest soil during biological reclamation. Izv. Akad. Nauk Ser. Biol. 32, 109–115.

Sun, H., Liao, C., Chen, L., Cheng, Q., Zheng, Y., Wang, C., Xie, Y., Chen, C., Li, P., 2023. Potential for volatile fatty acid production via anaerobically-fermenting rice straw pretreated with silage effluent and phenyllactic acid. Bioresour. Technol. 369, 128355. https://doi.org/https://doi.org/10.1016/j.biortech.2022.128355

Suthar, S., 2006. Potential utilization of guar gum industrial waste in vermicompost production. Bioresour. Technol. 97, 2474–2477.

Sutherland, R.A., 2000. Bed sediment-associated trace metals in an urban stream, Oahu, Hawaii. Environ. Geol. 39, 611–627.

Suvedha, A., Brindha Devi, G., Latha, R., Revathi, K., 2024. Identification of Cadmium (CD) metal binding sites in _ Eudrilus eugeniae using Insilico protocols. African J. Biomed. Res. 27, 2372–2376.

Swain, P., Biswal, T., Panda, R., 2018. A SHORT REVIEW ON SOLID WASTE GENERATIONS, RECYCLING AND MANAGEMENT IN THE PRESENT SCENARIO OF INDIA. https://doi.org/10.13140/RG.2.2.17912.47366

Swati, A., Hait, S., 2017. Fate and bioavailability of heavy metals during vermicomposting of various organic wastes—A review. Process Saf. Environ. Prot. 109, 30–45. https://doi.org/10.1016/j.psep.2017.03.031

Syed Hassan, S.S., Jawad, A.H., Habeeb, O.A., 2021. Characterization Study of Petroleum Oily Sludge Produced from North Refineries Company Baiji to Determine the Suitability for Conversion into Solid Fuel. Egypt. J. Chem. 64, 2775–2781.

Tabatabai, M.A., Bremner, J.M., 1969. Use of p-nitrophenyl phosphate for assay of soil phosphatase activity. Soil Biol. Biochem. 1, 301–307. https://doi.org/https://doi.org/10.1016/0038-0717(69)90012-1

Taeporamaysamai, O., Ratanatamskul, C., 2016. Co-composting of various organic substrates from municipal solid waste using an on-site prototype vermicomposting reactor. Int. Biodeterior. Biodegradation 113, 357–366.

Taiwo, E.A., Otolorin, J.A., 2009. Oil recovery from petroleum sludge by solvent extraction. Pet. Sci. Technol. 27, 836–844. https://doi.org/10.1080/10916460802455582

Tang, J.-C., Shibata, A., Zhou, Q., Katayama, A., 2007. Effect of temperature on reaction rate and microbial community in composting of cattle manure with rice straw. J. Biosci. Bioeng. 104, 321–328.

Tang, R., Li, X., Mo, Y., Ma, Y., Ding, C., Wang, J., Zhang, T., Wang, X., 2019. Toxic responses of metabolites, organelles and gut microorganisms of Eisenia fetida in a soil with chromium contamination. Environ. Pollut. 251, 910–920.

Tanirbergenova, S., Tagayeva, A., Rossi, C.O., Porto, M., Caputo, P., Kanzharkan, E., Tugelbayeva, D., Zhylybayeva, N., Tazhu, K., Tileuberdi, Y., 2024. Studying the Characteristics of Tank Oil Sludge. Processes 12.

Temjen, W., Singh, M.R., Ajungla, T., 2022. Effect of shifting cultivation and fallow on soil quality index in Mokokchung district, Nagaland, India. Ecol. Process. 11, 42.

Teng, Q., Zhang, D., Yang, C., 2021. A review of the application of different treatment processes for oily sludge. Environ. Sci. Pollut. Res. 28, 121–132.

Teshome, K., Aklilu, S., Zewdu, A., 2025. Impact of Fertilization on Antioxidant Activity, Microbiological Quality, and Sensory Attributes of Tomato (Solanum lycopersicum L.) Cultivated in Ethiopia's Central Rift Valley. Food Sci. Nutr. 13, e70609.

Tessier, A., Campbell, P.G.C., Bisson, M., 1979. Sequential extraction procedure for the speciation of particulate trace metals. Anal. Chem. 51, 844–851.

Thakur, S.S., Lone, A.R., Yellaboina, S., Tambat, S., Yadav, A.N., Jain, S.K., Yadav, S., 2022. Metagenomic insights into the gut microbiota of Eudrilus eugeniae (Kinberg) and its potential roles in agroecosystem. Curr. Microbiol. 79, 295.

Tian, M., Yu, R., Guo, S., Yang, W., Liu, S., Du, H., Liang, J., Zhang, X., 2024. Effect of Vermicompost Application on the Soil Microbial Community Structure and Fruit Quality in Melon (Cucumis melo). Agronomy 14, 2536.

Tian, Y., Chen, L., Gao, L., Michel Jr, F.C., Keener, H.M., Klingman, M., Dick, W.A., 2012. Composting of waste paint sludge containing melamine resin and the compost's effect on vegetable growth and soil water quality. J. Hazard. Mater. 243, 28–36.

Tiwari, R.K., Singh, S., Pandey, R.S., Sharma, B., 2016. Enzymes of earthworm as indicators of pesticide pollution in soil. Adv. Enzym. Res. 4, 113.

Toor, M.D., Anwar, A., Koleva, L., Eldesoky, G.E., 2024. Effects of vermicompost on soil microbiological properties in lettuce rhizosphere: An environmentally friendly approach for sustainable green future. Environ. Res. 243, 117737.

Tripathi, G., Bhardwaj, P., 2004. Decomposition of kitchen waste amended with cow manure using an epigeic species (Eisenia fetida) and an anecic species (Lampito mauritii). Bioresour. Technol. 92, 215–218. https://doi.org/https://doi.org/10.1016/j.biortech.2003.08.013

Usmani, Z., Kumar, V., Mritunjay, S.K., 2017. Vermicomposting of coal fly ash using epigeic and epi-endogeic earthworm species: nutrient dynamics and metal remediation. RSC Adv. 7, 4876–4890.

Usta, A.N., Guven, H., 2024. Vermicomposting organic waste with Eisenia fetida using a continuous flow-through reactor: Investigating five distinct waste mixtures. J. Environ. Chem. Eng. 12, 114384. https://doi.org/https://doi.org/10.1016/j.jece.2024.114384

Varol, M., 2011. Assessment of heavy metal contamination in sediments of the Tigris River (Turkey) using pollution indices and multivariate statistical techniques. J. Hazard. Mater. 195, 355–364.

Vasileiadou, A., 2023. Sustainable energy production from grape marc: from thermo-analytical and chemical analysis to kinetic modeling and environmental impact assessment. Energy, Ecol. Environ. 8, 471–484.

Vavouraki, A.I., Kornaros, M., 2023. Vermi-Conversion of Anaerobic Sludges by Eisenia fetida Earthworms. Fermentation 9, 512.

Vdovenko, S., Boichenko, S., Kochubei, V., 2015. Composition and properties of petroleum sludge produced at the refineries. Chem. Chem. Technol. 9, 257–260. https://doi.org/10.23939/chcht09.02.257

Velásquez-Chávez, T.E., Sáenz-Mata, J., Quezada-Rivera, J.J., Palacio-Rodríguez, R., Muro-Pérez, G., Servín-Prieto, A.J., Hernández-López, M., Preciado-Rangel, P., Salazar-Ramírez, M.T., Ontiveros-Chacón, J.C., 2025. Bacterial and Physicochemical Dynamics During the Vermicomposting of Bovine Manure: A Comparative Analysis of the Eisenia fetida Gut and Compost Matrix. Microbiol. Res. (Pavia). 16, 177.

Verma, S., Kuila, A., 2019. Bioremediation of heavy metals by microbial process. Environ. Technol. Innov. 14, 100369. https://doi.org/https://doi.org/10.1016/j.eti.2019.100369

Viana, F.F., de Castro Dantas, T.N., Rossi, C.G.F.T., Dantas Neto, A.A., Silva, M.S., 2015. Aged oil sludge solubilization using new microemulsion systems: Design of experiments. J. Mol. Liq. 210, 44–50. https://doi.org/https://doi.org/10.1016/j.molliq.2015.02.042

Vyas, P., Sharma, S., Gupta, J., 2022. Vermicomposting with microbial amendment: implications for bioremediation of industrial and agricultural waste. BioTechnologia 103, 203–215.

Wang, H., Kuang, S., Lang, Q., Yu, W., 2018. Effects of Aged Oil Sludge on Soil Physicochemical Properties and Fungal Diversity Revealed by High-Throughput Sequencing Analysis. Archaea 2018, 9264259.

Wang, L.K., Hung, Y.-T., Li, K.H., 2009. Vermicomposting process, in: Biological Treatment Processes. Springer, pp. 715–732.

Wang, S., Liu, P., Wang, M., Cui, Y., Tuo, Y., Zhao, B., Wang, N., 2024. Evaluation of chemical properties and humification process during co-composting of spent mushroom substrate (Pleurotus ostreatus) and pig manure under different mass ratios. Int. Biodeterior. Biodegradation 193, 105858. https://doi.org/https://doi.org/10.1016/j.ibiod.2024.105858

Wang, W., Zhu, X., Chang, L., Zhang, Y., Zhang, S., Wu, D., 2021. How do earthworms affect the soil organic carbon fractions and CO2 emissions after incorporation of different maize straw-derived materials. J. Soils Sediments 21, 1–13. https://doi.org/10.1007/s11368-021-03006-w

Wang, X.-X., Zhao, F., Zhang, G., Zhang, Y., Yang, L., 2017. Vermicompost improves tomato yield and quality and the biochemical properties of soils with different tomato planting history in a greenhouse study. Front. Plant Sci. 8, 1978.

Wang, X., Wang, Q., Wang, S., Li, F., Guo, G., 2012. Effect of biostimulation on community level physiological profiles of microorganisms in field-scale biopiles composed of aged oil sludge. Bioresour. Technol. 111, 308–315.

https://doi.org/10.1016/j.biortech.2012.01.158

Wang, Z., Chen, Z., Niu, Y., Ren, P., Hao, M., 2021. Feasibility of vermicomposting for spent drilling fluid from a nature-gas industry employing earthworms Eisenia fetida. Ecotoxicol. Environ. Saf. 214, 111994. https://doi.org/https://doi.org/10.1016/j.ecoenv.2021.111994

Weissmannová, H.D., Pavlovský, J., 2017. Indices of soil contamination by heavy metals–methodology of calculation for pollution assessment (minireview). Environ. Monit. Assess. 189, 616.

Wonnapinij, P., Sriboonlert, A., Surat, W., 2022. Exploration of microbial communities in the guts and casts of Eudrilus eugeniae, Perionyx excavatus, and Eisenia fetida. Folia Microbiol. (Praha). 67, 329–337.

Wu, D., Chen, C., Liu, Y., Zhang, G., Yang, L., 2023. Vermicompost improves tomato yield and quality by promoting carbohydrate transport to fruit under salt stress. Horticulturae 9, 1015.

Wu, G., Duan, C., Li, H., Li, M., Liu, C., 2025. Cadmium stress drives remodeling of earthworm mucus metabolism: Hormetic antioxidant response and synergistic amino acid defence mechanisms. Environ. Res. 283, 122151. https://doi.org/https://doi.org/10.1016/j.envres.2025.122151

Xiao, R., Liu, X., Ali, A., Chen, A., Zhang, M., Li, R., Chang, H., Zhang, Z., 2021. Bioremediation of Cd-spiked soil using earthworms (Eisenia fetida): Enhancement with biochar and Bacillus megatherium application. Chemosphere 264, 128517.

Xie, D., Wu, W., Hao, X., Jiang, D., Li, X., Bai, L., 2016. Vermicomposting of sludge from animal wastewater treatment plant mixed with cow dung or swine manure using Eisenia fetida. Environ. Sci. Pollut. Res. 23, 7767–7775.

Xing, Y., Xie, Y., Wang, X., 2025. Enhancing soil health through balanced fertilization: a pathway to sustainable agriculture and food security. Front. Microbiol. 16, 1536524.

Xu, G., Hu, T., Wei, H., Cheng, L., Wang, H., Fang, B., 2021. Response surface optimization, combustion characteristics and kinetic analysis of mixed fuels of Fenton/CaO conditioned municipal sewage sludge and rice husk. J. Environ. Manage. 296, 113181.

Yadav, J., Gupta, R.K., Kumar, D., 2017. Changes in C: N ratio of different substrates during vermicomposting. Ecol. Environ. Conserv. 23, 367–371.

Yadav, R., Kumar, R., Gupta, R.K., Kaur, T., Kour, A., Kaur, S., Rajput, A., 2023. Heavy metal toxicity in earthworms and its environmental implications: A review. Environ. Adv. 12, 100374.

Yang, L., Zhao, F., Chang, Q., Li, T., Li, F., 2015. Effects of vermicomposts on tomato yield and quality and soil fertility in greenhouse under different soil water regimes. Agric. Water Manag. 160, 98–105. https://doi.org/https://doi.org/10.1016/j.agwat.2015.07.002

Yefremova, S., Kablanbekov, A., Satbaev, B., Zharmenov, A., 2023. Rice Husk-Based Adsorbents for Removal of Metals from Aqueous Solutions. Materials (Basel). 16, 7353.

Yeh, C.K., Lin, C., Shen, H.C., Cheruiyot, N.K., Camarillo, M.E., Wang, C.L., 2020. Optimizing food waste composting parameters and evaluating heat generation. Appl. Sci. 10, 2284.

Yiga, V.A., Lubwama, M., Olupot, P.W., 2023. Pyrolysis, kinetics and thermodynamic analyses of rice husks/clay fiber-reinforced polylactic acid composites using thermogravimetric analysis. J. Therm. Anal. Calorim. 148, 3457–3477. https://doi.org/10.1007/s10973-022-11927-y

Yusefi, M., Khalid, M., Yasin, F.M., Abdullah, L.C., Ketabchi, M.R., Walvekar, R., 2018. Performance of cow dung reinforced biodegradable poly (Lactic Acid) biocomposites for structural applications. J. Polym. Environ. 26, 474–486.

Yuvaraj, A., Karmegam, N., Thangaraj, R., 2018. Vermistabilization of paper mill sludge by an epigeic earthworm Perionyx excavatus: mitigation strategies for sustainable environmental management. Ecol. Eng. 120, 187–197.

Yuvaraj, A., Karmegam, N., Tripathi, S., Kannan, S., Thangaraj, R., 2020. Environment-friendly management of textile mill wastewater sludge using epigeic earthworms: Bioaccumulation of heavy metals and metallothionein production. J. Environ. Manage. 254, 109813. https://doi.org/10.1016/j.jenvman.2019.109813

Zahedifar, M., 2023. Assessing alteration of soil quality, degradation, and resistance indices under different land uses through network and factor analysis. CATENA 222, 106807. https://doi.org/https://doi.org/10.1016/j.catena.2022.106807

Zainal, N.S., Mohamad, Z., Mustapa, M.S., Badarulzaman, N.A., Salim, Z.A.S.A., Masirin, M.I., 2018. Study of characteristics of rice husk and silica obtained from rice husk. Int. J. Chem. Eng. Appl. 9, 158–162.

Zannat, A., Hussain, M.A., Abdullah, A.H.M., Hossain, M.I., Saifullah, M., Safhi, F.A., Alshallash, K.S., Mansour, E., ElSayed, A.I., Hossain, M.S., 2023. Exploring genotypic variability and interrelationships among growth, yield, and quality characteristics in diverse tomato genotypes. Heliyon 9.

Zhang, H., Li, J., Zhang, Y., Huang, K., 2020. Quality of vermicompost and microbial community diversity affected by the contrasting temperature during vermicomposting of dewatered sludge. Int. J. Environ. Res. Public Health 17, 1748.

Zhang, J., Li, J., Thring, R.W., Hu, X., Song, X., 2012. Oil recovery from refinery oily sludge via ultrasound and freeze/thaw. J. Hazard. Mater. 203–204, 195–203. https://doi.org/10.1016/j.jhazmat.2011.12.016

Zhang, M., Liu, Y., Wei, Q., Liu, L., Gu, X., Gou, J., Wang, M., 2023. Effects of biochar and vermicompost on growth and economic benefits of continuous cropping pepper at karst yellow soil region in Southwest China. Front. Plant Sci. 14, 1238663.

Zhang, S., Song, J., Gao, H., Zhang, Q., Lv, M.-C., Wang, S., Liu, G., Pan, Y.-Y., Christie, P., Sun, W., 2016. Improving prediction of metal uptake by Chinese cabbage (Brassica pekinensis L.) based on a soil-plant stepwise analysis. Sci. Total Environ. 569–570, 1595–1605. https://doi.org/https://doi.org/10.1016/j.scitotenv.2016.07.007

Zhang, S., Wu, J., Nie, Q., Duan, X., Yi, X., 2022. Environmental Risk Analysis Based on Characterization of Ground Oily Sludge. Materials (Basel). 15, 9054.

Zhang, X., Zhou, J., Xu, Z., Zhu, P., Liu, J., 2021. Characterization of heavy metals in textile sludge with hydrothermal carbonization treatment. J. Hazard. Mater. 402, 123635. https://doi.org/https://doi.org/10.1016/j.jhazmat.2020.123635

Zhang, Yanliang, Huang, C., Zhao, J., Hu, L., Yang, L., Zhang, Yuanyuan, Sang, W., 2024. Insights into tolerance mechanisms of earthworms (Eisenia fetida) in copper-contaminated soils by integrating multi-omics analyses. Environ. Res. 252, 118910. https://doi.org/https://doi.org/10.1016/j.envres.2024.118910

Zhou, C., Wang, Jia, Xu, T., Pei, K., Ma, B., Li, Q., Liu, Y., Ding, X., Han, Y., Wang, Junqiang, 2025. Manure substitution for chemical nitrogen enhances soil quality without compromising maize yield: a short-term field experiment in Northeast China. Front. Plant Sci. 16, 1694608.

Zhou, Y., Zhang, D., Zhang, Y., Ke, J., Chen, D., Cai, M., 2021. Evaluation of temperature on the biological activities and fertility potential during vermicomposting of pig manure employing Eisenia fetida. J. Clean. Prod. 302, 126804. https://doi.org/https://doi.org/10.1016/j.jclepro.2021.126804

Zhu, N., 2007. Effect of low initial C/N ratio on aerobic composting of swine manure with rice straw. Bioresour. Technol. 98, 9–13.

Zhu, N., Zhu, Y., Kan, Z., Li, B., Cao, Y., Jin, H., 2021. Effects of two-stage microbial inoculation on organic carbon turnover and fungal community succession during co-composting of cattle manure and rice straw. Bioresour. Technol. 341, 125842.

Zhu, W., Du, W., Shen, X., Zhang, H., Ding, Y., 2017. Comparative adsorption of Pb2+ and Cd2+ by cow manure and its vermicompost. Environ. Pollut. 227, 89–97.

Zorpas, A.A., Loizidou, M., 2008. Sawdust and natural zeolite as a bulking agent for improving quality of a composting product from anaerobically stabilized sewage sludge. Bioresour. Technol. 99, 7545–7552.

BIODATA OF THE CANDIDATE

Snigdha Nath

Ph.D. Scholar

Department of Environmental Science

Mizoram University

E-mail: snigdhonath@gmail.com

Contact No.: +91-7002904667

OrcID: 0009-0002-0523-9291

ResearchGate: https://www.researchgate.net/profile/Snigdha-Nath-2

1. Academic profile

- **Master of Science:** Department of Ecology and Environmental Science, Pondicherry University, Puducherry (2018-2020).

- **Bachelor of Science:** Department of Biotechnology, Cotton University, Guwahati (Assam) (2015-2018).

- **Higher Secondary:** Cotton College, Guwahati, Assam (2013-2015).

2. Conferences/seminars attended

National Conferences

- Oral paper presentation at the National Seminar on Environmental Management: Issues and Challenges in North East India, Department of Environmental Science, Pachhunga University College, Aizawl, Mizoram India.
- Oral paper presentation at the National Conference on Emerging Trends in Environmental Research (NACETER 2023), Department of Environmental Science, Manipur University, Manipur, India.
- Oral paper presentation at the National Conference on Sustainable Solutions: Navigating Climate Change and Natural Resources, Department of Environmental Science, Mizoram University, Aizawl India.

International Conferences

- Oral paper presentation at International Conference on Environmental hazards Mountainous regions: Problems and prospects, Pachhunga University College, Aizawl, Mizoram India.

- Oral paper presentation at ICSSR Sponsored International Conference on Traditional Knowledge (Exploring Traditional Knowledge: Bridging Past and Future) held on 22nd & 23rd March 2024 organized at Nagaon University, Assam, India.
- Oral paper presentation at International Conference on Recent Advances in Environmental Research, Biodiversity Conservation and Sustainable Development, Department of Environmental Science, Pachhunga University College, Aizawl, Mizoram India.

3. Publications

Research papers

i. Nath, S., & Das, S. (2026). Species-specific benefits in bioremediation of oil refinery sludge via large-scale vermicomposting process: a detailed comparison between Eisenia fetida and Eudrilus eugeniae. *Chemosphere*, *394*, 144782.

ii. Nath, S., & Das, S. (2025). Exploring the Reusability of Oil Refinery Sludge Post Blending with Natural Bulking Agents: Comparing the Suitability of Rice Husk and Cow Dung Manure. *Environmental Quality Management*, *35*(2), e70203.

iii. Nath, S., Dutta, U., Tangjang, S., & Das, S. (2025). Assessing the compost-ability of oil refinery sludge in the presence or absence of earthworms: An eco-friendly approach of biodegradation. *International Biodeterioration & Biodegradation*, *198*, 105987.

iv. Nath, S., & Das, S. (2024). Aqueous extracts of composted oil refinery sludge and their possible environmental impacts. *Water Science & Technology*, *90*(2), 524-548.

Review paper

v. Nath, S., Qureshi, A., & Das, S. (2023). Role of bulking agents, process optimization, and different earthworm species in the vermiremediation process of industrial wastes: A review. *Notulae Scientia Biologicae*, *15*(2), 11490-11490.

Book chapters

vi. Nath, S., & Das, S. (2026). Comparison of advantages among crop-sensing technology, optical sensor, and digital agriculture technologies for nitrogen management. In *Point Source Nitrogen Pollution* (pp. 305-331). Elsevier.

vii. Nath, S., & Das, S. (2025). Technological System to Increase the Rate of Plastic Collections from Soil. In *Handbook of Microplastic Pollution in the Environment* (pp. 155-185). CRC Press.

viii. Nath, S., Singh, K. K., Tangjang, S., & Das, S. (2024). Industrial solid wastes and environment: an overview on global generation, implications, and available management options. *Technical Landfills and Waste Management: Volume 1: Landfill Impacts, Characterization and Valorisation*, 221-246.

In communication

Research paper

ix. Nath, S., & Das, S. (2026). Repurposing vermicomposted oil refinery sludge in the cultivation of tomato and cabbage: focus on the process safety and environmental implications. *Physics and Chemistry of the Earth. Elsevier.* (Under review)

In collaboration

Research papers

x. Nath, S., Babu, K.N., Dar, A.A., & Parthasarathy, N. (2022). Increasing liana biomass and carbon stocks in tropical dry evergreen forests of southern India. *Notulae Scientia Biologicae*, *14*(3), 11279-11279.

xi. Nath, S., Babu, K. N., Dilshad, K., Dar, A. A., & Parthasarathy, N. (2022). Impact of anthropogenic disturbances on the liana diversity and need for conservation of resource valued species-evidences from Indian tropical dry evergreen forests. *Taiwania*, *67*(1), 129-139.

xii. Dar, A. A., Babu, K. N., Dilshad, K., Nath, S., & Parthasarathy, N. (2023). Temporal changes in tree community structure and carbon stocks in a human-impacted tropical dry evergreen forest, South India. *Acta Ecologica Sinica*, *43*(4), 701-711.

PARTICULARS OF THE CANDIDATE

Name of the student: Snigdha Nath

Degree: Doctor of Philosophy (Ph.D.)

Title of thesis: Prospect of vermicomposting on transforming oil refinery sludge into valuable organic manure

Date of admission:	21/08/2021
Date of approval in DRC:	31/03/2022
Date of approval in BoS:	25/05/2022
Date of approval in school board:	10/06/2022
Date of consideration in academic council:	13/07/2022
MZU Registration No.:	2200136
MZU Enrolment No.:	MZU2107936
Ph.D. Roll No.:	ES/Ph.D./c.w./21/79
Ph.D. Registration No. and Date:	MZU/PhD/1888 of 21/08/2021

ABSTRACT

PROSPECT OF VERMICOMPOSTING ON TRANSFORMING OIL REFINERY SLUDGE INTO VALUABLE ORGANIC MANURE

A THESIS SUBMITTED IN PARTIAL FULFILLMENT OF THE REQUIREMENTS FOR THE DEGREE OF DOCTOR OF PHILOSOPHY

SNIGDHA NATH

MZU REGISTRATION NO.: 2200136

Ph.D. REGISTRATION NO.: MZU/PhD/1888 of 21/08/2021

DEPARTMENT OF ENVIRONMENTAL SCIENCE

SCHOOL OF EARTH SCIENCES AND NATURAL RESOURCES MANAGEMENT

FEBRUARY, 2026

PROSPECT OF VERMICOMPOSTING ON TRANSFORMING OIL REFINERY SLUDGE INTO VALUABLE ORGANIC MANURE

BY

SNIGDHA NATH

DEPARTMENT OF ENVIRONMENTAL SCIENCE

Supervisor

Dr. SUBHASISH DAS

Submitted

In partial fulfillment of the requirement of the Degree of Doctor of Philosophy in Environmental Science, Mizoram University, Aizawl.

ABSTRACT

Oil refinery sludge (ORS) is an industrial waste generated during the crude-oil extraction and refining processes of the petroleum refineries. The chemical composition of ORS is highly heterogenous, mainly characterized by high concentrations of potentially toxic heavy metals and recalcitrant hydrocarbons. Because of the ever-growing global population and increasing energy demands, the production of petro-based fuels and other intermediates has substantially increased. As a consequent, the generation of ORS has also tremendously aggravated in the petroleum refineries, making the treatment and management of this hazardous sludge an extremely difficult task. In this context, bioremediation avenues have emerged as viable and economically feasible methods to address the undesirable effects of environmental pollution caused by industrial wastes. Among the various bioremediation methods, the potential of earthworms vis-à-vis vermicomposting technology has not yet been examined adequately for the sanitization of a potentially hazardous waste like ORS. Considering the successful precedent works in industrial sludge vermiremediation, the potential of earthworms in bio-transforming ORS is an underexplored research area that requires thorough investigation. Specifically, the lack of systematic data on the remediation efficiency and metabolic performance of two physiologically different earthworm species with regards to ORS mitigation serves as the major research gap of this study. To address these research gaps, the current study was carried out with the following objectives:

i. To convert the oil refinery sludge through vermicomposting.
ii. To compare the potential of *Eisenia fetida* and *Eudrilus eugenia*e to produce vermicompost.
iii. To analyze the impact of vermicompost on the growth and yield of Cabbage and Tomato plant.

The entire experimental work was carried out via four systematic phases: Phase I: Characterization experiment, Phase II: Bioconversion experiment, Phase III: Large-scale composting experiment, and Phase IV: Field experiment. The characterization experiment (Phase I) proposed an eco-friendly approach to counter-balance the chemical and structural heterogeneity of ORS by blending it with natural bulking agents: rice husk (RH) and cow dung manure (CDM) (in 1:1 ratio; w/v). The structural, thermal, and chemical attributes of these two substrates (ORS + RH and ORS + CDM) were studied in detail to choose the appropriate bulking material for the bioconversion experiment (Phase II). From the results, it was observed that the pH, C: N and C:P ratios of ORS + RH were optimum with lesser heavy metal

concentrations than ORS + CDM. The SEM-EDX micrographs revealed good microstructural integrity, porosity, and higher SiO_2 bi-layers on the surface of ORS + RH and better elemental retention than ORS + CDM. The TGA-DTG curves revealed showed distinct stages of mass loss for both the samples. In addition, ORS + RH showed a more thermal reactive profile, with better combustion efficiency (5.2×10^{-07} $\%^2$ $◦C^{-3}$ min^{-2}) than ORS + CDM (2.30×10^{-07} $\%^2$ $◦C^{-3}$ min^{-2}). The FTIR analysis attributed the presence of alcohols, thiols, isocyanates, hydrocarbons, and halogenated compounds more prominently in ORS + CDM. The GC-MS analysis detected 581 compound signatures in total, wherein 63 and 139 were unique to ORS + RH and ORS + CDM, respectively. A higher pollution potential was also depicted by ORS + CDM than its ORS + RH counterpart. From the findings, it was inferred that RH was a suitable bulking material in ORS reusability and valorization. Therefore, ORS + RH was chosen as the composting substrate in the next phase (Phase II).

In the bioconversion experiment (Phase II), the efficiency of three composting systems, viz., *Eisenia*-system (with *Eisenia fetida* - EF), *Eudrilus*-system (with *Eudrilus eugeniae* - EE), and non-earthworm system (AC) was investigated for ORS bioconversion. Accordingly, these three systems were categorized into nine different treatments: EF_1, EF_2, EF_3, EE_1, EE_2, EE_3, AC_1, AC_2, and AC_3. In addition, compost teas were produced from the composts of these treatments to assess their ecotoxicity and health hazard risks. The earthworm-based systems recorded greater increment in available nutrients and reduction of heavy metals than the non-earthworm system. The *Eudrilus*-system recorded an increment in total bacterial count by 10%, while P-solubilizing bacteria increased by 5-folds in the *Eisenia*-system. Among the various treatments, EF_2 and EE_2 outperformed the other treatments in terms of nutrient increment, metal reduction, microbial, and enzymatic activity. The clean index (> 4) and fertility index (> 3.1) of earthworm-sourced composts reflected their high manurial potential. The compost quality index (CQI > 7) indicated that the presence of earthworms greatly facilitated the bioconversion of ORS due to higher humification and microbial diversity. In addition, higher economic benefit was observed in terms of net present value (US $ 203.08), benefit-to-cost ratio (0.63) and pay-back time (1 year and 6 months) in the *Eudrilus*-system. Also, the compost teas of the earthworm-based systems, especially EF_2 and EE_2, demonstrated the lowest environmental and health hazard risks compared to the other compost teas. Principal component analysis identified water holding capacity, total C, N, P, K, and earthworm growth as the major contributors to CQI. From the results, it was inferred that the earthworm-based systems efficiently bio-converted ORS into a fortified organic manure compared to non-earthworm system. Based on the findings, EF_2 and EE_2 were chosen as the two best treatments for the next phase, i.e. large-scale composting experiment (Phase III).

In the large-scale composting experiment (Phase III), a 90-day mesocosm experiment was conducted by upscaling the two best treatments of the bioconversion experiment to study the efficacy of the two species *Eisenia fetida* (EF) and *Eudrilus eugeniae* (EE). Detailed changes in physicochemical properties, heavy metal speciation (in gut and compost), and carbon fractions of the two ORS vermicomposts were evaluated. From the results, it was observed that EE yielded a 1.5-fold higher N increment than EF. In addition, EE reduced Ni's bioavailable fraction and residual fraction by 55.9 % and 39.4 %, respectively. EE also showed an 11 % higher reduction in labile C pool than EF, with 1.95 % increment in its humic acid fraction (HAC). The gut bioaccumulation was 20-47 % higher in EE than EF across heavy metals. Moreover, the removal efficiency of heavy metals with EE was 24 % higher than EF. The higher vermiremediation benefit index (VBI) for EE (1.68) compared to EF (1.45) confirmed the differences in the physiological adaptations of the two species, which facilitated NPK mineralization and metal detoxification. Principal component analysis attributed earthworm growth, gut accumulation, and metal reduction to EE's higher VBI. From the results, it was inferred that both the species were comparable in performance in terms of ORS vermicomposting. However, the physiological adaptations of *E. eugeniae* made it more advantageous in adapting to the toxic composting environment of ORS.

In the field experiment (Phase IV), the efficacy of the two ORS-vermicomposts (*Eisenia fetida* - EF and *Eudrilus eugeniae* - EE) produced from the large-scale composting experiment (Phase III) was assessed in the cultivation of two winter crops: tomato and cabbage. Eight different treatments were utilized in this experiment with a negative control (soil without amendment), positive control (with inorganic fertilizer - NPK_{100}), and the two vermicomposts applied at three different concentrations i.e., 25%, 50%, and 100% (EF_{25}, EF_{50}, EF_{100}, EE_{25}, EE_{50}, and EE_{100}). Accordingly, changes in the physicochemical attributes, metal concentrations in soils and their uptake in crops, and morphometric and phytochemical changes in crops were evaluated. The total N increment in the EE_{100}-applied tomato soils was 14.03% higher than the inorganic fertilizer (NPK_{100}). The overall availability of P increased by 20% in the vermicompost-treated soils. Both the ORS-vermicomposts induced an overall 14.15% lower metal concentrations in soil than NPK_{100}, with 13.25-15.35% lower metal uptake in crops. The overall biochemical content in the crops was also 10.6% higher with EF and EE applications. The higher soil quality index (SQI) in the vermicompost-treated soils (0.60-0.69) compared to

NPK_{100} (0.48) validated both EF and EE's efficient nutritional output and metal reduction potential. Principal component analysis established that the increase in NPK and decline in the heavy metals were the major factors that contributed to SQI. The results indicated that ORS-derived vermicomposts could potentially substitute inorganic fertilizers in terms of their use as organic amendments. However, more research is warranted to assess the long-term sustainability of the soils amended by ORS-vermicompost.